UCLouvain
Institute for Information
and Communication Technologies,
Electronics and Applied Mathematics

Multi-function multi-point wireless networks: Interference analysis and management

Guillaume Thiran

Thesis submitted in partial fulfillment
of the requirements for the degree of
Docteur en Sciences de l'ingénieur et Technologies

Dissertation committee:

Prof. Luc Vandendorpe (UCLouvain, advisor)
Prof. Jérôme Louveaux (UCLouvain)
Prof. Samson Lasaulce (Khalifa University)
Prof. Marc Moonen (KULeuven)
Prof. Robert Schober (FAU Erlangen-Nuremberg)
Prof. David Bol (UCLouvain, chair)

Version of 2024.

Acknowledgments

This work would not have been possible without the support of many people, to whom I would like to express my gratitude.

First, I wish to extend my sincere thanks to all the jury members for their thorough review and for the insightful discussions we shared.

I am especially grateful to Prof. Luc Vandendorpe, who has supervised my work during four years. I have the feeling that we moved from a traditional supervision to a true collaboration, whose climax is probably the works pursued to harness the near-field effect in wireless networks.

My gratitude also goes to Dr. Ivan Stupia, who introduced me to the field of game theory for wireless communications. Yet, the discussions I had with Ivan always sharpened my understanding, helping me to discard the flawed or irrelevant elements and to bring fresh perspectives into the picture.

Since many years, Dr. François De Saint Moulin and (soon-to-be Dr.) Florian Quatresooz have been my daily work companions. They shared with me the joys, challenges, and excitements which are inherent to any research project, and this is why I want to thank them here.

My thanks also go to all my colleagues with whom I have collaborated for research or teaching activities, or simply discussed around a cup of coffee. They really made my four years of PhD an enjoyable and convivial experience.

As those who know me are aware, my family holds a significant place in my life. My PhD does not derogate to the rule, and this is why I want to thank them for their support throughout these four years.

I want to conclude by reserving a special thank you for my wife Céline, who has probably been the most impacted by my PhD journey. I have always been able to rely on her support, encouragements and understanding, even when the demands of the PhD encroached upon our personal lives.

Abstract

Emerging networks are envisioned to sustain not only the communication service, but also other applications such as sensing, localisation, or physical layer security. These multiple functions inherently connect many points, these points being devices, users, access points, computation servers, etc. The several network functions and the multiple points however share the same physical resources, and they thus interfere with each other. This thesis consequently addresses the problem of multi-function multi-point interference analysis and management, along three research directions.

The first studied paradigm considers that the network nodes are autonomous, locally optimising their own resource allocation according to their several functions. Yet, since the resources are shared, the nodes interact together. It must therefore be ensured that they reach a stable point, if possible whatever their preferences among their different functions. This problem is formalised as the convergence of the best response dynamics associated with a competitive game. Several ways of formulating such a game are investigated, and the associated convergence conditions are developed. The theoretical frameworks are moreover applied to two instances of multi-function multi-point networks: a joint radar and communication network, and a multi-level random access scheme.

The second considered research direction focuses on the joint optimisation of the resource allocation of a set of coupled nodes. To that aim, a joint optimisation problem must be formulated, and solution methods must be provided. This approach is applied to a cell-free network in which secure communications must be established thanks to beamforming design. Next, a joint radar and communication application is also optimised thanks to the beamforming design, with a focus on the fairness of the resource allocation among the radar targets and communication users.

Finally, as a third way to handle the interference, the near-field effect is exploited. This effect enables to distinguish radar targets along the range direction of an antenna array. The near-field range estimation problem is hence studied, for two target models, namely the point and extended target models. The maximum-likelihood estimator is obtained, and the associated performance bounds are derived, being the ambiguity function and the Cramér-Rao bound. Closed-form expressions are obtained, in which the parameters' impact is highlighted. Among others, this leads to simple expressions of the range resolution, precision, and the near-field effective region.

Acronyms and Notations

List of Acronyms

AM Alternating Maximisation
AP Access Point
AWGN Additive White Gaussian Noise
BR Best Response
BRD Best Response Dynamics
CDMA Code Division Multiple Access
CF Cell-Free
CRB Cramér-Rao Bound
CSI Channel State Information
DSL Digital Subscriber Line
ET Extended Target
FDMA Frequency Division Multiple Access
FF Far-Field
GNE Generalised Nash Equilibrium
GNEP Generalised Nash Equilibrium Problem
GSS Golden-Section Search
GT Game Theory
HPBW Half-Power BeamWidth
ISI Inter-Symbol Interference
IWFA Iterative WaterFilling Algorithm
JRC Joint Radar and Communication
KKT Karush-Kuhn-Tucker
LHS Left-Hand Side

LoS Line-of-Sight
MF Multi-Function
MF MP Multi-Function Multi-Point
MI Mutual Information
MIMO Multiple-Input Multiple-Output
ML Maximum Likelihood
MO Multi-Objective
MOG Multi-Objective Game
MOGT Multi-Objective Game Theory
MOO Multi-Objective Optimisation
MP Multi-Point
MUI Multi-User Interference
MVDR Minimum Variance Distortionless Response
NE Nash Equilibrium
NEP Nash Equilibrium Problem
NF Near-Field
OFDM Orthogonal Frequency Division Multiplexing
P2P Point-to-Point
PDF Probability Density Function
PNE Pareto-Nash Equilibrium
PoA Price-of-Anarchy
PSD Power Spectral Density
PSLR Peak-to-Side-lobe Level Ratio
PT Point Target
RA Random Access
RE Resource Element
RHS Right-Hand Side
RMS Root-Mean-Square
SDMA Space Division Multiple Access
SF Single-Function
SIMO Single-Input Multiple-Output
SINR Signal-to-Noise-plus-Interference Ratio
SNR Signal-to-Noise Ratio
SO Single-Objective
SOO Single-Objective Optimisation
SP Single-Point
SWIPT Simultaneous Wireless Information and Power Transfer
TDMA Time Division Multiple Access
UE User Equipment

ULA Uniform Linear Array

⋆ List of Notations

a or A	Scalar
$\mathbf{a}$	Column vector
$\mathbf{A}$	Matrix
$\mathcal{A}$	Set
$\mathbf{1}_N$	Column vector of size N with all elements equal to 1
$\mathbf{I}_m$	Identity matrix of size m
$\mathbf{0}_{m\times n}$	Zero matrix of size $m \times n$
$\mathbf{1}_{m\times n}$	Matrix of size $m \times n$ with all elements equal to 1
$\emptyset$	Empty set
$\mathbb{R}$	Set of the real numbers
$\mathbb{R}^+$	Set of the non-negative real numbers
$\mathbb{C}$	Set of the complex numbers
$\mathbb{R}^m$	Set of the size-m real vectors
$\mathbb{R}^{m\times n}$	Set of the $m \times n$ real matrices
$\mathbb{C}^m$	Set of the size-m complex vectors
$\mathbb{C}^{m\times n}$	Set of the $m \times n$ complex matrices
$\mathrm{sign}\{a\}$	Sign of a (for a real)
$\mathrm{Re}\{a\}$	Real part of a
$\mathrm{Im}\{a\}$	Imaginary part of a
$\arg\{a\}$	Argument of a
$\lvert a\rvert$	Absolute value of a
$[a_1, \ldots, a_N]^\top = [a_i]_{i=1}^N$	Vector formed by the elements $a_1, \ldots, a_N$
$[\mathbf{a}]_i$	ith element of $\mathbf{a}$

$[\mathbf{A}]_{i,j}$	(i,j)th element of $\mathbf{A}$
$\mathbf{A}^\top$	Transpose of $\mathbf{A}$
$\mathbf{A}^\star$	Complex conjugate of $\mathbf{A}$
$\mathbf{A}^\mathrm{H}$	Hermitian of $\mathbf{A}$
$\mathbf{A}^{-1}$	Inverse of $\mathbf{A}$ (for $\mathbf{A}$ nonsingular)
$\mathbf{A}^+$	Moore-Penrose generalised inverse of $\mathbf{A}$
$\mathbf{A}^s$	Symmetric part of $\mathbf{A}$: $\mathbf{A}^s = \left(\mathbf{A} + \mathbf{A}^\mathrm{H}\right)/2$
$\mathrm{Tr}\{\cdot\}$	Trace operator (for square matrices)
$\mathcal{R}\{\cdot\}$	Range operator
$\mathrm{rank}\{\cdot\}$	Rank operator
$\|\cdot\|$	Matrix norm
$\|\cdot\|_2$	2-norm vector norm
$\|\cdot\|_F$	Frobenius matrix norm
$\lambda_{\min}(\mathbf{A})$	Minimum eigenvalue of $\mathbf{A}$ (for $\mathbf{A}$ Hermitian)
$\lambda_{\max}(\mathbf{A})$	Maximum eigenvalue of $\mathbf{A}$ (for $\mathbf{A}$ Hermitian)
$\sigma_{\min}(\mathbf{A})$	Minimum singular value of $\mathbf{A}$
$\sigma_{\max}(\mathbf{A})$	Maximum singular value of $\mathbf{A}$
$\kappa(\mathbf{A})$	Condition number of $\mathbf{A}$: $\kappa(\mathbf{A}) = \sigma_{\max}(\mathbf{A})/\sigma_{\min}(\mathbf{A})$
$\sigma_k(\mathbf{A})$	k-th singular value of $\mathbf{A}$
$>, \geq, \leq, <$	element-wise relationships
$\mathbf{A} \succ \mathbf{0}$	$\mathbf{A}$ is positive definite
$\mathbf{A} \succeq \mathbf{0}$	$\mathbf{A}$ is positive semidefinite
$\mathrm{Diag}(\mathbf{a})$	Diagonal matrix with $\mathbf{A}_{ii} = \mathbf{a}_i$
$\mathbf{A}_1 \otimes \mathbf{A}_2$	Kronecker product of $\mathbf{A}_1$ and $\mathbf{A}_2$
$\mathrm{vec}(\mathbf{A})$	Vectorization of the matrix $\mathbf{A}$
$\{a_1, \ldots, a_N\} = \{a_i\}_{i=1}^N$	Set of the elements $a_1, \ldots, a_N$
$[a_1; a_2]$	Closed interval between a_1 and a_2
$]a_1; a_2[$	Open interval between a_1 and a_2
$\mathcal{P}^\mathcal{A}$	Power set of $\mathcal{A}$

$\lvert\mathcal{A}\rvert$	Cardinality of $\mathcal{A}$
$\operatorname{int}\mathcal{A}$	Interior of $\mathcal{A}$
$\operatorname{conv}\mathcal{A}$	Convex hull of $\mathcal{A}$
$\operatorname{span}\{\mathbf{a}_1,\ldots,\mathbf{a}_N\}$	Set spanned by the vectors $\mathbf{a}_1,\ldots,\mathbf{a}_N$
$\mathcal{A}_1 \times \mathcal{A}_2$, $\times_{i=1}^{N}\mathcal{A}_i$	Cartesian product of $\mathcal{A}_1$ and $\mathcal{A}_2$, and $\mathcal{A}_1,\ldots,\mathcal{A}_N$
$\mathcal{A}_1 \cup \mathcal{A}_2$, $\bigcup_{i=1}^{N}\mathcal{A}_i$	Union of $\mathcal{A}_1$ and $\mathcal{A}_2$, and $\mathcal{A}_1,\ldots,\mathcal{A}_N$
$\mathcal{A}_1 \cap \mathcal{A}_2$, $\bigcap_{i=1}^{N}\mathcal{A}_i$	Intersection of $\mathcal{A}_1$ and $\mathcal{A}_2$, and $\mathcal{A}_1,\ldots,\mathcal{A}_N$
$\mathcal{C}^k$	Set of k-times continuously differentiable functions
$\frac{\partial f}{\partial x}$	Partial derivative of the function f with respect to x
$\frac{\partial^2 f}{\partial y \partial x}$	Second-order partial derivative of the function f with respect to x and y
$\frac{\partial^2 f}{\partial x^2}$	Second-order partial derivative of the function f with respect to x
$\boldsymbol{\nabla}_{\mathbf{x}} f$	Gradient of the function f with respect to $\mathbf{x}$, arranged as a column vector: $[\boldsymbol{\nabla}_{\mathbf{x}} f]_i = \frac{\partial f}{\partial x_i}$
$\boldsymbol{\nabla}_{\mathbf{x}}^{\top}\mathbf{f}$	Gradient of the vector function $\mathbf{f}$ with respect to $\mathbf{x}$, arranged as: $\left[\boldsymbol{\nabla}_{\mathbf{x}}^{\top}\mathbf{f}\right]_{i,j} = \frac{\partial f_i}{\partial x_j}$
$\boldsymbol{\nabla}_{\mathbf{yx}}^2 f$	Jacobian matrix of the function f with respect to $\mathbf{x}$ and $\mathbf{y}$: $\left[\boldsymbol{\nabla}_{\mathbf{yx}}^2 f\right]_{i,j} = \frac{\partial^2 f}{\partial y_j \partial x_i}$
$\mathbb{P}[X]$	Probability of the event X
$\mathbb{E}_Y\{X\}$	Expectation of X over the random variable Y
$\mathbb{1}(X)$	Indicator function of the event X
$\delta(x)$	Dirac delta function
$\delta[n]$	Discrete-time impulse function
Δ^N	N-dimensional simplex
$\operatorname{sinc}(x)$	Cardinal sine function $\operatorname{sinc}(x) = \frac{\sin(\pi x)}{\pi x}$
$[\cdot]^+$	$\max\{\cdot, 0\}$
$\mathcal{O}(\cdot)$	Big-O notation

Contents

List of Figures

1 Introduction

The first generations of wireless networks have been designed to optimise the communication performance of the wireless links existing between the core network and the User Equipments (UEs). To that aim, the paradigm has been to provide a network architecture under which each UE communicates with the core network through a virtual Point-to-Point (P2P) link. The two building blocks of this architecture are the following:

- Each UE communicates with the core network via a unique Access Point (AP) at a time, and close APs utilise orthogonal frequency resources;
- The UEs associated with the same AP communicate on orthogonal time, frequency, code, or space resources.

The first point has therefore led to the introduction of the cellular concept, while the second pushed the design of the Time Division Multiple Access (TDMA), Frequency Division Multiple Access (FDMA), Code Division Multiple Access (CDMA), and Space Division Multiple Access (SDMA) schemes. Together, these two elements enable to avoid the interference from the users of the neighbouring cells (inter-cell interference), as well as from the other UEs of the same cell (intra-cell interference). This makes each communication link an instance of a P2P interference-free channel, for which the associated signal processing is therefore facilitated.

The cellular concept hence leads to a Single-Function (SF) Single-Point (SP) perspective, since the network is build focusing on the communication function only, and the communications take place between a single point to another single point. This idealistic vision must be nuanced, since interference occurs between the cells utilising the same frequency resources. To that aim, inter-cell interference coordination mechanisms [1] have been designed to alleviate this issue, especially for the cell-edge users. These mechanisms are however more of an ad-hoc mechanism than a true Multi-Point (MP) approach.

From single-function to multi-function networks Emerging networks differentiate from the early network generations by sustaining other functions than the communication function only. The different envisioned services include the following.

- **Communication function:** The wireless network still supports the communication between the nodes of the network. These communications are however not limited to the AP-UE links, but also include device-to-device communications [2], communications between vehicles and other vehicles [3], and with the infrastructure [4], among others. In a general way, these communications are qualified as *everything-to-everything*.
- **Sensing function:** Wireless signals can be utilised to probe the environment. This function covers thus the positioning services [5] whose aim is to detect and estimate the position and velocity of the nodes of the network. When utilising high carrier frequencies such as the THz band, the network can provide imaging capabilities [6], whose goal is to provide a high-resolution image of the environment. Yet another sensing service is the crowd monitoring application [7] which gathers information about the crowd density and movement.
- **Security function:** The network may provide security of the communications at the physical layer level. Such security services include among others privacy by avoiding the eavesdropping of the communication, fingerprinting services, and secret key distillation [8].
- **Power transfer function:** For nodes which are not connected to the power grid, such as sensors, the network can wirelessly send power, especially when the nodes are located close to the emitting antennas [9].

- **Computing function:** By deploying computing servers inside, or at the edge of the core network, wireless networks are envisioned to support computing services [10]. This may enable the devices to offload their computation tasks to servers with higher computation capabilities, hence targetting an improvement of the energy consumption, latency, accuracy, etc.

- **Caching function:** The information content required by neighbouring nodes at a given time is often similar. Therefore, the network can provide a caching service, which brings the popular content in storage units located close to the nodes [11]. This then enables to reduce the latency and the communication load within the core network.

Emerging networks are thus envisioned to connect points which should support multiple functions. These networks are therefore termed Multi-Function (MF). Moreover, since the connected points are no longer limited to UEs, they are abstractly named *nodes* in this thesis.

From single-point to multi-point networks The evolution from SF to MF networks has for consequence the change from a SP to a MP perspective. Indeed, the cellular concept was suited for vertical communications, occurring between a UE and its associated AP. Yet, the multiple functions make this vertical communication model outdated.

- The communications may indeed take place in an horizontal manner between the nodes, such as in device-to-device [2], vehicle-to-vehicle [3], or machine-to-machine communications [12].

- A single node may access the core network through several APs, in a so-called *cell-free* architecture [13]. Among others, this enables to provide a more uniform performance compared to the cellular architecture, especially for the UEs which were located at the cell-edge.

- Another envisioned network architecture is the multi-tier architecture [14]. This framework still considers the cell concept, but each point of the space may be covered by several cells of different size, named the different tiers.

Therefore, the network should not anymore be modelled as a set of parallel P2P links. Instead, a true MP perspective must be considered.

Interference analysis and management in multi-function multi-point networks In a Multi-Function Multi-Point (MF MP) network, the heterogeneity of the devices and of the network functions call for a flexible interference management. This interference management can partly rely on the allocation of orthogonal resources to the different nodes, similarly to the approach followed in the cellular paradigm. Yet, as the cell concept fades out, interference will likely occur between nodes which are close to each other, especially considering resource-limited networks. Moreover, the considered resources are no longer only radio-resources, but they also include the computing resources, the caching resources, and the other resources required by the different functions. In this context, the world *interference* is used as an abstract way to refer to any kind of coupling between the nodes, or between the functions. It covers the traditional wireless interference, the coupling exiting between nodes accessing the same resource, and it also covers the interactions existing between the conflicting functions of the network. **Consequently, the goal of this thesis is to analyse and manage the interference in MF MP networks.** To that aim, three complementary directions are explored, which are namely the autonomous interference analysis and management, the optimisation-based interference management, and the near-field-based interference analysis. These research directions are summarised in Table 1.1, and detailed below.

	Interference management and analysis in MF MP networks		
Research directions	Autonomous	Optimisation-based	Near-field-based
Interference analysis	×		×
Interference management	×	×	
Challenges	Identify the structural parameters governing the interactions	Formulate the optimisation problem, and solve it	Obtain performance bounds for NF-based radar systems

Table 1.1 Summary of the research directions considered in this thesis

Autonomous interference analysis and management In this first approach, the perspective is to support the flexibility of the network by enabling the nodes to autonomously manage the interference. To that aim, each node can be considered as selfish, performing his resource allocation to optimise his own performance without considering the performance of the other nodes. The choice of one of them however impacts the interference experienced by the other nodes. Given a change of strategy of one node, the others could therefore be willing to update their resource allocation, which could in turn impacts the other nodes, and so on.

In this perspective, the challenge does not lie in the optimisation problem each node faces. Indeed, these problems are by essence SP, with existing solutions for most wireless scenarios. However, the difficulty lies in the fact that the MP character of the network makes the nodes coupled together. Therefore, they interact with each other, and these interactions are not always guaranteed to eventually settle to a stable resource allocation. Such problem falls into the field of the Game Theory (GT) [15], which among others enable to analyse the interactions between competitive agents. **Hence, the aim of the autonomous interference analysis and management approach is to develop a game-theoretic framework able to identify the structural parameters which govern the interactions between the nodes of a MF MP network.**

Optimisation-based interference management It must be emphasised that the autonomous approach is not an optimisation technique. It ensures the interactions between the nodes settle to a stable point, but this point might not be optimal for the network. **Therefore, the second research direction of this thesis focuses on interference management schemes which globally optimise the performance of a MF MP network.**

This problem is tackled by considering a set of MF nodes interacting with each other. Then, an optimisation problem must be formulated, which encompasses the performance metrics of all the considered nodes. A first challenge of this approach is to ensure the formulation of the optimisation problem balances the performance of the different nodes in the desired way. Depending on the cases, the desired trade-off can be the fairness among the nodes, or at the other extreme, the maximisation of the performance of one node with minimal performance requirements for the others. Whatever the selected formulation, the resulting optimisation problem is inherently high-dimensional since it includes the resources of all the considered nodes. A second difficulty lies therefore in providing solution schemes with a low complexity.

Near-field-based interference analysis One drawback of the optimisation-based approach is that it leads to interference management schemes which are heavy both in terms of information centralisation and computational load, especially when many nodes are considered. When there are numerous nodes, the autonomous approach may also be jeopardised, since the resulting analysis could be too complex to be performed, or the interactions could not settle to an equilibrium. As discussed above, the orthogonal resource allocation procedure of cellular network could consequently still be considered, in order to form smaller groups of interfering nodes. Then, the autonomous and the optimisation-based interference management techniques could be applied to these smaller clusters.

To that aim, the traditional time, frequency, code resources can be utilised. Considering nodes equipped with antenna arrays, the space resource can also be leveraged upon in order to discriminate between different propagation angles. The emerging networks additionally offer the possibility to orthogonalise the space dimension not only in the angular domain, but also in the range domain. This is achieved using the so-called *glsnf* effect, which arises for low propagation ranges, high carrier frequencies and large array dimensions.

At the time of writing this thesis, the exploitation of the Near-Field (NF) effect in wireless networks is a very active research domain. Providing a complete answer to the interference management schemes enabled by the NF effect in MF MP network is therefore out of the scope of this thesis. **Nevertheless, as first step towards this goal, the third research direction focuses on the radar function of MF MP networks. More precisely, it studies NF-based radar systems, with an emphasis on the associated performance bounds.** Obtaining such bounds opens the way to the understanding of how densely the range resource can be exploited, and therefore how it can prevent the nodes to interfere with each other.

1.1 Contributions

Given these three research directions, the general contributions of this thesis are the following.

- For the autonomous approach, a general multi-objective game-theoretic framework is developed to model the interactions between multi-function nodes. Focusing on the application to wireless networks, the critical challenge is identified to be the convergence of the best response dynamics towards an equilibrium. Convergence conditions are obtained for different modelling of the nodes' behaviour.

- When each node optimises a weighted-sum of its performance metrics, the obtained convergence conditions hold whatever the weights' value. Since the weights depict the node preferences, these conditions are named *preference-agnostic*.
- If each node optimises a single metric with all others set as constraints, the game-theoretic problem becomes a *generalised Nash equilibrium problem*. Convergence conditions for the best response dynamics are obtained for generalised Nash equilibrium problems whose strategy sets are polyhedral with variable right-hand sides. Since these conditions depend on the constraint thresholds set by the node, they are termed *preference-aware*.
- Between the two above extremes, the nodes could optimise a partial weighted-sum of their metrics, with the other set as constraints. Convergence conditions are also obtained in this case, which are agnostic about the weight of the partial weighted-sum, but dependent on the constraint thresholds.

For each modelling, the obtained frameworks are applied to two multi-function multi-point networks. The first one is an instance of a joint radar and communication network, while the second studies a random access protocol with multiple activity levels. The analysis reveals levers on which the network designer can act to ensure the convergence of the interactions between the nodes.

- In the optimisation-based interference management perspective, two instances of multi-function multi-point networks are considered. The first one is the case of a cell-free network providing at the same time communication services to the legitimate users, while preventing information leakage towards the eavesdroppers. The second instance is a joint radar and communication network, in which a radar system must detect several targets, and receive the uplink communication signals of several users. For both instances, the beamformers associated with the antenna arrays are optimised. The first step towards this goal is the formulation of an optimisation problem which encompasses the performance metrics of all the considered nodes. Then, optimisation procedures for these optimisation problems are designed, and analysed numerically.

- Finally, a near-field radar system is studied, being a first step towards near-field-based interference management. An estimator of the range of a target is provided, which leverages both on the near-field effect and on the traditional round-trip delay of the radar waveform. Two target models are studied, namely the point and the extended target models. The latter model accounts for the fact that in the near-field region, targets may have a significant size. Performance bounds are obtained for the developed range estimator through an analysis of the associated ambiguity function and Cramér-Rao Bound. From these bounds, engineering quantities are derived, being the radar near-field resolution, precision, the peak-to-sidelobe ratio, and the effective field region.

1.2 Thesis organisation

To support the above contributions, the thesis is organised as follows.

Regarding the autonomous part, the general multi-objective game-theoretic framework is developed in Chapter 2. Then, the different flavours of the node modelling are analysed in the subsequent chapters. Chapter 3 studies nodes optimising a weighted-sum of their objective, Chapter 4 nodes optimising a single objective with the others set as constraints, and Chapter 5 the intermediate cases. Then, Chapter 6 draws the conclusions of the autonomous interference analysis and management part, both regarding the developed theoretical frameworks, and the insights gained on the MF MP scenarios.

Then, the second part is divided in two chapters pursuing an optimisation-based interference management approach. Chapter 7 studies the secure beamforming design in a cell-free network, while Chapter 8 tackles the case of the joint radar and communication use-case.

Finally, the near-field range estimation problem is studied in Chapter 9, both for the estimator design and the performance analysis.

Part I

Autonomous interference analysis and management

2

Modelling the interactions between multi-function nodes: the general picture

The author is very grateful to Dr. Ivan Stupia, for bringing to the author attention the autonomous interference management perspective, and for the close and constructive mentoring of the research carried out in this direction. The material of the autonomous part has led to the following research papers [16–18].

In the first part of this thesis, the autonomous interference analysis and management paradigm is explored. As discussed in the introduction, the philosophy behind this paradigm is to consider each node as a selfish entity optimising its own performance, and to let the nodes interact together. The challenge then lies in obtaining conditions ensuring that these interactions eventually settle to a stable point.

The framework suited to such study is the GT. This field of research studies the interactions between competitive agents named the *players*, such interactions being encompassed by what is known as a *game*. For this reason, the terms *node* and *player* will be used interchangeably in this part of the thesis. While originating from the field of economics, GT has since then been applied to various domains, including wireless communications.

Studying wireless networks through the lens of GT requires however to make the wireless world and the GT world meet. The wireless scenarios must be abstracted into games, and the required hypotheses and results provided by the GT must be translated back to the wireless world. To that aim, this chapter sets the scene for the autonomous interference management part by providing the following elements.

- It provides first an overview of the GT terminology, formalisms and notations, which are instrumental to the modelling of wireless networks. It also identifies the properties a game should benefit from in order to be applicable to wireless scenarios.

- The wireless scenarios considered in this thesis are not only MP, they are also MF. This means that each node might have several objective functions which should be optimised together. Therefore, the concept of multi-objective game is defined. Such a multi-objective game can be studied through families of single-objective games, being named the *scalarised game* families. Different versions of such families are defined, and equivalence results between the multi-objective and the scalarised games are provided.

- Two MF MP wireless scenarios are described, for which the nodes' interactions can be analysed with the GT. The first scenario is an instance of a Joint Radar and Communication (JRC) system, while the second models a multi-level random access protocol.

The above elements constitute the contributions of this chapter, yet these latter lies at a conceptual level. Indeed, the challenge of this chapter is to make the wireless requirements and specificities meet the theoretical framework of GT. However, no novel technical results are provided in this chapter, these contributions being instead the focus of the next chapters.

As far as this chapter is concerned, it is structured as follows. First, Section 2.1 introduces the GT concepts instrumental to the analysis of wireless networks, while Section 2.2 covers the related state-of-the-art. The concepts of multi-objective and scalarised games are defined in Section 2.3. Finally, the two MF MP scenarios considered in this part are described in Section 2.4, and the introduced theoretical concepts illustrated on these scenarios.

2.1 Primer on single-objective game theory for wireless networks

To begin the autonomous interference management part, this section provides a brief introduction to the framework of GT, with a focus on the elements relevant for wireless networks. As the interactions between the nodes may take different forms, two types of games are first described in Section 2.1.1 and Section 2.1.2, these games being the Nash Equilibrium Problems (NEPs) and Generalised Nash Equilibrium Problems (GNEPs). Then, the specificities of GT for wireless networks are discussed in Section 2.1.3 and Section 2.1.4, as well as the perspective considered in this thesis.

2.1.1 Nash Equilibrium Problem

A NEP describes the competitive interactions between a set of nodes, named the *players*, which try to optimise their own performance while being coupled together.

To translate the above into the mathematical domain, the following notations are introduced. The number of players is denoted Q, and the set of players is defined as $\Omega \triangleq \{1, \dots, Q\}$. Each qth player controls an n_q-dimensional vector of real variables, grouped into the vector $\mathbf{x}_q \in \mathbb{R}^{n_q}$, and named its *strategy*. This strategy is constrained to belong to the *strategy set* $\mathcal{X}_q \subseteq \mathbb{R}^{n_q}$. To account for the strategy of the other players, the strategy profile $\mathbf{x}_{-q} \triangleq [\mathbf{x}_q]_{r \neq q}$ is introduced, as well as the corresponding set $\mathcal{X}_{-q} \triangleq \bigtimes_{q \neq r} \mathcal{X}_r$. Similarly, the *global strategy profile* is denoted and defined as $\mathbf{x} \triangleq [\mathbf{x}_q]_{q \in \Omega}$, with the set $\mathcal{X} \triangleq \bigtimes_{q \in \Omega} \mathcal{X}_q$. To highlight the impact of the other players on the qth player, the global strategy profile can be written as $\mathbf{x} = (\mathbf{x}_q, \mathbf{x}_{-q})$. This notation is introduced for the sake of clarity, but it however does not mean the strategy of the players are re-ordered. In other words, for two players q and r, $(\mathbf{x}_q, \mathbf{x}_{-q})$ and $(\mathbf{x}_r, \mathbf{x}_{-r})$ correspond to the same global strategy profile $\mathbf{x}$. The performance of each qth player is assessed with an *objective function* denoted $u_q \colon \mathcal{X} \to \mathbb{R}$, which depends at the same time on the strategy of the considered player $\mathbf{x}_q$, and on the one of the others $\mathbf{x}_{-q}$. This is why they are defined on the global strategy set $\mathcal{X}$. Without loss of generality, these functions are considered to be minimised.

Before moving to the definition of NEPs, it must be stressed out the strategies defined above are coined in the GT literature under the name *pure strategies*. The term *pure* refers to the fact that such a strategy is a deterministic element of the strategy set of the player. In a general case, a player might however want to adopt a probabilistic behaviour. This is the case for instance in the rock-paper-scissor game: a pure strategy would be to always play rock, while a mixed strategy would be to assign a 1/3 probability to each of the three choices.

Definition 2.1: Pure and mixed strategies [15]

Given a strategy set $\mathcal{X}_q$ for the qth player,

- a *pure strategy* is an element $\mathbf{x}_q \in \mathcal{X}_q$;
- a *mixed strategy* is a probability distribution over $\mathcal{X}_q$. All pure strategies are also mixed strategies;
- a *strictly mixed strategy* is a mixed strategy which is not a pure strategy.

Remark 2.1

In this thesis, only pure strategies are considered. The strictly mixed strategies are discarded from the analysis for two reasons.

- A game with finite strategy sets and mixed strategies can always be transformed into another game, named the *mixed extension*, for which the strategy sets are convex and compact, and in which only pure strategies need to be considered [19]. This will be illustrated on one of the wireless applicative scenario in Section 2.4.2;
- If the strategy sets are compact convex sets, then under strict convexity assumptions, it can be shown that the strictly mixed strategies are always suboptimal with respect to pure strategies. In that case, they can therefore be discarded without loss of generality [20, Theorem 3], and the game can thus be simplified into a NEP with only pure strategies.

Therefore, in the following, the GT concepts (equilibrium points, best responses) will always be defined in terms of pure strategies, unless explicitly stated.

A NEP is thus characterised by a set of player Ω, the players' strategy sets $\{\mathcal{X}_q\}_{q\in\Omega}$, and the players' objective functions $\{u_q\}_{q\in\Omega}$. It is hence denoted as $\mathcal{G} \triangleq \left\langle \Omega, \{\mathcal{X}_q\}_{q\in\Omega}, \{u_q\}_{q\in\Omega} \right\rangle$, and formally defined in the below definition.

Definition 2.2: Nash equilibrium problem [15]

A Nash equilibrium problem $\mathcal{G} = \left\langle \Omega, \{\mathcal{X}_q\}_{q\in\Omega}, \{u_q\}_{q\in\Omega} \right\rangle$ modelises the interactions between the players indexed in Ω. The behaviour of the qth player is described by the following single-objective optimisation problem:

$$\begin{aligned} \text{minimise}_{\mathbf{x}_q} \quad & u_q\left(\mathbf{x}_q, \mathbf{x}_{-q}\right), \\ \text{s.t.} \quad & \mathbf{x}_q \in \mathcal{X}_q, \end{aligned} \tag{2.1}$$

in which $\mathbf{x}_{-q}$ is considered as a fixed parameter.

For each qth player, given $\mathbf{x}_{-q} \in \mathcal{X}_{-q}$, the strategies which minimise the above are grouped into the Best Response (BR) set, denoted $\mathcal{BR}_q\left(\mathbf{x}_{-q}\right)$ and defined as

$$\mathcal{BR}_q\left(\mathbf{x}_{-q}\right) \triangleq \left\{\mathbf{x}_q \in \mathcal{X}_q | \nexists \mathbf{y}_q \in \mathcal{X}_q \text{ s.t. } u_q\left(\mathbf{y}_q, \mathbf{x}_{-q}\right) < u_q\left(\mathbf{x}_q, \mathbf{x}_{-q}\right)\right\}. \tag{2.2}$$

In other words, this latter is a set-valued mapping $\mathcal{BR}_q \colon \mathcal{X}_{-q} \to \mathcal{P}^{\mathcal{X}_q}$, with the notation $\mathcal{P}^{\mathcal{S}}$ denoting the power set of $\mathcal{S}$, i.e., the set of all its subsets. When whatever $\mathbf{x}_{-q} \in \mathcal{X}_{-q}$, a unique BR exists, then the BR mapping becomes a regular function denoted $\mathbf{BR}_q \colon \mathcal{X}_{-q} \to \mathcal{X}_q$. Such BR mappings group thus the strategies which can be rationally played by the players, considering the strategy of the others as fixed. Therefore, the equilibrium of a NEP is a global strategy profile $\mathbf{x}^{(\mathrm{E})} \in \mathcal{X}$ such that each player has a strategy belonging to its BR set. This equilibrium concept is named the Nash Equilibrium (NE) concept [15], and it is formally defined as follows.

Definition 2.3: Nash Equilibrium [15]

Given a NEP $\mathcal{G} = \left\langle \Omega, \{\mathcal{X}_q\}_{q\in\Omega}, \{u_q\}_{q\in\Omega} \right\rangle$, a strategy profile $\mathbf{x}^{(\mathrm{E})} \in$

$\mathcal{X}$ satisfying

$$\mathbf{x}_q^{(\mathrm{E})} \in \mathcal{BR}_q\left(\mathbf{x}_{-q}^{(\mathrm{E})}\right), \quad \forall q \in \Omega, \tag{2.3}$$

is named a Nash equilibrium.

Intuitively, a NE is thus a point at which no player has an interest in modifying its strategy unilaterally. For a NEP $\mathcal{G}$, the set of NE is denoted $\mathcal{E}(\mathcal{G})$.

2.1.2 Generalised Nash equilibrium problem

In a NEP, the interaction of the players lies in the objective functions. GNEPs broaden the above by considering the case of strategy sets also depending on the other players, as originally introduced by Debreu [21, 22].

Additionally to the fixed set $\mathcal{X}_q$, the *strategy-dependent strategy set* $\tilde{\mathcal{X}}_q(\mathbf{x}_{-q})$ is therefore introduced for each qth player, these sets being such that $\tilde{\mathcal{X}}_q(\mathbf{x}_{-q}) \subseteq \mathcal{X}_q$ whatever $\mathbf{x}_{-q} \in \mathcal{X}_{-q}$. In other words, the fixed sets are outer bounds for the moving strategy sets. In terms of mathematical objects, these latter are set-valued mappings defined as $\tilde{\mathcal{X}}_q \colon \mathcal{X}_{-q} \to \mathcal{P}^{\mathcal{X}_q}$. In GNEPs, the objective function definition must be refined in order to include cases in which for a given $\mathbf{x}_{-q} \in \mathcal{X}_{-q}$, the objective function is only defined on $\tilde{\mathcal{X}}_q(\mathbf{x}_{-q})$, and not on $\mathcal{X}_q$. To that aim, the set $\mathcal{Y}_q$ is introduced as the set of strategy profiles which are feasible for the qth player given the strategy of the others:

$$\mathcal{Y}_q(\mathbf{x}_{-q}) \triangleq \left\{\mathbf{x} \in \mathcal{X} \middle| \mathbf{x}_{-q} \in \mathcal{X}_{-q}, \mathbf{x}_q \in \tilde{\mathcal{X}}_q(\mathbf{x}_{-q})\right\}. \tag{2.4}$$

With this definition, the objective functions of the qth player is defined as $u_q \colon \mathcal{Y}_q \to \mathbb{R}$.

The constitutive elements of a GNEP are thus the set of player Ω, the moving strategy sets $\left\{\tilde{\mathcal{X}}_q(\mathbf{x}_q)\right\}_{q\in\Omega}$, and the objective functions $\{u_q\}_{q\in\Omega}$. The associated GNEP is thus denoted $\tilde{\mathcal{G}} = \left\langle \Omega, \left\{\tilde{\mathcal{X}}_q\right\}_{q\in\Omega}, \{u_q\}_{q\in\Omega}\right\rangle$, the *tilde* notation highlighting the generalised character of such problem.

	Player set	Strategy sets	Objective functions
NEP $\mathcal{G}$	Ω	$\mathcal{X}_q$	$u_q : \mathcal{X} \to \mathbb{R}$
GNEP $\tilde{\mathcal{G}}$	Ω	$\mathcal{X}_q$ $\tilde{\mathcal{X}}_q\left(\mathbf{x}_{-q}\right) : \mathcal{X}_{-q} \to \mathcal{P}^{\mathcal{X}_q}$ $\mathcal{Y}_q \subseteq \mathcal{X}$	$u_q : \mathcal{Y}_q \to \mathbb{R}$

Table 2.1 Comparison of the defining elements of a NEP and a GNEP.

Definition 2.4: Generalised Nash equilibrium problem [23, 24]

A generalised Nash equilibrium problem $\tilde{\mathcal{G}} = \left\langle \Omega, \left\{\tilde{\mathcal{X}}_q\right\}_{q\in\Omega}, \left\{u_q\right\}_{q\in\Omega} \right\rangle$ modelises the interactions between the players indexed in Ω. The behaviour of the qth player is described by the following single-objective optimisation problem:

$$\begin{aligned} \text{minimise}_{\mathbf{x}_q} \quad & u_q\left(\mathbf{x}_q, \mathbf{x}_{-q}\right), \\ \text{s.t.} \quad & \mathbf{x}_q \in \tilde{\mathcal{X}}_q\left(\mathbf{x}_{-q}\right), \end{aligned} \tag{2.5}$$

in which $\mathbf{x}_{-q}$ is considered as a fixed parameter.

In order to better grasp the defining elements of a NEP and a GNEP, they are compared in Table 2.1, and illustrated in Example 2.1. As it can be observed by comparing Table 2.1 to the GNEP notation, only the moving strategy sets are present in the triplet notation. The sets $\mathcal{Y}_q\left(\mathbf{x}_{-q}\right)$ are indeed fully described by the moving strategy sets, while the sets $\mathcal{X}_q$ can be build from $\tilde{\mathcal{X}}_q\left(\mathbf{x}_{-q}\right)$ so has to ensure $\tilde{\mathcal{X}}_q\left(\mathbf{x}_{-q}\right) \subseteq \mathcal{X}_q$ whatever $\mathbf{x}_{-q} \in \mathcal{X}_{-q}$, for all players.

As for NEPs, the minimisers of the above are grouped into the BR mapping, defined as

$$\begin{aligned} &\mathcal{BR}_q\left(\mathbf{x}_{-q}\right) \\ &\quad \triangleq \left\{\mathbf{x}_q \in \tilde{\mathcal{X}}_q\left(\mathbf{x}_{-q}\right) \middle| \nexists \mathbf{y}_q \in \tilde{\mathcal{X}}_q\left(\mathbf{x}_{-q}\right) \text{ s.t. } u_q\left(\mathbf{y}_q, \mathbf{x}_{-q}\right) < u_q\left(\mathbf{x}_q, \mathbf{x}_{-q}\right)\right\}. \end{aligned} \tag{2.6}$$

As it can be noticed, the same notation is used to denote the BR mapping of a GNEP and the one of a NEP, as both BRs are defined similarly. Similarly to NEPs, the BR mapping of the qth player will be denoted $\mathbf{BR}_q\left(\mathbf{x}_{-q}\right)$ if it is single-valued whatever $\mathbf{x}_{-q} \in \mathcal{X}_{-q}$. With these elements, the equilibria of a GNEP, named the *Generalised Nash Equilibria (GNEs)*, are defined as follows, and grouped into the set $\mathcal{E}\left(\tilde{\mathcal{G}}\right)$.

Definition 2.5: Generalised Nash Equilibrium [24]

Given a GNEP $\tilde{\mathcal{G}} = \left\langle \Omega, \left\{\tilde{\mathcal{X}}_q\right\}_{q\in\Omega}, \left\{u_q\right\}_{q\in\Omega}\right\rangle$, a strategy profile $\mathbf{x}^{(\mathrm{E})} \in \mathcal{X}$ satisfying

$$\mathbf{x}_q^{(\mathrm{E})} \in \mathcal{BR}_q\left(\mathbf{x}_{-q}^{(\mathrm{E})}\right), \quad \forall q \in \Omega, \tag{2.7}$$

is named a generalised Nash equilibrium.

To conclude this section, Example 2.1 illustrates the above concepts.

Example 2.1

A two-player GNEP $\tilde{\mathcal{G}}^c$ parametrised by $0 < c < 1.5$ is considered. The players' objective functions and strategy sets are defined as

$$\begin{cases} u_1\left(x_1, x_2\right) = \left(x_1 - cx_2 + 1\right)^2, \\ \mathcal{X}_1 = \tilde{\mathcal{X}}_1\left(x_2\right) = \left[-2; 2\right], \end{cases} \qquad \begin{cases} u_2\left(x_2, x_1\right) = \left(x_2 + cx_1\right)^2, \\ \mathcal{X}_2 = \left[1 - 2c; 3 + c\right], \\ \tilde{\mathcal{X}}_2\left(x_1\right) = \left[1 - cx_1; 3 - c\frac{x_1}{2}\right]. \end{cases}$$

The first player is thus a classic NEP player, while the second is characteristic of GNEPs since his strategy set depends on x_1. Figure 2.1 depicts the different strategy sets of this GNEP. Among others, the difference between $\mathcal{X}$ and $\mathcal{Y}_2$ can be noticed, since

$$\begin{aligned} \mathcal{X} &= \mathcal{Y}_1 = \left[-2; 2\right] \bigtimes \left[1 - 2c; 3 + c\right], \\ \mathcal{Y}_2 &= \left\{\left[x_1, x_2\right]^\top \in \mathbb{R}^2 \middle| x_1 \in \left[-2; 2\right], \ 1 - cx_1 \le x_2 \le 3 - c\frac{x_1}{2}\right\}. \end{aligned}$$

For this example, by inspection, the BRs are obtained as

$$\mathrm{BR}_1\left(x_2\right) = \min\left\{\max\left\{cx_2 - 1, -2\right\}, 2\right\}, \quad \mathrm{BR}_2\left(x_1\right) = 1 - cx_1,$$

as also represented in the figure. Analysing the fixed points of these BR mappings, it appears the GNEP has a unique equilibrium given by $\mathbf{x}\left(\mathrm{E}\right) = \left[\frac{c-1}{c^2+1}, \frac{c+1}{c^2+1}\right]^\top$.

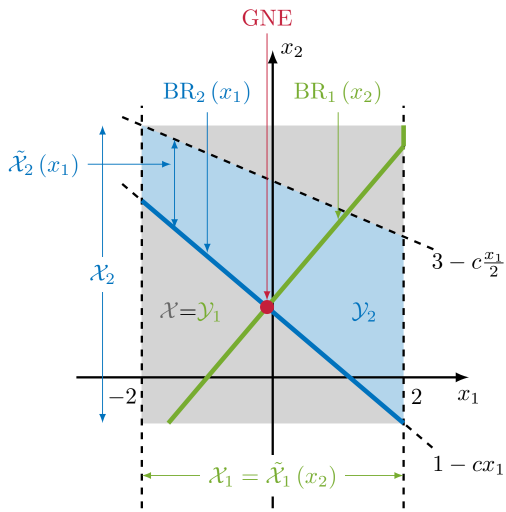

Fig. 2.1 Illustration of the strategy sets, BRs and equilibrium of the GNEP defined in Example 2.1, for $c = 0.85$.

2.1.3 Game theory for wireless networks, and considered point-of-view

In this part of the thesis, the interactions occurring in wireless networks will be studied through NEPs and GNEPs. Contrarily to what the names may hint, there is much more to study in these problems than the mere computation of the equilibria. This section formulates thus requirements on these problems for them to be applicable to wireless scenarios.

- **Equilibrium existence**: the games must have at least one equilibrium, otherwise the players will not be able to reach a stable state.

- **Equilibrium unicity**: this requirement is not mandatory, but can be desirable in certain contexts. First, it avoids the design of equilibrium selection procedures, needed when several equilibria exist. Secondly, if iterative procedures are designed to reach an equilibrium, the unicity enables to have a predictable outcome for the game whatever the iterations order and the starting point. Finally, again considering iterative procedures, this requirement enables to cope with adversarial players. Indeed, if several equilibria exist, some equilibria could suit better a player than the others. Therefore, this player might try to push the iterations towards these preferred equilibria by acting in an adversarial manner, even if the game has already converged to another equilibrium.

- **Equilibrium computation, or convergence of a learning dynamics**: If an equilibrium exists, then it remains to bring the players to this equilibrium. This can be done by a central authority, which would compute the equilibrium and communicate the resulting strategies to the players. Yet, in many cases, such information and computation centralisation is not possible. In that case, an equilibrium must be reached iteratively. This iterative process is named the *learning dynamics* and its convergence must be assessed.

- **Required side-information**: Associated with the above is the information required to compute the equilibrium in the centralised case, or the one needed by the players to implement the learning dynamics in the autonomous case.

- **Price-of-anarchy**: Due their competitive nature, NEs exhibit performance losses with respect to a global optimum jointly computed across the players. The Price-of-Anarchy (PoA) [25] measures this performance loss, and is thus of interest when analysing the performance of a GT approach.

In light of the above, two main questions arise. First, one should decide whether the equilibria are computed in a centralised manner, or if the players must reach them autonomously. In the latter case, the second question amounts at determining which learning dynamics will be considered. **As detailed in the below discussion, this thesis considers the autonomous approach with as dynamics the Best Response Dynamics (BRD)**, this dynamics letting the players update their strategy according to their BR.

Centralised versus autonomous equilibrium computation This thesis defends the point of view that computing an equilibrium in a centralised manner in wireless networks is not realistic. Indeed, such approach is possible only if the players' information can be centralised. However, if the information of all nodes is available, then it is also possible to perform a joint optimisation. Except in peculiar cases, such joint optimisation provides a point which improves the objective function of all players, compared to the equilibrium of a game. Moreover, since centralised equilibrium computations are very often based on reformulations into equivalent optimisation problems, both approaches are likely to have a similar numerical complexity. Therefore, the centralised optimisation approach offers a better performance, while not necessarily being more complex than the centralised GT approach. This is why this work focuses on the cases in which an equilibrium is reached autonomously by the players.

Remark 2.2: Decision, computation and information autonomy

The above discussion advocates for the autonomous approach over the centralised one. This autonomy applies to three levels. First, the decisions are performed locally by each node based on some local rule. Secondly, it is considered the nodes have enough computational power to behave according to their local rule. Thirdly, the nodes are assumed to be able to *efficiently* gather the information required to make their decision.

Regarding the information part, a full autonomy is difficult to achieve. Indeed, the nodes need at some point to gather information about the strategy implemented by the other players. This is why this remark emphasises the *efficiency* rather than the *autonomy* of the nodes with respect to the information. Depending on the type of learning dynamics, and on the specific game instances, the side-information exchanges which are required can then be discussed. This will be done below for the two wireless scenarios described in Section 2.4.

Learning dynamics Designing algorithms converging towards an equilibrium is known in the literature as the problem of *learning in games*. An overview of existing algorithms is provided in [19, Table 6.2], algorithms differing in terms of compatible game classes, convergence conditions, type of equilibrium and required side-information. In this thesis, the case of games with continuous strategy sets is tackled, as opposed to games in which players have a finite set of actions. Among the dynamics described in [19, Table 6.2], only two of them are suited to the computation of (generalised) NEs in such games: the BRD and the Brown fictitious play [26]. Informally, the BRD amounts at letting players update their strategy according to their BR, at any time. The Brown fictitious play tackles the case of mixed strategies, in which the probability distribution of the strategies of the players is determined based on the dynamics history, and then the players compute a BR probability distribution on their strategy set. In the NEPs and GNEPs defined in Definitions 2.2 and 2.4, the players however only consider their pure strategies. In that case, the probability density learning of the Brown fictitious play is not needed, and the BRD appears thus as the best choice.

Beside this first point, we feel that there is a fundamental difference between the BRD and the other dynamics. The BRD indeed sticks to the definition of the player behaviour given by the optimisation problems (2.1) and (2.5). On the contrary, the other dynamics modify the behaviour of the players in order to make them learn the equilibrium. In wireless scenarios, the nodes might however not be aware of the game characteristics, such as the number of players, or the strategy sets of the others players. They even might not be conscious that they are interacting with the other nodes of the network, and thus that they are part of a game. A typical example of such setting is the power allocation on Orthogonal Frequency Division Multiplexing (OFDM) tones in an interference channel [27–29], which has been widely studied under a GT perspective. To maximise their capacity, the nodes implement a waterfilling operation which depends on the total noise-plus-interference power and on the channel coefficient of each tone. To implement the waterfilling operation, this power is measured at the receiver, but this receiver does not differentiate the impact of the other nodes. In fact, he might not differentiate between a change in the power allocation of the other nodes, and a change of channel coefficients. This implies that in such setting, the interactions of the node can be modelled as the BRD of a competitive game, even if the players are not conscious they belong to such game. This difference between the BRD and the other dynamics is a second reason why the BRD is considered in this thesis.

A few other reasons motivate the study of the BRD only. One of them is that the BRD is particularly attractive in what is named *aggregative games* [30], which are games in which the objective function of one player depends on an aggregate quantity of the other players' strategies. Thus, only the aggregate quantity must thus be known by a player to implement the BRD. As below examples will show, many wireless situations correspond to aggregative games, the aggregate quantity being for instance the total interference power impacting a player. Yet another advantage of the BRD is that when it converges, it is heuristically observed to converge quickly towards a NE [19].

For these reasons, the totally asynchronous BRD is considered in this work, as formally defined in the next section. The drawback of studying solely this dynamics is that its convergence is not guaranteed for all games. Therefore, the underlying perspective of this thesis is to identify sufficient conditions under which convergence can be ensured. These conditions enable then to identify structural parameters (interference limits, allowed number of players, etc) which are levers to control the players' interaction. In other words, the goal of the next chapters is to identify macro-parameters able to manage the interference between the players, the interference being either classical wireless interference, or other forms of player interactions.

Remark 2.3

The above discussion does not put the PoA of a competitive scheme as a central point of the analysis. Nevertheless, the competitive perspective of this thesis might be considered irrelevant if the PoA of the reached equilibrium is too high, and this independently of whether the BRD converges or not.
Obtaining a priori guarantees or bounds on the PoA would thus be of paramount interest. Yet, to the author knowledge, there exists no general result which enables to analyse the objective functions and strategy sets of a game, and to deduce from this the PoA of the game. Instead, in the wireless literature, the PoA is usually obtained in a different manner for each considered system model. When such a model is relatively simple, this PoA analysis can be theoretical, based on ad-hoc arguments. In that case, a priori bounds can be obtained which measure the worst-case efficiency of the competitive approach. In many cases, such theoretical analysis is however not possible. Yet, a numerical evaluation can be performed by comparing the reached equilibrium with the point obtained by solving numerically a centralised optimisation problem [31, 32].
In the following chapters, our goal is rather to develop general theoretical frameworks which can then be applied to specific wireless scenarios. This is the reason why the PoA analysis is left for future works.

2.1.4 Best response dynamics

In the totally asynchronous BRD name, the terms *totally asynchronous* mean that players update their strategy at any time, and possibly with outdated information about the other players' strategy. To describe these effects, each qth player is associated with a set $\mathcal{N}_q \subseteq \{1, 2, \ldots\}$ of its update times and with the times $\left\{\{\tau_r^q(n)\}_{r\neq q}\right\}_{n\in\mathcal{N}_q}$. The time index $\tau_r^q(n)$ denotes the fact that at time n, the qth player knows the strategy of the rth player which has been used at time $\tau_r^q(n)$, and not the current one. Naturally, these times are such that $\tau_r^q(n) \in \{0, 1, \ldots, n\}$, as players can only use past and current information. Let $\mathbf{x}_q^{(n)}$ be the strategy of the qth player at time n, and define the strategy profile of other players as seen at time n by the qth player as $\mathbf{x}_{-q}^{(\boldsymbol{\tau}^q(n))} \triangleq \left\{\mathbf{x}_r^{(\tau_r^q(n))}\right\}_{r\neq q}$. With these definitions, the totally asynchronous BRD is described by Algorithm 1.

Algorithm 1 Totally asynchronous best response dynamics

Set $\mathbf{x}^{(0)} \in \mathcal{X}$.
for $n = 1 \to \infty$ **do**
  for $q = 1, \ldots, Q$ **do**
    if $n \in \mathcal{N}_q$ **then**
      Set $\mathbf{x}_q^{(n)} = \mathbf{BR}_q\left(\mathbf{x}_{-q}^{(\boldsymbol{\tau}^q(n))}\right)$.
    else
      $\mathbf{x}_q^{(n)} = \mathbf{x}_q^{(n-1)}$.

As it can be observed, the algorithm is described in terms of a single-valued function $\mathbf{BR}_q(\mathbf{x}_{-q})$, instead of the BR set $\mathcal{BR}_q(\mathbf{x}_{-q})$. This is only valid when whatever $\mathbf{x}_{-q}$, the BR set is never empty, and always contains a single element. To deal with multivalued BRs, the BRD can be modified by letting players select one of the strategy uniformly at random among the optimal responses [19, Section 5.2]. In this thesis, the non-emptiness and convexity hypotheses which will be required by the subsequent analysis will make sure that such case does not occur, hence the algorithm is given in its single-valued form.

In the totally asynchronous case, assumptions are needed to prevent some of the players from stopping the updates of their strategy, and from using too old information about the other players' strategy. The below assumption is hence introduced [33], naturally holding in any practical scenario.

Assumption 2.1: Best response dynamics

For each qth player,

- his strategy is updated infinitely often: $|\mathcal{N}_q| = \infty$;
- the outdated information about any rth player is eventually purged from the system: $\lim_{k\to\infty} \tau_r^q(n_k) = \infty$ with $\{n_k\}$ an increasing sequence in $\mathcal{N}_q$.

Being particular cases of the above, the synchronous and sequential flavours of the BRD have respectively $\mathcal{N}_q = \{q, Q+q, 2Q+q, \ldots\}$ and $\mathcal{N}_q = \{q, q+Q, q+2Q, \ldots\}$, and they require the players to have up-to-date information when they are allowed to update their strategy: $\tau_r^q(n) = n$, $\forall n \in \mathcal{N}_q$, $\forall q, r \in \Omega$ with $q \neq r$.

To illustrate the above definitions, the behaviour of the BRD of Example 2.1 is investigated in the below example. As expected, the BRD does not always converge, the challenge being in the identification of structural parameters enabling the control of such convergence.

Example 2.2

The sequential BRD of Example 2.1, obtained with $\mathcal{N}_1 = \{2, 4, 6, \ldots\}$ and $\mathcal{N}_2 = \{1, 3, 5, \ldots\}$, is depicted in Figure 2.2, its behaviour depending on the parameter c. When $0 \leq c < 1$ (case (a)), the BRD always converges towards the equilibrium. When $c = 1$, (Case (b)), then the BRD gets stuck in cycles. The same behaviour is observed when $1 < c \leq 1.5$ (case (c)), except that in this case, all starting points lead to the same cycle. Finally, when $c > 2$, then the strategy set of the second-player is empty for low values of x_1, and therefore the BRD becomes undefined. It can moreover be checked that the same behaviour occurs for the synchronous BRD in which $\mathcal{N}_1 = \mathcal{N}_2 = \{1, 2, 3, \ldots\}$, and for the asynchronous BRD.
The above analysis reveals that the parameter c acts as a macro-parameter controlling the player interactions. This parameter can in fact be observed to measure in some sense the players' coupling, for instance by looking at the optimisation problem definitions. Players are independent when $c = 0$, slightly coupled for small c's while they become highly coupled as c increases. Far from being a coincidence,

this link between player coupling and convergence of the BRD will be formalised in the below chapters of the thesis.

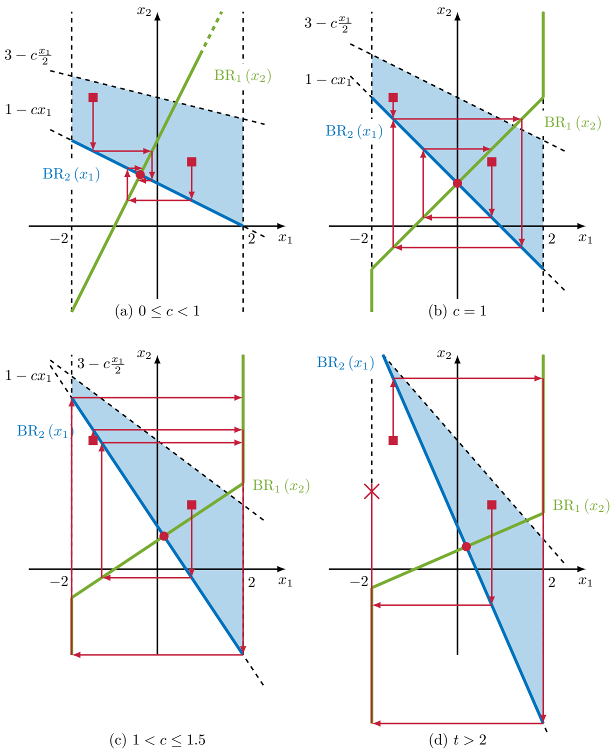

Fig. 2.2 BRD of the GNEP of Example 2.1, for four parameters c. The strategy sets' representation are identical to those of Figure 2.1. The sequential BRD is displayed with red arrows, from two different starting points. On panel (d), the cross represents the fact that the second player has no feasible strategy at that point, and thus cannot implement a BR.

In this section, the BRD has been defined, both in its totally asynchronous version, and in its synchronous and sequential flavours. In the following, the question will be to determine whether the BRD converges or not. A related question, which has not yet been discussed, is the speed at which convergence occurs. While relevant for the synchronous and sequential BRDs, this question can however not be answered for the totally asynchronous BRD. Indeed, Assumption 2.1 states its requirements in terms of times growing to infinity, both for the update times and the outdating of the information. Therefore, convergence results will be stated in terms of the limit point of the strategies of the players as the time grows to infinity. The below definition formalises this convergence concept.

Definition 2.6: BRD convergence

The totally asynchronous BRD is said to converge to an equilibrium $\mathbf{x}^{(\mathrm{E})} \in \mathcal{X}$ if whatever $q \in \Omega$, whatever the initial strategy profile $\mathbf{x}_q^{(0)} \in \mathcal{X}_q$, whatever the update times $\mathcal{N}_q \in \{1, 2, \ldots\}$ and measure times $\left\{\{\tau_r^q(n)\}_{r \neq q}\right\}_{n \in \mathcal{N}_q}$ satisfying Assumption 2.1, with $\tau_r^q(n) \in \{0, \ldots, n\}$, the below limit exists and is equal to the equilibrium strategy:

$$\lim_{n \to \infty} \mathbf{x}_q^{(n)} = \mathbf{x}_q^{(\mathrm{E})}.$$

If one wants to obtain information about the convergence speed in the asynchronous case, the requirements of Assumption 2.1 must be modified in order to only allow a partial asynchronism, as described in [33, Section 6.3.5, Chapter 7]. More precisely, a maximum delay B must be required to exist, limiting the maximum time a player can stay without updating its strategy, and without measuring the one of the others. In that case, convergence rate could be obtained for the partially asynchronous BRD. Another possibility offered by the partial asynchronism framework is that in some cases, the totally asynchronous BRD could diverge, while the partially asynchronous one could be proven to converge for a finite or small enough delay B. These opportunities constitute very interesting research directions, but they are not covered in this thesis.

2.2 (G)NEPs for wireless networks: state-of-the-art

Modelling the interactions occurring in wireless networks as NEPs or GNEPs is a well-established approach, which has been used in various scenarios. This section first provides an overview of these wireless scenarios in Section 2.2.1. Some of them are instances of MF networks, yet it is argued below that the performed analyses do not fully encompass the Multi-Objective (MO) character of the interactions. Hence, Section 2.2.2 presents the mathematical basis which can be leveraged upon in order to obtain such Multi-Objective Game Theory (MOGT) results.

2.2.1 Competitive interactions in wireless networks

One of the earliest application of GT in wireless systems has been the analysis of the power control problem in cellular networks [34–42]. In such setting, the players are the UEs which must choose their transmit power such that at the corresponding receiver, their Signal-to-Noise-plus-Interference Ratio (SINR) is high enough, or other related metrics.

The advent of Digital Subscriber Line (DSL) and OFDM systems has brought new challenges, since the power of one UE is spread over the multiple tones, and the inter-user interference occur in a tone-by-tone fashion. In that case, the power allocation which maximises the sum-rate while fulfilling power constraints has a waterfilling expression, the water level depending on the interference-plus-noise power of each tone. Such interference makes thus the UEs coupled, motivating the analysis of the coupling with GT. Generalising the power control problems, the competitive interactions of the UEs have therefore been studied in [28, 29, 43–53]. These works have popularised the use of the BRD in DSL and OFDM interference channels, the dynamics being known as the Iterative WaterFilling Algorithm (IWFA) due to the BR expression.

The emergence of Multiple-Input Multiple-Output (MIMO) systems has once again raised the question of the power allocation and precoder design across the antennas. Similarly to the OFDM systems, the precoder maximising the channel capacity while fulfilling power constraints has a waterfilling-like expression. The interactions between the precoders have been analysed in [32, 54], once again naming the BRD as the IWFA. Synthesising this line of research, [55] provides a survey of the state-of-the-art tools employed to analyse the BRD convergence.

While the use of GT for game theory stems from the communication rate maximisation, it has since then been applied to many other scenarios. MF scenarios include JRC systems [56, 57], Simultaneous Wireless Information and Power Transfer (SWIPT) networks [58, 59], cell-free massive MIMO systems [60], Wi-Fi and cellular communications coexistence [61], federated learning networks [62–65], etc. Yet, as discussed in the below paragraph, the above works assume that the preferences of the players among their different functions are known and fixed, while this is usually not the case in practical scenarios.

2.2.2 Multi-objective game theory - the case of incomplete preferences

In MF wireless applications, the players are characterised by several metrics, such as the rate, consumed power, harvested power, radar detection probability, etc. To handle several metrics, the players can be modelled as optimising one of them, with the other as constraints. They can also optimise a weighted scalar function of the metrics, such as a weighted-sum, a weighted maximum, etc. In both cases, the player behaviour is thus dependent on some parameters, which are either the constraint thresholds, or the weights of the objective functions. These parameters depict the preference of the players among their metrics. If the game analysis depend on the value of these parameters, then this analysis depend on the player preferences, which are thus assumed to be known to the game modeller. In such setting, the players are said to have *complete preferences*, and the game analysis is said in this thesis to be *preference-aware*.

This raises the question of whether it is possible to analyse the interactions between players with *incomplete preferences*, with an analysis being hence termed *preference-agnostic*. Such situation has been first analysed in 1959 by Lloyd Shapley [66], coined under the name of a game with vector payoffs. In such game, the players optimise the several metrics without specifying the relative importance of the metrics. Their behaviour is thus encompassed by a Multi-Objective Optimisation (MOO) problem, whose optimal points are those which are Pareto-optimal. Instead of the traditional NE concept, such games thus lead to the definition of Pareto-Nash Equilibria (PNEs).

As it is already shown in [66] for finite zero-sum games, these PNEs can be reached as the NE of a NEP, in which the objective function is a weighted-sum of the original objective with well-chosen weights. Pursuing this line of research, [67–80] have studied the equivalences between the PNEs and the NEs of associated NEPs, these latter being named the *scalarised games*. Depending on convexity, continuity and finiteness assumptions, different family of scalarised games can be considered.

These equivalences motivate the study of Multi-Objective Games (MOGs) from their scalarised counterparts. However, as discussed in Section 2.1.3, wireless applications require other properties than the existence of an equilibrium. Among others, one can wonder how one can ensure the convergence of the BRD for all scalarised games. This would enable to have results holding whatever the preferences of the players, in order to truly encompass the MO character of the interactions.

To the author knowledge, such question has however not yet been tackled in the mathematical literature, and it has thus not been applied to MF wireless scenarios. The remaining part of this chapter, and the following ones, explore therefore this research direction.

2.3 Multi-objective and scalarised games

Leveraging on the mathematical literature on games with incomplete preference, this section first formally defines such games, named MOGs, in Section 2.3.1. Then, different flavours of scalarised games are described in Section 2.3.2, being instances of NEPs and GNEPs. Finally, Section 2.3.3 provides the equivalences existing between the equilibria of the scalarised games, and those of the MOGs.

2.3.1 Multi-objective games

In a MOG, the performance of each player is assessed with multiple objective functions. The number of functions of the qth player is denoted L_q, the lth objective function of the qth player being written as $u_{q,l} \colon \mathcal{X} \to \mathbb{R}$. These functions are grouped into the vector function $\mathbf{u}_q \triangleq [u_{q,l}]_{l=1}^{L_q}$. Given these MO functions, the interactions of the MF players are encompassed by the MOG $\mathcal{G}^{(\mathrm{MO})} \triangleq \left\langle \Omega, \{\mathcal{X}_q\}_{q\in\Omega}, \{\mathbf{u}_q\}_{q\in\Omega} \right\rangle$, defined as follows.

Definition 2.7: Multi-objective game

A multi-objective game $\mathcal{G}^{(\mathrm{MO})} = \left\langle \Omega, \{\mathcal{X}_q\}_{q\in\Omega}, \{\mathbf{u}_q\}_{q\in\Omega} \right\rangle$ modelises the interactions between the players indexed in Ω. The behaviour of the qth player is described by the following multi-objective optimisation problem:

$$\begin{aligned} \operatorname{minimise}_{\mathbf{x}_q} \quad & \mathbf{u}_q\left(\mathbf{x}_q, \mathbf{x}_{-q}\right), \\ \text{s.t.} \quad & \mathbf{x}_q \in \mathcal{X}_q, \end{aligned} \tag{2.8}$$

in which $\mathbf{x}_{-q}$ is considered as a fixed parameter.

Remark 2.4

To simplify the discussion, fixed strategy sets are considered for the MOGs. Nevertheless, most part of the below results can be extended in a straightforward manner to the case of strategy sets depending on the other players.

Remark 2.5

The terminology considered in this thesis is the following.
The *single-objective* or *multi-objective* character of a game depends on the number of metrics characterising a player, regardless of whether they are included in the objective function, or set as constraints.
Differently, the *NEP* and *GNEP* terminology differentiates between games in which the strategy set of one player depends on the others, and those with fixed strategy sets. It is thus purely a mathematical consideration.
Therefore, both characterisations are independent, one depending on the players' metrics, and the other on the optimisation problems' structure.

The above definition states that a player *coordinates* its L_q objective functions, while it *competes* with the other players through the impact of $\mathbf{x}_{-q}$. Let us first study the intra-player coordination part, that is, the way the multiple objectives are coordinated together. To that aim, the minimisers of (2.8) must be defined. A point $\mathbf{x}_q$ is considered as a rational choice for the qth player given $\mathbf{x}_{-q}$ if it is strongly Pareto-optimal. This means that compared to $\mathbf{x}_q$, no other strategy is able to improve one of the objective without degrading at least one of the others, as formally stated in the below definition.

Definition 2.8: Strongly Pareto-optimal point [81]

Given the multi-objective optimisation problem

$$\text{minimise}_{\mathbf{x}} \quad \mathbf{u}\left(\mathbf{x}\right) \quad \text{s.t.} \quad \mathbf{x} \in \mathcal{X},$$

with $\mathbf{u} = [u_l]_{l=1}^{L}$, a point $\mathbf{x}^{\star} \in \mathcal{X}$ is said to be strongly Pareto-optimal if

$$\nexists \mathbf{y} \in \mathcal{X} \quad \text{s.t.} \quad \begin{cases} \forall l \in \mathcal{L}, & u_l(\mathbf{y}) \leq u_l(\mathbf{x}^\star), \\ \exists l \in \mathcal{L} \quad \text{s.t.} & u_l(\mathbf{y}) < u_l(\mathbf{x}^\star). \end{cases} \tag{2.9}$$

For the qth player, given $\mathbf{x}_{-q}$, the set of strongly Pareto-optimal points is denoted $\mathcal{P}_q(\mathbf{x}_{-q})$, the dependency on $\mathbf{x}_{-q}$ highlighting the competitive character of the MOG. Mimicking the BR mapping of NEPs and GNEPs, this set represents the rational choices the qth player has in order to respond to $\mathbf{x}_{-q}$. If its current strategy $\mathbf{x}_q$ does not belong to $\mathcal{P}_q(\mathbf{x}_{-q})$, then he will have an interest in changing its strategy. Conversely, the equilibria of a MOG are defined as the points which are Pareto-optimal for all players.

Definition 2.9: Strong Pareto-Nash Equilibrium [66]

Given a multi-objective game $\mathcal{G}^{(\mathrm{MO})} = \left\langle \Omega, \{\mathcal{X}_q\}_{q\in\Omega}, \{\mathbf{u}_q\}_{q\in\Omega} \right\rangle$, a strategy profile $\mathbf{x}^{(\mathrm{E})} \in \mathcal{X}$ satisfying

$$\mathbf{x}_q^{(\mathrm{E})} \in \mathcal{P}_q\left(\mathbf{x}_{-q}^{(\mathrm{E})}\right), \quad \forall q \in \Omega, \tag{2.10}$$

is named a strong Pareto-Nash equilibrium.

For a game $\mathcal{G}^{(\mathrm{MO})}$, the associated set of PNE is denoted as $\mathcal{E}\left(\mathcal{G}^{(\mathrm{MO})}\right)$. The concept of PNE merges thus the concept of Pareto-optimality for the intra-player coordination, and the one of NE for the inter-player competition. It should be noted that equivalent weak concepts can be defined similarly, but that they are not relevant for rational users. Indeed, at such weak profiles, players might find another strategy which improve one of the objective without degrading the others. Therefore, in the following, the names *Pareto-optimal* and *PNE* will always refer to their strong flavour.

Remark 2.6

It should be emphasised that a PNE $\mathbf{x}^{(\mathrm{E})}$ is not Pareto-optimal for the global function $[\mathbf{u}_q]_{q\in\Omega}$ and the set $\mathcal{X}$. Indeed, the definition of a PNE ensures that each $\mathbf{x}_q^{(\mathrm{E})}$ is Pareto-optimal for $\mathbf{u}_q$ and $\mathcal{X}_q$, given $\mathbf{x}_{-q}$. However, by coordinating all players and objective functions, a point improving all the objective functions compared to $\mathbf{x}^{(\mathrm{E})}$ may be found.

2.3.2 From multi-objective to single-objective games

While (2.8) indeed abstracts MF autonomous players interacting with each other, it does not fully describe how these multiple functions are articulated one with respect to the others. This in turns implies that given $\mathbf{x}_{-q}$, the qth player has the possibility to select any strategy belonging to $\mathcal{P}_q(\mathbf{x}_{-q})$. Additional elements must therefore be included in the player description in order to precise which strategy should be selected. Such refinement of the players' behaviours is achieved by translating the MOO problems into Single-Objective Optimisation (SOO) problems. This process is named a *scalarisation*, and several flavours can be investigated [82, 83].

Weighted-sum scalarised games A first possibility is the weighted-sum scalarisation approach, in which the scalar function reads as

$$u_q^{\boldsymbol{\lambda}_q} \triangleq \sum_{l=1}^{L_q} \lambda_{q,l} u_{q,l}, \tag{2.11}$$

with $\lambda_{q,l}$ a weight representing the preference of the qth player for its lth objective function. These preferences are grouped into the vector $\boldsymbol{\lambda}_q \triangleq [\lambda_{q,l}]_{l=1}^{L_q}$, which must be non-negative and sum to one. The set of M-dimensional non-negative vectors summing to one is thus defined as follows, being named the M-dimensional simplex,

$$\Delta^M \triangleq \left\{ \boldsymbol{\lambda} \in \mathbb{R}^M \middle| \lambda_m \geq 0 \, \forall m = 1, \ldots, M, \quad \sum_{m=1}^{M} \lambda_m = 1 \right\}. \tag{2.12}$$

The scalarisation vector therefore satisfies $\boldsymbol{\lambda}_q \in \Delta^{L_q}$. Grouping the preferences of all players, the global weight profile is defined as $\boldsymbol{\Lambda} \triangleq \{\boldsymbol{\lambda}_q\}_{q=1}^{Q}$, belonging to the set $\Delta^{\times} \triangleq \bigtimes_{q=1}^{Q} \Delta^{L_q}$. The weighted-sum scalarised game associated with a MOG is thus a NEP with the same players and strategy sets, but with these weighted-sum scalarised objective functions.

Definition 2.10: Weighted-sum scalarised game

The weighted-sum scalarised game associated with a MOG $\mathcal{G}^{(\mathrm{MO})} = \left\langle \Omega, \{\mathcal{X}_q\}_{q\in\Omega}, \{\mathbf{u}_q\}_{q\in\Omega} \right\rangle$ and the weight profile $\mathbf{\Lambda} \in \Delta^\times$ is the NEP defined as $\mathcal{G}^{\mathbf{\Lambda}} \triangleq \left\langle \Omega, \{\mathcal{X}_q\}_{q\in\Omega}, \left\{ u_q^{\boldsymbol{\lambda}_q} \right\}_{q\in\Omega} \right\rangle$.

ϵ-constraint scalarised games In this second scalarisation flavour, one of the L_q objective functions of a player is considered as more important than the others. Without loss of generality, the index of this function is considered to be $l = 1$ for all players. Then, while this first function is optimised, the others are associated with maximum requirements $\epsilon_{q,l}$. As for the weighted-sum scalarised games, the constraint thresholds of the qth player are grouped into the vector $\boldsymbol{\epsilon}_q \triangleq [\epsilon_{q,l}]_{l=2}^{L_q}$, and the global threshold profile is defined as $\mathbf{E} \triangleq \{\boldsymbol{\epsilon}_q\}_{q=1}^{Q}$. This later thus belongs to $\mathbb{R}^\times \triangleq \bigtimes_{q=1}^{Q} \mathbb{R}^{L_q - 1}$. With these thresholds, the qth player MOO problem (2.8) becomes

$$\begin{aligned} \text{minimise}_{\mathbf{x}_q} \quad & u_{q,1}\left(\mathbf{x}_q, \mathbf{x}_{-q}\right), \\ \text{s.t.} \quad & \mathbf{x}_q \in \mathcal{X}_q, \\ & u_{q,l}\left(\mathbf{x}_q, \mathbf{x}_{-q}\right) \leq \epsilon_{q,l}, \quad \forall l = 2, \ldots, L_q. \end{aligned} \tag{2.13}$$

The strategy set mapping of the qth player is therefore defined as

$$\tilde{\mathcal{X}}_q^{\boldsymbol{\epsilon}_q}\left(\mathbf{x}_{-q}\right) \triangleq \left\{ \mathbf{x}_q \in \mathcal{X}_q | u_{q,l}\left(\mathbf{x}_q, \mathbf{x}_{-q}\right) \leq \epsilon_{q,l}, \quad \forall l = 2, \ldots, L_q \right\}. \tag{2.14}$$

With these elements, the ϵ-constraint scalarised game associated with a MOG is defined as follows.

Definition 2.11: ϵ-constraint scalarised game

The ϵ-constraint scalarised game associated with a MOG $\mathcal{G}^{(\mathrm{MO})} = \left\langle \Omega, \{\mathcal{X}_q\}_{q\in\Omega}, \{\mathbf{u}_q\}_{q\in\Omega} \right\rangle$ and the threshold profile $\mathbf{E} \in \mathbb{R}^\times$ is the GNEP defined as $\tilde{\mathcal{G}}^{\mathbf{E}} \triangleq \left\langle \Omega, \left\{ \tilde{\mathcal{X}}_q^{\boldsymbol{\epsilon}_q} \right\}_{q\in\Omega}, \{u_{q,1}\}_{q\in\Omega} \right\rangle$.

Constraint satisfaction games Pushing the ϵ-constraint philosophy to its extreme, another way of transforming a MOG is to consider all the objective functions as constraints. In that case, the threshold profile is denoted

$\boldsymbol{\epsilon}_q^{\mathrm{sat}} \triangleq \left[\epsilon_{q,l}^{\mathrm{sat}}\right]_{l=1}^{L_q}$, and the global threshold profile as $\mathbf{E}^{\mathrm{sat}} \triangleq \left\{\boldsymbol{\epsilon}_q^{\mathrm{sat}}\right\}_{q=1}^{Q}$. Such threshold profile belongs to the set $\mathbb{R}^{\times,\mathrm{sat}} \triangleq \bigtimes_{q=1}^{Q} \mathbb{R}^{L_q}$. The optimisation problem of the qth player reads then as

$$\begin{aligned} \operatorname{minimise}_{\mathbf{x}_q} \quad & 1, \\ \text{s.t.} \quad & \mathbf{x}_q \in \mathcal{X}_q. \\ & u_{q,l}\left(\mathbf{x}_q, \mathbf{x}_{-q}\right) \leq \epsilon_{q,l}^{\mathrm{sat}}, \quad \forall l = 1, \ldots, L_q. \end{aligned} \tag{2.15}$$

The above optimisation problem (2.15) means that the qth player is interested in finding any strategy that satisfies all the constraints, all of such strategy giving him a performance of 1. Similarly to the above definitions, the strategy set mapping of the players is introduced as

$$\tilde{\mathcal{X}}_q^{\boldsymbol{\epsilon}_q^{\mathrm{sat}}}\left(\mathbf{x}_{-q}\right) \triangleq \left\{\mathbf{x}_q \in \mathcal{X}_q \middle| u_{q,l}\left(\mathbf{x}_q, \mathbf{x}_{-q}\right) \leq \epsilon_{q,l}^{\mathrm{sat}}, \quad \forall l = 1, \ldots, L_q\right\}. \tag{2.16}$$

The game resulting from the above is therefore named a *constraint satisfaction game* [19], being an instance of a GNEP.

Definition 2.12: Constraint satisfaction game

The constraint satisfaction game associated with a MOG $\mathcal{G}^{(\mathrm{MO})} = \left\langle \Omega, \left\{\mathcal{X}_q\right\}_{q\in\Omega}, \left\{\mathbf{u}_q\right\}_{q\in\Omega} \right\rangle$ and the threshold profile $\mathbf{E}^{\mathrm{sat}} \in \mathbb{R}^{\times,\mathrm{sat}}$ is the GNEP defined as $\tilde{\mathcal{G}}^{\mathbf{E}^{\mathrm{sat}}} \triangleq \left\langle \Omega, \left\{\tilde{\mathcal{X}}_q^{\boldsymbol{\epsilon}_q^{\mathrm{sat}}}\right\}_{q\in\Omega}, \left\{1\right\}_{q\in\Omega} \right\rangle$.

Remark 2.7

Such formulation is rather unusual in the wireless communication literature. Yet, as pointed out in [19], it can be argued to be a better model of the interests of the points in a wireless environment: often, such points have requirements coming from their applications which must be met. However, they are usually not interested in optimising one or several metrics till the last decimals.

Hybrid sum-constraint scalarised game The three above scalarisation formulations can be generalised into a unique representation, being named the hybrid sum-constraint scalarised games. In this general hybrid approach, the players optimise a partial weighted-sum of the objective functions, with the others as constraint. For each qth player, let $0 \leq l_q^{(h)} \leq L_q$ be such that the functions $u_{q,l}$ are kept in the objective if $l \leq l_q^{(h)}$, while they become constraints otherwise. Each player is associated with partial weight profiles $\boldsymbol{\lambda}_q^{(h)} \in \Delta^{l_q^{(h)}}$, and with partial threshold profiles $\boldsymbol{\epsilon}_q^{(h)} \in \mathbb{R}^{L_q - l_q^{(h)}}$. The corresponding global profiles are denoted $\boldsymbol{\Lambda}^{(h)}$ and $\mathbf{E}^{(h)}$, with the associated sets being respectively defined as $\Delta^{\times,(h)} \triangleq \bigtimes_{q=1}^{Q} \Delta^{l_q^{(h)}}$ and $\mathbb{R}^{\times,(h)} \triangleq \bigtimes_{q=1}^{Q} \mathbb{R}^{L_q - l_q^{(h)}}$. Given such profiles, the partial weighted-sum scalarised function and constraint sets are given by

$$u_q^{\boldsymbol{\lambda}_q^{(h)}}\left(\mathbf{x}_q, \mathbf{x}_{-q}\right) \triangleq \sum_{l=1}^{l_q^{(h)}} \lambda_{q,l}^{(h)} u_{q,l}\left(\mathbf{x}_q, \mathbf{x}_{-q}\right), \tag{2.17}$$

$$\tilde{\mathcal{X}}_q^{\boldsymbol{\epsilon}_q^{(h)}}\left(\mathbf{x}_{-q}\right) \triangleq \left\{\mathbf{x}_q \in \mathcal{X}_q \middle| u_{q,l}\left(\mathbf{x}_q, \mathbf{x}_{-q}\right) \leq \epsilon_{q,l}^{(h)},\ \forall l = l_q^{(h)} + 1, \ldots, L_q\right\}. \tag{2.18}$$

The hybrid sum-constraint scalarised game is then defined as follows.

Definition 2.13: Hybrid sum-constraint scalarised game

The hybrid sum-constraint scalarised game associated with a MOG $\mathcal{G}^{(\mathrm{MO})} = \left\langle \Omega, \left\{\mathcal{X}_q\right\}_{q\in\Omega}, \left\{\mathbf{u}_q\right\}_{q\in\Omega} \right\rangle$, the hybrid indices $\left\{l_q^{(h)}\right\}_{q=1}^{Q}$ with $0 \leq l_q^{(h)} \leq L_q$, the weight profile $\boldsymbol{\Lambda}^{(h)} \in \Delta^{\times,(h)}$, and the threshold profile $\mathbf{E}^{(h)} \in \mathbb{R}^{\times,(h)}$ is the GNEP defined as $\tilde{\mathcal{G}}^{\boldsymbol{\Lambda}^{(h)},\mathbf{E}^{(h)}} \triangleq \left\langle \Omega, \left\{\tilde{\mathcal{X}}_q^{\boldsymbol{\epsilon}_q^{(h)}}\right\}_{q\in\Omega}, \left\{u_q^{\boldsymbol{\lambda}_q^{(h)}}\right\}_{q\in\Omega} \right\rangle$.

Such hybrid sum-constraint scalarised game encompasses thus the particular cases of the weighted-sum scalarised games when $l_q^{(h)} = L_q$, the ϵ-constraint scalarised games when $l_q^{(h)} = 1$, and the constraint satisfaction games when $l_q^{(h)} = 0$, for all $q \in \Omega$. It is also emphasised the hybrid index $l_q^{(h)}$ might be different for each qth player, and that therefore not all players should be scalarised in the same manner.

Weighted-Chebyshev scalarised games Finally, a last scalarisation possibility is discussed here, being the weighted-Chebyshev scalarisation. In such scalarisation, the weighted maximum of the objective functions is minimised, the qth player solving thus the following SOO problem

$$\begin{aligned} \text{minimise}_{\mathbf{x}_q} \quad & \max_{l=1,\dots,L_q} \left\{\gamma_{q,l} u_{q,l}\left(\mathbf{x}_q, \mathbf{x}_{-q}\right)\right\}, \\ \text{s.t.} \quad & \mathbf{x}_q \in \mathcal{X}_q, \end{aligned} \tag{2.19}$$

with $\gamma_{q,l}$ the non-negative weights associated with each objective function, summing to one. It can be noted that the above has links with the ϵ-constraint scalarisation, since (2.19) can be rewritten as

$$\begin{aligned} \text{minimise}_{\mathbf{x}_q} \quad & \eta_q, \\ \text{s.t.} \quad & \mathbf{x}_q \in \mathcal{X}_q, \\ & \gamma_{q,l} u_{q,l}\left(\mathbf{x}_q, \mathbf{x}_{-q}\right) \leq \eta_q, \quad \forall l = 1, \dots, L_q, \end{aligned} \tag{2.20}$$

The difference lies in the fact the thresholds η_q are optimised in the weighted-Chebyshev scalarisation, while they are fixed in the ϵ-constraint scalarisation.

From the two above representations, it can be observed a weighted-Chebyshev scalarised game may either be represented as a NEP or a GNEP. Yet, it turns out that both formulations are difficult to handle in the below analysis. In the first case, this is due to the fact that the objective functions are not smooth, and that therefore the framework of Chapter 3 does not apply. In the second case, the problem comes from the constraint structure, which is not covered by the results of Chapter 4. Therefore, such scalarisation will not be studied further below. Adapting the frameworks of Chapters 3 and 4 to such scalarisation is however an interesting research direction.

2.3.3 Equilibrium point equivalence

Above, the concept of MOG has been introduced, as well as several ways of transforming it into a NEP or a GNEP. The question of the equivalence between the PNE of a MOG and the equilibria of the associated scalarised games is now addressed.

Equivalences in multi-objective optimisation This question mirrors the one arising in MOO, i.e., without considering competitive interactions on top of the MO problems. Indeed, depending on the assumptions made on the objective functions, the scalarisation methods may, or may not, be able to reach all the Pareto-optimal points by varying the scalarisation parameters (i.e., the weights and constraint thresholds). Such equivalences are detailed in [83–85], and for the methods described above, they can be described as follows:

- If the objective functions are strictly convex, and the strategy sets are convex, then the weighted-sum scalarisation method is able to reach all the Pareto-optimal points, and conversely.
- If the solution of the optimisation problems resulting from the ϵ-constraint scalarisation is unique whatever the constraint threshold, then this scalarisation method is able to reach all the Pareto-optimal points, and conversely. Such uniqueness can be ensured among others when the strategy set is convex, and the function kept as an objective strictly quasi-convex. The same holds for the Chebyshev scalarisation method.
- As the constraint satisfaction perspective does not push the objectives towards their optimum, such relationships however do not hold.

An illustrative example of these relationships is given in Figure 2.3, both for convex and quasi-convex objective functions, for the optimisation problem

$$\begin{aligned} \text{minimise}_{\mathbf{x}} \quad & \left[u_1\left(\mathbf{x}\right), u_2\left(\mathbf{x}\right)\right]^\top, \\ \text{s.t.} \quad & \mathbf{x} \in \mathcal{X}. \end{aligned}$$

In this figure, the grey area represents the possible values of $\left[u_1\left(\mathbf{x}\right), u_2\left(\mathbf{x}\right)\right]^\top$ for $\mathbf{x}$ in the strategy set. The Pareto frontier is the left boundary of this area, depicted with a dark grey line. The point reached by the weighted-sum scalarisation is obtained by translating to the left a line whose slope is governed by the scalarisation weights. Regarding the ϵ-constraint method, it selects the leftmost point which is below the constraint threshold ϵ_2. The Chebyshev method reaches the point of a line originating from the origin with a slope depending on the scalarisation weights, such that all points below and to the left of this point do not below to the grey area. Finally, the constraint satisfaction method finds any point below the two constraint thresholds, even if such point is not Pareto-optimal. As it can be observed on the right panel of this figure, the weighted-sum scalarisation is not able to sweep through all the Pareto-optimal points when the objective functions are strictly quasi-convex, but not convex.

Equivalences for multi-objective games Motivated by the above equivalences, the below assumption is introduced for the hybrid scalarised game

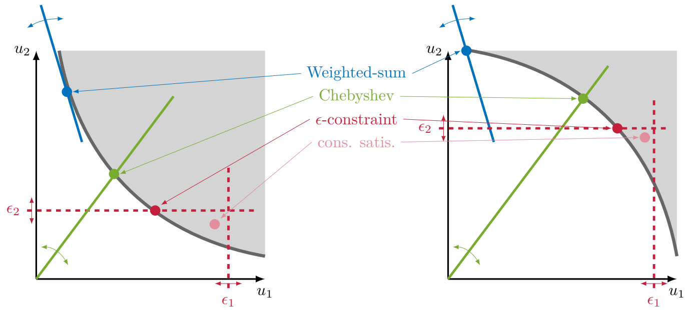

(a) Strictly convex objectives (b) Strictly quasi-convex objectives

Fig. 2.3 Relationships between scalarisation methods and Pareto-optimality, for strictly convex and quasi-convex objective functions, and a convex strategy set.

associated with a MOG $\mathcal{G}^{(\mathrm{MO})}$ and the hybrid indices $\left\{l_q^{(h)}\right\}_{q=1}^{Q}$.

Assumption 2.2: Convexity and non-emptiness

Whatever $q \in \Omega$,

- $\mathcal{X}_q$ is non-empty, closed and convex;
- $u_{q,l}$ is strictly convex in $\mathbf{x}_q \in \mathcal{X}_q$, whatever $\mathbf{x}_{-q} \in \mathcal{X}_{-q}$, and whatever $l = 1, \ldots, l_q^{(h)}$.
- $u_{q,l}$ is quasi-convex in $\mathbf{x}_q \in \mathcal{X}_q$, whatever $\mathbf{x}_{-q} \in \mathcal{X}_{-q}$, and whatever $l = l_q^{(h)} + 1, \ldots, L_q$.

The above assumption ensures that the hybrid strategy sets are convex, since one possible definition of quasi-convexity is the following:

$$f(\mathbf{x}) \text{ is quasi-convex} \iff \{\mathbf{x} | f(\mathbf{x}) \leq \alpha\} \text{ is convex, } \forall \alpha \in \mathbb{R}.$$

Given this assumption, the below theorem states the equivalence between the PNEs of a MOG, and the sets of NE of the hybrid sum-constraint scalarised games, when all hybrid indices are such that $l_q^{(h)} \geq 1$. It thus includes as particular cases the weighted-sum and ϵ-constraint scalarised games, but does not cover the constraint satisfaction games.

Theorem 2.1: Equilibrium points' equivalence

Let the MOG $\mathcal{G}^{(\mathrm{MO})}$ and the hybrid indices $\left\{l_q^{(h)}\right\}_{q=1}^{Q}$ satisfy Assumption 2.2, with $l_q^{(h)} \geq 1$ whatever $q \in \Omega$. The equilibrium points of the hybrid sum-constraint scalarised game $\tilde{\mathcal{G}}^{\mathbf{\Lambda}^{(h)},\mathbf{E}^{(h)}} = \left\langle \Omega, \left\{\mathcal{X}_q^{\boldsymbol{\epsilon}_q^{(h)}}\right\}_{q\in\Omega}, \left\{u_q^{\boldsymbol{\lambda}_q^{(h)}}\right\}_{q\in\Omega}\right\rangle$, with $\mathbf{\Lambda}^{(h)} \in \Delta^{\times,(h)}$ and $\mathbf{E}^{(h)} \in \mathbb{R}^{\times,(h)}$, satisfy

$$\mathcal{E}\left(\mathcal{G}^{(\mathrm{MO})}\right) = \bigcup_{\substack{\mathbf{\Lambda}^{(h)} \in \Delta^{\times,(h)},\\ \mathbf{E}^{(h)} \in \mathbb{R}^{\times,(h)}}} \mathcal{E}\left(\tilde{\mathcal{G}}^{\mathbf{\Lambda}^{(h)},\mathbf{E}^{(h)}}\right). \tag{2.21}$$

Proof. See Section 2.6.1. □

The equilibrium equivalences provided by the above theorem are the corner stone of this part of the thesis: when analysing MF competitive players, it must be ensured they reach a PNE. Yet, the drawback of MOGs is that they do not fully describe the behaviour of the players, since given $\mathbf{x}_{-q}$, they might select several strategies. The above theorem enables to analyse the PNE of a MOG by considering instead a given hybrid representation, i.e., by performing a weighted-sum of some of the objectives and setting the others as constraints. Such representation is parametrised by the weights and constraint thresholds. The above ensures then that whatever the weights and thresholds, the reached NE is a PNE. Conversely, any PNE can be reached for some weights and thresholds. This motivates thus the study of MO interactions through their scalarised counterparts.

Remark 2.8

In the above theorem, it must be pointed that for some thresholds $\mathbf{E}^{(h)}$, the scalarised GNEP might not admit any equilibrium, for instance if the thresholds are too stringent.
Another comment on the above theorem is that the equivalence holds for fixed hybrid indices $\left\{l_q^{(h)}\right\}_{q=1}^{Q}$. Thus, all the PNEs can be reached by varying the weights $\mathbf{\Lambda}^{(h)}$ and thresholds $\mathbf{E}^{(h)}$ whatever the chosen

representation. Among others, this means that the weighted-sum scalarised games benefit from such equivalence, as well as ϵ-constraint scalarised games.

2.4 Applicative multi-function multi-point use-cases

Throughout this part of the thesis which focuses on autonomous interference analysis and management, the developed theoretical frameworks will be illustrated on two instances of MF MP wireless networks. The first is a JRC scenario, in which the two functions are the communication, and the radar task. The second studies a Random Access (RA) protocol, in which the devices must choose between several activity levels. These two scenarios are thus described below as MOGs. Instead of defining the associated scalarised games in this section, they will be introduced in the next chapters, when the corresponding analysis will be performed.

2.4.1 JRC scenario

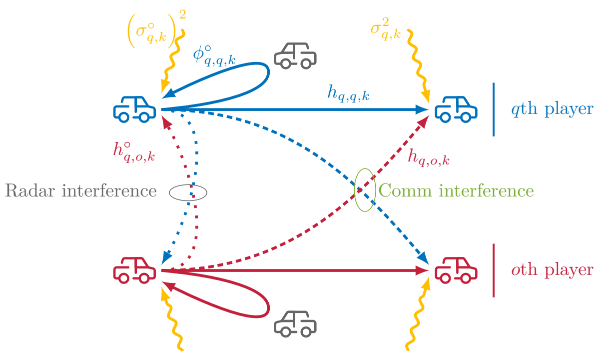

Fig. 2.4 JRC scenario. The direct links are denoted with solid arrows and the interfering links of respectively the communication and radar part with dashed and dotted arrows.

Players As represented in Figure 2.4, a set of Q cars wish to communicate with their respective neighbour with an OFDM waveform, and to gather radar information about their environment based on the received echo. In that setting, the qth player is thus constituted by the qth emitting car and by the corresponding receiver. This receiver can feedback information to the emitter of the same pair, among other on the channel coefficient and received interference.

Strategy sets In a co-design paradigm [86, 87], a single waveform is used for both functions: the sent signal carries information to the receiver while its radar echo provides sensing capabilities to the emitting car. To that aim, each qth emitting car splits its power budget P_q on the K OFDM subcarriers. Denoting by $\mathbf{p}_q = [p_{q,k}]_{k=1}^{K}$ the power allocation of the qth car, it belongs thus to the strategy set

$$\mathcal{X}_q = \left\{ \mathbf{p}_q \in \mathbb{R}^K \middle| \mathbf{p}_q \geq \mathbf{0}, \sum_{k=1}^{K} p_{q,k} = P_q \right\}. \tag{2.22}$$

Objective functions In line with [87–92], an information-theoretic point of view is considered to evaluate the communication and radar performance. Treating the interference as noise, the communication capacity reads for the qth car as

$$R_q(\mathbf{p}) = \sum_{k=1}^{K} \ln \left(1 + \frac{|h_{q,q,k}|^2 p_{q,k}}{\sigma_{q,k}^2 + \sum_{o \neq q} |h_{q,o,k}|^2 p_{o,k}} \right), \tag{2.23}$$

where $h_{q,o,k}$ is the complex channel coefficient between emitter o and receiver q on the kth tone and $\sigma_{q,k}^2$ is the noise power for the qth receiver on the kth tone. For the radar metric, the estimation rate has been widely used in radar systems [93–98] to optimally design radar waveforms. Measured as the Mutual Information (MI) between the radar echo and the target response, it reads as [87, 95]

$$R_q^{\circ}(\mathbf{p}) = \sum_{k=1}^{K} \ln \left(1 + \frac{\mathbb{E}\left\{ \left| \phi_{q,q,k}^{\circ} \right|^2 \right\} p_{q,k}}{\left(\sigma_{q,k}^{\circ} \right)^2 + \sum_{o \neq q} \left| h_{q,o,k}^{\circ} \right|^2 p_{o,k}} \right), \tag{2.24}$$

with $\phi_{q,q,k}^{\circ}$ the channel coefficient of the round-trip radar channel, $h_{q,o,k}^{\circ}$ the channel between the oth emitter and the qth emitter on the kth tone, and $\left(\sigma_{q,k}^{\circ}\right)^2$ the noise power on the kth tone at the qth emitter. Contrarily to the communication coefficients, $\phi^{\circ}_{q,q,k}$ depends on the unknown target response from the radar information is extracted, and this is why the information-theoretic analysis models it as a random quantity. Defining the normalised noise power and channel gains as $a_{q,k} = \sigma^2_{q,k}/|h_{q,q,k}|^2$, $b_{q,o,k} = |h_{q,o,k}|^2/|h_{q,q,k}|^2$, $a^{\circ}_{q,k} = \left(\sigma^{\circ}_{q,k}\right)^2/\mathbb{E}\left\{\left|\phi^{\circ}_{q,q,k}\right|^2\right\}$, $b^{\circ}_{q,o,k} = \left|h^{\circ}_{q,o,k}\right|^2/\mathbb{E}\left\{\left|\phi^{\circ}_{q,q,k}\right|^2\right\}$, the MO objective function of the qth player is given by

$$\mathbf{u}_q\left(\mathbf{p}\right) = \begin{bmatrix} -\sum_{k=1}^{K} \ln\left(1 + \frac{p_{q,k}}{a_{q,k}+\sum_{o\neq q} b_{q,o,k}p_{o,k}}\right) \\ -\sum_{k=1}^{K} \ln\left(1 + \frac{p_{q,k}}{a^{\circ}_{q,k}+\sum_{o\neq q} b^{\circ}_{q,o,k}p_{o,k}}\right) \end{bmatrix}. \tag{2.25}$$

JRC MOG, and associated side-information exchange The JRC network is thus described by $\mathcal{G}^{(\mathrm{MO})} = \left\langle \Omega, \left\{\mathcal{X}_q\right\}_{q\in\Omega}, \left\{\mathbf{u}_q\right\}_{q\in\Omega}\right\rangle$, with the strategy sets and objective functions defined in (2.22) and (2.25). The above game definition shows that the optimisation problem of the qth user is fully parametrised by the aggregate noise-plus-interference powers on each tone, for the communication and radar functions. These normalised powers are respectively denoted

$$\xi_{q,k}\left(\mathbf{p}_{-q}\right) = a_{q,k} + \sum_{o\neq q} b_{q,o,k}p_{o,k}, \tag{2.26}$$

$$\xi^{\circ}_{q,k}\left(\mathbf{p}_{-q}\right) = a^{\circ}_{q,k} + \sum_{o\neq q} b^{\circ}_{q,o,k}p_{o,k}, \tag{2.27}$$

for the communication and radar part. From a practical point of view, this means only the aggregate noise-plus-interference powers must be measured at the receivers. This is achieved by feeding back the SINR experienced by each receiver to the corresponding emitter, as it would be done for any OFDM power allocation scheme. However, no inter-player information exchange is required, the BRD of any scalarised game being therefore particularly well-suited to this scenario.

Remark 2.9

If instead of a GT analysis, a global optimisation was performed, one should be aware of the gain of the channel between each emitter and each receiver, even those of another pair. Estimating all cross-channel gains is however resource consuming, and is not supported in traditional wireless scenarios. Thus, such optimisation is not considered in this work. For the same reasons, computing the NE in a centralised way requires information which is not available.

Remark 2.10

For this scenario, totally decentralised techniques such as reinforcement learning algorithms could be considered [19]. Yet, they usually require to evaluate the metrics in order to determine whether a strategy profile is better than another. Since the aggregate noise-plus-interference power is needed to compute the rates, such algorithms would be based on the same information as the BRD.

2.4.2 Multi-level random access protocol

Players and RA protocol In the considered scenario, Q nodes must communicate with an AP. The communication load is assumed to be low, an example of such a network being for instance the case of distributed sensors centralising their collected data. In such networks, the sensors must fulfil this communication function, but their primary function is to acquire the data. For such a low communication load, RA protocols are relevant, and a slotted RA scheme is therefore considered. In such setting, common time slots are shared by the nodes, which have some probability, named the access probability, to try to transmit a packet to the AP at each time slot. This probability must be carefully designed, as if several nodes are active during the same time slot, then all communications are lost.

Below, the competitive interactions existing between players selecting their *best* access probability will be analysed, modelling their interactions as a BRD. Other characteristics than the BRD convergence could also be analysed within a GT framework. The interested reader is referred to [19], in which these different GT aspects are developed and applied to a RA scenario, among others.

Strategy sets Differently from traditional RA schemes, the considered scheme is a multi-level RA protocol. The difference with respect to the traditional protocol, in which nodes have one idle and one active level, lies in the fact that each qth node has $A_q + 1$ levels. The 0th one is the idle state while the A_q others differ in terms of power and rate. The rate and consumed power of the a_qth activity level are respectively denoted R_{q,a_q} and P_{q,a_q}, with the idle state being such that $(R_{q,0}, P_{q,0}) = (0, P_{\text{idle},q})$. Without loss of generality, the states are assumed to be sorted with increasing rates, this ordering also corresponding to the consumed power ordering. Thus, the maximum rate and consumed power of the qth player are R_{q,A_q} and P_{q,A_q}. At each time slot, each device thus draws one of its state according to a probability profile $\mathbf{x}_q = \left[x_{q,a_q}\right]_{a_q=0}^{A_q}$ on its activity levels. This probability profile is constrained to the set

$$\mathcal{X}_q = \left\{ \mathbf{x}_q \in \mathbb{R}^{A_q+1} \middle| \begin{array}{ll} 1 - x_q^{\max} \leq x_{q,0} & \\ 0 \leq x_{q,a_q}, & \forall a_q = 1, \ldots, A_q \\ \sum_{a_q=0}^{A_q} x_{q,a_q} = 1 & \end{array} \right\} \tag{2.28}$$

in which one can recognise the probability simplex Δ^{A_q+1}, with an additional lower bound on $x_{q,0}$. This lower bound depends on the maximum active probability $x_q^{\max}$, and it is introduced to avoid channel congestion. It translates the sharing of the communication resource among the nodes, to prevent one of them to occupy all communication slots.

Objective functions For each qth node, two objectives are considered, being the average consumed power, and average uplink rate. The uplink rate is relative to the communication function of the nodes, while the consumed power objective enables to save energy for the other functions. The average consumed power reads as

$$\overline{P}_q\left(\mathbf{x}_q\right) \triangleq \sum_{a_q=0}^{A_q} x_{q,a_q} P_{q,a_q}. \tag{2.29}$$

The consumed power only depends on the strategy profile $\mathbf{x}_q$ of the qth node. On the contrary, the average uplink rate is also impacted by the ones of the others $\mathbf{x}_{-q}$. Indeed, if several nodes try to transmit during the same time slot, a collision occurs and all the transmissions are assumed to be lost. Thus, the communication of the qth node is successful only if all other nodes are inactive. The success probability of the qth device when it is transmitting, denoted $\theta_q\left(\mathbf{x}_{-q}\right)$, is hence given by

$$\theta_q\left(\mathbf{x}_{-q}\right) \triangleq \prod_{r \neq q} x_{r,0}. \tag{2.30}$$

With these elements, the average rate of the qth user is given by

$$\overline{R}_q\left(\mathbf{x}_q, \mathbf{x}_{-q}\right) \triangleq \theta_q\left(\mathbf{x}_{-q}\right) \sum_{a_q=1}^{A_q} x_{q,a_q} R_{q,a_q}. \tag{2.31}$$

The MO objective function of the qth player is therefore defined as

$$\mathbf{u}_q\left(\mathbf{x}\right) \triangleq \begin{bmatrix} \frac{\overline{P}_q(\mathbf{x}_q)-P_{\text{idle},q}}{P_{q,A_q}-P_{\text{idle},q}} \\ -\frac{\overline{R}_q(\mathbf{x}_q,\mathbf{x}_{-q})}{R_{q,A_q}} \end{bmatrix} = \begin{bmatrix} \mathbf{p}_q^\top \\ -\theta_q\left(\mathbf{x}_{-q}\right)\mathbf{r}_q^\top \end{bmatrix} \mathbf{x}_q, \tag{2.32}$$

with $\mathbf{p}_q$ and $\mathbf{r}_q$ given by

$$\mathbf{p}_q \triangleq \left[0, \quad \frac{P_{q,1}-P_{\text{idle},q}}{P_{q,A_q}-P_{\text{idle},q}}, \quad \ldots, \quad \frac{P_{q,A_q-1}-P_{\text{idle},q}}{P_{q,A_q}-P_{\text{idle},q}}, \quad 1\right]^\top, \tag{2.33}$$

$$\mathbf{r}_q \triangleq \left[0, \quad \frac{R_{q,1}}{R_{q,A_q}}, \quad \ldots, \quad \frac{R_{q,A_q-1}}{R_{q,A_q}}, \quad 1\right]^\top. \tag{2.34}$$

In the above, the objective functions have been normalised by the maximum consumed power and rates, in order to avoid the objective functions to have different scales. Hence, the normalised objective functions are respectively the normalised excess consumed power, and the normalised rate.

RA MOG, and associated side-information exchange With these elements, the RA resource allocation process is encompassed by the MOG $\mathcal{G}^{(\mathrm{MO})} = \left\langle \Omega, \left\{\mathcal{X}_q\right\}_{q\in\Omega}, \left\{\mathbf{u}_q\right\}_{q\in\Omega} \right\rangle$, with the strategy sets and objective functions defined in (2.28) and (2.32). In this game, the strategy of the players is a probability profile on a discrete number of activity levels. It thus looks like a game with finite strategy sets, in which players are allowed to play mixed strategies. The below remark formalises this observation by showing the RA MOG is the mixed extension of a finite game. The RA scenario therefore echoes Remark 2.1, and the subsequent analysis will show how to analyse a MOG with a finite number of actions and mixed strategies, through the lens of its mixed extension.

Remark 2.11

Let the finite MOG $\mathcal{H}^{(\mathrm{MO})}$ be defined as $\mathcal{H}^{(\mathrm{MO})} \triangleq \left\langle \Omega, \left\{\mathcal{A}_q\right\}_{q\in\Omega}, \left\{\left[-r_q, p_{\text{exc},q}^\top\right]\right\}_{q\in\Omega} \right\rangle$, with the finite strategy sets $\mathcal{A}_q = \{0, \ldots, A_q\}$, and the objective function of the qth player for the activity profile $(a_1, \ldots, a_Q)$ given by

$$r_q(a_1, \ldots, a_Q) = x_{q,\max} r_{q,a_q} \prod_{r \neq q} \left(1 - x_{r,\max} \mathbb{1}(a_r \neq 0)\right),$$

$$p_{\mathrm{exc},q}(a_1, \ldots, a_Q) = x_{q,\max} p_{q,a_q},$$

with $\mathbb{1}(\cdot)$ the indicator function. In the above, the quantities r_{q,a_q} and p_{q,a_q} are the elements of the rate and power vectors defined in (2.33) and (2.34). A mixed strategy of the qth player is a probability profile $\mathbf{v}_q \in \Delta^{A_q+1}$ on its activity levels. The average first objective value of the qth player is then given by

$$\sum_{a_1=1}^{A_1} \cdots \sum_{a_Q=1}^{A_Q} v_{1,a_1} \ldots v_{Q,a_Q} \left(-r_q(a_1, \ldots, a_Q)\right),$$

and similarly for the second objective. Let

$$\mathbf{x}_q \triangleq x_{q,\max} \mathbf{v}_q + \left[1 - x_{q,\max}, 0, \ldots, 0\right]^\top.$$

Then $\mathbf{v}_q \in \Delta^{A_q+1} \iff \mathbf{x}_q \in \mathcal{X}_q$ with $\mathcal{X}_q$ defined in (2.28). Moreover, the average rate and power obtained with the probability profiles $\mathbf{v}_1, \ldots, \mathbf{v}_Q$ are equal to those defined (2.31) and (2.29), since

$$\begin{aligned}
&\overline{R}_q(\mathbf{x}_q, \mathbf{x}_{-q}) \\
&= \sum_{a_q=1}^{A_q} v_{q,a_q} x_{q,\max} R_{q,a_q} \prod_{r \neq q} \left(1 - x_{r,\max} + x_{r,\max} v_{r,0}\right), \\
&= \sum_{a_q=1}^{A_q} v_{q,a_q} x_{q,\max} R_{q,a_q} \prod_{r \neq q} \sum_{a_r=0}^{A_r} v_{r,a_r} \left(1 - x_{r,\max} \mathbb{1}(a_r \neq 0)\right), \\
&= R_{q,A_q} \sum_{a_1=0}^{A_q} \cdots \sum_{a_Q=0}^{A_Q} v_{1,a_1} \ldots v_{Q,a_Q} r_q(a_1, \ldots, a_Q), \\
&\overline{P}_q(\mathbf{x}_q) = P_{\mathrm{idle},q} + \sum_{a_q=0}^{A_q} v_{q,a_q} x_{q,\max} \left(P_{q,a_q} - P_{\mathrm{idle},q}\right).
\end{aligned}$$

This thus shows that the RA game is the mixed extension of the MOG $\mathcal{H}^{(\mathrm{MO})}$.

Regarding the side-information exchange, as for the JRC scenario, the impact of the other players is condensed into aggregate quantities. For the qth player, its behaviour only depends on its success probability $\theta_q\left(\mathbf{x}_{-q}\right)$. Two possibilities can be envisioned to give this knowledge to the qth player.

First, such success probability can be estimated from the acknowledgment information the user gets from the access point. Such feedback mechanism is indeed present in RA schemes to indicate to the devices which packets must be retransmitted. The advantage of getting the success probability information in this manner is that it does not increase the amount of signalling with respect to traditional protocols. The drawback is however that the estimated probabilities depend on the collision realisations, and they are thus noisy.

Thus, a second mechanism can be designed, which requires only minimal side-information exchange. Periodically, each qth node appends a header containing $x_{q,0}$ to the transmitted packet. Then, the AP computes the value $X \triangleq \prod_{q=1}^{Q} x_{q,0}$ based on the received probabilities. Next, X is sent together with the feedback information to each node. It should be noted that as X is common to all nodes, it can also be broadcasted. Each node can finally compute the success probability of its a_qth activity level as $\theta_q\left(\mathbf{x}_{-q}\right) = \frac{X}{x_{q,0}}$. By transmitting the product X instead of all $x_{q,0}$'s, the header sizes are constant whatever the number of nodes Q.

2.5 Chapter summary

This chapter initiates the analysis of the interactions in MF MP networks. First, Section 2.1 defines two types of interaction modelling: the NEPs and GNEPs. The analyses which need to be performed on these problems to make them adequate for wireless applications are then discussed. These applications motivate the study of the totally asynchronous BRD as a way for the multiple nodes to a reach a stable point. Nevertheless, as the state-of-the-art of Section 2.2 emphasises, convergence guarantees for the BRD of MF players are lacking.

In Section 2.3, the framework of MOGs is defined. Several ways of refining the behaviour of the players are introduced through the different flavours of scalarised games. The equivalences between the equilibria of a MOG and the ones of the associated scalarised games are formally stated, building on the mathematical literature.

Finally, two instances of MF MP networks are introduced, one covering the power allocation in a JRC network, and the second the design of a multi-level RA scheme.

As a graphical summary, the different kind of scalarised games associated with a MOG are summarised in Figure 2.5, with an emphasis on those for which equilibrium equivalences hold. The goal of the next chapters will be the study the different scalarisations, with as aim the obtention of convergence conditions for the totally asynchronous BRD. To fully embrace the MF character of the nodes, such conditions should ideally be agnostic from the scalarisation weights (the λ's) and the constraint thresholds (the ϵ's). However, as the below chapters will show, this will be achieved for the scalarisation weights, but not for the constraint thresholds.

As depicted in the figure, Chapter 3 studies the weighted-sum scalarised game family and provide conditions agnostic from the weights. The ϵ-constraint representation is studied in Chapter 4 for fixed, known thresholds, as it turns out BRD convergence results for GNEPs are sparse in the literature. Chapter 5 then discusses the reasons which make very challenging the extension of the obtained results to conditions independent of the constraint thresholds. This chapter also merges the results of Chapters 3 and 4 in order to study general hybrid games, including the constraint satisfaction games. The results obtained in all these chapters are furthermore applied to the two introduced MF MP scenarios.

2.6 Proofs

2.6.1 Proof of Theorem 2.1

In the weighted-sum case, i.e., when the hybrid indices are such that $l_q^{(h)} = L_q$, the proof is given in [77].

In the ϵ-constraint case, i.e., when the hybrid indices are such that $l_q^{(h)} = 1$, the theorem is proven in two steps. First, it is shown that all PNEs of $\mathcal{G}^{(\mathrm{MO})}$ are an NE of one of the ϵ-constraint games, and then the converse is proven. Let $\mathbf{x}^{(\mathrm{E})} \in \mathcal{X}$ be a PNE of $\mathcal{G}^{(\mathrm{MO})}$: $\mathbf{x}^{(\mathrm{E})} \in \mathcal{E}\left(\mathcal{G}^{(\mathrm{MO})}\right)$. Then, consider

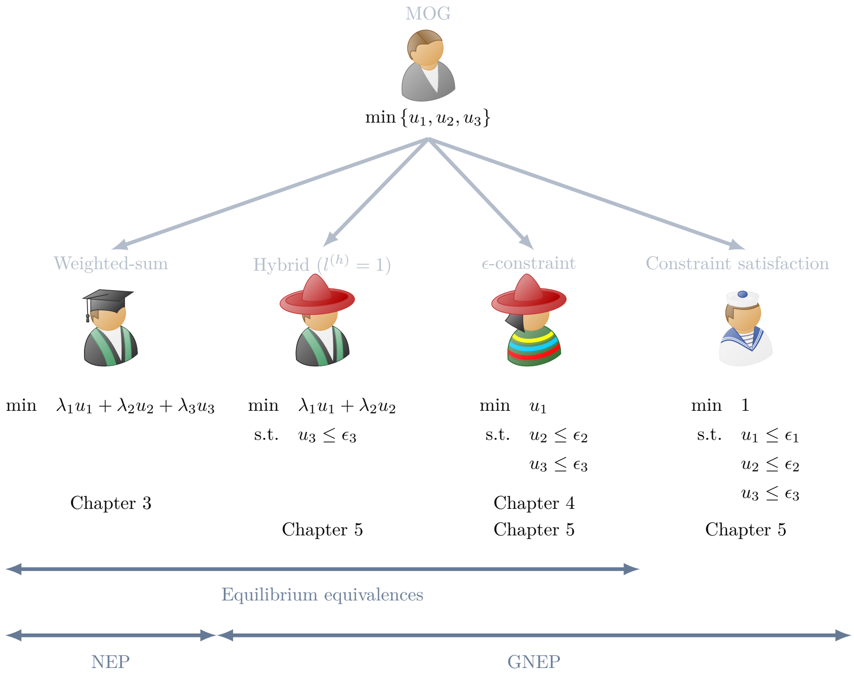

Fig. 2.5 Overview of the MOGT challenges addressed in the following chapters, depending on the manner a player chooses to articulate its different metrics.

the ϵ-constraint gain with $\epsilon_{q,l} \triangleq u_{q,l}\left(\mathbf{x}^{(\mathrm{E})}\right)$. From the definition of a PNE, $\mathbf{x}_q^{(\mathrm{E})}$ belongs to $\mathcal{BR}_q^{\boldsymbol{\epsilon}_q}(\mathbf{x}_{-q})$ for each qth player, and therefore $\mathbf{x}^{(\mathrm{E})}$ is a NE of the ϵ-constraint game. In the reverse direction, let $\mathbf{x}^{(\mathrm{E})}$ be a NE of an ϵ-constraint game for given constraint thresholds. As shown in [82], such equilibrium point is Pareto-optimal for all players, considering the strategy of the others as fixed. Hence, it is also a PNE of the MOG.

In the general hybrid case, the proof is readily obtained by merging the development obtained for the weighted-sum and the ϵ-constraint scalarised games.

3

Preference-agnostic weighted-sum game

This chapter focuses on the weighted-sum scalarised game representation of a MOG. The goal is to obtain conditions which ensure that the totally asynchronous BRD converges to a NE of the scalarised game, whatever the scalarisation weights. This justifies thus the words *preference-agnostic* of this chapter title. In details, the contributions are the following.

- The concept of *underlying game* is introduced, being the games obtained when each player selects one of its objective functions. It is shown that any weighted-sum scalarised game can be expressed as a convex combination of these underlying games, whose number is $N_{\text{und}} = \prod_{q=1}^{Q} L_q$.
- From this representation, conditions are obtained, guaranteeing that whatever the scalarisation weights, a NE exists, is unique, and that the totally asynchronous BRD converges towards it. Whereas analysing all scalarised games requires to study a continuum of games, these conditions are only based on the N_{und} underlying games.
- As the number of underlying games might still be large, conditions enabling to remove some of them are provided. These conditions show

that when an objective of one player is coupled with the other players more weakly than another of its objective, then the underlying games corresponding to the weakly coupled objective can be removed. Among others, this implies that for games with 2 players, a single underlying game can be analysed.

- The above results are extended to the case of players with preference subsets. In these cases, the scalarisation weights of each qth player belong to a subset Θ_q of the simplex Δ^{L_q}. When the subset is a polyhedron, this chapter shows how to transform the MOG with preference subsets into another MOG without preference information, hence on which the above results can be applied.
- Finally, the developed theoretical framework is applied to the JRC scenario and the multi-level RA problem introduced in Section 2.4. For the JRC scenario, it is shown that the BRD converges whatever the scalarisation weights if the interfering links between the pairs are not too strong. For the RA application, the theoretical framework of this chapter requires to add a regularisation term to the objective function. Then, the analysis reveals a trade-off between the approximation quality and the BRD convergence guarantees.

The above contributions are developed in the below sections as follows. First, Section 3.1 provides a state-of-the-art on the frameworks enabling to obtain convergence conditions for the BRD of NEPs. Then, the underlying games are defined in Section 3.2, and the convex combination results are stated. Building on this, Section 3.3 provides the conditions which ensure BRD convergence whatever the scalarisation weights. Section 3.4 extends the above results to the case of preference subsets. Finally, Section 3.5 applies the developed theoretical framework to the JRC scenario and the multi-level RA problem.

Before jumping to the NEP state-of-the-art, three levels of assumptions are introduced for the MOGs. These assumptions involve standard convexity, continuity and differentiability properties, which are required by the below frameworks and thus introduced here.

Assumption 3.1: Assumptions for equilibrium existence

For each qth player,

- $\mathcal{X}_q$ is non-empty, closed, convex and bounded;

and $\forall \mathbf{x} \in \mathcal{X}$, $\forall l_q = 1, \ldots, L_q$,

- $u_{q,l_q}(\mathbf{x}_q, \mathbf{x}_{-q})$ is convex in $\mathbf{x}_q$;
- $u_{q,l_q}(\mathbf{x}_q, \mathbf{x}_{-q})$ is $\mathcal{C}^0$ in $\mathbf{x}$.

Assumption 3.2: Assumptions for equilibrium unicity

For each qth player,

- $\mathcal{X}_q$ is non-empty, closed and convex;

and $\forall \mathbf{x} \in \mathcal{X}$, $\forall l_q = 1, \ldots, L_q$,

- $u_{q,l_q}(\mathbf{x}_q, \mathbf{x}_{-q})$ is convex in $\mathbf{x}_q$;
- $u_{q,l_q}(\mathbf{x}_q, \mathbf{x}_{-q})$ is $\mathcal{C}^1$ in $\mathbf{x}_q$.

Assumption 3.3: Assumptions for BRD convergence

For each qth player,

- $\mathcal{X}_q$ is non-empty, closed and convex;

and $\forall \mathbf{x} \in \mathcal{X}$, $\forall l_q = 1, \ldots, L_q$,

- $u_{q,l_q}(\mathbf{x}_q, \mathbf{x}_{-q})$ is strongly convex in $\mathbf{x}_q$;
- $u_{q,l_q}(\mathbf{x}_q, \mathbf{x}_{-q})$ is $\mathcal{C}^1$ in $\mathbf{x}_q$;
- $\boldsymbol{\nabla}_{\mathbf{x}_q} u_{q,l_q}(\mathbf{x}_q, \mathbf{x}_{-q})$ is $\mathcal{C}^1$ in $\mathbf{x}_q$ and $\mathbf{x}_{-q}$.

3.1 Single-objective NEP framework: state-of-the-art

In order to provide convergence guarantees for the BRD, the frameworks can be separated into two categories: those which relies on the BR expressions, and those which depend on the objective function and constraint set properties.

In the first category, one possibility is to show that the BR mapping is a *standard function*, meaning that it satisfies positivity, scalability, and monotonicity properties [40]. This approach has been considered in [36,41,42], mainly for power control problems. Another direction consists in proving the BR mapping is a *contraction*. Informally, this property means that if the players respond to two strategy profiles $\mathbf{x}$ and $\mathbf{y} \in \mathcal{X}$, then the distance between the player responses is always smaller than the distance between $\mathbf{x}$ and $\mathbf{y}$. In that case, fixed-point theorems imply that the BRD converges to the unique NE [33]. This contraction approach has been instrumental to the analysis of resource allocation schemes on interference channels, either for power control [35, 38], OFDM power allocation [28, 44, 49, 50, 53] and MIMO precoding [32, 54]. The caveat with these two approaches (standard function and contraction) is that they require to have a closed-form, or almost closed-form expression of the BR of the players. Yet, this is specific to the considered problems, and these frameworks thus are not good candidates for this chapter, which seeks general results.

The second category of frameworks thus provides convergence guarantees directly from the expression of the objective functions, and of the strategy sets. The framework developed in [55] belongs to this category. It in fact provides conditions on the objective functions and strategy sets ensuring that the BR mapping is a contraction, hence implying BRD convergence. Another advantage of this framework is that it consists in a systematic procedure: the second derivatives of the objective functions are computed, then their maximum norm on the strategy set are obtained to build a convergence matrix, and the properties of this matrix are analysed. Such step-by-step procedure avoids the need to use an ad-hoc reasoning specific to every tackled problem. Therefore, this framework is developed in details in this section, as it will be instrumental to the preference-agnostic results provided in this chapter.

To that aim, a NEP $\mathcal{G} = \left\langle \Omega, \{\mathcal{X}_q\}_{q\in\Omega}, \{u_q\}_{q\in\Omega} \right\rangle$ can be classified depending on the properties of the strategy sets and objective functions [55]. For this purpose, the qth player gradient mapping is introduced as $\mathbf{F}_q(\mathbf{x}) \triangleq \boldsymbol{\nabla}_{\mathbf{x}_q} u_q(\mathbf{x})$, the global gradient mapping as $\mathbf{F}(\mathbf{x}) \triangleq [\mathbf{F}_q(\mathbf{x})]_{q=1}^{Q}$ and the (q,r)th Jacobian matrix as $\mathbf{J}_r\mathbf{F}_q(\mathbf{x}) \triangleq \boldsymbol{\nabla}_{\mathbf{x}_r}^{\top}\mathbf{F}_q(\mathbf{x})$, under respectively first and second order differentiability assumptions. The convergence matrix $\boldsymbol{\Upsilon}$ is then defined as

$$[\boldsymbol{\Upsilon}]_{qr} \triangleq \begin{cases} \alpha_q & \text{if } q = r, \\ -\beta_{q,r} & \text{otherwise,} \end{cases} \tag{3.1}$$

with

$$\begin{aligned} \alpha_q &\triangleq \min_{\mathbf{x}\in\mathcal{X}} \lambda_{\min}\left(\mathbf{J}_q\mathbf{F}_q\left(\mathbf{x}\right)\right), \\ \beta_{q,r} &\triangleq \max_{\mathbf{x}\in\mathcal{X}} \sigma_{\max}\left(\mathbf{J}_r\mathbf{F}_q\left(\mathbf{x}\right)\right). \end{aligned} \tag{3.2}$$

In the above $\lambda_{\min}(\mathbf{A})$ is the minimum eigenvalue of the (symmetric) matrix $\mathbf{A}$, while $\sigma_{\max}(\mathbf{A})$ is the maximum singular value of the matrix (possibly non-symmetric). With these elements, the six following game classes[1] are introduced. These classes, represented in Figure 2.1, provide existence, unicity and convergence guarantees [55] which are instrumental to the MO results. In the below definitions, the symmetric part of a real matrix is denoted and defined as $\mathbf{A}^s \triangleq \left(\mathbf{A}+\mathbf{A}^\top\right)/2$, and the principal minors of a matrix are the determinants of the submatrices obtained by deleting some of the rows and the corresponding columns.

- $\mathcal{G}$ is **strictly monotone** if it fulfils Assumption 3.2 and its gradient mapping $\mathbf{F}$ is strictly monotone on $\mathcal{X}$: $\forall \mathbf{x},\mathbf{y}\in\mathcal{X}$, $\mathbf{x}\neq\mathbf{y}$,

$$(\mathbf{x}-\mathbf{y})^\top(\mathbf{F}(\mathbf{x})-\mathbf{F}(\mathbf{y}))>0.$$

- $\mathcal{G}$ is **P** if it fulfils Assumption 3.2 and its gradient mapping $\mathbf{F}$ is a P-function on $\mathcal{X}=\bigtimes_{q=1}^{Q}\mathcal{X}_q$: $\forall \mathbf{x},\mathbf{y}\in\mathcal{X}$, $\mathbf{x}\neq\mathbf{y}$,

$$\max_{q\in\Omega}(\mathbf{x}_q-\mathbf{y}_q)^\top(\mathbf{F}_q(\mathbf{x})-\mathbf{F}_q(\mathbf{y}))>0.$$

- $\mathcal{G}$ is **strongly monotone** if it fulfils Assumption 3.2 and its gradient mapping $\mathbf{F}$ is strongly monotone on $\mathcal{X}$: $\exists\, c>0$ s.t. $\forall \mathbf{x},\mathbf{y}\in\mathcal{X}$,

$$(\mathbf{x}-\mathbf{y})^\top(\mathbf{F}(\mathbf{x})-\mathbf{F}(\mathbf{y}))\geq c\,\|\mathbf{x}-\mathbf{y}\|_2^2.$$

- $\mathcal{G}$ is **uniformly P** if it fulfils Assumption 3.2 and its gradient mapping $\mathbf{F}$ is a uniform P-function on $\mathcal{X}=\bigtimes_{q=1}^{Q}\mathcal{X}_q$: $\exists\, d>0$ s.t. $\forall \mathbf{x},\mathbf{y}\in\mathcal{X}$,

$$\max_{q\in\Omega}(\mathbf{x}_q-\mathbf{y}_q)^\top(\mathbf{F}_q(\mathbf{x})-\mathbf{F}_q(\mathbf{y}))\geq d\,\|\mathbf{x}-\mathbf{y}\|_2^2.$$

- $\mathcal{G}$ is $\succ^s_{\boldsymbol{\Upsilon}}$ if it fulfils Assumption 3.3 and the symmetric part of its convergence matrix $\boldsymbol{\Upsilon}$ is positive definite, i.e., if $\lambda_{\min}(\boldsymbol{\Upsilon}^s)>0$.

[1] The $\succ^s_{\boldsymbol{\Upsilon}}$-class is not studied in [55], but corresponding implications can readily be derived following similar steps as in [55, Appendix B].

- $\mathcal{G}$ is $\mathbf{P}_{\boldsymbol{\Upsilon}}$ if it fulfils Assumption 3.3 and its convergence matrix $\boldsymbol{\Upsilon}$ is P, i.e., if all its principal minors are strictly positive.

The guarantees provided by these classes are stated in the three below propositions.

Proposition 3.1: Existence [15, 20]

Let the NEP $\mathcal{G} = \left\langle \Omega, \{\mathcal{X}_q\}_{q\in\Omega}, \{u_q\}_{q\in\Omega} \right\rangle$ fulfils Assumption 3.1. Then, it admits a pure NE. If furthermore the objective functions are strictly convex, then no strictly mixed NE exists.

Proposition 3.2: Unicity [55]

Let the NEP $\mathcal{G} = \left\langle \Omega, \{\mathcal{X}_q\}_{q\in\Omega}, \{u_q\}_{q\in\Omega} \right\rangle$ fulfils Assumption 3.2. Then at most one NE exists if $\mathcal{G}$ is strictly monotone or P, and a unique NE exists if $\mathcal{G}$ is strongly monotone or uniformly P.

Proposition 3.3: Convergence [55]

Let the NEP $\mathcal{G} = \left\langle \Omega, \{\mathcal{X}_q\}_{q\in\Omega}, \{u_q\}_{q\in\Omega} \right\rangle$ fulfils Assumption 2.2. Then, the totally asynchronous BRD converges to the unique NE in the sense of Definition 2.6 if $\mathcal{G}$ is $\succ^s_{\boldsymbol{\Upsilon}}$ or $\mathrm{P}_{\boldsymbol{\Upsilon}}$.

It should be noted that parts of Assumptions 3.1 to 3.3 can be relaxed, or replaced by other assumptions. Yet, as the below results anyway require these assumptions, and as these latter are often satisfied by wireless problems, the relaxations will not be considered in this work. The guarantees provided by the above propositions are depicted in Figure 3.1. It appears that the P-classes always give broader conditions than their monotone counterpart, yet they often turn out to be more difficult to study. The same complexity-broadness trade-off happens for the computation of α_q and $\beta_{q,r}$. At the price of narrower convergence conditions, any lower-bound $\overline{\alpha}_q \leq \alpha_q$ and upper-bound $\overline{\beta}_{q,r} \geq \beta_{q,r}$ can be used to build the matrix $\overline{\boldsymbol{\Upsilon}}$. Indeed, as $\overline{\boldsymbol{\Upsilon}} \leq \boldsymbol{\Upsilon}$, the positive definiteness of $\overline{\boldsymbol{\Upsilon}}^s$ implies the one of $\boldsymbol{\Upsilon}^s$ [99, 4.11.9], and similarly for the P-property [99, Fact 4.11.8].

Regarding the P-property of the $\boldsymbol{\Upsilon}$ matrix, it is defined above as the fact that all the principal minors are strictly positive. This property can be

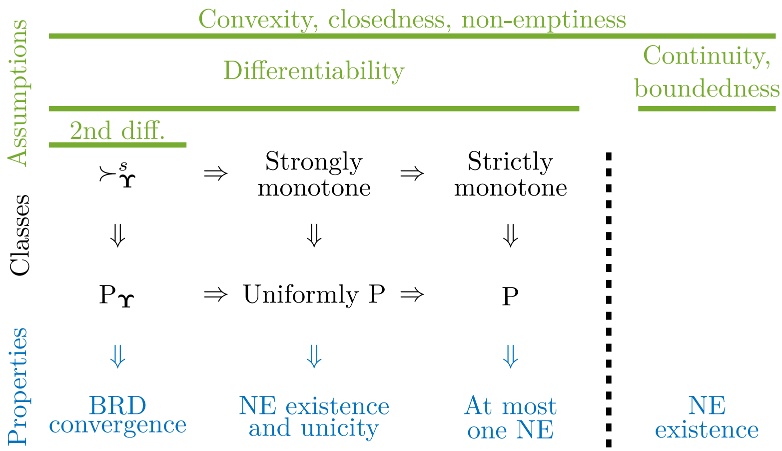

Fig. 3.1 NEP game classes, required assumptions and ensured properties [55].

linked to the spectral radius of the matrix $\boldsymbol{\Gamma} \in \mathbb{R}^{Q\times Q}$, defined as

$$[\boldsymbol{\Gamma}]_{qr} \triangleq \begin{cases} 0 & \text{if } q = r, \\ \frac{\beta_{q,r}}{\alpha_q} & \text{otherwise.} \end{cases} \tag{3.3}$$

The spectral radius of a matrix $\mathbf{A}$, denoted $\rho(\mathbf{A})$ is the largest modulus of the eigenvalues of the matrix.

Proposition 3.4: P-property [100, Fact F17]

Let $\boldsymbol{\Upsilon}$ be defined in (3.1), and $\boldsymbol{\Gamma}$ defined in (3.3). Then,

$$\boldsymbol{\Upsilon} \text{ is P} \quad \iff \quad \rho(\boldsymbol{\Gamma}) < 1. \tag{3.4}$$

As both matrices ($\boldsymbol{\Upsilon}$ and $\boldsymbol{\Gamma}$) provide BRD convergence guarantees, they are both named *convergence matrices*. Below, the letter $\boldsymbol{\Upsilon}$ will always refer to the convergence matrix defined in (3.1), while the letter $\boldsymbol{\Gamma}$ will always correspond to the definition (3.3). To gain insights into the above matrix properties, yet another equivalent formulation can be provided, which translates into a kind of diagonal dominance. This thus show that to have convergence guarantees, the off-diagonal elements $\beta_{q,r}$ should be significantly smaller than the diagonal ones α_q.

Proposition 3.5: Diagonal dominance [55, Corollary 31]

The matrix $\mathbf{\Upsilon}$ is P, or equivalently $\rho\left(\mathbf{\Gamma}\right) < 1$, if and only if $\exists\, \mathbf{w} \in \mathbb{R}^Q$, $\mathbf{w} > \mathbf{0}$ such that one of the two below conditions is satisfied :

$$\sum_{r \neq q} w_r \beta_{q,r} < w_q \alpha_q, \quad \forall q \in \Omega,$$
$$\sum_{q \neq r} w_q \beta_{q,r} < w_r \alpha_r, \quad \forall r \in \Omega.$$

To conclude the presentation of the BRD convergence conditions, it must be stressed out the game classes of Figure 3.1 only provide sufficient conditions for respectively the NE existence, unicity, and the convergence of the BRD. When the conditions are not fulfilled, nothing can therefore be said about these three properties, at least given the framework of [55]. In that case, other frameworks can be employed to try to obtain BRD convergence guarantees. One example of such problem has been analysed in [101, 102] for a multiple access channel. In that case, it is shown the game does not belong to the $P_{\mathbf{\Upsilon}}$ class, while the BRD is proven to converge using another framework.

From the author point of view, such effect is common to almost all GT frameworks applied to wireless networks. There does not exist a single framework which differentiates between the games for which the BRD converges, and those for which it does not. Therefore, when facing a GT scenario, one must find the right framework to analyse it, if such framework exists. In this thesis, the framework of [55] has been considered, since it has been possible to extend it to the MO case, as it will be shown in the below sections.

3.2 Underlying games

Given a MOG $\mathcal{G}^{(\mathrm{MO})}$ and a weight profile $\mathbf{\Lambda} \in \Delta^{\times}$, the weighted-sum scalarised game $\mathcal{G}^{\mathbf{\Lambda}}$ is defined in Definition 2.10. This specific weighted-sum NEP can be analysed within the framework defined above, by finding conditions ensuring it belongs to the game classes of Figure 3.1. Yet, to fully encompass the MO character of the players, such procedure must be done for all weighted-sum scalarised games, i.e., for all weight profiles $\mathbf{\Lambda} \in \Delta^{\times}$. Studying such a continuum of games is however challenging. Hence, the concept of underlying game is introduced in this section, since it will enable to move the focus from the infinite number of scalarised games to a finite number of underlying games.

In an underlying game, each qth player selects one of its objective functions, his choice being denoted by the index $\pi_q \in \{1, \dots, L_q\}$. The vector $\boldsymbol{\pi} \triangleq [\pi_q]_{q=1}^{Q}$, belonging to the set defined as $\Pi \triangleq \bigtimes_{q=1}^{Q} \{1, \dots, L_q\}$ thus parametrises the NEP $\mathcal{G}^{(\boldsymbol{\pi})} = \left\langle \Omega, \{\mathcal{X}_q\}_{q\in\Omega}, \{u_{q,\pi_q}\}_{q\in\Omega} \right\rangle$. This game is named the underlying game associated with $\boldsymbol{\pi}_q$. There exists only a finite number $N_{\text{und}} \triangleq \prod_{q=1}^{Q} L_q$ of underlying games. Yet, they summarise in some sense the whole weighted-sum scalarised game family, as shown by the below lemmas.

First, Lemma 3.1 expresses the gradient mapping of the scalarised game $\mathcal{G}^{\boldsymbol{\Lambda}}$ as a convex combination of the one of the underlying games. To that aim, the mappings of the weighted-sum scalarised game $\mathcal{G}^{\boldsymbol{\Lambda}}$ and the underlying game $\mathcal{G}^{(\boldsymbol{\pi})}$ are respectively written as

$$\mathbf{F}^{\boldsymbol{\Lambda}}(\mathbf{x}) \triangleq \left[\mathbf{F}_q^{\boldsymbol{\lambda}_q}(\mathbf{x})\right]_{q=1}^{Q} = \left[\boldsymbol{\nabla}_{\mathbf{x}_q} u_q^{\boldsymbol{\lambda}_q}(\mathbf{x})\right]_{q=1}^{Q}, \tag{3.5}$$

$$\mathbf{F}^{(\boldsymbol{\pi})}(\mathbf{x}) \triangleq \left[\mathbf{F}_{q,\pi_q}(\mathbf{x})\right]_{q=1}^{Q} = \left[\boldsymbol{\nabla}_{\mathbf{x}_q} u_{q,\pi_q}(\mathbf{x})\right]_{q=1}^{Q}. \tag{3.6}$$

The weights of the convex combination depend on the weight profile $\boldsymbol{\Lambda}$. For each objective selection $\boldsymbol{\pi} \in \Pi$, they are defined as $\gamma^{(\boldsymbol{\pi})} \triangleq \prod_{q=1}^{Q} \lambda_{q,\pi_q}$. These weights are non-negative, and they sum to one since

$$\begin{aligned}
\sum_{\boldsymbol{\pi}\in\Pi} \gamma^{(\boldsymbol{\pi})} &= \sum_{\pi_1=1}^{L_1} \sum_{\pi_2=1}^{L_2} \cdots \sum_{\pi_{Q-1}=1}^{L_{Q-1}} \sum_{\pi_Q=1}^{L_Q} \prod_{q=1}^{Q} \lambda_{q,\pi_q}, \\
&= \underbrace{\sum_{\pi_1=1}^{L_1} \lambda_{1,\pi_1}}_{=1} \underbrace{\sum_{\pi_2=1}^{L_2} \lambda_{2,\pi_2}}_{=1} \cdots \underbrace{\sum_{\pi_{Q-1}=1}^{L_{Q-1}} \lambda_{Q-1,\pi_{Q-1}}}_{=1} \underbrace{\sum_{\pi_Q=1}^{L_Q} \lambda_{Q,\pi_Q}}_{=1}.
\end{aligned}$$

The above thus shows that $\gamma^{(\boldsymbol{\pi})} \in \Delta^{N_{\text{und}}}$, with $\Delta^{N_{\text{und}}}$ the N_{und}-dimensional simplex, as defined in (2.12). This emphasises the fact that the below lemma expresses the gradient mapping of the scalarised game as a convex combination of the one of the underlying games.

Lemma 3.1

Let $\mathcal{G}^{(\mathrm{MO})} = \left\langle \Omega, \{\mathcal{X}_q\}_{q\in\Omega}, \{\mathbf{u}_q\}_{q\in\Omega} \right\rangle$ satisfy Assumption 3.2. Then, $\forall \mathbf{\Lambda} \in \Delta^{\times}$, the gradient mappings of the scalarised and underlying games are such that, $\forall \mathbf{x} \in \mathcal{X}$,

$$\mathbf{F}^{\mathbf{\Lambda}}(\mathbf{x}) = \begin{bmatrix} \sum_{\pi_1=1}^{L_1} \lambda_{1,\pi_1} \mathbf{F}_{1,\pi_1}(\mathbf{x}) \\ \vdots \\ \sum_{\pi_Q=1}^{L_Q} \lambda_{Q,\pi_Q} \mathbf{F}_{Q,\pi_Q}(\mathbf{x}) \end{bmatrix} = \sum_{\boldsymbol{\pi}\in\Pi} \gamma^{(\boldsymbol{\pi})} \mathbf{F}^{(\boldsymbol{\pi})}(\mathbf{x}).$$

Proof. The first equality follows from the mapping definition, while the second is proven in Section 3.7.1. □

Example 3.1

The convex combination interpretation provided by Lemma 3.1 is illustrated on a game with $Q = 2$ players, each with two objectives: $L_1 = L_2 = 2$. The scalarisation weights of the first (resp. second) player are $\lambda_{1,1}$ and $\lambda_{1,2}$ (resp. $\lambda_{2,1}$ and $\lambda_{2,2}$), the weights of any player summing to one. In Figure 3.2, it can indeed been observed the scalarised game $\mathcal{G}^{\mathbf{\Lambda}}$ has coordinates corresponding to the scalarisation weights. In this figure, the 4 corners correspond to cases for which one of the player selects a single objective, i.e., to the underlying games. With these elements, the scalarised game can also be specified by the area of the four rectangles, which are the weights $\gamma^{(\boldsymbol{\pi})}$, since $\gamma^{([1,1])} = \lambda_{1,1}\lambda_{2,1}$, and similarly for the other weights. As it can be verified, when one of these rectangles covers the full unit square, then the scalarised game boils down to one of the underlying games.

As Figure 3.1 shows, the above lemma will enable to study the NE existence and unicity. As for the convergence conditions, they depend on the convergence matrix defined for a NEP in (3.1). Applying this definition for the scalarised game $\mathcal{G}^{\mathbf{\Lambda}}$ and the underlying game $\mathcal{G}^{(\boldsymbol{\pi})}$, their convergence matrices are respectively denoted $\mathbf{\Upsilon}^{\mathbf{\Lambda}}$ and $\mathbf{\Upsilon}^{(\boldsymbol{\pi})}$. The lines of the matrices are furthermore referred to as $\mathbf{\Upsilon}^{\mathbf{\Lambda}} = \left[\boldsymbol{\upsilon}_1^{\boldsymbol{\lambda}_1}, \ldots, \boldsymbol{\upsilon}_Q^{\boldsymbol{\lambda}_Q}\right]^{\top}$ and $\mathbf{\Upsilon}^{(\boldsymbol{\pi})} = \left[\boldsymbol{\upsilon}_{1,\pi_1}, \ldots, \boldsymbol{\upsilon}_{Q,\pi_Q}\right]^{\top}$. With these definitions, a result similar to the convex combination expression of the gradient mapping can be obtained for

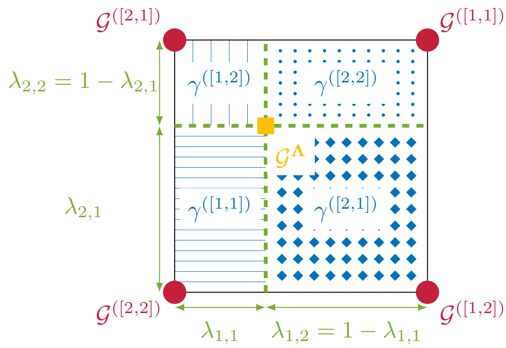

Fig. 3.2 Representation of the convex combination interpretation of the scalarised (yellow square) and underlying (red circles) games, for two players, each with two objectives. The scalarisation weights are represented with the green arrows, while the weights of the underlying games correspond to the area of the four hatched rectangles.

the convergence matrices. The difference is that only an inequality can be obtained.

Lemma 3.2

Let $\mathcal{G}^{(\mathrm{MO})} = \left\langle \Omega, \{\mathcal{X}_q\}_{q\in\Omega}, \{\mathbf{u}_q\}_{q\in\Omega} \right\rangle$ satisfy Assumption 3.3. Then, $\forall \mathbf{\Lambda} \in \Delta^{\times}$, the convergence matrices of the scalarised and underlying games are such that

$$\mathbf{\Upsilon}^{\mathbf{\Lambda}} \geq \sum_{\boldsymbol{\pi}\in\Pi} \gamma^{(\boldsymbol{\pi})} \mathbf{\Upsilon}^{(\boldsymbol{\pi})} = \begin{bmatrix} \sum_{\pi_1=1}^{L_1} \lambda_{1,\pi_1} \boldsymbol{\upsilon}_{1,\pi_1}^{\top} \\ \vdots \\ \sum_{\pi_Q=1}^{L_Q} \lambda_{Q,\pi_Q} \boldsymbol{\upsilon}_{Q,\pi_Q}^{\top} \end{bmatrix}.$$

Proof. See Section 3.7.2. □

3.3 Preference-agnostic existence, unicity and convergence conditions

In Section 3.1, six game classes have been defined based on [55], providing guarantees on the NE existence, NE unicity and BRD convergence towards a NE. Then, underlying games have been introduced in Section 3.2 and any scalarised has been shown to be a kind of convex combination of the underlying games. In this section, it is shown that the guarantees one can provide on the whole scalarised game family can be expressed in terms of the underlying games' classes. The advantage of this result follows from the fact that the number of underlying games is finite, while there are a continuum of scalarised games.

First, Theorem 3.1 provides guarantees on the existence of a NE whatever the scalarisation weights.

Theorem 3.1: NE Existence for $\mathcal{G}^{\mathbf{\Lambda}}$

Let $\mathcal{G}^{(\mathrm{MO})} = \left\langle \Omega, \{\mathcal{X}_q\}_{q\in\Omega}, \{\mathbf{u}_q\}_{q\in\Omega} \right\rangle$ satisfy Assumption 3.1. Then, $\forall \mathbf{\Lambda} \in \Delta^{\times}$, the scalarised game $\mathcal{G}^{\mathbf{\Lambda}} = \left\langle \Omega, \{\mathcal{X}_q\}_{q\in\Omega}, \left\{u_q^{\boldsymbol{\lambda}_q}\right\}_{q\in\Omega} \right\rangle$ admits a pure NE. If furthermore the objective functions are strictly convex, then no strictly mixed NE exists.

Proof. Since a non-negative weighted-sum of (strictly) convex functions stays (strictly) convex, assumptions of Proposition 3.1 hold for the scalarised game whatever the weights. □

Then, the focus is put on the 6 game classes of Figure 3.1. Stated informally, the below theorem shows that if all underlying games belong to a given class, then all weighted-sum scalarised games belong to it too, and conversely.

Theorem 3.2: Classes relationships for $\mathcal{G}^{\mathbf{\Lambda}}$

Let $\mathcal{G}^{(\mathrm{MO})} = \left\langle \Omega, \{\mathcal{X}_q\}_{q\in\Omega}, \{\mathbf{u}_q\}_{q\in\Omega} \right\rangle$ satisfy Assumption 3.2. Then, the below equivalences between the scalarised and underlying game families hold:

a) $\mathcal{G}^{\mathbf{\Lambda}}$ is strictly monotone $\forall \mathbf{\Lambda} \in \Delta^{\times}$
$\iff \mathcal{G}^{(\boldsymbol{\pi})}$ is strictly monotone $\forall \boldsymbol{\pi} \in \Pi$;

b) $\mathcal{G}^{\mathbf{\Lambda}}$ is P $\forall \mathbf{\Lambda} \in \Delta^{\times} \iff \mathcal{G}^{(\boldsymbol{\pi})}$ is P $\forall \boldsymbol{\pi} \in \Pi$;

c) $\mathcal{G}^{\mathbf{\Lambda}}$ is strongly monotone $\forall \mathbf{\Lambda} \in \Delta^{\times}$
$\iff \mathcal{G}^{(\boldsymbol{\pi})}$ is strongly monotone $\forall \boldsymbol{\pi} \in \Pi$;

d) $\mathcal{G}^{\mathbf{\Lambda}}$ is uniformly P $\forall \mathbf{\Lambda} \in \Delta^{\times}$
$\iff$ $\mathcal{G}^{(\boldsymbol{\pi})}$ is uniformly P $\forall \boldsymbol{\pi} \in \Pi$.

If Assumption 3.3 holds,

e) $\mathcal{G}^{\mathbf{\Lambda}}$ is $\succ^{s}_{\mathbf{\Upsilon}}$ $\forall \mathbf{\Lambda} \in \Delta^{\times} \iff \mathcal{G}^{(\boldsymbol{\pi})}$ is $\succ^{s}_{\mathbf{\Upsilon}}$ $\forall \boldsymbol{\pi} \in \Pi$;

f) $\mathcal{G}^{\mathbf{\Lambda}}$ is $\mathrm{P}_{\mathbf{\Upsilon}}$ $\forall \mathbf{\Lambda} \in \Delta^{\times} \iff \mathcal{G}^{(\boldsymbol{\pi})}$ is $\mathrm{P}_{\mathbf{\Upsilon}}$ $\forall \boldsymbol{\pi} \in \Pi$.

Proof. See Section 3.7.3. □

The above theorem provides a powerful way to study NE existence, unicity and convergence of the totally asynchronous BRD while being agnostic about the preferences of the players. It moves the effort from studying all scalarised games, each involving a possibly complicated weighted-sum of several objectives, to the study of the underlying games, whose number is finite, each involving a single objective per player. This point of view is moreover supported by the fact that many NEPs have already been studied in the literature, paving the way to an easy analysis of MO interactions. Finally, the above theorem is tight: to ensure $\mathcal{G}^{\mathbf{\Lambda}}$ belongs to one class for all scalarisation profiles, verifying all underlying games belong to that class is necessary and sufficient.

The above strengths of the developed framework must nevertheless be discussed in terms of scalability, regarding both the number of objective functions and number of players. As far as the analysis complexity is concerned, since there are $N_{\text{und}} = \prod_{q=1}^{Q} L_q$ underlying games, checking all of them becomes prohibitive for large numbers of players and objectives. Even if the analysis can be performed, the class conditions usually are harder and harder to fulfil when the number of players increases. These two effects thus lead in practice to a player number limit, which must be kept in mind when studying MOGs. If this raises difficulties for the considered application, then ad-hoc mechanisms must be designed to ensure the number of interacting users remains moderate. Such ad-hoc mechanisms may be provided by the other parts of this thesis which study other way of managing the interference between nodes.

The above comment must be nuanced for the $\mathrm{P}_{\mathbf{\Upsilon}}$ class, this class being the one providing convergence guarantees. Indeed, in some cases, the number of underlying games which need to be checked can be reduced. To that aim, the following definition is introduced.

Definition 3.1: Weaker/stronger coupling

In a MOG $\mathcal{G}^{(\mathrm{MO})} = \left\langle \Omega, \{\mathcal{X}_q\}_{q\in\Omega}, \{\mathbf{u}_q\}_{q\in\Omega} \right\rangle$, let $q \in \Omega$, $l, l' \in \{1,\dots,L_q\}$, and let $\alpha_{q,l}$ and $\beta_{q,r,l}$ (resp. $\alpha_{q,l'}$ and $\beta_{q,r,l'}$) be the elements of the convergence matrix (3.1) associated with the lth objective (resp. l'th) of the qth player. The objective function $u_{q,l'}$ is said to be **coupled more weakly** than $u_{q,l}$, or said otherwise, $u_{q,l}$ **coupled more strongly** than $u_{q,l'}$, if

$$\forall r \neq q, \qquad \frac{\beta_{q,r,l'}}{\alpha_{q,l'}} \leq \frac{\beta_{q,r,l}}{\alpha_{q,l}}. \tag{3.7}$$

When considering games with 2 players, a single inequality (3.7) must be fulfilled, and therefore one of the objective is always coupled more strongly than all the others, for each player. However, when $Q \geq 3$, then it may happen none of the objectives satisfy the above. For instance, for the first player in a game with 3 players, if $\beta_{1,2,1}/\alpha_{1,1} = \beta_{1,3,1}/\alpha_{1,1} = 1$, and $\beta_{1,2,2}/\alpha_{1,2} = 2$, $\beta_{1,3,2}/\alpha_{1,2} = 0.5$. In mathematical terms, the above is a partial ordering [99, Def. 1.3.8].

For each qth player, let $\mathcal{L}_q^w \subset \{1,\dots,L_q\}$ be only composed of objectives which are coupled more weakly than one of the objectives in $\{1,\dots,L_q\} \setminus \mathcal{L}_q^w$. The set of underlying games, excluding the objectives which are coupled more weakly than others, is then defined as $\underline{\Pi} \triangleq \bigtimes_{q=1}^{Q} \{1,\dots,L_q\} \setminus \mathcal{L}_q^w$. The below proposition shows that this reduced set of underlying games provides the same information as the complete set, regarding the $\mathrm{P}_{\boldsymbol{\Upsilon}}$ class only.

Proposition 3.6: Reduced set of underlying games

Let $\mathcal{G}^{(\mathrm{MO})} = \left\langle \Omega, \{\mathcal{X}_q\}_{q\in\Omega}, \{\mathbf{u}_q\}_{q\in\Omega} \right\rangle$ satisfy Assumption 3.3. Then,

$$\mathcal{G}^{(\boldsymbol{\pi})} \text{ is } \mathrm{P}_{\boldsymbol{\Upsilon}} \ \forall \boldsymbol{\pi} \in \Pi \quad \Longleftrightarrow \quad \mathcal{G}^{(\boldsymbol{\pi})} \text{ is } \mathrm{P}_{\boldsymbol{\Upsilon}} \ \forall \boldsymbol{\pi} \in \underline{\Pi}. \tag{3.8}$$

Proof. This result follows from the link between the P-property and the spectral radius of the matrix defined in (3.3), and from [99, Fact 4.11.18]. $\square$

The above proposition might in some cases greatly reduce the number of underlying games which need to be analysed to ensure the whole scalarised game family belongs to the $\mathrm{P}_{\boldsymbol{\Upsilon}}$ class, since the objectives which are coupled more weakly than others can be discarded from the analysis. Extending

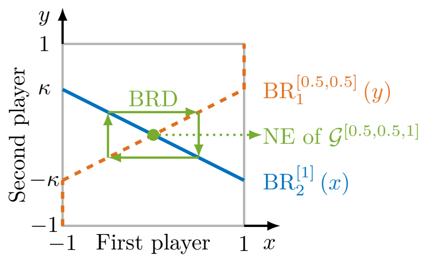

Fig. 3.3 BR mappings, NE and BRD of Example 3.2 for the scalarised game with equal weights.

it to the other classes of Figure 3.1 is an interesting definition for future works, which however requires defining relevant coupling measures, similarly to Definition 3.1.

To conclude this section, it is noted that in the above results, the existence, unicity and convergence properties are obtained from the game classes of Figure 3.1, these classes providing sufficient but not necessary conditions. Theorem 3.2 shows then that if all underlying games belong to a given class, then all scalarised games belong to it too. This raises the question of whether such equivalences hold for the properties themselves. For instance, if all underlying games have a BRD converging to a NE, does the BRD of any scalarised game converges too? The answer to this question is negative, as shown in the following example.

Example 3.2

Let us consider a 2-player game $\mathcal{G}^{(\mathrm{MO})}$ parametrised by $\kappa < 1$ with $\mathcal{X}_1 = \mathcal{X}_2 = [-1; 1]$, in which the first player has two objectives

$$u_{1,1}(x, y) = e^{x - \frac{y}{\kappa}}, \qquad u_{1,2}(x, y) = e^{\frac{y}{\kappa} - x},$$

while the second player has a single objective

$$u_{2,1}(y, x) = (y + \kappa x)^2 .$$

Associated with this MOG, there are two underlying games, respectively when the first player selects its first or second objective function. The BR mapping of the first player for the two underlying games are respectively $\mathrm{BR}_{1,1}(y) = -1$ and $\mathrm{BR}_{1,2}(y) = 1$, being independent of the strategy of the second player. This implies that the BRD of the two underlying games converges, since once the first player has implemented its BR, the second player sets its strategy to $\mathrm{BR}_{2,1}(x) = -\kappa x$ and the equilibrium is reached. Considering the weighted-sum scalarised game in which the first player has equal weights $\boldsymbol{\lambda}_1 = [0.5, 0.5]$, its objective function and BR are given by

$$u_1^{[0.5,0.5]}(x,y) = \cosh\left(x - \frac{y}{\kappa}\right),$$
$$\mathrm{BR}_1^{[0.5,0.5]}(y) = \min\left\{\max\left\{\frac{y}{\kappa}, -1\right\}, 1\right\},$$

while the one of the second player remains unchanged. The BRs are depicted in Figure 3.3, as well as the BRD. As it can be observed, for the chosen starting point, the BRD gets stuck in the cycle $(x,y) = \left(\frac{1}{2}, \frac{-\kappa}{2}\right) \to \left(\frac{-1}{2}, \frac{-\kappa}{2}\right) \to \left(\frac{-1}{2}, \frac{\kappa}{2}\right) \to \left(\frac{1}{2}, \frac{\kappa}{2}\right) \to \left(\frac{1}{2}, \frac{-\kappa}{2}\right)$ for the chosen starting point. This shows that in general, the BRD convergence for all underlying games does not imply convergence for the scalarised game. Modifying the $\frac{y}{\kappa}$ or κx terms into the objective functions, similar examples are obtained for the existence and unicity of a NE.

The above example also shows that the BR of a scalarised game might be very different from the one of the underlying games. Hence, the frameworks which obtain the unicity and convergence conditions from the properties of the BR are difficult to generalise to MOGT.

3.4 Extension to subsets of preferences

The above results have been obtained by considering that the scalarisation weights of the qth player could be any weight profile belonging to Δ^{L_q}. This corresponds to having absolutely no knowledge of the preferences of the player among its objectives. At the other extreme, when one knows the player preferences, a single scalarisation profile may be considered, leading to a unique NEP. This section considers the intermediate situation between these two extremes, in which the qth player weights are known to belong to a subset of Δ^{L_q}, denoted Θ_q, as represented in Figure 3.4. The global weight profile belongs then to the set $\Theta^\times$ defined as $\Theta^\times \triangleq \bigtimes_{q=1}^{Q} \Theta_q$.

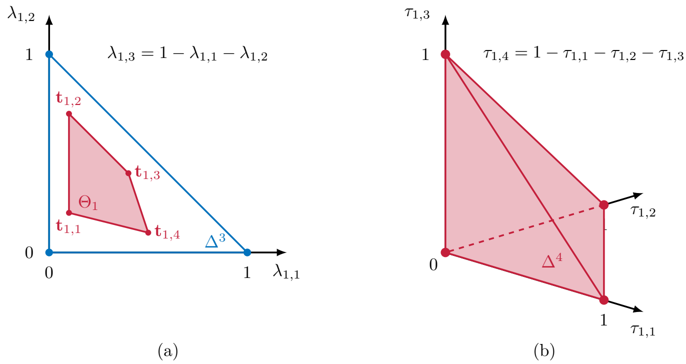

Fig. 3.4 On panel (a), illustration of the subset of preference of the first player Θ_1, this player having $L_1 = 3$ objective functions. On panel (b), representation of Θ_1 as a 4-dimensional simplex.

The results of the above sections leverages on the fact a scalarised game $\mathcal{G}^{\boldsymbol{\Lambda}}$ can be seen as a convex combination of the underlying games, these latter corresponding the corners of the simplices. When the preference subset Θ_q is a convex polyhedron, it is thus tempting to try to express any scalarised game as a convex combination of the games obtained at the vertices of the polyhedron. This section provides such a result by defining a modified MOG $\mathcal{G}^{(\mathrm{MO}),v}$ for which the preference subsets Θ_q are translated into simplices, this enabling a direct application of the results of the above sections. To that aim, the below assumption is introduced.

Assumption 3.4: Polyhedron

Whatever $q \in \Omega$, $\Theta_q \subseteq \Delta^{L_q}$ is a convex polyhedron, i.e., it can be described as the convex hull of its T_q vertices denoted $\left\{\mathbf{t}_{q,1}, \dots, \mathbf{t}_{q,T_q}\right\}$, with $\mathbf{t}_{q,t_q} \in \Delta^{L_q}$ for all $t_q = 1, \dots, T_q$:

$$\Theta_q = \operatorname{conv}\left\{\mathbf{t}_{q,1}, \dots, \mathbf{t}_{q,T_q}\right\}.$$

The above implies that if $\boldsymbol{\lambda}_q \in \Theta_q$, then it exists a weight vector $\boldsymbol{\tau}_q \in \Delta^{T_q}$ such that

$$\boldsymbol{\lambda}_q = \left[\mathbf{t}_{q,1}, \dots, \mathbf{t}_{q,T_q}\right] \boldsymbol{\tau}_q = \sum_{t_q=1}^{T_q} \tau_{q,t_q} \mathbf{t}_{q,t_q} \tag{3.9}$$

In other words, any scalarisation weight vector can be expressed a convex combination of the vertices of the polyhedron. The objective function corresponding to each polyhedron vertex is defined as

$$v_{q,t_q}(\mathbf{x}) \triangleq \mathbf{t}_{q,t_q}^{\top}\mathbf{u}_q(\mathbf{x}) = \sum_{l_q=1}^{L_q}\left[\mathbf{t}_{q,t_q}\right]_{l_q} u_{q,l_q}(\mathbf{x}), \tag{3.10}$$

being a convex combination of the original objective functions. The vector objective function is furthermore defined as $\mathbf{v}_q = \left[v_{q,t_q}(\mathbf{x})\right]_{t_q=1}^{T_q} \in \mathbb{R}^{T_q}$, and the weighted-sum objective function associated with the weight profile $\boldsymbol{\tau}_q \in \Delta^{T_q}$ is denoted $v_q^{\boldsymbol{\tau}_q}(\mathbf{x}) \triangleq \sum_{t_q=1}^{T_q} \tau_{q,t_q} v_{q,t_q}(\mathbf{x})$.

For a pair $(\boldsymbol{\lambda}_q, \boldsymbol{\tau}_q)$ satisfying (3.9), the two scalarised functions are identical:

$$u_q^{\boldsymbol{\lambda}_q}(\mathbf{x}) = \boldsymbol{\lambda}_q^{\top}\mathbf{u}_q(\mathbf{x}) = \boldsymbol{\tau}_q^{\top}\begin{bmatrix}\mathbf{t}_{q,1}^{\top}\mathbf{u}_q(\mathbf{x}) \\ \vdots \\ \mathbf{t}_{q,T_q}^{\top}\mathbf{u}_q(\mathbf{x})\end{bmatrix} = \boldsymbol{\tau}_q^{\top}\mathbf{v}_q(\mathbf{x}) = v_q^{\boldsymbol{\tau}_q}(\mathbf{x}).$$

Thus, the objective functions of the scalarised games can either be expressed as a combination of the original objective functions, or as a combination of the objective functions obtained at the vertices of the polyhedron. In this latter representation, the global weight profile is denoted as $\mathbf{T} \triangleq \{\boldsymbol{\tau}_q\}_{q=1}^{Q}$, belonging to the set $\Delta^{\times,v} \triangleq \bigtimes_{q=1}^{Q} \Delta^{T_q}$. The modified MOG is thus defined as $\mathcal{G}^{(\mathrm{MO}),v} = \left\langle \Omega, \{\mathcal{X}_q\}_{q\in\Omega}, \{\mathbf{v}_q\}_{q\in\Omega}^{Q}\right\rangle$, its weighted-sum scalarised games being denoted $\mathcal{G}^{\mathbf{T},v} = \left\langle \Omega, \{\mathcal{X}_q\}_{q\in\Omega}, \left\{v_q^{\boldsymbol{\tau}_q}\right\}_{q\in\Omega}^{Q}\right\rangle$ for $\mathbf{T} \in \Delta^{\times,v}$. Based on these definitions, Proposition 3.7 formalises the fact that studying all weighted-sum scalarised games with the preference subset $\Theta^{\times}$ is equivalent to studying a modified MOG with no preference information.

Proposition 3.7: Preference subset equivalent game

Given a MOG $\mathcal{G}^{(\mathrm{MO})} = \left\langle \Omega, \{\mathcal{X}_q\}_{q\in\Omega}, \{\mathbf{u}_q\}_{q\in\Omega}\right\rangle$ and the preference subset $\Theta^{\times} \subseteq \Delta^{\times}$ satisfying Assumption 3.4, let $\mathcal{G}^{(\mathrm{MO}),v}$ be the associated modified MOG. Let $\mathcal{G}^{\boldsymbol{\Lambda}}$ be the weighted-sum scalarised game associated with $\mathcal{G}^{(\mathrm{MO})}$ and $\boldsymbol{\Lambda} \in \Theta^{\times}$, and $\mathcal{G}^{\mathbf{T},v}$ the one associated with $\mathcal{G}^{(\mathrm{MO}),v}$ and $\mathbf{T} \in \Delta^{\times,v}$ Then,

$$\bigcup_{\boldsymbol{\Lambda}\in\Theta^{\times}} \{\mathcal{G}^{\boldsymbol{\Lambda}}\} = \bigcup_{\mathbf{T}\in\Delta^{\times,v}} \{\mathcal{G}^{\mathbf{T},v}\}. \tag{3.11}$$

The above proposition enables to apply Theorems 3.1 and 3.2 to a MOG with preference information, by first translating it into the associated modified MOG without preference information. Let $\pi_q^v \in \{1,\ldots,T_q\}$ denote the selection of the qth player among the modified objective functions, $\boldsymbol{\pi}^v \triangleq \left[\pi_1^v,\ldots,\pi_Q^v\right]$ the global selection, and $\Pi^v \triangleq \bigtimes_{q=1}^{Q} \{1,\ldots,T_q\}$ the set of all possible selections. The modified underlying game associated with $\boldsymbol{\pi}^v \in \Pi^v$ is denoted and defined as $\mathcal{G}^{(\boldsymbol{\pi}^v),v} = \left\langle \Omega, \{\mathcal{X}_q\}_{q\in\Omega}, \left\{v_{q,\pi_q^v}\right\}_{q\in\Omega}^{Q} \right\rangle$. Theorem 3.2 show that to obtain BRD convergence guarantees, one must study the convergence matrix of each of the modified underlying games. Such convergence matrix can either be obtained from the definition (3.1), or a lower-bound can be computed with Lemma 3.2, with the weight profiles $\boldsymbol{\lambda}_q$ replaced by the polyhedron vertices $\mathbf{t}_{q,\pi_q^v}$. Since only a lower-bound is provided by the second approach, the obtained convergence conditions will be narrower than those obtained with the exact computation. This will be illustrated on the JRC scenario in Section 3.5.1.

The above procedure is possible when the preference subset of each player is a convex polyhedron. If the preference subsets are not convex polyhedra, but can be represented as a finite union of convex polyhedra, then the above results can be extended by considering each polyhedron separately. Extensions to other types of preference subsets, such as a disk, are a direction for future works, even though the added value of such an analysis seems to be limited at first sight.

3.5 Application to the multi-function multi-point use-cases

The theoretical results of this chapter are applied to the two MF MP use-cases defined in Section 2.4. For each use-case, it is first checked whether the equivalence between the PNEs of the MOG and the NEs of the weighted-sum scalarised games holds. Then, efficient way of computing the BR of the scalarised games are provided, as this ensures the players are able to interact according to the BRD. Finally, convergence conditions for the BRD are obtained by building the convergence matrices of the underlying games.

3.5.1 JRC scenario

Equilibrium point equivalence For the JRC scenario described in Section 2.4.1, it can be checked Assumption 2.2 is fulfilled, since the strategy sets are non-empty, closed and convex, and each qth objective function is strictly convex (even strongly convex) in the strategy $\mathbf{p}_q$. From Theorem 2.1, this thus shows that by varying the global weight profile in $\Delta^{\times}$, the NEs of the scalarised game spans all PNEs of the MOG, and conversely. This thus motivates the study of the JRC MO competitive interactions through the weighted-sum scalarised game family.

Weighted-sum scalarised game and BR In the JRC MOG, the players all have two objective functions, and thus the preference of the qth player is characterised by the weight profile $\boldsymbol{\lambda}_q = [\lambda_{q,1}, \lambda_{q,2}]^\top \in \Delta^2$. The global weight profile is given by $\boldsymbol{\Lambda} = [\boldsymbol{\lambda}_q]_{q=1}^{Q} \in \Delta^{\times}$, with $\Delta^{\times} = \bigtimes_{q=1}^{Q} \Delta^2$. With these elements, the optimisation problem of the qth player corresponding to the weighted-sum scalarised game $\mathcal{G}^{\boldsymbol{\Lambda}}$ is given by

$$\begin{aligned} \text{minimise}_{\mathbf{p}_q} \quad & -\textstyle\sum_{k=1}^{K} \left(\lambda_{q,1} \ln\left(1 + \frac{p_{q,k}}{\xi_{q,k}(\mathbf{p}_{-q})}\right) + \lambda_{q,2} \ln\left(1 + \frac{p_{q,k}}{\xi^{\circ}_{q,k}(\mathbf{p}_{-q})}\right)\right) \\ \text{s.t.} \quad & p_{q,k} \geq 0 \quad \forall k = 1, \ldots, K, \\ & \textstyle\sum_{k=1}^{K} p_{q,k} = P_q, \end{aligned} \tag{3.12}$$

with the noise-plus-interference normalised powers defined in (2.27). The unique minimiser of the above is the BR of the qth player, denoted $\mathbf{BR}_q^{\boldsymbol{\lambda}_q}(\mathbf{p}_{-q})$. This BR has a waterfilling-like expression, given by [87]

$$\left[\mathbf{BR}_q^{\boldsymbol{\lambda}_q}(\mathbf{p}_{-q})\right]_k = \left[\delta_q\left(1 + \sqrt{\gamma_{q,k}}\right) - \frac{\xi_{q,k} + \xi^{\circ}_{q,k}}{2}\right]^{+}, \tag{3.13}$$

$$\text{with } \gamma_{q,k} = \left(\frac{\xi_{q,k} - \xi^{\circ}_{q,k}}{2\delta} + \lambda_{q,2} - \lambda_{q,1}\right)^2 + 4\lambda_{q,1}\lambda_{q,2},$$

with $[\cdot]^{+} = \max\{\cdot, 0\}$, and the dependency of $\xi_{q,k}$, $\xi^{\circ}_{q,k}$ and $\gamma_{q,k}$ on $\mathbf{p}_{-q}$ being omitted for clarity. In the above, δ_q is the water level, which must satisfy the maximum power constraint with an equality: $\sum_{k=1}^{K}\left[\mathbf{BR}_q^{\boldsymbol{\lambda}_q}(\mathbf{p}_{-q})\right]_k = P_q$.

This water level can be efficiently computed for instance with the binary search method. This almost closed-form BR expression, together with the equilibrium point equivalences, call for the study of convergence conditions for the BRD.

Preference-agnostic convergence conditions The JRC MOG satisfies the convexity and differentiability requirements of Assumptions 3.1 to 3.3, respectively for equilibrium existence, unicity and BRD convergence. Therefore, the results of Theorem 3.1 shows that whatever the scalarisation weights, the weighted-sum scalarised game admits a pure NE, and no strictly mixed NE. Regarding the game relationships of Figure 3.1, Theorem 3.2 show that to ensure all scalarised games belong to a given class, it is sufficient to verify all underlying games belong to that class.

Therefore, the underlying games of the JRC scenario are studied. The objective selected by the qth player is denoted π_q, being equal to 1 for the communication objective, and 2 for the radar part. In the underlying game parametrised by $\boldsymbol{\pi} = [\pi_q]_{q=1}^{Q}$, each player minimises thus the following objective function

$$u_q^{(\pi_q)}(\mathbf{p}) = -\sum_{k=1}^{K} \ln\left(1 + \frac{p_{q,k}}{\hat{a}_{q,k} + \sum_{o\neq q} \hat{b}_{q,o,k} p_{o,k}}\right), \tag{3.14}$$

with the generic coefficients $(\hat{a}_{q,k}, \hat{b}_{q,o,k})$ equal to $(a_{q,k}, b_{q,o,k})$ if $\pi_q = 1$, and to $(a^{\circ}_{q,k}, b^{\circ}_{q,o,k})$ if $\pi_q = 2$. In order to ensure BRD convergence, the $P_{\boldsymbol{\Upsilon}}$ class is studied, depending on the convergence matrix of the underlying game (3.1). Taking advantage of the NEP analysis of [55], the convergence matrix elements are obtained as

$$\alpha_{q,\pi_q} = \min_{k=1,\dots,K} \left\{ \frac{1}{\left(\hat{a}_{q,k} + \sum_{o=1}^{Q} \hat{b}_{q,o,k} P_o\right)^2} \right\}, \tag{3.15}$$

$$\beta_{q,r,\pi_q} = \max_{k=1,\dots,K} \left\{ \frac{\hat{b}_{q,r,k}}{\hat{a}^2_{q,k}} \right\}, \tag{3.16}$$

as detailed in Section 3.7.4. The P-property of the convergence matrix associated with each selection profile $\boldsymbol{\pi}$ can now be checked to ensure BRD convergence. In general, Proposition 3.6 cannot be leveraged upon in this case to reduce the number of underlying games to analyse. Indeed, the above expressions of α_{q,π_q} and β_{q,r,π_q} do not enable to identify objectives which are coupled more weakly than others, if any. Yet, for specific values of the coefficients $\hat{a}_{q,k}$ and $\hat{b}_{q,r,k}$, it might be possible to do so.

Building on the diagonal dominance interpretation of the P-property, as provided by Proposition 3.5, the analysis shows that the $\hat{b}_{q,o,k}$ coefficients should be small to have a matrix benefitting from the P-property. This thus reveals the following insight on the JRC interactions.

Insight 3.1: Low interference

For the weighted-sum scalarised games, the BRD of the JRC scenario is likely to converge when the interfering link gains are significantly smaller than the direct link gains, that is when

$$\begin{aligned} \left|h_{q,r,k}\right|^2 &\ll \left|h_{q,q,k}\right|^2, \\ \left|h^{\circ}_{q,r,k}\right|^2 &\ll \mathbb{E}\left\{\left|\phi^{\circ}_{q,q,k}\right|^2\right\}. \end{aligned}$$

Preference subsets The above convergence conditions have been obtained considering all possible weights of the players. The case of a partial knowledge of the players' preferences is now investigated, by considering that each qth player has a minimum communication weight $t_{q,\mathrm{C}}$, and a minimum radar weight $t_{q,\mathrm{R}}$. In other word, the weight profile of the qth player belongs to

$$\Theta_q = \operatorname{conv}\left\{\begin{bmatrix} t_{q,\mathrm{C}} \\ 1-t_{q,\mathrm{C}} \end{bmatrix}, \begin{bmatrix} 1-t_{q,\mathrm{R}} \\ t_{q,\mathrm{R}} \end{bmatrix}\right\}, \tag{3.17}$$

with $t_{q,\mathrm{C}} + t_{q,\mathrm{R}} \leq 1$. The modified objective functions are thus

$$
\begin{aligned}
v_{q,1}(\mathbf{p}) = -\sum_{k=1}^{K} \Bigg(t_{q,\mathrm{C}} \ln \left(1 + \frac{p_{q,k}}{\xi_{q,k}(\mathbf{p}_{-q})}\right) \\
+ (1 - t_{q,\mathrm{C}}) \ln \left(1 + \frac{p_{q,k}}{\xi^{\star}_{q,k}(\mathbf{p}_{-q})}\right) \Bigg), \\
v_{q,2}(\mathbf{p}) = -\sum_{k=1}^{K} \Bigg((1 - t_{q,\mathrm{R}}) \ln \left(1 + \frac{p_{q,k}}{\xi_{q,k}(\mathbf{p}_{-q})}\right) \\
+ t_{q,\mathrm{R}} \ln \left(1 + \frac{p_{q,k}}{\xi^{\circ}_{q,k}(\mathbf{p}_{-q})}\right) \Bigg).
\end{aligned}
$$

Then, the convergence matrix associated with each selection between these modified objective functions can be computed following the same steps as those of Section 3.7.4. For instance, considering the qth player selects $\pi^v_1 = 1$, the elements of the convergence matrix are given by

$$
\begin{aligned}
\alpha^v_{q,1} &= \min_{k=1,\ldots,K} \left\{ \frac{t_{q,\mathrm{C}}}{\left(a_{q,k} + \sum_{o=1}^{Q} b_{q,o,k} P_o\right)^2} + \frac{1 - t_{q,\mathrm{C}}}{\left(a^{\circ}_{q,k} + \sum_{o=1}^{Q} b^{\circ}_{q,o,k} P_o\right)^2} \right\}, \\
\beta^v_{q,r,1} &= \max_{k=1,\ldots,K} \left\{ t_{q,\mathrm{C}} \frac{b_{q,r,k}}{a^2_{q,k}} + (1 - t_{q,\mathrm{C}}) \frac{b^{\circ}_{q,r,k}}{\left(a^{\star}_{q,k}\right)^2} \right\}.
\end{aligned}
$$

It should be noted that using Lemma 3.2 instead of the exact computations would have led to

$$
\begin{aligned}
t_{q,\mathrm{C}} \min_{k=1,\ldots,K} \left\{ \frac{1}{\left(a_{q,k} + \sum_{o=1}^{Q} b_{q,o,k} P_o\right)^2} \right\} \\
+ (1 - t_{q,\mathrm{C}}) \min_{k=1,\ldots,K} \left\{ \frac{1}{\left(a^{\circ}_{q,k} + \sum_{o=1}^{Q} b^{\circ}_{q,o,k} P_o\right)^2} \right\} \leq \alpha^v_{q,1}, \\
t_{q,\mathrm{C}} \max_{k=1,\ldots,K} \left\{ \frac{b_{q,r,k}}{a^2_{q,k}} \right\} + (1 - t_{q,\mathrm{C}}) \max_{k=1,\ldots,K} \left\{ \frac{b^{\circ}_{q,r,k}}{\left(a^{\star}_{q,k}\right)^2} \right\} \geq \beta^v_{q,r,1},
\end{aligned}
$$

which lower- and upper-bound the actual elements, and thus provide convergence conditions which are less tight.

Numerical analysis The above developments are applied to a JRC scenario with $Q = 8$ players and $K = 16$ OFDM tones, with $P_q = 1$ and $\sigma^2_{q,k} = \left(\sigma^\circ_{q,k}\right)^2 = 10^{-2}$ for all players and tones. All channel coefficients $h_{q,r,k}$, $\phi^\circ_{q,q,k}$ and $h^\circ_{q,r,k}$ are complex normal independent random variables, with unit variance for the direct links and with variance η for the cross ones.

Thus, for each draw of the coefficients, a different MOG is obtained, with different scalarised and underlying games. For each of the draw, it can be determined whether all underlying games belong to the $\mathrm{P}_{\boldsymbol{\Upsilon}}$ class, this being named the *MO conditions*. For a specific weight profile $\boldsymbol{\Lambda}$, it can also be checked whether this specific weighted-sum scalarised game belongs to the considered class. Figure 3.5 depicts the probability for these games to belong to the $\mathrm{P}_{\boldsymbol{\Upsilon}}$ class, as a function of the interfering power ratio η. It is observed that as predicted by Theorem 3.2, the MO conditions are tight in the sense that they cannot be strengthened while still being valid for all scalarised games. In that sense, they are a worst case analysis, ensuring the existence, unicity and convergence properties for the worst weight profile users can select. This figure also highlights the fact that convergence conditions are likely to be satisfied for low η, i.e., when the interference is not too strong, validating Insight 3.1. As far as the equilibrium quality is concerned, it is thus observed that fortunately, the class of games for which the BRD converges is likely to benefit from high communication and radar rates, since convergence occurs for low interference factors η.

3.5.2 Multi-level RA scenario

Regularised game and equilibrium point equivalence In the multi-level RA scenario, the objective functions of the qth player are linear in its strategy profile. Thus, they do not fulfil the strict convexity requirement of Theorem 2.1, and therefore there is no equilibrium equivalence. Moreover, when building the convergence matrices, this linearity makes the diagonal elements equal to 0, since they depend on the second derivative of the objective function. Hence, leveraging on the diagonal dominance interpretation of the P-property given by Proposition 3.5, this shows that the framework of this chapter cannot provide convergence guarantees for the RA game, in its current form.

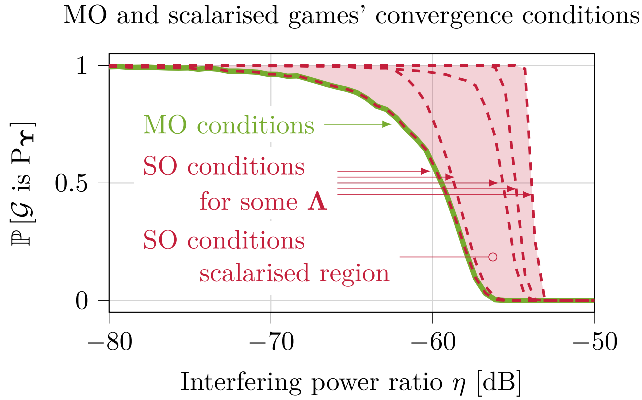

Fig. 3.5 Probability for the sufficient MO convergence conditions to be satisfied. The green solid curve depicts the probability all underlying games belong to that class, the dashed red ones are the probability a specific scalarised game belongs to it and the red area is the region obtained when sweeping through all scalarised games.

To circumvent this problem, the objective functions are regularised with strongly convex terms, hence reading as

$$\mathbf{u}_q^{\dagger}(\mathbf{x}) = \mathbf{u}_q(\mathbf{x}) + \eta_q \frac{\|\mathbf{x}_q\|_2^2}{2} \mathbf{1}_2, \tag{3.18}$$

with the regularisation parameter $\eta_q > 0$. This parameter governs the trade-off between the approximation quality and the strong convexity parameter of the objective function, since $\forall \mathbf{x} \in \mathcal{X}$,

$$\left\|\mathbf{u}_q(\mathbf{x}) - \mathbf{u}_q^{\dagger}(\mathbf{x})\right\|_2 \leq \frac{\eta_q}{\sqrt{2}} \tag{3.19}$$

$$\lambda_{\min}\left(\boldsymbol{\nabla}^2_{\mathbf{x}_q\mathbf{x}_q} u^{\dagger}_{q,1}(\mathbf{x})\right) = \lambda_{\min}\left(\boldsymbol{\nabla}^2_{\mathbf{x}_q\mathbf{x}_q} u^{\dagger}_{q,2}(\mathbf{x})\right) = \eta_q. \tag{3.20}$$

Thus, the regularised game $\mathcal{G}^{(\mathrm{MO}),\dagger} = \left\langle \Omega, \{\mathcal{X}_q\}_{q\in\Omega}, \{\mathbf{u}_q^{\dagger}\}_{q\in\Omega} \right\rangle$ is studied in the following. The regularised objective functions are strongly convex, this regularised game hence satisfying Assumption 2.2. Thus, it benefits from the equilibrium point equivalence proven in Theorem 2.1.

Weighted-sum scalarised game and BR As for the JRC scenario, the preference of the qth player is characterised by the weight profile $\boldsymbol{\lambda}_q =$

$[\lambda_{q,1}, \lambda_{q,2}]^\top \in \Delta^2$, and the global weight profile is given by $\boldsymbol{\Lambda} \in \Delta^\times$ with $\Delta^\times = \bigtimes_{q=1}^{Q} \Delta^2$. The optimisation problem of the qth player reads as

$$\begin{aligned} \text{minimise}_{\mathbf{x}_q} \quad & \left(\lambda_{q,1}\mathbf{p}_q^\top - \lambda_{q,2}\theta_q\left(\mathbf{x}_{-q}\right)\mathbf{r}_q^\top\right)\mathbf{x}_q + \tfrac{\eta_q}{2}\left\|\mathbf{x}_q\right\|_2^2 \\ \text{s.t.} \quad & 1 - x_q^{\max} \leq x_{q,0}, \\ & 0 \leq x_{q,a_q}, \quad \forall a_q = 1, \ldots, A_q, \\ & \textstyle\sum_{a_q=0}^{A_q} x_{q,a_q} = 1. \end{aligned} \tag{3.21}$$

As shown in Section 3.7.5, the BR mappings have also a waterfilling-like expression. The BR of the qth player, $\mathbf{BR}_q^{\boldsymbol{\lambda}_q,\dagger}\left(\mathbf{x}_{-q}\right)$, reads indeed as

$$\left[\mathbf{BR}_q^{\boldsymbol{\lambda}_q,\dagger}\left(\mathbf{x}_{-q}\right)\right]_0 = \left[z_{q,0} - 1 + x_{q,\max} - \mu_q\right]^+ + 1 - x_{q,\max}, \tag{3.22}$$

$$\left[\mathbf{BR}_q^{\boldsymbol{\lambda}_q,\dagger}\left(\mathbf{x}_{-q}\right)\right]_{a_q} = \left[z_{q,a_q} - \mu_q\right]^+, \quad \forall a_q = 1, \ldots, A_q, \tag{3.23}$$

with $\mathbf{z}_q \triangleq \frac{-\lambda_{q,1}\mathbf{p}_q + \lambda_{q,2}\theta_q(\mathbf{x}_{-q})\mathbf{r}_q}{\eta_q}$ and the water level μ_q chosen such that $\sum_{a_q=0}^{A_q}\left[\mathbf{BR}_q^{\boldsymbol{\lambda}_q,\dagger}\left(\mathbf{x}_{-q}\right)\right]_{a_q} = 1$.

Preference-agnostic convergence conditions As for the JRC scenario, the regularised RA game satisfies Assumptions 3.1 to 3.3. Thus, Theorems 3.1 and 3.2 hold, ensuring the existence of a pure NE, and guaranteeing all scalarised games belong to a given class if and only if all underlying games belong to the same class. In an underlying game, each player is associated with an index $\pi_q \in \{1, 2\}$ denoting the selection between the power objective ($\pi_q = 1$) or the rate objective ($\pi_q = 2$).

Focusing on BRD convergence, the convergence matrix of the underlying games are studied. As shown in Section 3.7.6, if $\pi_q = 1$, i.e., when the power objective is chosen,

$$\alpha_{q,1} = \eta_q, \quad \beta_{q,r,1} = 0, \quad \forall r \neq q. \tag{3.24}$$

When $\pi_q = 2$, the rate objective is selected, and

$$\alpha_{q,2} = \eta_q, \tag{3.25}$$

$$\beta_{q,r,2} = \frac{\sqrt{\sum_{a_q=0}^{A_q} R_{q,a_q}^2}}{R_{q,A_q}} = \sqrt{1 + \sum_{a_q=1}^{A_q-1}\left(\frac{R_{q,a_q}}{R_{q,A_q}}\right)^2}, \quad \forall r \neq q. \tag{3.26}$$

From these expressions, it appears Proposition 3.6 can be applied, since for all players, the rate objective is coupled more strongly than the power objective, since $\beta_{q,r,1}/\alpha_{q,1} = 0 \leq \beta_{q,r,2}/\alpha_{q,2}$. Therefore, this implies that a single underlying game must be studied to ensure the whole scalarised game family belongs to the $\mathrm{P}_{\boldsymbol{\Upsilon}}$ class. This underlying game is the one obtained when all players maximise their rate only.

From the diagonal dominance interpretation of the P-property given by Proposition 3.5, this analysis reveals the following insights.

Insight 3.2: Number of activity levels

For the weighted-sum scalarised games, the BRD of the RA scenario is likely to converge when each player has few intermediate activity levels, beside the idle and full power levels.

Insight 3.3: Approximation quality

For the weighted-sum scalarised games, the BRD of the RA scenario is likely to converge when the regularisation parameters are large, at the price of approximating more roughly the original power and rate objectives.

3.6 Chapter summary

This chapter studies the weighted-sum scalarised games associated with a MOG. In order to truly encompass the MO character of the player interactions, the goal is to obtain results which do not depend on the player preferences among their objectives, i.e., which are agnostic about the scalarisation weights.

To that aim, the concept of underlying game is defined, which are the games corresponding to the extreme preferences of the players. Instead of analysing all games of the weighted-sum scalarised game family, this chapter shows that it is sufficient to analyse the underlying games only. In some cases, it is even possible to remove some of the underlying games from the analysis, by leveraging on the coupling strength between the players. As a final theoretical contribution, this chapter shows how to tackle the case of polyhedral preference subsets, by translating the original MOG into another

MOG without preference information.

These theoretical contributions are then applied on the two MF MP scenarios. For the JRC network, the analysis reveals that the interactions between the players converge to a stable point when the interference remains moderate. As far as the multi-level RA scheme is concerned, an approximate regularised version of the game is studied, as otherwise the framework of this chapter does not apply. This regularised game analysis reveals the trade-off between the approximation quality and the number of activity levels that the player have at their disposition.

This chapter thus provides a first way to analyse MO interactions, through the lens of the weighted-sum scalarised game family. As the scenarios have shown, the considered framework however has limitations, for instance when some of the objective functions are linear. This thus calls for the analysis of other scalarised game family, which are the subject of the following chapters.

3.7 Proofs

3.7.1 Proof of Lemma 3.1

The convex combination expression of the gradient mapping of a scalarised game is obtained by developing the gradient of the qth player weighted-sum objective as

$$\begin{aligned}
\boldsymbol{\nabla}_{\mathbf{x}_q} u_q^{\boldsymbol{\lambda}_q}(\mathbf{x}) &= \sum_{l_q=1}^{L_q} \lambda_{q,l_q} \boldsymbol{\nabla}_{\mathbf{x}_q} u_{q,l_q}(\mathbf{x}), \\
&= \left(\prod_{r\neq q}\left(\sum_{l_r=1}^{L_r} \lambda_{r,\pi_r}\right)\right) \sum_{l_q=1}^{L_q} \lambda_{q,l_q} \boldsymbol{\nabla}_{\mathbf{x}_q} u_{q,l_q}(\mathbf{x}), \\
&= \sum_{l_1=1}^{L_1} \cdots \sum_{l_Q=1}^{L_Q} \lambda_{1,\pi_1} \dots \lambda_{q,l_q} \boldsymbol{\nabla}_{\mathbf{x}_q} u_{q,l_q}(\mathbf{x}), \\
&= \sum_{\boldsymbol{\pi}\in\Pi} \gamma^{(\boldsymbol{\pi})} \boldsymbol{\nabla}_{\mathbf{x}_q} u_{q,\pi_q}(\mathbf{x}),
\end{aligned} \tag{3.27}$$

using the fact that $\sum_{l_r=1}^{L_r} \lambda_{r,\pi_r} = 1$ and the definition of $\gamma^{(\boldsymbol{\pi})} = \lambda_{1,\pi_1} \dots \lambda_{Q,\pi_Q}$. The introduction of the other players' weights enables to have the same coefficient $\gamma^{(\boldsymbol{\pi})}$ for all players and thus to express the full gradient mapping as

$$\mathbf{F}^{\boldsymbol{\Lambda}}(\mathbf{x}) = \sum_{\boldsymbol{\pi}\in\Pi} \gamma^{(\boldsymbol{\pi})} \begin{bmatrix} \boldsymbol{\nabla}_{\mathbf{x}_1} u_1^{(\pi_1)}(\mathbf{x}) \\ \vdots \\ \boldsymbol{\nabla}_{\mathbf{x}_Q} u_{Q,\pi_Q}(\mathbf{x}) \end{bmatrix} = \sum_{\boldsymbol{\pi}\in\Pi} \gamma^{(\boldsymbol{\pi})} \mathbf{F}^{(\boldsymbol{\pi})}(\mathbf{x}), \tag{3.28}$$

concluding the proof.

3.7.2 Proof of Lemma 3.2

The convex combination inequality for the convergence matrix is obtained by showing the convergence matrix lines satisfy $\boldsymbol{\upsilon}_q^{\boldsymbol{\lambda}_q} \geq \sum_{\pi_q=1}^{L_q} \lambda_{q,\pi_q} \boldsymbol{\upsilon}_{q,\pi_q}$. Then, steps similar to those of Section 3.7.1 enable to factor the weights $\gamma^{(\boldsymbol{\pi})}$, leading to the desired result. To obtain the line inequality, the diagonal matrix elements, respectively denoted for the scalarised games and underlying games as $\alpha_q^{\boldsymbol{\lambda}_q}$ and α_{q,π_q}, are bounded as

$$\begin{aligned} \alpha_q^{\boldsymbol{\lambda}_q} &= \min_{\mathbf{x}\in\mathcal{X}} \lambda_{\min}\left(\sum_{\pi_q=1}^{L_q} \lambda_{q,\pi_q} \mathbf{J}_q \mathbf{F}_{q,\pi_q}(\mathbf{x})\right), \\ &\geq \sum_{\pi_q=1}^{L_q} \lambda_{q,\pi_q} \min_{\mathbf{x}\in\mathcal{X}} \lambda_{\min}\left(\mathbf{J}_q \mathbf{F}_{q,\pi_q}(\mathbf{x})\right), \\ &= \sum_{\pi_q=1}^{L_q} \lambda_{q,\pi_q} \alpha_{q,\pi_q}, \end{aligned} \tag{3.29}$$

where [99, Fact 5.12.2] has been used to show the minimum eigenvalue of a sum of Hermitian matrices is lower-bounded by the sum of the minimum eigenvalues, the Hermitian property of the diagonal Jacobian matrices being ensured by Assumption 3.3. The property [99, Fact 5.12.2] also bounds the maximum singular value of a sum of Hermitian matrices. Letting the off-diagonal elements of the convergence matrices be denoted as $\beta_{q,r}^{\boldsymbol{\lambda}_q}$ and

β_{q,r,π_q}, this leads to

$$\begin{aligned}\beta_{q,r}^{\boldsymbol{\lambda}_q} &= \max_{\mathbf{x}\in\mathcal{X}} \sigma_{\max}\left(\sum_{\pi_q=1}^{L_q} \lambda_{q,\pi_q} \mathbf{J}_r \mathbf{F}_{q,\pi_q}(\mathbf{x})\right), \\ &\leq \sum_{\pi_q=1}^{L_q} \lambda_{q,\pi_q} \max_{\mathbf{x}\in\mathcal{X}} \sigma_{\max}\left(\mathbf{J}_r \mathbf{F}_{q,\pi_q}(\mathbf{x})\right) \\ &= \sum_{\pi_q=1}^{L_q} \lambda_{q,\pi_q} \beta_{q,r,\pi_q}. \end{aligned} \tag{3.30}$$

3.7.3 Proof of Theorem 3.2

For the six statements of Theorem 3.2, if $\mathcal{G}^{\mathbf{\Lambda}}$ belongs to a given class whatever $\mathbf{\Lambda} \in \Delta^{\times}$, all underlying games belong to that class since these latter are a subset of the scalarised ones. It remains thus to show that if all underlying games belong to a class, all scalarised games are also part of that class.

Strict monotonicity See strong monotonicity.

P-property See uniform P-property.

Strong monotonicity If each underlying game is strongly monotone, there exists $c > 0$ such that $\forall \mathbf{x}, \mathbf{y} \in \mathcal{X}$,

$$\begin{aligned}&(\mathbf{x}-\mathbf{y})^\top \left(\mathbf{F}^{\mathbf{\Lambda}}(\mathbf{x}) - \mathbf{F}^{\mathbf{\Lambda}}(\mathbf{y})\right) \\ &\quad= \sum_{\boldsymbol{\pi}\in\Pi} \gamma^{(\boldsymbol{\pi})} (\mathbf{x}-\mathbf{y})^\top \left(\mathbf{F}^{(\boldsymbol{\pi})}(\mathbf{x}) - \mathbf{F}^{(\boldsymbol{\pi})}(\mathbf{y})\right), \\ &\quad\geq \sum_{\boldsymbol{\pi}\in\Pi} \gamma^{(\boldsymbol{\pi})} c \left\|\mathbf{x}-\mathbf{y}\right\|_2^2 = c \left\|\mathbf{x}-\mathbf{y}\right\|_2^2, \end{aligned} \tag{3.31}$$

where the gradient mapping has been developed using Lemma 3.1. This shows $\mathbf{F}^{\mathbf{\Lambda}}$ is c-strongly monotone $\forall \mathbf{\Lambda} \in \Delta^{\times}$.

Uniform P-property By contradiction, let us assume every underlying game is uniformly P with constant d but that the scalarised game is not:

$\exists \mathbf{x}, \mathbf{y} \in \mathcal{X}$ such that $\forall q \in \Omega$,

$$(\mathbf{x}_q - \mathbf{y}_q)^\top \left(\mathbf{F}_q^{\boldsymbol{\lambda}_q}(\mathbf{x}) - \mathbf{F}_q^{\boldsymbol{\lambda}_q}(\mathbf{y})\right) < d \|\mathbf{x} - \mathbf{y}\|_2^2 . \tag{3.32}$$

From Lemma 3.1, this translates in

$$\sum_{\pi_q=1}^{L_q} \lambda_{q,\pi_q} (\mathbf{x}_q - \mathbf{y}_q)^\top \left(\mathbf{F}_{q,\pi_q}(\mathbf{x}) - \mathbf{F}_{q,\pi_q}(\mathbf{y})\right) < d \|\mathbf{x} - \mathbf{y}\|_2^2 ,$$

implying that for all $q \in \Omega$, $\exists \pi_q \in \mathcal{L}_q$ such that

$$(\mathbf{x}_q - \mathbf{y}_q)^\top \left(\mathbf{F}_{q,\pi_q}(\mathbf{x}) - \mathbf{F}_{q,\pi_q}(\mathbf{y})\right) < d \|\mathbf{x} - \mathbf{y}\|_2^2 . \tag{3.33}$$

Grouping the indices for which the strict lower inequality holds into $\boldsymbol{\pi} = [\pi_1, \ldots, \pi_Q]$, the above implies that the corresponding underlying game $\mathcal{G}^{(\boldsymbol{\pi})}$ is not uniformly P with constant d, contradicting the original assumption.

$\succ^s_{\boldsymbol{\Upsilon}}$-property As $\boldsymbol{\Upsilon}^{\boldsymbol{\Lambda}} \geq \sum_{\boldsymbol{\pi} \in \Pi} \gamma^{(\boldsymbol{\pi})} \boldsymbol{\Upsilon}^{(\boldsymbol{\pi})}$ from Lemma 3.2, their symmetric part also satisfies such an equality as well as their minimum eigenvalue [99, Fact 5.12.2]. If all underlying games are such that $\left(\boldsymbol{\Upsilon}^{(\boldsymbol{\pi})}\right)^s \succ \mathbf{0}$ whatever $\boldsymbol{\pi} \in \Pi$, this thus implies $\left(\boldsymbol{\Upsilon}^{\boldsymbol{\Lambda}}\right)^s \succ \mathbf{0}$, proving the claim.

$\mathrm{P}_{\boldsymbol{\Upsilon}}$-property The first part of the proof amounts at showing the matrix $\sum_{\boldsymbol{\pi} \in \Pi} \gamma^{(\boldsymbol{\pi})} \boldsymbol{\Upsilon}^{(\boldsymbol{\pi})}$ is a P-matrix. Since off-diagonal elements are non-positive, the characterisation provided in [100] is considered: $\boldsymbol{\Upsilon}$ is a P-matrix if it does not reverse the sign of non-zero vectors:

$$\forall \mathbf{e} \in \mathbb{R}^Q, \mathbf{e} \neq \mathbf{0}, \quad \exists q \in \Omega \quad \text{s.t.} \quad e_q \left[\boldsymbol{\Upsilon} \mathbf{e}\right]_q > 0. \tag{3.34}$$

Following the same steps as for the uniform P-property proof, the P-property of the matrix is obtained. As Lemma 3.2 shows that $\boldsymbol{\Upsilon}^{\boldsymbol{\Lambda}} \geq \sum_{\boldsymbol{\pi} \in \Pi} \gamma^{(\boldsymbol{\pi})} \boldsymbol{\Upsilon}^{(\boldsymbol{\pi})}$, this implies $\boldsymbol{\Upsilon}^{\boldsymbol{\Lambda}}$ is also a P-matrix [99, Fact 4.11.8], concluding the proof.

3.7.4 JRC game analysis

The goal of this appendix is to obtain conditions on $\hat{a}_{q,k}$, $\hat{b}_{q,o,k}$ and P_q ensuring the underlying game $\mathcal{G}^{(\boldsymbol{\pi})}$ belongs to the $\mathrm{P}_{\boldsymbol{\Upsilon}}$-class. Starting from the underlying game definition (3.14), the qth player gradient mapping $\mathbf{F}_{q,\pi_q}$

is obtained as

$$\mathbf{F}_{q,\pi_q}(\mathbf{p}) = \left[\frac{-1}{\hat{a}_{q,k} + \sum_{o\neq q}\hat{b}_{q,o,k}p_{o,k} + p_{q,k}}\right]_{k=1}^{K}, \tag{3.35}$$

and the Jacobian matrices are computed as

$$\mathbf{J}_q\mathbf{F}_{q,\pi_q}(\mathbf{p}) = \mathrm{Diag}\left(\left[\frac{1}{\left(\hat{a}_{q,k}+\sum_{o\neq q}\hat{b}_{q,o,k}p_{o,k}+p_{q,k}\right)^2}\right]_{k=1}^{K}\right),$$
$$\mathbf{J}_r\mathbf{F}_{q,\pi_q}(\mathbf{p}) = \mathrm{Diag}\left(\left[\frac{\hat{b}_{q,r,k}}{\left(\hat{a}_{q,k}+\sum_{o\neq q}\hat{b}_{q,o,k}p_{o,k}+p_{q,k}\right)^2}\right]_{k=1}^{K}\right).$$

This leads to

$$\begin{aligned}\alpha_{q,\pi_q} &= \min_{\mathbf{p}\in\mathcal{X}}\min_{k=1,\dots,K}\left\{\frac{1}{\left(\hat{a}_{q,k} + \sum_{o\neq q}\hat{b}_{q,o,k}p_{o,k} + p_{q,k}\right)^2}\right\},\\ &\geq \min_{k=1,\dots,K}\left\{\frac{1}{\left(\hat{a}_{q,k} + \sum_{o\neq q}\hat{b}_{q,o,k}P_o + P_q\right)^2}\right\},\end{aligned} \tag{3.36}$$

and

$$\begin{aligned}\beta_{q,r,\pi_q} &= \max_{\mathbf{p}\in\mathcal{X}}\max_{k=1,\dots,K}\left\{\frac{\hat{b}_{q,r,k}}{\left(\hat{a}_{q,k} + \sum_{o\neq q}\hat{b}_{q,o,k}p_{o,k} + p_{q,k}\right)^2}\right\},\\ &\leq \max_{k=1,\dots,K}\left\{\frac{\hat{b}_{q,r,k}}{\hat{a}_{q,k}^2}\right\},\end{aligned} \tag{3.37}$$

providing the desired result.

3.7.5 Multi-level RA BR computation

In order to compute the BR expression, the qth player regularised scalarised objective function can be rewritten as

$$u_q^{\boldsymbol{\lambda}_q,\dagger}(\mathbf{x}) = C_1 \left\| \mathbf{x}_q - \frac{-\lambda_{q,1}\mathbf{p}_q + \lambda_{q,2}\theta_q(\mathbf{x}_{-q})\mathbf{r}_q}{\eta_q} \right\|_2^2 + C_2, \tag{3.38}$$

with C_1 and C_2 constants independent of $\mathbf{x}_q$. From the above, it can be observed that the BR of the qth player is the projection of $\mathbf{z}_q = \frac{-\lambda_{q,1}\mathbf{p}_q+\lambda_{q,2}\theta_q(\mathbf{x}_{-q})\mathbf{r}_q}{\eta_q}$ on the strategy set $\mathcal{X}_q$. As described in Remark 2.11, defining $\mathbf{v}_q \in \mathbb{R}^{A_q+1}$ as $\mathbf{x}_q \triangleq x_{q,\max}\mathbf{v}_q + \left[1 - x_{q,\max}, 0, \ldots, 0\right]^\top$, the following is obtained:

$$\Pi_{\mathcal{X}_q}(\mathbf{z}_q) = x_{q,\max}\Pi_{\Delta^{A_q+1}}\left(\frac{\mathbf{z}_q}{x_{q,\max}} - \frac{1}{x_{q,\max}}\begin{bmatrix} 1 - x_{q,\max} \\ 0 \\ \vdots \\ 0 \end{bmatrix}\right) + \begin{bmatrix} 1 - x_{q,\max} \\ 0 \\ \vdots \\ 0 \end{bmatrix},$$

with the projection operator $\Pi_{\mathcal{S}}(\mathbf{z})$ being defined as $\Pi_{\mathcal{S}}(\mathbf{z}) \triangleq \arg\min_{\mathbf{x}\in\mathcal{S}} \|\mathbf{x}-\mathbf{z}\|_2$. The projection of $\mathbf{w} \in \mathbb{R}^N$ on the simplex is computed as [103]

$$\left[\Pi_{\Delta^{A_q+1}}(\mathbf{w})\right]_i = \left[w_i - \mu\right]^+, \quad \forall i = 1, \ldots, N, \text{ with } \mu \,\text{s.t.} \sum_{i=1}^{N}\left[w_i - \mu\right]^+ = 1.$$

Plugging this expression into $\Pi_{\mathcal{X}_q}(\mathbf{z}_q)$, the BR expression is obtained.

3.7.6 Multi-level RA game analysis

When the power regularised objective is selected, the gradient mapping reads as

$$\mathbf{F}_{q,1}(\mathbf{x}) = \mathbf{p}_q + \eta_q\mathbf{x}_q,$$

leading to

$$\mathbf{J}_q\mathbf{F}_{q,1}(\mathbf{x}) = \eta_q\mathbf{I}_{A_q+1}, \quad \mathbf{J}_r\mathbf{F}_{q,1}(\mathbf{x}) = \mathbf{0}_{(A_q+1)\times(A_q+1)},$$

providing the desired result. When the rate objective is selected, the gradient mapping is given by

$$\mathbf{F}_{q,2}\left(\mathbf{x}\right) = -\theta_q\left(\mathbf{x}_{-q}\right)\mathbf{r}_q + \eta_q \mathbf{x}_q,$$

and thus to

$$\begin{aligned}
\mathbf{J}_q\mathbf{F}_{q,2}\left(\mathbf{x}\right) &= \eta_q \mathbf{I}_{A_q+1}, \\
\mathbf{J}_r\mathbf{F}_{q,2}\left(\mathbf{x}\right) &= -\mathbf{r}_q\left(\boldsymbol{\nabla}_{\mathbf{x}_r}\theta_q\left(\mathbf{x}_{-q}\right)\right)^\top, \\
&= -\mathbf{r}_q\begin{bmatrix}\prod_{o\neq q,r} x_{o,0} & 0 & \dots & 0\end{bmatrix}.
\end{aligned}$$

Therefore,

$$\begin{aligned}
&\sigma_{\max}\left(\mathbf{J}_r\mathbf{F}_{q,2}\left(\mathbf{x}\right)\right) = \left\|\mathbf{r}_q\right\|_2 \prod_{o\neq q,r} x_{o,0}, \\
\iff &\max_{\mathbf{x}\in\mathcal{X}} \sigma_{\max}\left(\mathbf{J}_r\mathbf{F}_{q,2}\left(\mathbf{x}\right)\right) = \left\|\mathbf{r}_q\right\|_2,
\end{aligned}$$

concluding the RA game analysis.

4

Preference-aware ϵ-constraint game

In this chapter, the MO interactions between the players are tackled through the lens of the ϵ-constraint scalarised games. These games are instances of GNEPs, and they unfortunately benefit from sparser results from the literature that the NEPs, especially regarding the BRD convergence. Therefore, this chapter first tackles the case of fixed constraint thresholds, as if one was aware of the preferences of the players between their objective functions. This thus explains the words *preference-aware* of the title of this chapter. For such fixed thresholds, this chapter provides the following contributions.

- A class of GNEPs, named the GNEPs with polyhedral strategy sets and variable Right-Hand Sides (RHSs) is delimited. Additionally to the constraint set structure, this class is delimited by standard convexity, continuity, and constraint qualification assumptions. Moreover, a novel assumption is introduced, named the *set insensitivity to perturbations*. This assumption ensures that the sets of constraints which can be active at the same time are not modified by infinitesimally small perturbations.
- For this class, sufficient convergence conditions are provided for the totally asynchronous BRD. These conditions depend on the objective

functions and strategy set expressions. They hence can be extracted in a systematic way from the optimisation problem structures, following a step-by-step procedure. To the author knowledge, these conditions are the first result providing convergence guarantees for the BRD of GNEPs which are neither NEPs, nor generalised potential games.

- The MF MP scenarios introduced in Section 2.4 are analysed with the above framework. It is shown that unfortunately, the sum-rate objectives of the JRC network do not lead to a GNEP with polyhedral strategy sets with variable RHSs. The multi-level RA problem however can be analysed with the developed framework. When the rate metric is set as constraint, the analysis reveals that the BRD of this problem is likely to converge when the rate requirement is low, and when the activity levels have significantly different rates.

To achieve this, this chapter is organised as follows. First, Section 4.1 provides a state-of-the-art on the GNEPs, with a focus on the convergence of learning dynamics towards a GNE. Then, the class of GNEPs tackled in this chapter is delimited in Section 4.2, while the BRD convergence conditions are provided in Section 4.3. Finally, the developed theoretical framework is applied on the MF MP use-cases in Section 4.4.

4.1 BRD convergence for GNEPs: state-of-the-art

The study of GNEPs dates back to the works of Debreu [21, 22], in which the problem was known as an *abstract economy problem*. Since then, many properties of the equilibrium points (existence, uniqueness, stability), as well as algorithms enabling to find such equilibria, have been studied [23, 24, 104, 105]. Most of these algorithms are based on reformulations of a GNEP into an equivalent problem, which can then be solved using tailored, centralised methods [106–111]. A particular class of GNEPs, named the *jointly convex GNEPs*, benefits from stronger equivalences and simpler algorithms. This class is defined below, consisting of the GNEPs in which all players have the same constraints.

Definition 4.1: Jointly convex GNEP [24]

A GNEP $\tilde{\mathcal{G}} = \left\langle \Omega, \{\tilde{\mathcal{X}}_q\}_{q\in\Omega}, \{u_q\}_{q\in\Omega} \right\rangle$ is said to be jointly convex if there exists a non-empty, closed convex set $\mathcal{D}$ such that $\forall q \in \Omega$, $\forall \mathbf{x}_{-q} \in \overline{\mathcal{X}}_{-q}$,

$$\tilde{\mathcal{X}}_q\left(\mathbf{x}_{-q}\right) = \left\{\mathbf{x}_q \in \mathbb{R}^{n_q} | \left(\mathbf{x}_q, \mathbf{x}_{-q}\right) \in \mathcal{D}\right\}.$$

In order to grasp the particularity of this class, let us consider that given $\mathbf{x} \in \mathcal{D}$, the qth player changes its strategy from $\mathbf{x}_q$ to $\mathbf{y}_q$, making sure its own constraints are fulfilled: $\mathbf{y}_q \in \tilde{\mathcal{X}}_q\left(\mathbf{x}_{-q}\right)$. Since $\mathcal{D}$ is shared by all players, the new strategy profile $\left(\mathbf{y}_q, \mathbf{x}_{-q}\right)$ is such that $\mathbf{x}_r \in \tilde{\mathcal{X}}_r\left(\mathbf{x}_{-r}\right)$ for all the rth players. In other words, the change of strategy of one player cannot make the constraints of the others violated. The constraints appear thus as *joint* constraints across all players, justifying the name of this GNEP class.

Among the results related to the jointly convex GNEPs, the work of Rosen [23] is emphasised here as it is the first work providing uniqueness and convergence guarantees for a learning dynamics of a GNEP. This dynamics is based on the gradients of the objective and constraint functions, and one of its appealing characteristics is that the resulting computations can partly be performed individually by the nodes. Following this research direction, schemes which let each node performs its own computations have been developed, named *decomposition methods* in the GNEP literature. One of these methods consist is reaching the equilibria of a GNEP by solving a sequence of parametrised NEPs [112]. If the algorithm used to solve the NEPs can be decomposed among the players, then the GNEP algorithm is an instance of a decomposition method. More recently, in [113, 114], decomposition methods based on projection and proximal operators have been shown to converge to an equilibrium. While avoiding the sharing of players' local information, the above methods are still demanding in terms of computations and convergence speed. They involve multi-layer loops, in which the inner loop solves parametrised problems till convergence, while the outer loop updates the parameters in order to drift towards an equilibrium. Additionally, coordination is still required in order to synchronise the loops entrance and exit.

For the reasons developed in Section 2.1.3, wireless networks call instead for the study of the BRD, being the most straightforward decomposition method. Yet, there currently exists no theoretical convergence guarantees for the BRD of general GNEPs. Practice has shown it often reaches an equilibrium [24], but counterexamples have also been exhibited [115]. It is therefore considered in [24] as *at most, a good and simple heuristic*. Three exceptions must however be pointed out. First, for specific wireless scenarios, BRD convergence guarantees have been obtained using ad-hoc arguments [27, 116, 117]. However, as the developments are specific to the considered scenarios, they cannot be applied to other problems. The second particular class is the class of NEPs, for which the convergence guarantees of [55] hold. Finally, the last particular case is the class of the *generalised potential games*, for which the convergence of a regularised version of the BRD can be ensured [115, 118]. This class is characterised by the fact that even if the players are not aware of that, they jointly minimise a function $\Phi(\mathbf{x})$, named the potential, on a set $\mathcal{D}$.

Definition 4.2: Generalised potential game [115]

A GNEP $\tilde{\mathcal{G}} = \left\langle \Omega, \left\{\tilde{\mathcal{X}}_q\right\}_{q\in\Omega}, \left\{u_q\right\}_{q\in\Omega} \right\rangle$ is said to be a generalised potential game if:

- there exists a non-empty, closed set $\mathcal{D}$ such that $\forall q \in \Omega$, $\forall \mathbf{x}_{-q} \in \overline{\mathcal{X}}_{-q}$,

$$\tilde{\mathcal{X}}_q\left(\mathbf{x}_{-q}\right) = \left\{\mathbf{x}_q \in \mathbb{R}^{n_q} \middle| \left(\mathbf{x}_q, \mathbf{x}_{-q}\right) \in \mathcal{D}\right\};$$

- there exists a continuous function $\Phi(\mathbf{x}) : \mathcal{D} \to \mathbb{R}$ such that $\forall q \in \Omega$, $\forall \mathbf{x}_{-q} \in \overline{\mathcal{X}}_{-q}$, $\forall \mathbf{x}_q, \mathbf{y}_q \in \tilde{\mathcal{X}}_q\left(\mathbf{x}_{-q}\right)$,

$$u_q\left(\mathbf{x}_q, \mathbf{x}_{-q}\right) - u_q\left(\mathbf{y}_q, \mathbf{x}_{-q}\right) = \Phi\left(\mathbf{x}_q, \mathbf{x}_{-q}\right) - \Phi\left(\mathbf{y}_q, \mathbf{x}_{-q}\right).$$

With respect to the jointly convex GNEPs, the generalised potential games have the additional requirement of the potential function[1], but they do not require the set $\mathcal{D}$ to be convex. The corresponding class relationships are depicted in Figure 4.1, with the class of the *GNEPs with polyhedral strategy sets and variable RHSs* being the class studied in this thesis, being defined in the next section. It can be noted that the GNEP toy example of Example 2.1 and the MF MP scenarios defined in Section 2.4 are neither

[1] Definition 4.2 considers an exact potential function for the sake of simplicity. A more general class definition is provided in [115], still with convergence guarantees for the regularised BRD.

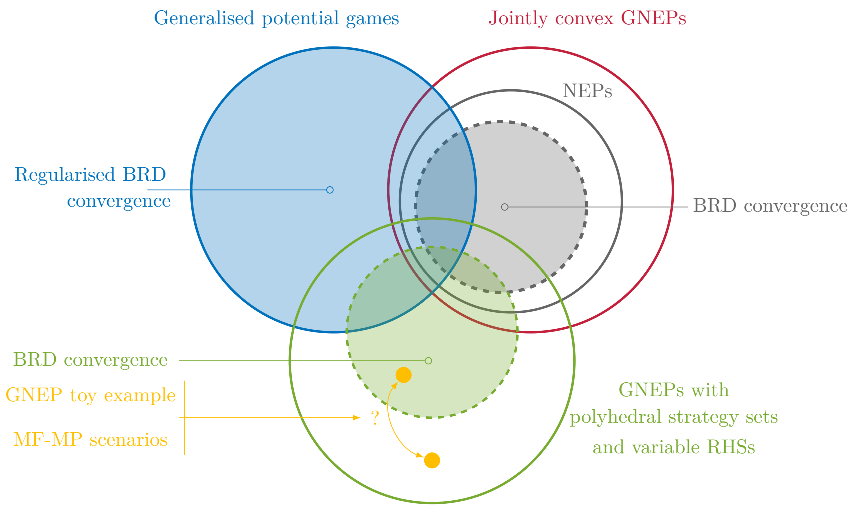

Fig. 4.1 Illustration of the relationships between the classes of GNEPs. The filled areas are the GNEPs for which the convergence of the BRD can be guaranteed. The GNEP toy example of Example 2.1, and the MF MP scenarios are represented with the amber dots.

jointly convex GNEPs, nor generalised potential games. Hence, the question which will be answered in this chapter is determining whether the BRD of these scenarios converges to an equilibrium.

4.2 Considered GNEP class

The GNEPs tackled in this work are limited to the class which we name *GNEPs with polyhedral strategy sets and variable RHSs*, as defined below.

Definition 4.3: GNEP with polyhedral strategy sets and variable RHSs

A GNEP $\tilde{\mathcal{G}} = \left\langle \Omega, \left\{\tilde{\mathcal{X}}_q\right\}_{q\in\Omega}, \left\{u_q\right\}_{q\in\Omega} \right\rangle$ is said to be a GNEP with polyhedral strategy sets and variable RHSs if $\forall q \in \Omega$, $\forall \mathbf{x}_{-q} \in \overline{\mathcal{X}}_{-q}$, the strategy set mappings can be written as

$$\tilde{\mathcal{X}}_q\left(\mathbf{x}_{-q}\right) = \left\{ \mathbf{x}_q \in \mathbb{R}^{n_q} \;\middle|\; \begin{array}{ll} \mathbf{p}_{q,i}^\top \mathbf{x}_q \leq \gamma_{q,i}\left(\mathbf{x}_{-q}\right), & \forall i \in \mathcal{I}_q \\ \tilde{\mathbf{p}}_{q,j}^\top \mathbf{x}_q = \tilde{\gamma}_{q,j}\left(\mathbf{x}_{-q}\right), & \forall j \in \mathcal{J}_q \end{array} \right\}, \tag{4.1}$$

with $\mathcal{I}_q \triangleq \{1, \ldots, I_q\}$ and $\mathcal{J}_q \triangleq \{1, \ldots, J_q\}$ the sets of inequality and equality constraints, $\mathbf{p}_{q,i}, \tilde{\mathbf{p}}_{q,i} \in \mathbb{R}^{n_q}$ the linear constraint vectors, and $\gamma_{q,i} \colon \mathcal{X}_{-q} \to \mathbb{R}$, $\tilde{\gamma}_{q,j} \colon \mathcal{X}_{-q} \to \mathbb{R}$ the possibly non-linear RHS functions which depend on the other players.

The sets $\mathcal{I}_{qr}^\circ \subseteq \mathcal{I}_q$ and $\mathcal{J}_{qr}^\circ \subseteq \mathcal{J}_q$ are furthermore introduced as the sets of constraints for which the RHS function depends on the strategy of the rth player. The GNEPs are moreover assumed to satisfy the three below assumptions, the first one being similar to those for NEPs, and the second and last preventing the strategy-sets to have pathologic structures. The two first are standard in the GNEP literature.

Assumption 4.1: NEP-like assumptions

For each qth player,

- $\mathcal{X}_q$ is non-empty, closed, convex and bounded;
- $\forall \mathbf{x}_{-q} \in \mathcal{X}_{-q}$, $\tilde{\mathcal{X}}_q\left(\mathbf{x}_{-q}\right)$ is non-empty.

Furthermore, $\forall \mathbf{x} \in \mathcal{Y}_q$,

- $u_q\left(\mathbf{x}_q, \mathbf{x}_{-q}\right)$ is strongly convex in $\mathbf{x}_q$;
- $u_q\left(\mathbf{x}_q, \mathbf{x}_{-q}\right)$ is $\mathcal{C}^1$ in $\mathbf{x}_q$;
- $\boldsymbol{\nabla}_{\mathbf{x}_q} u_q\left(\mathbf{x}_q, \mathbf{x}_{-q}\right)$ is $\mathcal{C}^1$ in $\mathbf{x}_q$ and $\mathbf{x}_{-q}$;
- $\left\{\gamma_{q,i}\left(\mathbf{x}_{-q}\right)\right\}_{i \in \mathcal{I}_q}$ and $\left\{\tilde{\gamma}_{q,j}\left(\mathbf{x}_{-q}\right)\right\}_{j \in \mathcal{J}_q}$ are $\mathcal{C}^1$ in $\mathbf{x}_{-q}$.

Assumption 4.2: Constraint qualification

For each qth player,

- $\forall \mathbf{x}_{-q} \in \mathcal{X}_{-q}$, the Slater constraint qualification holds for

$\tilde{\mathcal{X}}_q(\mathbf{x}_{-q})$, i.e., $\exists \mathbf{x}_q \in \tilde{\mathcal{X}}_q(\mathbf{x}_{-q})$ such that $\forall i \in \mathcal{I}_q$, $\mathbf{p}_{q,i}^\top \mathbf{x}_q < \gamma_{q,i}(\mathbf{x}_{-q})$.

- The family $\{\tilde{\mathbf{p}}_{q,j}\}_{j\in\mathcal{J}_q}$ is linearly independent.

To state the last assumption, given $\mathbf{x}$, the set of active inequality constraints is defined as

$$\mathcal{I}_q^{\mathbf{x}} \triangleq \left\{ i \in \mathcal{I}_q \middle| \mathbf{p}_{q,i}^\top \mathbf{x}_q = \gamma_{q,i}(\mathbf{x}_{-q}) \right\}. \tag{4.2}$$

Then, the ensemble of all sets of linearly independent constraints which can be active at the same time, with at least one depending on the rth player is introduced as

$$\mathfrak{I}_{qr}^\dagger \triangleq \left\{ \mathcal{I} \subseteq \mathcal{I}_q \middle| \begin{array}{l} \exists \mathbf{x} \in \mathcal{Y}_q \text{ s.t. } \mathcal{I} = \mathcal{I}_q^{\mathbf{x}} \\ \left\{ \{\mathbf{p}_i\}_{i\in\mathcal{I}}, \{\tilde{\mathbf{p}}_j\}_{j\in\mathcal{J}} \right\} \text{ is linearly independent} \\ \mathcal{I} \cap \mathcal{I}_{qr}^\circ \neq \emptyset \text{ or } \mathcal{J} \cap \mathcal{J}_{qr}^\circ \neq \emptyset \end{array} \right\}. \tag{4.3}$$

The problem is also looked at when the inequality constraints are perturbed by $\mathbf{v}_q \in \mathbb{R}^{I_q}$, and the following sets are defined similarly to the above:

$$\mathcal{K}_q^{\mathbf{x},\mathbf{v}_q} \triangleq \left\{ i \in \mathcal{I}_q \middle| \mathbf{p}_{q,i}^\top \mathbf{x}_q = \gamma_{q,i}(\mathbf{x}_{-q}) + v_{q,i} \right\}, \tag{4.4}$$

$$\mathfrak{K}_{qr}^\dagger \triangleq \left\{ \mathcal{I} \subseteq \mathcal{I}_q \middle| \begin{array}{l} \forall \epsilon > 0, \exists \mathbf{x} \in \mathcal{Y}_q, \mathbf{v}_q \in \mathbb{R}^{I_q} \\ \qquad\qquad \text{with } \|\mathbf{v}_q\|_2 \leq \epsilon \text{ s.t. } \mathcal{I} = \mathcal{K}_q^{\mathbf{x},\mathbf{v}_q} \\ \left\{ \{\mathbf{p}_i\}_{i\in\mathcal{I}}, \{\tilde{\mathbf{p}}_j\}_{j\in\mathcal{J}} \right\} \text{ is linearly independent} \\ \mathcal{I} \cap \mathcal{I}_{qr}^\circ \neq \emptyset \text{ or } \mathcal{J} \cap \mathcal{J}_{qr}^\circ \neq \emptyset \end{array} \right\}. \tag{4.5}$$

Assumption 4.3: Set insensitivity to perturbations

For each pair (q, r) of players with $q \neq r$, $\mathfrak{K}_{qr}^\dagger = \mathfrak{I}_{qr}^\dagger$.

The above assumption means that when considering infinitesimally small perturbations, the sets of possibly active constraints are not modified. To better grasp this last assumption, the below example illustrates its impact.

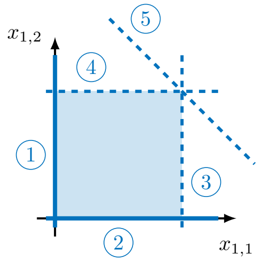

Fig. 4.2 Strategy set of Example 4.1, the constraint index being denoted by circled numbers. The moving constraints are depicted with dashed lines.

Example 4.1

Let us consider a two-player GNEP, in which the first player controls a size-2 vector $\mathbf{x}_1 \triangleq [x_{1,1}, x_{1,2}]^\top$ and the second a scalar strategy $x_2 \in \mathcal{X}_2 = [0\,;\,1]$. The strategy set of the first reads as

$$\mathcal{X}_1(x_2) \triangleq \left\{ \mathbf{x}_1 \in \mathbb{R}^2 \left| \begin{array}{l} [-1 \quad 0]\,\mathbf{x}_1 \le 0 \\ [0 \quad -1]\,\mathbf{x}_1 \le 0 \\ [1 \quad 0]\,\mathbf{x}_1 \le x_2 \\ [0 \quad 1]\,\mathbf{x}_1 \le x_2 \\ [1 \quad 1]\,\mathbf{x}_1 \le 2x_2 \end{array} \right. \right\},$$

being represented in Figure 4.2. Constraint 5 can be seen to be redundant with the others. As constraints 3, 4 and 5 depends on the second player, this gives $\mathcal{I}^\circ_{12} = \{3, 4, 5\}$. Depending on $\mathbf{x}$, the set $\mathcal{I}^{\mathbf{x}}_q \in \{\emptyset, \{1\}, \{1,2\}, \{2\}, \{2,3\}, \{3\}, \{3,4,5\}, \{4\}, \{4,1\}\}$. Removing the linearly dependent constraints, and the sets which do not depend on the second player, $\mathfrak{I}^\dagger_{12} = \{\{2,3\}, \{3\}, \{4\}, \{4,1\}\}$. Yet, considering infinitesimal perturbations of constraints 3, 4 and 5, $\mathcal{K}^{\mathbf{x},\mathbf{v}}_q \in \{\emptyset, \{1\}, \{1,2\}, \{2\}, \{2,3\}, \{3\}, \{3,4,5\}, \{4\}, \{4,1\}\} \cup \{\{3,4\}, \{4,5\}, \{3,5\}\}$. This gives $\mathfrak{K}^\dagger_{12} = \{\{2,3\}, \{3\}, \{4\}, \{4,1\}\} \cup \{\{3,4\}, \{4,5\}, \{3,5\}\}$, which is different from $\mathfrak{I}^\dagger_{12}$. This is an example of a pathological case in which the constraint sets are sensitive to infinitesimally small perturbations, and which are thus not covered by this thesis. As it can be noticed, this happens because the fifth constraint follows the third and fourth one whatever x_2, and therefore is redundant. If one considers the same problem but with the fifth constraint removed, then this equivalent formulation becomes insensitive to perturbations.

4.3 BRD convergence conditions

In the above section, the class of GNEPs which are considered in this thesis is delimited. Yet, as represented in Figure 4.1, not all GNEPs belonging to that class benefit from BRD convergence. Therefore, this section provides sufficient conditions which ensure that the totally asynchronous BRD converges towards an equilibrium. As for the NEPs, these conditions depend on a convergence matrix $\boldsymbol{\Gamma} \in \mathbb{R}^{Q\times Q}$, which translates both the objective functions' interaction and the strategy sets' interaction. The elements of this matrix are obtained as

$$[\boldsymbol{\Gamma}]_{qr} \triangleq \sqrt{\left(\left[\boldsymbol{\Gamma}^{\mathrm{obj}}\right]_{qr}\right)^2 + \left(\left[\boldsymbol{\Gamma}^{\mathrm{cons}}\right]_{qr}\right)^2}, \tag{4.6}$$

with $\boldsymbol{\Gamma}^{\mathrm{obj}}, \boldsymbol{\Gamma}^{\mathrm{cons}} \in \mathbb{R}^{Q\times Q}$. The objective part is computed as

$$\left[\boldsymbol{\Gamma}^{\mathrm{obj}}\right]_{qr} \triangleq \begin{cases} \max_{\mathbf{x}\in\mathcal{Y}_q} \dfrac{\sigma_{\max}\left(\boldsymbol{\nabla}^2_{\mathbf{x}_q\mathbf{x}_r} u_q(\mathbf{x})\right)}{\lambda_{\min}\left(\boldsymbol{\nabla}^2_{\mathbf{x}_q\mathbf{x}_q} u_q(\mathbf{x})\right)} & \text{if } q \neq r, \\ 0 & \text{otherwise.} \end{cases} \tag{4.7}$$

The constraint part is build as

$$\left[\boldsymbol{\Gamma}^{\mathrm{cons}}\right]_{qr} \triangleq \begin{cases} C_{qr} & \text{if } q \neq r, \\ 0 & \text{otherwise,} \end{cases} \tag{4.8}$$

with, when $q \neq r$,

$$C_{qr} \triangleq \max_{\substack{\mathbf{x}\in\mathcal{Y}_q \\ \mathcal{I}\in\mathfrak{I}^{\dagger}_{qr}}} \left\{\kappa\left(\boldsymbol{\nabla}^2_{\mathbf{x}_q\mathbf{x}_q} u_q\left(\mathbf{x}\right)\right) \sigma_{\max}\left(\left(\mathbf{E}_{qr,\mathcal{I}}\boldsymbol{\Pi}_{qr,\mathcal{I}}\right)^{+} \mathbf{G}_{qr,\mathcal{I}}\left(\mathbf{x}_{-q}\right)\right)\right\}, \tag{4.9}$$

where $\kappa(\cdot) \triangleq \frac{\lambda_{\max}(\cdot)}{\lambda_{\min}(\cdot)}$ is the condition number of a symmetric matrix and $(\cdot)^+$ the Moore-Penrose inverse operator. For each $\mathcal{I} \in \mathfrak{I}_{qr}^{\dagger}$, the above matrices are defined as

$$\mathbf{E}_{qr,\mathcal{I}} \triangleq \begin{bmatrix} \left\{\mathbf{p}_{q,i}^{\top}\right\}_{i\in\mathcal{I}_{qr}^{(e)}} \\ \left\{\tilde{\mathbf{p}}_{q,j}^{\top}\right\}_{j\in\mathcal{J}_{qr}^{\circ}} \end{bmatrix}, \qquad \mathbf{F}_{qr,\mathcal{I}} \triangleq \begin{bmatrix} \left\{\mathbf{p}_{q,i}^{\top}\right\}_{i\in\mathcal{I}_{qr}^{(f)}} \\ \left\{\tilde{\mathbf{p}}_{q,j}^{\top}\right\}_{j\in\mathcal{J}_q\setminus\mathcal{J}_{qr}^{\circ}} \end{bmatrix},$$

$$\mathbf{\Pi}_{qr,\mathcal{I}} \triangleq \mathbf{I} - \mathbf{F}_{qr,\mathcal{I}}^{\top}\left(\mathbf{F}_{qr,\mathcal{I}}\mathbf{F}_{qr,\mathcal{I}}^{\top}\right)^{-1}\mathbf{F}_{qr,\mathcal{I}},$$

$$\mathbf{G}_{qr,\mathcal{I}}\left(\mathbf{x}_{-q}\right) \triangleq \begin{bmatrix} \left\{\mathbf{\nabla}_{\mathbf{x}_r}^{\top}\gamma_{q,i}\left(\mathbf{x}_{-q}\right)\right\}_{i\in\mathcal{I}_{qr}^{(e)}} \\ \left\{\mathbf{\nabla}_{\mathbf{x}_r}^{\top}\tilde{\gamma}_{q,j}\left(\mathbf{x}_{-q}\right)\right\}_{j\in\mathcal{J}_{qr}^{\circ}} \end{bmatrix},$$

with the inequality constraint indices partitioned between $\mathcal{I}_{qr}^{(e)} \triangleq \mathcal{I} \cap \mathcal{I}_{qr}^{\circ}$, and $\mathcal{I}_{qr}^{(f)} \triangleq \mathcal{I} \setminus \mathcal{I}_{qr}^{(e)}$. The matrix $\mathbf{\Pi}_{qr,\mathcal{I}}$ is the projector onto the null space of $\mathbf{F}_{qr,\mathcal{I}}$, being well-defined since the constraint sets of $\mathfrak{I}_{qr}^{\dagger}$ are linearly independent, ensuring $\mathbf{F}_{qr,\mathcal{I}}$ is full row rank. If $\mathbf{F}_{qr,\mathcal{I}}$ is empty, the above must be understood as $\mathbf{\Pi}_{qr,\mathcal{I}} = \mathbf{I}$. The definition of the convergence matrix $\mathbf{\Gamma}$ enables to state the main theorem of this chapter, guaranteeing convergence of the totally asynchronous BRD associated with a GNEP.

Theorem 4.1: Convergence of the BRD of GNEPs

If a GNEP with polyhedral strategy sets and variable RHSs fulfils Assumptions 4.1 to 4.3 , and if it satisfies $\rho(\mathbf{\Gamma}) < 1$, then

- it admits a unique equilibrium $\mathbf{x}(\mathrm{E})$;
- the totally asynchronous BRD, converges to the equilibrium $\mathbf{x}(\mathrm{E})$ in the sense of Definition 2.6;
- the iterates $\mathbf{x}^{(n)}$ of the synchronous BRD converges linearly to $\mathbf{x}(\mathrm{E})$ with a rate $\rho(\mathbf{\Gamma})$:

$$\left\|\mathbf{x}^{(n)} - \mathbf{x}(\mathrm{E})\right\| \leq C\left(\rho(\mathbf{\Gamma})\right)^n \left\|\mathbf{x}^{(0)} - \mathbf{x}(\mathrm{E})\right\|,$$

C being a constant depending on the choice of norm.

Proof. The proof amounts at showing that the GNEP BR mapping $\mathbf{BR}(\mathbf{x}) : \mathcal{X} \to \mathcal{X}$ is a contraction under some well-chosen block-maximum norm, $\mathcal{X}$ being a compact set. Then, from [33, Chapter 3 and 6], the above theorem is obtained. The challenge lies in proving that $\rho(\boldsymbol{\Gamma}) < 1$ provides a sufficient condition for the contraction property of the BR mapping, as detailed in Section 4.6.1. □

The above theorem provides a sufficient condition for the convergence of the totally asynchronous BRD. To the author's knowledge, it is the first result providing a framework able to study the convergence of the totally asynchronous BRD of a GNEP which is not a NEP. The following comments can be made on the obtained convergence conditions.

- As far as the existence is concerned, it holds under Assumptions 4.1 and 4.2 only, whatever the spectral radius value [24, Theorem 6]. A GNEP for which existence holds but not convergence is of little interest in an autonomous wireless scenario. This is why the existence result is provided together with the convergence conditions in Theorem 4.1.

- When building the convergence matrix, it must be kept in mind that any upper-bound for the off-diagonal elements can also be considered. This will lead to a convergence matrix $\tilde{\boldsymbol{\Gamma}}$ with a greater spectral radius [99, Fact 4.11.18], and thus $\rho\left(\tilde{\boldsymbol{\Gamma}}\right) < 1$ also provides existence and convergence guarantees. This might be useful as identifying the maximum over $\mathcal{Y}_q$ and $\mathfrak{I}^{\dagger}_{qr}$ might be challenging. However, the looser the upper-bounds are, the narrower the convergence guarantees will be.

- Theorem 4.1 can be applied to a NEP fulfilling Assumption 4.1, in which case the convergence matrix boils down to $\boldsymbol{\Gamma} = \boldsymbol{\Gamma}^{\text{obj}}$. This convergence matrix can be compared to the one defined in Section 3.1 specifically for NEPs according to the results of [55], denoted here $\boldsymbol{\Gamma}^{\text{NEP}}$. The matrix elements satisfy

$$\begin{aligned}\left[\boldsymbol{\Gamma}^{\text{obj}}\right]_{qr} &= \max_{\mathbf{x}\in\mathcal{X}} \frac{\sigma_{\max}\left(\boldsymbol{\nabla}^2_{\mathbf{x}_q\mathbf{x}_r} u_q(\mathbf{x})\right)}{\lambda_{\min}\left(\boldsymbol{\nabla}^2_{\mathbf{x}_q\mathbf{x}_q} u_q(\mathbf{x})\right)} \\ &\leq \frac{\max_{\mathbf{x}\in\mathcal{X}} \sigma_{\max}\left(\boldsymbol{\nabla}^2_{\mathbf{x}_q\mathbf{x}_r} u_q(\mathbf{x})\right)}{\min_{\mathbf{x}\in\mathcal{X}} \lambda_{\min}\left(\boldsymbol{\nabla}^2_{\mathbf{x}_q\mathbf{x}_q} u_q(\mathbf{x})\right)} = \left[\boldsymbol{\Gamma}^{\text{NEP}}\right]_{qr}.\end{aligned}$$

  Therefore, the matrix $\boldsymbol{\Gamma}^{\text{obj}}$ provides broader conditions than the NEP matrix $\boldsymbol{\Gamma}^{\text{NEP}}$.

- Similarly to the NEP results of Section 3.1, Theorem 4.1 describes a systematic procedure for any GNEP with polyhedral strategy sets and variable RHSs. This procedure consists in building the convergence matrices of the objective part and constraint part, and then computing the spectral radius of $\mathbf{\Gamma}$. Hence, this step-by-step procedure is an off-the-shelf tool to analyse the convergence of the BRD of GNEPs.

The obtained convergence conditions can be understood intuitively, leveraging on the diagonal dominance interpretation provided by Proposition 3.5.

Remark 4.1

The convergence matrix $\mathbf{\Gamma}$ measures the coupling existing between the players.
Indeed, regarding the objective parts, the element $\sigma_{\max}\left(\nabla^2_{\mathbf{x}_q\mathbf{x}_r} u_q\left(\mathbf{x}\right)\right)$ is large when the objective function of the qth player is heavily impacted by the strategy of the rth one.
The same is observed for the constraint part, where this impact is measured by the derivative of the RHS functions through $\mathbf{G}_{qr,\mathcal{I}}\left(\mathbf{x}_{-q}\right)$.
The impact of the moving constraints also depends on the geometry of the qth optimisation problem, or said otherwise, it depends on whether translating a constraint heavily impacts the BR. This geometry is measured by the term $\left(\mathbf{E}_{qr,\mathcal{I}}\mathbf{\Pi}_{qr,\mathcal{I}}\right)^{+}$. The matrix $\mathbf{E}$ contains the orientation of the moving constraints, while $\mathbf{\Pi}$ is the projector onto the space orthogonal to the active fixed constraints. Thus, the matrix $\mathbf{E}_{qr,\mathcal{I}}\mathbf{\Pi}_{qr,\mathcal{I}}$ will be small when the moving constraints are almost parallel to the fixed ones. This then results in a large pseudo-inverse, and therefore a large matrix element. Finally, the term $\kappa\left(\nabla^2_{\mathbf{x}_q\mathbf{x}_q} u_q\left(\mathbf{x}\right)\right)$ measures whether the minimiser of the objective function is more sensitive to one element of $\mathbf{x}_q$ than another. In that case, a change of the strategy set has more impact in that direction, this being measured by the condition number.

In order to illustrate Theorem 4.1, it is applied to the toy example defined in Example 2.1.

Example 4.2

In the GNEP example introduced in Example 2.1 and studied in Example 2.2, the BRD has been been observed to converge when $c < 1$. This condition has been obtained by inspection in Example 2.2, and it is now compared to the obtained sufficient conditions. The GNEP has polyhedral strategy sets with variable RHSs, and it fulfils Assumptions 4.1 to 4.3. For the objective interaction part, computing the second order derivatives of the objective functions, the convergence matrix reads as

$$\boldsymbol{\Gamma}^{\text{obj}} = \begin{bmatrix} 0 & c \\ c & 0 \end{bmatrix}.$$

To analyse the constraint set interaction, the player-dependent active constraints sets are computed as $\mathfrak{I}^{\dagger}_{12} = \emptyset$, $\mathfrak{I}^{\dagger}_{21} = \{\{1\},\{2\}\}$. This gives $\mathbf{E}_{2,\{1\}} = -1$, $\mathbf{F}_{2,\{1\}} = \mathbf{0}_{0\times1}$, $\mathbf{G}_{21,\{1\}}\left(x_1\right) = c$, and $\mathbf{E}_{2,\{2\}} = 1$, $\mathbf{F}_{2,\{2\}} = \mathbf{0}_{0\times1}$, $\mathbf{G}_{21,\{2\}}\left(x_1\right) = \frac{-c}{2}$, and therefore

$$\boldsymbol{\Gamma}_{\text{cons}} = \begin{bmatrix} 0 & 0 \\ c & 0 \end{bmatrix}.$$

Finally, one can compute

$$\rho\left(\boldsymbol{\Gamma}\right) = \rho\left(\begin{bmatrix} 0 & c \\ \sqrt{2}c & 0 \end{bmatrix}\right) = \sqrt[4]{2}c,$$

from which it can be concluded the asynchronous BRD converges if $c < \frac{1}{\sqrt[4]{2}} \simeq 0.84$. Comparing this condition with the actual convergence which occurs when $c < 1$, it appears that as expected, the obtained convergence conditions are sufficient but not necessary.

4.4 Application to the multi-function multi-point use-cases

The developed framework, and especially Theorem 4.1, is applied in this section to the MF MP use-cases introduced in Section 2.4. First, the JRC scenario is considered. Unfortunately, the ϵ-constraint scalarised games related to this scenario do not belong to the class of GNEPs with polyhedral strategy set, as discussed in Section 4.4.1. Secondly, the multi-level RA scenario is analysed in Section 4.4.2. The ϵ-constraint scalarised games are first defined, then the assumptions verified, and finally the convergence matrix is build.

4.4.1 JRC scenario

ϵ-constraint game and BR In the JRC scenario, the two objective functions have the same form. Without loss of generality, the GNEP obtained by keeping the radar rate as an objective, and setting the communication one as a constraint, is considered. In that case, the optimisation problem of the qth player reads as

$$\begin{aligned} \text{minimise}_{\mathbf{p}_q} \quad & -\textstyle\sum_{k=1}^{K} \ln\left(1 + \frac{p_{q,k}}{a^{\circ}_{q,k} + \sum_{o \neq q} b^{\circ}_{q,o,k} p_{o,k}}\right) \\ \text{s.t.} \quad & p_{q,k} \geq 0 \quad \forall k = 1, \ldots, K, \\ & \textstyle\sum_{k=1}^{K} p_{q,k} = P_q, \\ & \textstyle\sum_{k=1}^{K} \ln\left(1 + \frac{p_{q,k}}{a_{q,k} + \sum_{o \neq q} b_{q,o,k} p_{o,k}}\right) \geq \epsilon_q. \end{aligned} \tag{4.10}$$

The above is a convex optimisation problem, which can be tackled with conic-programming solvers [119]. While possible, it is however pointed out that using such solvers might be computationally expensive for wireless nodes, hence making such modelling less attractive.

GNEP class A second problem with the ϵ-constraint scalarised games associated with the JRC scenario is that the resulting GNEPs do not have polyhedral strategy sets with variable RHSs, due to the rate constraint. Even by adding auxiliary varibles, it is not possible to transform the above into a form similar to (4.1) to the author knowledge. More precisely, it is not possible to obtain linear inequalities and equalities in all variables, including the auxiliary ones, while keeping the other player variables in the RHSs.

Unfortunately, the JRC example hence cannot be analysed within the developed GNEP framework. Extending the above results to sets with non-linear constraints constitutes therefore a interesting research direction.

4.4.2 Multi-level RA scenario

ϵ-constraint game and BR In the ϵ-constraint games associated with the RA MOG, the players either act according to

$$\begin{aligned} \text{minimise}_{\mathbf{x}_q} \quad & -\theta_q\left(\mathbf{x}_{-q}\right)\mathbf{r}_q^\top \mathbf{x}_q + \tfrac{\eta_q}{2}\left\|\mathbf{x}_q\right\|_2^2, \\ \text{s.t.} \quad & x_{q,0} \geq 1 - x_{q,\max}, \\ & x_{q,a_q} \geq 0, \quad \forall a_q = 1, \ldots, A_q, \\ & \mathbf{p}_q^\top \mathbf{x}_q \leq \epsilon_q, \\ & \textstyle\sum_{a_q=0}^{A_q} x_{q,a_q} = 1. \end{aligned} \tag{4.11}$$

or to

$$\begin{aligned} \text{minimise}_{\mathbf{x}_q} \quad & \mathbf{p}_q^\top \mathbf{x}_q + \tfrac{\eta_q}{2}\left\|\mathbf{x}_q\right\|_2^2, \\ \text{s.t.} \quad & x_{q,0} \geq 1 - x_{q,\max}, \\ & x_{q,a_q} \geq 0, \quad \forall a_q = 1, \ldots, A_q, \\ & \mathbf{r}_q^\top \mathbf{x}_q \geq \tfrac{\epsilon_q}{\theta_q(\mathbf{x}_{-q})}, \\ & \textstyle\sum_{a_q=0}^{A_q} x_{q,a_q} = 1. \end{aligned} \tag{4.12}$$

As it can be observed, the objective functions have been regularised in both cases with strongly convex terms to satisfy Assumption 4.1. The ϵ-constraint scalarisation game in which all players act according to (4.11) is named the *rate maximisation ϵ-constraint game*, while if they are all characterised by (4.12), it is named the *power minimisation ϵ-constraint gamee*. These two flavours are analysed below, while the case of heterogeneous players (some maximising the rate, the others minimising their power) can be analysed similarly.

In order for the players to obtain their BR, they must solve the above optimisation problems, which have a quadratic objective function and linear constraints. It can thus in both cases be efficiently solved using specialised solvers such as Mosek [119]. Also, rewritting the power objective as

$$\mathbf{p}_q^\top \mathbf{x}_q + \frac{\eta_q}{2}\left\|\mathbf{x}_q\right\|_2^2 = \frac{\eta_q}{2}\left\|\mathbf{x}_q + \frac{\mathbf{p}_q}{\eta_q}\right\|_2^2 - \frac{\left\|\mathbf{p}_q\right\|_2^2}{2\eta_q},$$

it is observed the above problem amounts to projecting $-\mathbf{p}_q/\eta_q$ on the player-dependent strategy set. Dedicated algorithms can therefore be employed, for instance the Dijkstra alternating projection method [120]. The same holds for the rate maximisation ϵ-constraint game.

Rate maximisation ϵ-constraint game First, it is considered all players select the rate as the objective function, and set the power as contraint, following the formulation (4.11). As the power objective does not depend on the other players, the rate-maximisation game is an instance of a NEP. This NEP has polyhedral strategy sets and it fulfils Assumptions 4.1 to 4.3. Building on Section 3.7.6, the associated convergence matrix is obtained as $\boldsymbol{\Gamma} = \boldsymbol{\Gamma}^{\text{obj}}$ with

$$\left[\boldsymbol{\Gamma}^{\text{obj}}\right]_{qr} \triangleq \begin{cases} \frac{\|\mathbf{r}_q\|_2}{\eta_q} = \frac{1}{\eta_q}\sqrt{1 + \sum_{a_q=1}^{A_q-1}\left(\frac{R_{q,a_q}}{R_{q,A_q}}\right)^2} & \text{if } q \neq r, \\ 0 & \text{otherwise.} \end{cases} \tag{4.13}$$

This matrix is the same as the one obtained for the weighted-sum scalarised games in Section 3.5, and thus it provides the identical insights given by Insights 3.2 and 3.3. As a reminder, those are the fact that BRD convergence is likely when the number of intermediate activity levels is small, and when the regularisation parameters are large.

Remark 4.2

If one notices that maximising $\mathbf{r}_q^\top \mathbf{x}_q$ is equivalent to maximising $\theta_q\left(\mathbf{x}_{-q}\right)\mathbf{r}_q^\top \mathbf{x}_q$, the players could be considered to instead act as

$$\begin{aligned} \text{minimise}_{\mathbf{x}_q} \quad & -\mathbf{r}_q^\top \mathbf{x}_q + \tfrac{\eta_q}{2}\left\|\mathbf{x}_q\right\|_2^2, \\ \text{s.t.} \quad & x_{q,0} \geq 1 - x_{q,\max}, \\ & x_{q,a_q} \geq 0, \quad \forall a_q = 1,\dots,A_q, \\ & \mathbf{p}_q^\top \mathbf{x}_q \leq \epsilon_q, \\ & \textstyle\sum_{a_q=0}^{A_q} x_{q,a_q} = 1. \end{aligned} \tag{4.14}$$

In that case, the players are not interacting anymore, and therefore the convergence of a learning dynamics is not anymore a concern.

Power minimisation ϵ-constraint game Contrarily to the rate maximisation game, the second flavour of the ϵ-constraint scalarised game, given by (4.12), is a true GNEP since the strategy sets are dependent on the other players. To analyse this GNEP, the notations of Section 4.2 are first identified and the required assumptions are verified. The set-valued mapping elements (4.1) are identified as $\mathcal{I}_q = \{1, \ldots, A_q + 2\}$,

$$\mathbf{p}_{q,i} = \begin{cases} -\mathbf{e}_i & \forall i = 1, \ldots, A_q + 1, \\ -\mathbf{r}_q & i = A_q + 2, \end{cases}$$

$$\gamma_{q,i}\left(\mathbf{x}_{-q}\right) = \begin{cases} x_q^{\max} - 1 & i = 1, \\ 0 & \forall i = 2, \ldots, A_q + 1, \\ -\frac{\epsilon_q}{\theta_q(\mathbf{x}_{-q})} & i = A_q + 2, \end{cases}$$

where $\mathbf{e}_i$ is the zero vector with a 1 at the ith index. The equality constraint leads to $\mathcal{J}_q = \{1\}$, $\tilde{\mathbf{p}}_{q,1} = \mathbf{1}_{A_q+1}$, and $\tilde{\gamma}_{q,1}\left(\mathbf{x}_{-q}\right) = 1$. The set of constraints depending on the other players are furthermore defined as $\mathcal{I}_{qr}^{\circ} = \{A_q + 2\}$, $\mathcal{J}_{qr}^{\circ} = \emptyset$.

Regarding the assumptions, the convexity, differentiability and linear independency parts of Assumptions 4.1 and 4.2 hold. However, to ensure the non-emptiness of $\tilde{\mathcal{X}}_q\left(\mathbf{x}_{-q}\right)$ and the Slater constraint qualification, one must show that whatever $\mathbf{x}_{-q} \in \mathcal{X}_{-q}$, there exists a strategy $\mathbf{x}_{-q}$ belonging to the strategy set, and at which no inequality constraint is active. This also enables tu ensure Assumption 4.3 is fulfilled. To that aim, it is sufficient to show that it exists $\nu > 0$ such that the strategy profile $\left[1 - x_q^{\max} + \nu, \nu, \ldots, \nu, x_q^{\max} - A_q\nu\right]$ fulfils the minimum rate constraint with a strict inequality, whatever the strategies of the other players. Considering the worst case scenario at which all other players have $x_{r,0} = 1 - x_r^{\max}$, this translates into

$$x_q^{\max} - \nu \sum_{a_q=1}^{A_q} \left(1 - \frac{R_{q,a_q}}{R_{q,A_q}}\right) > \frac{\epsilon_q}{\prod_{r \neq q}\left(1 - x_r^{\max}\right)}.$$

A positive ν satisfying the above thus exists for all players if

$$\max_{q=1,\ldots,Q} \left\{ \frac{\epsilon_q}{x_q^{\max}} \frac{1}{\prod_{r \neq q}\left(1 - x_r^{\max}\right)} \right\} < 1. \tag{4.15}$$

The Left-Hand Side (LHS) of the above, denoted ρ_{exist}, is named the existence number since as noted above, Assumptions 4.1 and 4.2 ensure an equilibrium exists. To gain insight into the above expression, the factor $\epsilon_q / x_q^{\max}$ can be rewritten as $\epsilon_q R_{q,A_q} / x_q^{\max} R_{q,A_q}$, $x_q^{\max} R_{q,A_q}$ being the maximum achievable average rate when no collision occurs. This ratio depicts thus the exigence of the FL communication demand compared to the devices' capability. The simplicity of the considered RA scheme comes with an additional $1/\prod_{r\neq q}(1-x_r^{\max})$ factor, translating the rate loss due to the collisions.

BRD convergence To ensure BRD convergence, Theorem 4.1 is applied. To that aim, the convergence matrix $\mathbf{\Gamma}$ must be build, as defined in (4.6). Then, to ensure BRD convergence, it is sufficient to have the spectral radius of this matrix smaller than 1. As shown in Section 4.6.2, the spectral radius of the convergence matrix is equal to

$$\rho\left(\mathbf{\Gamma}\right) = \frac{\sqrt{2}}{\prod_{q=1}^{Q}\left(1 - x_q^{\max}\right)} \rho\left(\tilde{\mathbf{\Gamma}}\right),$$

$$\text{with} \qquad \left[\tilde{\mathbf{\Gamma}}\right]_{qr} \triangleq \begin{cases} \frac{\epsilon_q R_{q,A_q}}{\min\limits_{a_q=0,\ldots,A_q-1} \left|R_{q,a_q} - R_{q,a_q+1}\right|} & \text{if } r \neq q, \\ 0 & \text{otherwise.} \end{cases}$$

Similarly to the existence number, the convergence number is defined as $\rho_{\text{conv}} \triangleq \rho\left(\mathbf{\Gamma}\right)$, Theorem 4.1 requiring it to be stricly smaller than 1.

Therefore, the existence and convergence numbers must be strictly smaller than 1 to ensure BRD convergence, this providing the following insights. Compared to those obtained for the weighted-sum scalarised family, the maximum active probabilities comes into play. The rate thresholds also have an impact, this showing that the analysis depends on the preference of the players. Finally, the successive activity level insight echoes Insight 3.2, with the added subtelty that more than the number of activity levels, this is their rate similarity which is important in this case.

Insight 4.1: Maximum active probability

For the power minimisation ϵ-constraint scalarised game, the BRD of the RA scenario is likely to converge when the maximum activity probabilities of the devices are low.

Insight 4.2: Rate requirement

For the power minimisation ϵ-constraint scalarised game, the BRD of the RA scenario is likely to converge when the rate requirements ϵ_q are significantly lower than the maximum active probabilities $x_q^{\max}$.

Insight 4.3: Successive activity levels

For the power minimisation ϵ-constraint scalarised game, the BRD of the RA scenario is likely to converge when the successive activity levels have significantly different rates.

4.5 Chapter summary

In this chapter, the ϵ-constraint scalarised games arising from a MOG are analysed. The carried-out analysis is said to be *preference-aware*, as the results of this chapter depend on the constraint thresholds selected by the players.

To provide such an analysis, a GNEP class has been delimited, named the GNEPs with polyhedral strategy sets and variable RHSs. For this class, sufficient convergence conditions for the totally asynchronous BRD have been derived. These conditions can be obtained following a step-by-step procedure which depends on the derivatives of the objective and strategy set functions. The developed theorem thus constitutes an off-the-shelf framework to analyse the convergence of the BRD of GNEPs.

These conditions have been applied to the MF MP scenarios of Section 2.4. Unfortunately, the JRC scenario does not fall within the considered class, and therefore the obtained results are not relevent. For the multi-level RA schemes, two ϵ-constraint games have been considered, depending on whether the players set the power or rate metric as a constraint. The insights provided by the analysis are that when the power is set as constraint, there is a trade-off between the approximation quality and the number of activity levels. In the other case, the analysis reveals that the maximum active probability, and the rate requirements of the players, should be low, while their activity levels should not have similar rates.

Both the theoretical analysis and its appplication to the MF MP use-cases have considered fixed constraint thresholds. The next chapter hence studies whether it is possible to obtain results independent of the preferences of the players. It also applies the results of Theorem 4.1 to the general hybrid scalarisation method, as well as to the constraint satisfaction games.

Regarding the possible future works, one major research direction would be to extend the above results to the case of non-linear constraints with variable RHSs. To that aim, one can notice that the linear constraints can be written as

$$\mathbf{p}_{q,i}^{\top}\mathbf{x}_q \leq \gamma_{q,i}\left(\mathbf{x}_{-q}\right) \iff -\mathbf{p}_{q,i}^{\top}\mathbf{x}_q + \gamma_{q,i}\left(\mathbf{x}_{-q}\right) \in \mathbb{R}^{+}.$$

with $\mathbb{R}^{+}$ the set of non-negative real numbers. Instead of this set, the above could be generalised to

$$-\mathbf{A}_{q,i}^{\top}\mathbf{x}_q + \boldsymbol{\gamma}_{q,i}\left(\mathbf{x}_{-q}\right) \in \mathcal{C}_{q,i},$$

with $\mathcal{C}_{q,i}$ a cone [121], and $\mathbf{A}_{q,i}$ and $\boldsymbol{\gamma}_{q,i}\left(\mathbf{x}_{-q}\right)$ of suitable dimensions. This formulation would enable to handle much more general constraints, such as quadratic ones, or sum-rate ones as in the JRC scenario. Whether or not the results of Theorem 4.1 could be generalised to this more general setting is thus a critical research question.

4.6 Proofs

4.6.1 Proof of Theorem 4.1

The proof of Theorem 4.1 consists in four steps. First, it is shown in Lemma 4.1 that the convergence can be linked to the spectral radius of a matrix whose off-diagonal elements are the Lipschitz constants of the BR mappings of the players. Then, Lemma 4.2 proves that under the considered assumptions, a finite Lipschitz constant exists for each pair of player. Next, Lemma 4.3 links the Lipschitz constant value to the norm of the gradient of the BR mapping. Finally, Lemma 4.6 provides an upper-bound on the gradient which only depends on the objective and constraint functions. Throughout the below proof, the lemmas are illustrated on Example 2.1.

Convergence matrix construction Given the BR mapping of the qth player $\mathbf{BR}_q\left(\mathbf{x}_{-q}\right)$ and considering another player r, let L_{qr} be the Lipschitz constant associated with $\mathbf{BR}_q(\mathbf{x}_{-q})$, considering it as a function of the rth player strategy only. That is, $\forall \left(\mathbf{x}_r, \mathbf{x}_{-(q,r)}\right), \left(\mathbf{y}_r, \mathbf{x}_{-(q,r)}\right) \in \mathcal{X}_{-q}$,

$$\left\|\mathbf{BR}_q\left(\mathbf{x}_r, \mathbf{x}_{-(q,r)}\right) - \mathbf{BR}_q\left(\mathbf{y}_r, \mathbf{x}_{-(q,r)}\right)\right\|_2 \leq L_{qr}\left\|\mathbf{x}_r - \mathbf{y}_r\right\|_2,$$

where $\mathbf{x}_{-(q,r)}$ denotes the vector $\mathbf{x}$ without the variables of the qth and rth player. Grouping all the constants into the matrix $\boldsymbol{\Xi} \in \mathbb{R}^{Q\times Q}$, defined as

$$[\boldsymbol{\Xi}]_{qr} \triangleq \begin{cases} L_{qr} & \text{if } r \neq q, \\ 0 & \text{otherwise,} \end{cases}$$

the following lemma gives a sufficient condition for the BR mapping to be a contraction.

Lemma 4.1

The BR mapping $\mathbf{BR}\colon \mathcal{X} \to \mathcal{X}$ satisfies

$$\left\|\mathbf{BR}(\mathbf{x}) - \mathbf{BR}(\overline{\mathbf{y}})\right\|_{\boldsymbol{\Xi}} \leq \rho(\boldsymbol{\Xi})\left\|\mathbf{x} - \overline{\mathbf{y}}\right\|_{\boldsymbol{\Xi}}, \quad \forall \mathbf{x}, \overline{\mathbf{y}} \in \mathcal{X}$$

with $\|\cdot\|_{\boldsymbol{\Xi}}$ a well-chosen block-maximum norm, whch depends on $\boldsymbol{\Xi}$. When $\rho(\boldsymbol{\Xi}) < 1$, the BR mapping is thus a contraction of modulus $\rho(\boldsymbol{\Xi})$.

Proof. Considering the BR mapping of the first player, given $\mathbf{x}_{-1}, \mathbf{y}_{-1}$, the vectors $\boldsymbol{\xi}^{(r)}$ are defined as

$$\boldsymbol{\xi}^{(r)} = \begin{cases} \mathbf{x}_{-1} & \text{if } r = 2, \\ [\mathbf{y}_2, \ldots, \mathbf{y}_{r-1}, \mathbf{x}_r, \ldots, \mathbf{x}_Q] & \text{if } 3 \leq r \leq Q, \\ \mathbf{y}_{-1} & \text{if } r = Q+1. \end{cases}$$

They enable to bound the BR difference as

$$\begin{aligned}
&\left\| \mathbf{BR}_1\left(\mathbf{x}_{-1}\right) - \mathbf{BR}_1\left(\mathbf{y}_{-1}\right)\right\|_2 \\
&\quad = \left\| \sum_{r=2}^{Q} \left(\mathbf{BR}_1\left(\xi^{(r)}\right) - \mathbf{BR}_1\left(\xi^{(r+1)}\right)\right)\right\|_2 , \\
&\quad \leq \sum_{r=2}^{Q} \left\| \mathbf{BR}_1\left(\xi^{(r)}\right) - \mathbf{BR}_1\left(\xi^{(r+1)}\right)\right\|_2 , \\
&\quad \leq \sum_{r=2}^{Q} L_{qr} \left\|\mathbf{x}_r - \mathbf{y}_r\right\|_2 ,
\end{aligned}$$

from the triangular inequality and the definition of the Lipschitz constant L_{qr}, since $\boldsymbol{\xi}^{(r+1)}$ is equal to $\boldsymbol{\xi}^{(r)}$ with $\mathbf{x}_r$ replaced by $\mathbf{y}_r$. Doing so similarly from the other players, and letting $f_q \triangleq \left\|\mathbf{BR}_q\left(\mathbf{x}_{-q}\right) - \mathbf{BR}_q\left(\mathbf{y}_{-q}\right)\right\|_2$, $e_q \triangleq \left\|\mathbf{x}_q - \mathbf{y}_q\right\|_2$, the following element-wise inequality is obtained

$$\mathbf{0} \leq \mathbf{f} \leq \boldsymbol{\Xi}\mathbf{e}, \quad \forall \mathbf{x}, \mathbf{y} \in \mathcal{X}.$$

As it can be shown by following similar steps than those of [55, Appendix C], the above implies the BR is a contraction with modulus $\rho\left(\boldsymbol{\Xi}\right)$ when such modulus is strictly smaller than 1, under a weighted block-maximum norm depending on $\boldsymbol{\Xi}$. □

The lemma enables to move the focus from the coupled interactions between the Q players together, to the interaction between each couple of players. It remains thus to i) prove the Lipschitz constants L_{qr} exist, and ii) obtain an expression for these constants. Before jumping to the next part of the proof, the lemma is applied to Example 2.1.

Example 4.3

From the expression of the BRs given in Example 2.1, the Lipschitz constants can be obtained as $L_{12} = L_{21} = c$, leading to $\rho\left(\boldsymbol{\Xi}\right) = c$. The lemma ensures thus BRD convergence when $c < 1$, being in this case both sufficient and necessary.

Lipschitz property of the best response mapping The goal of the the second part of the proof is to show that for all pairs q,r, the BR mapping of the qth player admits a finite Lipschitz constant L_{qr} w.r.t. the strategy of the rth player. To facilitate the proof notations, the optimisation problems of all pairs of players are abstracted into a generic problem $\mathcal{P}_{\mathbf{v}}(\mathbf{t})$ defined as

$$\begin{aligned} \mathbf{BR}_{\mathbf{v}}(\mathbf{t}) \triangleq \quad & \underset{\mathbf{x}}{\arg\min} && u(\mathbf{x}, \mathbf{t}) - \mathbf{x}^{\top}\mathbf{v}^{(a)} \\ & \text{s.t.} && \mathbf{x} \in \mathcal{X}_{\mathbf{v}}(\mathbf{t}), \end{aligned} \tag{4.16}$$

with

$$\mathcal{X}_{\mathbf{v}}(\mathbf{t}) \triangleq \left\{ \mathbf{x} \in \mathbb{R}^n \,\middle|\, \begin{array}{ll} \mathbf{p}_i^{\top}\mathbf{x} \leq \gamma_i(\mathbf{t}) + v_i^{(b)} & \forall i \in \mathcal{I} \\ \tilde{\mathbf{p}}_j^{\top}\mathbf{x} = \tilde{\gamma}_j(\mathbf{t}) + v_j^{(c)} & \forall j \in \mathcal{J} \end{array} \right\}.$$

with $\mathcal{I} \triangleq \{1, \ldots, I\}$ and $\mathcal{J} \triangleq \{1, \ldots, J\}$. In the above, $\mathbf{x} \in \mathcal{X} \subseteq \mathbb{R}^n$ mirrors the strategy of the qth player, $\mathbf{t} \in \mathcal{T} \subseteq \mathbb{R}^m$ the one of the rth player and $\mathbf{v}^{(a)} \in \mathbb{R}^n$, $\mathbf{v}^{(b)} \in \mathbb{R}^I$, $\mathbf{v}^{(c)} \in \mathbb{R}^J$ are additional perturbations instrumental to the next steps of the proof. The perturbation size is governed by a parameter ϵ since $\mathbf{v} = \left[\mathbf{v}^{(a)}, \mathbf{v}^{(b)}, \mathbf{v}^{(c)}\right]^{\top} \in \mathcal{V}^{\epsilon}$ with

$$\mathcal{V}^{\epsilon} = \left\{\mathbf{v} \in \mathbb{R}^{n+I+J} \middle| \|\mathbf{v}\|_2 \leq \epsilon\right\}.$$

The set $\mathcal{Z}^{\epsilon}$ is defined as $\mathcal{Z}^{\epsilon} = \{(\mathbf{x}, \mathbf{t}, \mathbf{v}) | \mathbf{x} \in \mathcal{X}_{\mathbf{v}}(\mathbf{t}), \mathbf{t} \in \mathcal{T}, \mathbf{v} \in \mathcal{V}^{\epsilon}\}$, and the sets $\mathcal{I}^{\circ} \subseteq \mathcal{I}$ and $\mathcal{J}^{\circ} \subseteq \mathcal{J}$ are moreover introduced as the constraints depending on $\mathbf{t}$, i.e. those for which the RHS function is not constant. Similarly to the game assumptions, the problem family $\mathcal{P}_{\mathbf{v}}(\mathbf{t})$ is assumed to satisfy the following.

Assumption 4.4

- The set $\mathcal{T}$ is compact, convex and non-empty;
- The unperturbed strategy set $\mathcal{X}_{\mathbf{0}}(\mathbf{t})$ is bounded, non-empty and fulfils the Slater constraint qualification, $\forall \mathbf{t} \in \mathcal{T}$;
- The family $\{\tilde{\mathbf{p}}_j\}_{j \in \mathcal{J}}$ is linearly independent;
- The RHS functions $\{\gamma_i(\mathbf{t})\}_{i \in \mathcal{I}}$ and $\{\tilde{\gamma}_j(\mathbf{t})\}_{j \in \mathcal{J}}$ are $\mathcal{C}^1$ in $\mathbf{t}$, $\forall \mathbf{t} \in \mathcal{T}$;
- Whatever $(\mathbf{x}, \mathbf{t}, \mathbf{0}) \in \mathcal{Z}^{\epsilon}$, the objective function $u(\mathbf{x}, \mathbf{t})$ is strongly convex and $\mathcal{C}^2$ in $\mathbf{x}$, and its gradient with respect to $\mathbf{x}$ is $\mathcal{C}^1$ in $\mathbf{t}$.

Comparing the above assumptions and generic optimisation problem (4.16) with Assumption 4.1, it appears the objective function of the players might not be defined, convex, or differentiable on the perturbed set. Yet, the Whitney extension theorem [122] ensures that the objective function of the qth player can be extended outside $\mathcal{X}_q$ while keeping a continuous function with continuous derivatives. Since the strong convexity property can be linked to the second derivative information, such extension is strongly convex for ϵ small enough. Hence, the generic objective function $u(\mathbf{x}, \mathbf{t})$ must be understood as the continuously differentiable extension of the player objective functions.

The below lemma then proves that under Assumption 4.4, a finite Lipschitz constant M_ϵ exists with respect to both $\mathbf{t}$ and $\mathbf{v}$. As a corollary, it proves that for $\mathbf{v} = \mathbf{0}$, a Lipschitz constant L exists with respect to $\mathbf{t}$ only, being the constant needed for the convergence matrix construction. Yet the fact that the BR mapping is Lipschitz also w.r.t $\mathbf{v}$ will be crucial for the next steps of the proof.

Lemma 4.2

If Assumption 4.4 is satisfied, the BR mapping of $\mathcal{P}_{\mathbf{v}}(\mathbf{t})$ admits $M_\epsilon < \infty$ such that $\forall \mathbf{t}, \mathbf{t}^{'} \in \mathcal{T}$, $\forall \mathbf{v}, \mathbf{v}^{'} \in \mathcal{V}^\epsilon$,

$$\left\|\mathbf{BR}_{\mathbf{v}}(\mathbf{t}) - \mathbf{BR}_{\mathbf{v}^{'}}\left(\mathbf{t}^{'}\right)\right\|_2 \leq M_\epsilon \left\| \begin{matrix} \mathbf{t} - \mathbf{t}^{'} \\ \mathbf{v} - \mathbf{v}^{'} \end{matrix} \right\|_2 .$$

This implies $\exists L < \infty$ such that $\forall \mathbf{t}, \mathbf{t}^{'} \in \mathcal{T}$,

$$\left\|\mathbf{BR}_{\mathbf{0}}(\mathbf{t}) - \mathbf{BR}_{\mathbf{0}}\left(\mathbf{t}^{'}\right)\right\|_2 \leq L \left\|\mathbf{t} - \mathbf{t}^{'}\right\|_2 .$$

Proof. The proof of Lemma 4.2 consists in two steps. First, it is shown that the boundedness, non-emptiness and constraint qualification assumption of $\mathcal{X}_0(\mathbf{t})$ can be extended to $\mathcal{X}_{\mathbf{v}}(\mathbf{t})$ for small enough perturbations, ensuring the BR mapping is well-defined. Then, the Lipschitz property of the mapping is proved.

For the first part, the boundedness property trivially holds since perturbations are themselves bounded. Then, it is noticed $\mathcal{X}_0(\mathbf{t})$ satisfies the regularity property introduced in [123]. Indeed, the Slater constraint qualification ensures there exists a point $\mathbf{x}$ such that all equality constraints are verified, and all inequality constraints are inactive. Moreover, the equality constraint family $\{\tilde{\mathbf{p}}_j\}_{j\in\mathcal{J}}$ is linearly independent. Then, using successively [123, Corollary 2, Theorem 2], the regularity of $\mathcal{X}_0(\mathbf{t})$ is obtained. From [123, Theorem 1], this implies small enough perturbations leave the system regular, implying in turn the existence of a point leaving the constraints inactive while satisfying the equality constraints. Hence, for ϵ small enough, $\mathcal{X}_{\mathbf{v}}(\mathbf{t})$ is bounded, non-empty and satisfies the Slater constraint qualification.

For the second part, since the optimisation problem $\mathcal{P}_{\mathbf{v}}(\mathbf{t})$ is strongly convex problem and satisfies the Slater constraint qualification, it admits a unique minimiser $\mathbf{BR}_{\mathbf{v}}(\mathbf{t})$ which is also the unique solution of the associated Karush-Kuhn-Tucker (KKT) conditions, for all $(\mathbf{t},\mathbf{v})\in\mathcal{T}\times\mathcal{V}^{\epsilon}$. Moreover, $\mathbf{BR}_{\mathbf{v}}(\mathbf{t})$ satisfies the Mangasarian-Fromovitz constraint qualification since this latter is implied by the Slater constraint qualification and the linear independency of the equality constraints [124, 125]. The constant rank constraint qualification furthermore holds at any point $(\mathbf{x},\mathbf{t},\mathbf{v})\in\mathcal{X}\times\mathcal{T}\times\mathcal{V}^{\epsilon}$ since linear constraints are considered [126]. Therefore, from [127, Theorem 3.6], this implies the BR mapping is Lipschitz continuous w.r.t. $(\mathbf{t},\mathbf{v})$ as the differentiability assumptions of the theorem hold. $\square$

The above lemma ensures that for each pair of player, the constant L_{qr} is finite. The next part of the proof thus focuses on computing this value. Before this, the above lemma is applied to Example 2.1.

Example 4.4

Focusing on the first player, the associated generic optimisation problem is given by

$$\begin{aligned}\mathrm{BR}_{\mathbf{v}}(t)= \quad & \arg\min_{x} && (x-ct+1)^2 - v_1 x\\ & \text{s.t.} && -2-v_2\le x\le 2+v_3,\end{aligned}$$

with $t\in\mathcal{T}=[1-2c;3+c]$. To make sure the strategy set remains non-empty, ϵ can for instance be chosen such that $\epsilon\le 0.1$. The associated BR is

$$\mathrm{BR}_{\mathbf{v}}(t)=\min\left\{\max\left\{ct-1+\frac{v_1}{2},-2-v_2\right\},2+v_3\right\}.$$

It can be checked that the above problem satisfies Assumption 4.4

and that its BR is Lipschitz w.r.t both t and $\mathbf{v}$, as predicted by the lemma.

Lipschitz constant as a function of the gradient Now that a finite Lipschitz constant has been proven to exists, this subsection shows that it can be linked to the gradient of the BR mapping. Hence, the Lipschitz constant, globally measuring how quickly a function varies, is linked to the gradient, locally measuring the rate of change of a function.

To that aim, two sets are introduced, $\operatorname{int}\mathcal{S}$ denoting the interior of the set $\mathcal{S}$. First, $\mathcal{T}_{\mathbf{0}}^{\mathrm{diff}} \triangleq \left\{\bar{\mathbf{t}} \in \operatorname{int}\mathcal{T} \middle| \boldsymbol{\nabla}_{\mathbf{t}}\mathbf{BR}_{\mathbf{0}}\left(\bar{\mathbf{t}}\right) \text{ exists}\right\}$ is defined as the differentiable points of the unperturbed BR mapping. Then, inspired from [128], the set of well-behaved points is defined as

$$\mathcal{W}^{\epsilon} \triangleq \{(\mathbf{t}, \mathbf{v}) \in \operatorname{int}\mathcal{T} \times \operatorname{int}\mathcal{V}^{\epsilon} | \\ \left.\begin{array}{l} \mathcal{P}_{\mathbf{v}}\left(\mathbf{t}\right) \text{ has lin. indep. constraints at } \mathbf{BR}_{\mathbf{v}}\left(\mathbf{t}\right) \\ \text{SCS holds for } \mathcal{P}_{\mathbf{v}}\left(\mathbf{t}\right) \text{ at } \mathbf{BR}_{\mathbf{v}}\left(\mathbf{t}\right) \end{array}\right\},$$

with *lin. indep.* abreviating *linearly independent*, and *SCS* standing for *Strict Complementary Slackness*. All well-behaved points are such that the BR mapping is differentiable [129], but the converse is not true: $(\mathbf{t}, \mathbf{0}) \in \mathcal{W}^{0} \implies \mathbf{t} \in \mathcal{T}_{\mathbf{0}}^{\mathrm{diff}}$. In the next part, an expression of the gradient will be obtained for the well-behaved point only, this explaining thus why the below lemma considers both $\mathcal{T}_{\mathbf{0}}^{\mathrm{diff}}$ and $\mathcal{W}^{\epsilon}$.

Lemma 4.3

The Lipschitz constant L of $\mathbf{BR}_{\mathbf{0}}\left(\mathbf{t}\right)$ w.r.t $\mathbf{t}$ is given by

$$\begin{aligned} L = &\sup_{\bar{\mathbf{t}} \in \mathcal{T}_{\mathbf{0}}^{\mathrm{diff}}} \sigma_{\max}\left(\boldsymbol{\nabla}_{\mathbf{t}}\mathbf{BR}_{\mathbf{0}}\left(\bar{\mathbf{t}}\right)\right) \\ &\leq \lim_{\epsilon \to 0^{+}} \sup_{\left(\bar{\mathbf{t}}, \bar{\mathbf{v}}\right) \in \mathcal{W}^{\epsilon}} \sigma_{\max}\left(\boldsymbol{\nabla}_{\mathbf{t}}\mathbf{BR}_{\bar{\mathbf{v}}}\left(\bar{\mathbf{t}}\right)\right). \end{aligned}$$

Proof. From Lemma 4.2, the unperturbed BR mapping $\mathbf{BR}_{\mathbf{0}}\left(\mathbf{t}\right)$ is Lipschitz continuous. Thus, for all $\bar{\mathbf{t}} \in \operatorname{int}\mathcal{T}$, its Clarke generalised gradient is defined as [130, 131]:

$$\overline{\boldsymbol{\nabla}}_{\mathbf{t}}\mathbf{BR}_{\mathbf{0}}\left(\bar{\mathbf{t}}\right) \triangleq \operatorname{conv}\left\{\mathbf{A} \in \mathbb{R}^{n \times m} \middle| \exists \mathbf{t}^{\rho} \to \bar{\mathbf{t}} \text{ with } \mathbf{t}^{\rho} \in \mathcal{T}_{\mathbf{0}}^{\mathrm{diff}}, \boldsymbol{\nabla}_{\mathbf{t}}\mathbf{BR}_{\mathbf{0}}\left(\mathbf{t}^{\rho}\right) \to \mathbf{A}\right\}.$$

The Lipschitz constant on $\operatorname{int}\mathcal{T}$ is then obtained as

$$L = \sup_{\bar{\mathbf{t}} \in \operatorname{int}\mathcal{T}} \max_{\mathbf{A} \in \overline{\boldsymbol{\nabla}}_{\mathbf{t}} \mathbf{BR}_{\mathbf{0}}\left(\bar{\mathbf{t}}\right)} \sigma_{\max}\left(\mathbf{A}\right),$$

from successively [132, Theorem 9.2, Proposition 9.24, Theorem 9.6.2] and the fact that the matrix norm induced by the vector euclidean norm is the maximum singular value of the matrix. Since [132, Theorem 9.58 and 2.33] shows that points in $\mathcal{T} \setminus \operatorname{int}\mathcal{T}$ do not modify the Lipshitz constant, the above is valid for $\mathcal{T}$, including its boundary. Since the generalised gradient is a limit point of a sequence of gradients at the differentiable points, the equality part of Lemma 4.3 is obtained.

Considering only well-behaved points in the above Clarke generalised gradient definition does not work. Indeed, the ill-behaved points (those which are not well-behaved) are not negligible in $\operatorname{int}\mathcal{T}$, the negligibility property being defined in [128]. Whatever $\mathbf{t} \in \operatorname{int}\mathcal{T}$, fixed, the set of ill-behaved point is however negligible in $\operatorname{int}\mathcal{V}^{\epsilon}$, since the differentiability assumptions of [128] are satisfied. This in turn implies that the set of ill-behaved points is negligible in $\operatorname{int}\mathcal{T} \times \operatorname{int}\mathcal{V}^{\epsilon}$. The projected generalised gradient of the BR mapping with respect to $\mathbf{t}$ at $\left(\bar{\mathbf{t}}, \mathbf{0}\right) \in \operatorname{int}\mathcal{T} \times \operatorname{int}\mathcal{V}^{\epsilon}$ can then be defined as

$$\begin{aligned}\boldsymbol{\pi}_{\mathbf{t}} \overline{\boldsymbol{\nabla}} \mathbf{BR}_{\mathbf{0}}\left(\bar{\mathbf{t}}\right) \triangleq \operatorname{conv}\Big\{\mathbf{A} \in \mathbb{R}^{n \times m} \Big| \, \exists \left(\mathbf{t}^{\rho}, \mathbf{v}^{\rho}\right) \to \left(\bar{\mathbf{t}}, \mathbf{0}\right) \\ \text{with } \left(\mathbf{t}^{\rho}, \mathbf{v}^{\rho}\right) \in \mathcal{W}^{\epsilon}, \boldsymbol{\nabla}_{\mathbf{t}} \mathbf{BR}_{\mathbf{v}^{\rho}}\left(\mathbf{t}^{\rho}\right) \to \mathbf{A}\Big\},\end{aligned}$$

where the sequence of converging gradient is allowed to explore the perturbations. The meaning of the $\boldsymbol{\pi}_{\mathbf{t}} \overline{\boldsymbol{\nabla}} \mathbf{BR}_{\mathbf{0}}\left(\bar{\mathbf{t}}\right)$ notation is that first the generalised gradient with respect to both $\mathbf{t}$ and $\mathbf{v}$ is computed as $\overline{\boldsymbol{\nabla}} \mathbf{BR}_{\mathbf{0}}\left(\bar{\mathbf{t}}\right)$, and then only the $\mathbf{t}$ part is kept through the $\boldsymbol{\pi}_{\mathbf{t}}$ operator. Such projected gradient satisfies [131, Proposition 2.3.16]

$$\overline{\boldsymbol{\nabla}}_{\mathbf{t}} \mathbf{BR}_{\mathbf{0}}\left(\bar{\mathbf{t}}\right) \subseteq \boldsymbol{\pi}_{\mathbf{t}} \overline{\boldsymbol{\nabla}} \mathbf{BR}_{\mathbf{0}}\left(\bar{\mathbf{t}}\right),$$

and thus the inequality part of the lemma is obtained. □

In the next part of the proof, Lemma 4.4 provides an expression of the BR gradient directly from the objective and constraint functions. Yet, such expression is only valid for the well-behaved points, and not all differentiable points. This explains why $\mathcal{W}^{\epsilon}$ is introduced, although only providing an upper-bound on the Lipschitz constant. Before moving to the next part of the proof, the above lemma is applied to Example 2.1.

Example 4.5

For the first player, the set of differentiable points is obtained as $\mathcal{T}_{\mathbf{0}}^{\text{diff}} = \text{int}\,\mathcal{T} \setminus \left\{\frac{-1}{c}, \frac{3}{c}\right\}$, and thus

$$L = \sup_{\bar{t} \in \mathcal{T}_{\mathbf{0}}^{\text{diff}}} \left|\nabla_t \text{BR}_{\mathbf{0}}\left(\bar{t}\right)\right| = \max\left\{0, c, 0\right\} = c.$$

To identify the well-behaved points, the KKT triplet is obtained as

$$\left(\text{BR}_{\mathbf{v}}\left(t\right), \mu^t_{\mathbf{v},1}, \mu^t_{\mathbf{v},2}\right) = \begin{cases} \left(-2 - v_2, -2 - 2ct - v_1 - 2v_2, 0\right) & \\ \qquad \text{if } ct \leq -1 - \frac{v_1}{2} - v_2, & \\ \left(ct - 1 + \frac{v_1}{2}, 0, 0\right) & \\ \qquad \text{otherwise}, & \\ \left(2 + v_3, 2ct - 6 + v_1 - 2v_3, 0\right) & \\ \qquad \text{if } ct \geq 3 - \frac{v_1}{2} + v_3, & \end{cases}$$

with $\mu^t_{\mathbf{v},1}$ and $\mu^t_{\mathbf{v},2}$ the multipliers associated with the first and second constraint. There exists no $(\mathbf{t}, \mathbf{v})$ for which the linear independency does not hold, but there exist points at which both the multiplier is zero and the associated constraint is active, i.e. points at which the strict complementary slackness does not hold:

$$\mathcal{W}^\epsilon = \left\{(t, \mathbf{v}) \in \text{int}\,\mathcal{T} \times \text{int}\,\mathcal{V}^\epsilon \,\middle|\, \left\{ \begin{array}{lcl} ct + \frac{v_1}{2} + v_2 & \neq & -1 \\ ct + \frac{v_1}{2} - v_3 & \neq & 3 \end{array} \right. \right\}.$$

The Lipschitz upper-bound, being exact in this case, is thus obtained as

$$L \leq \lim_{\epsilon \to 0^+} \sup_{\left(\bar{t}, \overline{\mathbf{v}}\right) \in \mathcal{W}^\epsilon} \left|\nabla_t \text{BR}_{\overline{\mathbf{v}}}\left(\bar{t}\right)\right| = \max\left\{0, c, 0\right\} = c.$$

Gradient expression from the optimisation problem This last step of the proof obtains an expression of the gradient from the objective and constraint functions. To that aim, the second-order derivatives of the objective function are introduced as

$$\mathbf{H}(\mathbf{x},\mathbf{t}) \triangleq \boldsymbol{\nabla}^2_{\mathbf{xx}} u(\mathbf{x},\mathbf{t}) \in \mathbb{R}^{n\times n},$$
$$\mathbf{K}(\mathbf{x},\mathbf{t}) \triangleq \boldsymbol{\nabla}^2_{\mathbf{xt}} u(\mathbf{x},\mathbf{t}) \in \mathbb{R}^{n\times m}.$$

On the constraint side, the set of active inequality constraints at $(\mathbf{x},\mathbf{t},\mathbf{v})$ is denoted as $\mathcal{I}^{\mathbf{t}}_{\mathbf{v}}(\mathbf{x}) \triangleq \left\{ i \in \mathcal{I} \middle| \mathbf{p}_i^\top \mathbf{x} = \gamma_i(\mathbf{t}) + v_i^{(b)} \right\}$ and the total number of active constraints as $r^{\mathbf{t}}_{\mathbf{v}}(\mathbf{x}) \triangleq \left|\mathcal{I}^{\mathbf{t}}_{\mathbf{v}}(\mathbf{x})\right| + J$. Then, the first-order constraint derivatives are grouped into the matrices

$$\mathbf{P}_{\mathcal{I}^{\mathbf{t}}_{\mathbf{v}}(\mathbf{x})} \triangleq \begin{bmatrix} \left\{\mathbf{p}_i^\top\right\}_{i\in\mathcal{I}^{\mathbf{t}}_{\mathbf{v}}(\mathbf{x})} \\ \left\{\tilde{\mathbf{p}}_j^\top\right\}_{j\in\mathcal{J}} \end{bmatrix} \in \mathbb{R}^{r^{\mathbf{t}}_{\mathbf{v}}(\mathbf{x})\times n},$$
$$\mathbf{S}_{\mathcal{I}^{\mathbf{t}}_{\mathbf{v}}(\mathbf{x})}(\mathbf{t}) \triangleq \begin{bmatrix} \left\{\boldsymbol{\nabla}^\top_{\mathbf{t}} \gamma_i(\mathbf{t})\right\}_{i\in\mathcal{I}^{\mathbf{t}}_{\mathbf{v}}(\mathbf{x})} \\ \left\{\boldsymbol{\nabla}^\top_{\mathbf{t}} \tilde{\gamma}_j(\mathbf{t})\right\}_{j\in\mathcal{J}} \end{bmatrix} \in \mathbb{R}^{r^{\mathbf{t}}_{\mathbf{v}}(\mathbf{x})\times m}.$$

Merging the objective and constraints part, the following idempotent matrices are defined as

$$\begin{aligned} &\mathbf{R}(\mathbf{x},\mathbf{t},\mathbf{v}) \\ &\triangleq \begin{cases} \left[\mathbf{I}_n - \mathbf{H}^{-1}\mathbf{P}^\top \left(\mathbf{P}\mathbf{H}^{-1}\mathbf{P}^\top\right)^+ \mathbf{P}\right]_{(\mathbf{x},\mathbf{t},\mathbf{v})} & \text{if } r^{\mathbf{t}}_{\mathbf{v}}(\mathbf{x}) > 0, \\ \mathbf{I}_n & \text{otherwise,} \end{cases} \\ &\mathbf{R}_\perp(\mathbf{x},\mathbf{t},\mathbf{v}) \triangleq \mathbf{I}_n - \mathbf{R}(\mathbf{x},\mathbf{t},\mathbf{v}), \end{aligned}$$

where $(\cdot)^+$ denotes the generalised inverse operator while $[\cdot]_{\mathbf{z}}$ means that all matrices inside the brackets are evaluated at $\mathbf{z}$. With these definitions, the gradient of the BR mapping is obtained in the following lemma.

Lemma 4.4

The gradient of $\mathbf{BR}_{\mathbf{v}}(\mathbf{t})$ with respect to $\mathbf{t}$ at a point $(\mathbf{t},\mathbf{v}) \in \mathcal{W}^\epsilon$ is given by

$$\boldsymbol{\nabla}_{\mathbf{t}} \mathbf{BR}_{\mathbf{v}}(\mathbf{t}) = \left[-\mathbf{R}\mathbf{H}^{-1}\mathbf{K} + \mathbf{R}_\perp \mathbf{P}^+ \mathbf{S}\right]_{(\mathbf{BR}_{\mathbf{v}}(\mathbf{t}),\mathbf{t},\mathbf{v})}.$$

Proof. The above is a direct consequence of [129, Section 4], showing that for well-behaved points,

$$\begin{aligned}&\boldsymbol{\nabla}_{\mathbf{t}}\mathbf{BR}_{\mathbf{v}}\left(\mathbf{t}\right)\\&=\left[-\mathbf{R}\mathbf{H}^{-1}\mathbf{K}+\mathbf{H}^{-1}\mathbf{P}^{\top}\left(\mathbf{P}\mathbf{H}^{-1}\mathbf{P}^{\top}\right)^{-1}\mathbf{S}\right]_{(\mathbf{BR}_{\mathbf{v}}(\mathbf{t}),\mathbf{t},\mathbf{v})}.\end{aligned}$$

When no constraint is active, the second term of the above is $\mathbf{0}$. When at least one is active, since at well-behaved points the linear independence of the constraints holds, $\mathbf{P}$ is full-row rank and thus a factor $\mathbf{P}\mathbf{P}^{+}=\mathbf{I}$ can be introduced to make $\mathbf{R}_{\perp}$ appear. □

Due to the intricate expression of $\mathbf{R}$, computing the maximum singular value of the above over all possible $(\mathbf{t},\mathbf{v})$ is challenging, although required by Lemma 4.3. Hence, the below lemma simplifies the expression and discards the dependency on the idempotent matrix $\mathbf{R}_{\mathbf{v}}^{\mathbf{t}}$. It also leverages the fact that for the constraints independent of $\mathbf{t}$, the lines of $\mathbf{S}$ are $\mathbf{0}$. To take into account this fact, the rows of $\mathbf{P}$ and $\mathbf{S}$ are permuted and partitioned as

$$\mathbf{P}=\begin{bmatrix}\mathbf{E}\\\mathbf{F}\end{bmatrix},\quad\text{and}\quad\mathbf{S}=\begin{bmatrix}\mathbf{G}\\\mathbf{0}\end{bmatrix},$$

with $\mathbf{E}$ and $\mathbf{G}$ the lines of the constraints dependent on $\mathbf{t}$, and $\mathbf{F}$ those of the fixed ones. The projector onto the null space of $\mathbf{F}$ is moreover introduced as $\mathbf{\Pi}=\mathbf{I}_n-\mathbf{F}^{\top}\left(\mathbf{F}\mathbf{F}^{\top}\right)^{-1}\mathbf{F}$, being well-defined for the well-behaved points.

Lemma 4.5

The maximum singular value of the gradient of $\mathbf{BR}_{\mathbf{v}}(\mathbf{t})$ with respect to $\mathbf{t}$ at a point $(\mathbf{t},\mathbf{v})\in\mathcal{W}^{\epsilon}$ is bounded by

$$\begin{aligned}&\sigma_{\max}\left(\boldsymbol{\nabla}_{\mathbf{t}}\mathbf{BR}_{\mathbf{v}}\left(\mathbf{t}\right)\right)\\&\leq\left[\sqrt{\frac{\sigma_{\max}^2\left(\mathbf{K}\right)}{\lambda_{\min}^2\left(\mathbf{H}\right)}+\kappa\left(\mathbf{H}\right)\sigma_{\max}^2\left(\left(\mathbf{E}\mathbf{\Pi}\right)^{+}\mathbf{G}\right)}\right]_{(\mathbf{BR}_{\mathbf{v}}(\mathbf{t}),\mathbf{t},\mathbf{v})}.\end{aligned}$$

Proof. The positive definite matrix $\mathbf{H}$ is factorised as $\mathbf{H}^{-1}=\mathbf{L}\mathbf{L}^{\top}$. Defining $\tilde{\mathbf{R}}=\mathbf{L}^{-1}\mathbf{R}\mathbf{L}$ and $\tilde{\mathbf{R}}_{\perp}=\mathbf{I}_n-\tilde{\mathbf{R}}$, these matrices are idempotent and symmetric (i.e., they are projectors). This enables to bound them as $\sigma_{\max}^2\left(\begin{bmatrix}\tilde{\mathbf{R}}&\tilde{\mathbf{R}}_{\perp}\end{bmatrix}\right)=\lambda_{\max}\left(\tilde{\mathbf{R}}\tilde{\mathbf{R}}^{\top}+\tilde{\mathbf{R}}_{\perp}\tilde{\mathbf{R}}_{\perp}^{\top}\right)=\lambda_{\max}\left(\mathbf{I}_n\right)=1$. Then, from [99, Cor. 9.6.4, Fact 9.14.14]

$$\begin{aligned}
&\sigma_{\max}\left(-\mathbf{R}\mathbf{H}^{-1}\mathbf{K}+\mathbf{R}_{\perp}\mathbf{P}^{+}\mathbf{S}\right)\\
&\quad=\sigma_{\max}\left(\mathbf{L}\begin{bmatrix}\tilde{\mathbf{R}} & \tilde{\mathbf{R}}_{\perp}\end{bmatrix}\begin{bmatrix}-\mathbf{L}^{\top}\mathbf{K}\\ \mathbf{L}^{-1}\mathbf{P}^{+}\mathbf{S}\end{bmatrix}\right),\\
&\quad\leq\sigma_{\max}\left(\mathbf{L}\right)\sqrt{\sigma^2_{\max}\left(\mathbf{L}^{\top}\mathbf{K}\right)+\sigma^2_{\max}\left(\mathbf{L}^{-1}\mathbf{P}^{+}\mathbf{S}\right)},\\
&\quad\leq\sigma_{\max}\left(\mathbf{L}\right)\sqrt{\sigma^2_{\max}\left(\mathbf{L}\right)\sigma^2_{\max}\left(\mathbf{K}\right)+\sigma^2_{\max}\left(\mathbf{L}^{-1}\right)\sigma^2_{\max}\left(\mathbf{P}^{+}\mathbf{S}\right)},\\
&\quad=\sqrt{\frac{\sigma^2_{\max}\left(\mathbf{K}\right)}{\lambda^2_{\min}\left(\mathbf{H}\right)}+\kappa\left(\mathbf{H}\right)\sigma^2_{\max}\left(\mathbf{P}^{+}\mathbf{S}\right)}.
\end{aligned}$$

From [99, Fact 6.1.6.xxx], any permutation matrix $\mathbf{\Sigma}$ is such that $\mathbf{P}^{+}\mathbf{S} = \left(\mathbf{\Sigma}\mathbf{P}\right)^{+}\mathbf{\Sigma}\mathbf{S}$, showing that the rows of $\mathbf{P}$ and $\mathbf{S}$ can be permuted with the same performutation. This thus makes the $\mathbf{E}$, $\mathbf{F}$ and $\mathbf{G}$ submatrices appear, leading to, from [99, Fact 6.1.6, 6.5.18, 2.17.3],

$$\begin{aligned}
\mathbf{P}^{+}\mathbf{S} &= \begin{bmatrix}\mathbf{E}\\ \mathbf{F}\end{bmatrix}^{+}\begin{bmatrix}\mathbf{G}\\ \mathbf{0}\end{bmatrix},\\
&=\begin{bmatrix}\mathbf{E}^{\top}\\ \mathbf{F}^{\top}\end{bmatrix}\begin{bmatrix}\mathbf{E}\mathbf{E}^{\top} & \mathbf{E}\mathbf{F}^{\top}\\ \mathbf{F}\mathbf{E}^{\top} & \mathbf{F}\mathbf{F}^{\top}\end{bmatrix}^{-1}\begin{bmatrix}\mathbf{G}\\ \mathbf{0}\end{bmatrix},\\
&=\left[\mathbf{E}^{\top}\left(\mathbf{E}\mathbf{\Pi}\mathbf{E}^{\top}\right)^{-1}-\left(\mathbf{I}_n-\mathbf{\Pi}\right)\mathbf{E}^{\top}\left(\mathbf{E}\mathbf{\Pi}\mathbf{E}^{\top}\right)^{-1}\right]\mathbf{G},\\
&=\left(\mathbf{E}\mathbf{\Pi}\right)^{+}\mathbf{G},
\end{aligned}$$

concluding the proof. □

The expression provided by Lemma 4.5 still depends on the optimisation problem solution $\mathbf{BR_v}\left(\mathbf{t}\right)$ which is in general not known. Moreover, the impact of the vanishingly small perturbations is not clear from the above expression. To circumvent this, the following set is introduced, grouping all possible sets of linearly independent active constraints, with at least one depending on $\mathbf{t}$:

$$\mathfrak{I}^{\dagger} = \left\{ \tilde{\mathcal{I}} \left| \begin{array}{l} \forall \epsilon > 0, \exists \left(\mathbf{x}, \mathbf{t}, \mathbf{v}\right) \in \mathcal{Z}^{\epsilon} \text{ s.t. } \tilde{\mathcal{I}} = \mathcal{I}_{\mathbf{v}}^{\mathbf{t}}\left(\mathbf{x}\right) \\ \left\{ \left\{\mathbf{p}_i\right\}_{i \in \tilde{\mathcal{I}}}, \left\{\tilde{\mathbf{p}}_j\right\}_{j \in \mathcal{J}} \right\} \text{ is linearly independent} \\ \tilde{\mathcal{I}} \cap \mathcal{I}^{\circ} \neq \emptyset \text{ or } \mathcal{J} \cap \mathcal{J}^{\circ} \neq \emptyset \end{array} \right. \right\}.$$

From the above definition, it can be noticed that for problems for which Assumption 4.3 holds, the above can be defined with $\mathbf{v} = \mathbf{0}$ without loss of generality.

Lemma 4.6

The Lipschitz constant of $\mathbf{BR_0}\left(\mathbf{t}\right)$ w.r.t $\mathbf{t}$ is bounded by

$$L^2 \leq \max_{\substack{\mathbf{t} \in \mathcal{T} \\ \mathbf{x} \in \mathcal{X}_{\mathbf{0}}(\mathbf{t})}} \left\{ \frac{\sigma_{\max}^2\left(\mathbf{K}\right)}{\lambda_{\min}^2\left(\mathbf{H}\right)} \right\} + \max_{\substack{\mathbf{t} \in \mathcal{T} \\ \mathbf{x} \in \mathcal{X}_{\mathbf{0}}(\mathbf{t})}} \left\{\kappa\left(\mathbf{H}\right)\right\} \max_{\substack{\tilde{\mathcal{I}} \in \mathfrak{I}^{\dagger} \\ \mathbf{t} \in \mathcal{T}}} \left\{ \sigma_{\max}^2 \left(\left(\mathbf{E\Pi}\right)^{+} \mathbf{G} \right) \right\}.$$

Proof. Considering the worst case active constraint set instead of the actual one, the Lipschitz constant is upper-bounded as

$$L^2 \leq \lim_{\epsilon \to 0^+} \sup_{\substack{(\mathbf{t}, \mathbf{v}) \in \mathcal{W}^{\epsilon} \\ \mathbf{x} = \mathbf{BR_v}(\mathbf{t})}} \frac{\sigma_{\max}^2\left(\mathbf{K}\right)}{\lambda_{\min}^2\left(\mathbf{H}\right)} + \kappa\left(\mathbf{H}\right) \max_{\tilde{\mathcal{I}} \in \mathfrak{I}^{\dagger}} \left\{ \sigma_{\max}^2 \left(\left(\mathbf{E\Pi}\right)^{+} \mathbf{G} \right) \right\}.$$

From the continuity of the BR mapping, of the derivatives, and of the maximum singular value and minimum eigenvalue operators, the above expression is continuous in both $\mathbf{t}$ and $\mathbf{v}$. Therefore, the vanishingly small perturbations can be discarded, and the whole set $\mathcal{T}$ can be considered. This leads to

$$L^2 \leq \max_{\substack{\mathbf{t} \in \mathcal{T} \\ \mathbf{x} = \mathbf{BR_0}(\mathbf{t})}} \frac{\sigma_{\max}^2\left(\mathbf{K}\right)}{\lambda_{\min}^2\left(\mathbf{H}\right)} + \kappa\left(\mathbf{H}\right) \max_{\tilde{\mathcal{I}} \in \mathfrak{I}^{\dagger}} \left\{ \sigma_{\max}^2 \left(\left(\mathbf{E\Pi}\right)^{+} \mathbf{G} \right) \right\}.$$

Since $\mathbf{BR_0}\left(\mathbf{t}\right)$ is yet difficult to obtain in closed form and to maximise upon, the maximum is instead taken over all $\mathbf{x} \in \mathcal{X}_{\mathbf{0}}\left(\mathbf{t}\right)$, concluding the proof of

Lemma 4.6. □

Example 4.6

The first player optimisation problem is such that $\mathfrak{I}^{\dagger} = \emptyset$ since no constraint depends on $\mathbf{t}$, and therefore the second term can be ignored. The Lipschitz constant upper-bound is thus given by

$$L \leq \max_{\substack{t\in[1-2c\,;\,3+c]\\ x\in[-2\,;\,2]}} \left\{ \frac{|-2c|}{2} \right\} = c,$$

the bound being in this case exact. For the second player, $\mathfrak{I}^{\dagger} = \{\{1\}, \{2\}\}$. Therefore,

$$L \leq \sqrt{\max_{\substack{t\in[-2\,;\,2]\\ x\in\left[1-ct\,;\,3-c\frac{t}{2}\right]}} \left\{ \frac{(2c)^2}{2^2} \right\} + \max\left\{ \frac{c^2}{4}, c^2 \right\}} = \sqrt{2}c.$$

In this case, the upper-bound overestimates the actual Lipschitz constant.

4.6.2 RA scenario analysis

First, it is noticed that as there is no objective function interactions, $\boldsymbol{\Gamma}^{\mathrm{obj}} = \mathbf{0}$ and thus one can focus on the constraint part. Moreover, the 2-norm objective leads to $\boldsymbol{\nabla}^2_{\mathbf{x}_q\mathbf{x}_q} u_q(\mathbf{x}) = \eta_q \mathbf{I}$ for the qth worker, with the associated condition number equal to 1. It remains to look at the linearly independent constraints sets which can be active at the same time, with at least one constraint depending on the other players. Such sets always include the (A_q+2)th constraint since it is the only one depending on the other players. To preserve a linearly independent set, considering an active (A_q+2)th constraint and the active equality constraint, only $A_q - 1$ lower bounds can be active at the same time. Therefore,

$$\mathfrak{I}^{\dagger}_{qr} = \{\mathcal{S} \subseteq \{1,\ldots,A_q+1\} | |\mathcal{S}| \leq A_q - 1\} \cup \{A_q + 2\}.$$

Given $\mathcal{I} \in \mathfrak{I}^{\dagger}_{qr}$, the indices of the active lower-bounds are defined as $\mathcal{I}^{\mathrm{a}} \triangleq \mathcal{I} \setminus \{A_q+2\}$ and their number is denoted by $N \triangleq |\mathcal{I}| - 1$. The variables not constrained by the lower bounds are indexed in $\mathcal{I}^{\mathrm{Na}} = \{1,\ldots,A_q+1\} \setminus \mathcal{I}^{\mathrm{a}}$, and their number is defined as $m \triangleq A_q + 1 - N$. The elements of $\mathbf{r}_q$ related respectively to the variables constrained by the lower bounds, and those for which it is not the case, are grouped into $\mathbf{r}_{q,\mathcal{I}^{\mathrm{a}}}$ and $\mathbf{r}_{q,\mathcal{I}^{\mathrm{Na}}}$. With these definitions, the matrices instrumental to the definition of the convergence matrix are obtained as

$$\mathbf{E}_{qr,\mathcal{I}} = \begin{bmatrix} -\mathbf{r}_{q,\mathcal{I}^{\mathrm{a}}}^{\top} & -\mathbf{r}_{q,\mathcal{I}^{\mathrm{Na}}}^{\top} \end{bmatrix}, \quad \mathbf{F}_{qr,\mathcal{I}} = \begin{bmatrix} -\mathbf{I}_N & \mathbf{0}_{N\times m} \\ \mathbf{1}_N^{\top} & \mathbf{1}_m^{\top} \end{bmatrix},$$
$$\mathbf{G}_{qr,\mathcal{I}}\left(\mathbf{x}_{-q}\right) = \begin{bmatrix} \frac{\epsilon_q}{\prod_{p\neq q} x_{p,0}} \frac{1}{x_{r,0}}, 0, \ldots, 0 \end{bmatrix}.$$

With respect to the definition provided in Theorem 4.1, one can notice that the columns of $\mathbf{E}_{qr,\mathcal{I}}$ and $\mathbf{F}_{qr,\mathcal{I}}$ have been permuted for the sake of simplicity, since permutation matrices can be introduced into $\sigma_{\max}\left(\left(\mathbf{E}_{qr,\mathcal{I}}\mathbf{\Pi}_{qr,\mathcal{I}}\right)^{+}\mathbf{G}_{qr,\mathcal{I}}\left(\mathbf{x}_{-q}\right)\right)$ without modifying its value. Using standard matrix theoretic properties for partitioned matrices, the projector $\mathbf{\Pi}_{qr,\mathcal{I}}$ is obtained as

$$\mathbf{\Pi}_{qr,\mathcal{I}} = \begin{bmatrix} \mathbf{0}_{N\times N} & \mathbf{0}_{N\times m} \\ \mathbf{0}_{m\times n} & \mathbf{I}_m - \frac{\mathbf{1}_m\mathbf{1}_m^{\top}}{m} \end{bmatrix}.$$

Letting $\xi_{qr} \triangleq \frac{\epsilon_q}{\prod_{p\neq q} x_{p,0}} \frac{1}{x_{r,0}}$, this leads to

$$\left(\mathbf{E}_{qr,\mathcal{I}}\mathbf{\Pi}_{qr,\mathcal{I}}\right)^{+}\mathbf{G}_{qr,\mathcal{I}}\left(\mathbf{x}_{-q}\right) =$$
$$\frac{\xi_{qr}}{\left\|\left(\mathbf{I}_m - \frac{\mathbf{1}_m\mathbf{1}_m^{\top}}{m}\right)\mathbf{r}_{q,\mathcal{I}^{\mathrm{Na}}}\right\|_2^2} \begin{bmatrix} \mathbf{0}_N & \mathbf{0}_{N\times A_r} \\ -\left(\mathbf{I}_m - \frac{\mathbf{1}_m\mathbf{1}_m^{\top}}{m}\right)\mathbf{r}_{q,\mathcal{I}^{\mathrm{Na}}} & \mathbf{0}_{m\times A_r} \end{bmatrix},$$

whose maximum singular value is obtained as

$$\begin{aligned} \sigma_{\max}\left(\left(\mathbf{E}_{qr,\mathcal{I}}\mathbf{\Pi}_{qr,\mathcal{I}}\right)^{+}\mathbf{G}_{qr,\mathcal{I}}\left(\mathbf{x}_{-q}\right)\right) &= \frac{\xi_{qr}}{\left\|\left(\mathbf{I}_m - \frac{\mathbf{1}_m\mathbf{1}_m^{\top}}{m}\right)\mathbf{r}_{q,\mathcal{I}^{\mathrm{Na}}}\right\|_2}, \\ &= \frac{\xi_{qr}}{\sqrt{\sum_{i\in\mathcal{I}^{\mathrm{Na}}} r_{q,i}^2 - \frac{\left(\sum_{i\in\mathcal{I}^{\mathrm{Na}}} r_{q,i}\right)^2}{m}}}. \end{aligned} \tag{4.17}$$

It remains to maximise the above with respect to the other players strategies, and to the constraint sets. For this latter, it is noticed that by removing a index i_0 from $\mathcal{I}^{\mathrm{Na}}$, the above quantity never decreases:

$$\left(\sum_{i\in\mathcal{I}^{\mathrm{Na}}} r_{q,i}^2 - \frac{\left(\sum_{i\in\mathcal{I}^{\mathrm{Na}}} r_{q,i}\right)^2}{m}\right) - \left(\sum_{i\in\mathcal{I}^{\mathrm{Na}}\setminus\{i_0\}} r_{q,i}^2 - \frac{\left(\sum_{i\in\mathcal{I}^{\mathrm{Na}}\setminus\{i_0\}} r_{q,i}\right)^2}{m-1}\right)$$
$$= \frac{\left(\sum_{i\in\mathcal{I}^{\mathrm{Na}}\setminus\{i_0\}} r_{q,i} - (m-1)\, r_{q,i_0}\right)^2}{m\,(m-1)}.$$

Thus, the smallest sets $\mathcal{I}^{\mathrm{Na}}$ must be considered, being at least of size 2 since $m = A_q + 2 - |\mathcal{I}| \geq 2$ for linearly independent constraint sets. Moreover, for sets with two elements, it can be observed that consecutive $r_{q,i}$'s will lead to the maximum of (4.17), if the $r_{q,i}$'s are sorted. In that case, the convergence matrix elements are obtained as

$$[\mathbf{\Gamma}^{\mathrm{cons}}]_{qr} = \frac{\epsilon_q}{\prod_{p\neq q}\left(1 - x_p^{\max}\right)} \frac{1}{\left(1 - x_r^{\max}\right)} \frac{\sqrt{2}}{\min_{i=0,\ldots,A_q-1} |r_{q,i} - r_{q,i+1}|}.$$

To conclude the convergence analysis, it is noticed that $\rho\left(\mathbf{\Gamma}\right) = \rho\left(\mathbf{T}\mathbf{\Gamma}\mathbf{T}^{-1}\right)$ whatever the invertible matrix $\mathbf{T}$ [99, Fact 4.45.xii], and that the desired expression is obtained with $\mathbf{T} = \mathrm{Diag}\left(\left[\frac{1}{1-x_1^{\max}}, \ldots, \frac{1}{1-x_Q^{\max}}\right]\right)$.

5

Preference-agnostic hybrid games

The above chapters have first outlined the MOG big picture, building on the idea that MO interactions can be studied from the associated scalarised game family. Next, the case of the weighted-sum scalarised games has been tackled, with conditions independent of the preference of the players among their objectives. As they were lacking in the literature, the previous chapter has then introduced convergence conditions for GNEPs, which have been applied to the ϵ-constraint scalarised games. These convergence conditions in fact can be applied to any hybrid scalarised game, in which the players minimise a partial weighted-sum of the objective functions, with the remaining ones as constraints. The caveat of such an analysis is that at this point, the conditions will depend on the preferences of the players, via the weighted-sum scalarisation weights and the constraint thresholds. The goal of this chapter is then to provide convergence guarantees for the BRD of hybrid scalarised games, which hold whatever the preferences of the players among their objectives. This goal is only partially achieved, as the obtained conditions will be independent of the weighted-sum weights, but will still rely on the knowledge of the constraint thresholds. In more details, the contributions of this chapter are the following.

- Focusing on ϵ-constraint scalarised games, the challenges of obtaining convergence guarantees independent of the constraint thresholds are discussed.

- For hybrid scalarised games, convergence guarantees are obtained in a partially preference-agnostic manner. More precisely, the convergence conditions are independent of the weighted-sum scalarisation weights, but still depend on the constraint thresholds. Such conditions naturally extend the results of Chapter 3, building on the definition of the underlying games.

- The case of the constraint satisfaction games is then tackled with the framework of Chapter 4. By designing the objective functions of the players, the GNEP convergence conditions are simplified, only depending on the strategy set interaction of the players. The designed objective functions have moreover the advantage of requiring no cooperation between the players, and to lead to efficient BR computations.

- The constraint satisfaction game framework is applied to the MF MP use-cases. As for the ϵ-constraint games, the JRC scenario does not belong to the considered GNEP class and thus cannot be analysed with the developed framework. As far as the multi-level RA scheme is concerned, the scheme reveals that the rate should depend in a nonlinear way on the consumed power in order to provide BRD convergence guarantees.

To that aim, Section 5.1 first applies the GNEP framework to the hybrid scalarised games, with fixed, known preferences. Then, Section 5.2 discusses the challenges of obtaining conditions which do not depend on the constraint thresholds. As a partially preference-agnostic result, Section 5.3 obtains convergence guarantees for a hybrid game, for fixed constraint thresholds but for all weighted-sum scalarisation weights. The constraint satisfaction games are then studied in Section 5.4, and applied to the MF MP use-cases in Section 5.5.

5.1 Preference-aware hybrid games

In this section, the GNEP convergence conditions provided in Theorem 4.1 are applied to the hybrid scalarised games, for known weighted-sum scalarisation weights and constraint thresholds. As a reminder of Definition 2.13, a hybrid sum-constraint scalarised game associated with a MOG $\mathcal{G}^{(\mathrm{MO})} =$

$\left\langle \Omega, \{\mathcal{X}_q\}_{q\in\Omega}, \{\mathbf{u}_q\}_{q\in\Omega} \right\rangle$ is parametrised by the hybrid indices $\left\{l_q^{(h)}\right\}_{q=1}^{Q}$, the weight profile $\mathbf{\Lambda}^{(h)} \in \Delta^{\times,(h)}$, and the threshold profile $\mathbf{E}^{(h)} \in \mathbb{R}^{\times,(h)}$. It is defined as the GNEP $\tilde{\mathcal{G}}^{\mathbf{\Lambda}^{(h)},\mathbf{E}^{(h)}} \triangleq \left\langle \Omega, \left\{ \tilde{\mathcal{X}}_q^{\boldsymbol{\epsilon}_q^{(h)}} \right\}_{q\in\Omega}, \left\{ u_q^{\boldsymbol{\lambda}_q^{(h)}} \right\}_{q\in\Omega} \right\rangle$, with the objective function and the player-dependent set defined as

$$u_q^{\boldsymbol{\lambda}_q^{(h)}}(\mathbf{x}_q, \mathbf{x}_{-q}) \triangleq \sum_{l=1}^{l_q^{(h)}} \lambda_{q,l}^{(h)} u_{q,l}(\mathbf{x}_q, \mathbf{x}_{-q}), \tag{5.1}$$

$$\tilde{\mathcal{X}}_q^{\boldsymbol{\epsilon}_q^{(h)}}(\mathbf{x}_{-q}) \triangleq \left\{ \mathbf{x}_q \in \mathcal{X}_q \middle| u_{q,l}(\mathbf{x}_q, \mathbf{x}_{-q}) \le \epsilon_{q,l}^{(h)}, \ \forall l = l_q^{(h)}+1, \ldots, L_q \right\}. \tag{5.2}$$

In this game, the qth player behaviour is thus modelled by the following optimisation problem

$$\begin{array}{rl} \text{minimise}_{\mathbf{x}_q} & \sum_{l=1}^{l_q^{(h)}} \lambda_{q,l}^{(h)} u_{q,l}(\mathbf{x}_q, \mathbf{x}_{-q}), \\ \text{s.t.} & \mathbf{x}_q \in \tilde{\mathcal{X}}_q^{\boldsymbol{\epsilon}_q^{(h)}}(\mathbf{x}_{-q}), \end{array} \tag{5.3}$$

Sticking with the GNEP class of Chapter 4, the hybrid games tackled in this section are those with polyhedral strategy sets and variable RHSs, which are formally defined as follows.

Definition 5.1: Hybrid scalarised game with polyhedral strategy sets and variable RHSs

A hybrid scalarised game $\tilde{\mathcal{G}}^{\mathbf{\Lambda}^{(h)},\mathbf{E}^{(h)}} \triangleq \left\langle \Omega, \left\{ \tilde{\mathcal{X}}_q^{\boldsymbol{\epsilon}_q^{(h)}} \right\}_{q\in\Omega}, \left\{ u_q^{\boldsymbol{\lambda}_q^{(h)}} \right\}_{q\in\Omega} \right\rangle$ is said to have polyhedral strategy sets and variable RHSs if $\forall q \in \Omega$, $\forall \mathbf{x}_{-q} \in \overline{\mathcal{X}}_{-q}$, the strategy set mappings can be written as

$$\tilde{\mathcal{X}}_q^{\boldsymbol{\epsilon}_q^{(h)}}(\mathbf{x}_{-q}) = \left\{ \mathbf{x}_q \in \mathbb{R}^{n_q} \middle| \begin{array}{ll} \mathbf{p}_{q,i}^\top \mathbf{x}_q \le \gamma_{q,i}^{\boldsymbol{\epsilon}_q^{(h)}}(\mathbf{x}_{-q}), & \forall i \in \mathcal{I}_q^{(h)} \\ \tilde{\mathbf{p}}_{q,j}^\top \mathbf{x}_q = \tilde{\gamma}_{q,j}(\mathbf{x}_{-q}), & \forall j \in \mathcal{J}_q \end{array} \right\}. \tag{5.4}$$

with $\mathcal{I}_q^{(h)}$ and $\mathcal{J}_q$ the sets of inequality and equality constraints, $\mathbf{p}_{q,i}, \tilde{\mathbf{p}}_{q,i} \in \mathbb{R}^{n_q}$ the linear constraint vectors, and $\gamma_{q,i}^{\boldsymbol{\epsilon}_q^{(h)}} : \mathcal{X}_{-q} \to \mathbb{R}$,

$\tilde{\gamma}_{q,j} : \mathcal{X}_{-q} \to \mathbb{R}$ the possibly non-linear RHS functions which depend on the other players.

As for the GNEPs, the hybrid scalarised games are assumed to satisfy the two following assumptions. In the second, the sets $\mathfrak{I}_{qr}^{\boldsymbol{\epsilon}_q^{(h)},\dagger}$ and $\mathfrak{K}_{qr}^{\boldsymbol{\epsilon}_q^{(h)},\dagger}$ are defined as in (4.3) and (4.5), yet applied to (5.4).

Assumption 5.1: Objective functions assumptions

For each qth player, $\forall l_q = 1, \ldots, l_q^{(h)}$, $\forall \mathbf{x} \in \mathcal{X}$,

- $u_{q,l_q}(\mathbf{x}_q, \mathbf{x}_{-q})$ is strongly convex in $\mathbf{x}_q$;
- $u_{q,l_q}(\mathbf{x}_q, \mathbf{x}_{-q})$ is $\mathcal{C}^1$ in $\mathbf{x}_q$;
- $\boldsymbol{\nabla}_{\mathbf{x}_q} u_{q,l_q}(\mathbf{x}_q, \mathbf{x}_{-q})$ is $\mathcal{C}^1$ in $\mathbf{x}_q$ and $\mathbf{x}_{-q}$;

Assumption 5.2: Strategy-set assumptions

For each qth player,

- $\mathcal{X}_q$ is non-empty, closed, convex and bounded;
- The family $\{\tilde{\mathbf{p}}_{q,j}\}_{j \in \mathcal{J}_q}$ is linearly independent;
- $\mathfrak{K}_{qr}^{\boldsymbol{\epsilon}_q^{(h)},\dagger} = \mathfrak{I}_{qr}^{\boldsymbol{\epsilon}_q^{(h)},\dagger}$ $\forall r \neq q$.

Moreover, $\forall \mathbf{x}_{-q} \in \mathcal{X}_{-q}$,

- $\exists\, \mathbf{x}_q \in \tilde{\mathcal{X}}_q^{\boldsymbol{\epsilon}_q^{(h)}}(\mathbf{x}_{-q})$ such that $\forall i \in \mathcal{I}_q^{(h)}$, $\mathbf{p}_{q,i}^\top \mathbf{x}_q < \gamma_{q,i}^{\boldsymbol{\epsilon}_q^{(h)}}(\mathbf{x}_{-q})$.
- $\left\{\gamma_{q,i}^{\boldsymbol{\epsilon}_q^{(h)}}(\mathbf{x}_{-q})\right\}_{i \in \mathcal{I}_q^{(h)}}$ and $\{\tilde{\gamma}_{q,j}(\mathbf{x}_{-q})\}_{j \in \mathcal{J}_q}$ are $\mathcal{C}^1$ in $\mathbf{x}_{-q}$.

In the above definition and assumptions, it can be noticed that the inequality RHS functions $\gamma_{q,i}^{\boldsymbol{\epsilon}_q^{(h)}}(\mathbf{x}_{-q})$ depend on the constraint thresholds, while the equality ones do not depend on them. This comes from the fact that for a MOG with fixed strategy sets, as those considered in this thesis, the hybrid scalarised games only add inequalities to the strategy sets. Another consequence of this is that the objective functions of the

MOG are considered defined on the whole set $\mathcal{X}$, as it can be observed in Assumption 5.1. Differently, in the GNEP framework of Chapter 4, they were only required to be defined on the set of strategy profiles which were feasible for the considered player, taking into account the moving constraints.

Remark 5.1

Assumption 5.1 is independent of the weighted-sum scalarised weights, similarly to those stated in Chapter 3 for the preference-agnostic weighted-sum games. On the contrary, Assumption 5.2 depends on the constraint thresholds. As it will be discussed in Section 5.2, this already hints the fact that obtaining BRD convergence results agnostic from the constraint thresholds is challenging.

For a hybrid scalarised game with polyhedral strategy sets and variables RHSs, which fulfils Assumptions 5.1 and 5.2, the convergence matrix can be build following the definition provided in Section 4.3. This convergence matrix is denoted $\mathbf{\Gamma}^{\mathbf{\Lambda}^{(h)},\mathbf{E}^{(h)}}$, depending thus on the weighted-sum scalarised weights and the constraint thresholds. Based on this, Theorem 4.1 can be applied, implying that the totally asynchronous BRD converges if $\rho\left(\mathbf{\Gamma}^{\mathbf{\Lambda}^{(h)},\mathbf{E}^{(h)}}\right) < 1$.

5.2 Fully preference-agnostic hybrid games

The above section provides the sufficient condition $\rho\left(\mathbf{\Gamma}^{\mathbf{\Lambda}^{(h)},\mathbf{E}^{(h)}}\right) < 1$ for the convergence of the BRD of a hybrid game. In order to account for the MO character of the players, this section thus focuses on obtaining conditions which would be fully preference-agnostic, hence being independent of $\mathbf{\Lambda}^{(h)}$ and $\mathbf{E}^{(h)}$. This thus also covers the case of preference-agnostic ϵ-constraint games.

However, obtaining conditions which do not require the knowledge of the constraint thresholds $\mathbf{E}^{(h)}$ turns out to be extremely challenging. The reasons are detailed below, this thesis hence not covering this research direction.

- Assumption 5.2 delimits the strategy sets which can be handled by the developed GNEP framework, among others with non-emptiness, constraint qualification and insensitivity to infinitesimal perturbations.

This assumption however depends on the selected constraint thresholds. In order to obtain results agnostic from the player preferences, one should find assumptions on the MOG which would ensure Assumption 5.2 is fulfilled whatever the *relevant* constraint threshold.

- The above word *relevant* refers to the fact that contrarily to the weighted-sum scalarisation weights, many constraint thresholds lead to a GNEP which does not admit an equilibrium. Therefore, given a MOG, one should identify a subset of $\mathbf{E}^{(h)}$ which includes all GNEPs admitting an equilibrium, but excludes all others. Doing so, Theorem 2.1 would still hold, and each studied hybrid scalarised game would admit an equilibrium.

- Yet another problem is that the BRD could not be defined, even for a GNEP admitting an equilibrium. This happens for instance for Example 2.1 when $c > 2$, as depicted in panel (d) of Figure 2.2. While the GNEP admits an equilibrium, the BRD reaches points at which one of the player has an empty strategy set. The fact that a GNEP might admit an equilibrium, but might also have its BRD undefined, thus limits the constraint thresholds for which BRD convergence guarantees can be provided. Except for GNEPs with few players having low-dimensional strategy sets, determining such a subset of thresholds is however challenging.

- Finally, if the above issues are addressed, it remains to analyse the impact of the constraint thresholds on the convergence matrix defined (4.6), in order to determine when such matrix has a spectral radius smaller than 1 whatever the thresholds. This impact lies on the one hand in the set of linearly independent constraints which can be active at the same time $\mathfrak{I}_{qr}^{\boldsymbol{\epsilon}_q^{(h)},\dagger}$. On the other hand, the thresholds impact the RHS functions' derivatives. Therefore, one would need to analyse of these impact translate into the convergence matrix elements, building on matrix theoretic properties.

For the above reasons, this research direction is not explored in this thesis. Hence, for the ϵ-constraint, hybrid, and constraint satisfaction scalarised games, the convergence results provided in this work will always be dependent on the constraint thresholds selected by the players.

5.3 Partially preference-agnostic hybrid games

The above section discusses the fact that it is difficult to have convergence results independent of the constraint thresholds for the hybrid games, and thus guarantees which are fully agnostic about the preferences of the player. It is however possible to obtain partially preference-agnostic results, in the sense that they depend on the constraint thresholds $\mathbf{E}^{(h)} \in \mathbb{R}^{\times,(h)}$ but not on the scalarisation weights $\mathbf{\Lambda}^{(h)} \in \Delta^{\times,(h)}$.

To that aim, similarly to Chapter 3, the underlying games associated with the hybrid scalarised game family are defined as follows. In an underlying game, each player has an index $\pi_q^{(h)} \in \left\{1, \ldots, l_q^{(h)}\right\}$ depicting the selection of one of its objective function, and the global selection profile is denoted $\boldsymbol{\pi}^{(h)} \triangleq \left[\pi_1^{(h)}, \ldots, \pi_Q^{(h)}\right]$. This global selection profile belongs to the set $\Pi^{(h)}$, defined as $\Pi^{(h)} \triangleq \bigtimes_{q=1}^{Q} \left\{1, \ldots, l_q^{(h)}\right\}$. The resulting underlying game is then defined as $\tilde{\mathcal{G}}^{\left(\boldsymbol{\pi}^{(h)}\right),\mathbf{E}^{(h)}} \triangleq \left\langle \Omega, \left\{\tilde{\mathcal{X}}_q^{\boldsymbol{\epsilon}_q^{(h)}}\right\}_{q\in\Omega}, \left\{u_{q,\pi_q^{(h)}}\right\}_{q\in\Omega} \right\rangle$. The convergence matrix associated with this underlying game is denoted $\mathbf{\Gamma}^{\left(\boldsymbol{\pi}^{(h)}\right),\mathbf{E}^{(h)}}$, following once again the definition (4.6).

With these definitions, the below proposition provides an equivalence similar to those of Chapter 3, yet for the hybrid scalarised games. It indeed shows that if the convergence matrices of all underlying games have a spectral radius smaller than 1, then it is the case for the hybrid games whatever the weighted-sum scalarisation weights.

Proposition 5.1

Let the MOG $\mathcal{G}^{(\mathrm{MO})}$, the hybrid indices $\left\{l_q^{(h)}\right\}_{q=1}^{Q}$, and the threshold profile $\mathbf{E}^{(h)} \in \mathbb{R}^{\times,(h)}$ satisfy Assumptions 5.1 and 5.2, with $l_q^{(h)} \geq 1$ whatever $q \in \Omega$. Let also consider the hybrid games have polyhedral strategy sets and variable RHSs. Then, they satisfy

$$\rho\left(\mathbf{\Gamma}^{\mathbf{\Lambda}^{(h)},\mathbf{E}^{(h)}}\right) < 1 \quad \forall \mathbf{\Lambda}^{(h)} \in \Delta^{\times,(h)} \iff \rho\left(\mathbf{\Gamma}^{\left(\boldsymbol{\pi}^{(h)}\right),\mathbf{E}^{(h)}}\right) < 1 \quad \forall \boldsymbol{\pi}^{(h)} \in \Pi^{(h)}. \tag{5.5}$$

Proof. See Section 5.7.1. □

The above proposition provides thus an efficient way to study BRD convergence for hybrid scalarised games, whatever the preferences of the players among a partial set of their objective functions. It can be noted that it however does not cover the constraint satisfaction games, since the hybrid indices are assumed to be greater or equal to 1. Indeed, as the objective functions of the constraint satisfaction games are constant, they are not strongly convex and therefore the assumptions of Theorem 4.1 are not satisfied.

5.4 Preference-aware constraint satisfaction games

Answering the above comment, this section studies the constraint satisfaction games. In these games, defined in Definition 2.12, the players are only interested in fulfilling requirements on their objective functions. In other words, each qth player has a player-dependent strategy set $\tilde{\mathcal{X}}_q^{\boldsymbol{\epsilon}_q^{\mathrm{sat}}}(\mathbf{x}_{-q})$, but his objective function is a constant whatever his strategy and the one of the other players. Additionally to contradicting the assumptions of Theorem 4.1, this formulation makes the BR mappings multivalued. That is, given $\mathbf{x}_{-q}$, the qth player might rationally play any strategy in $\tilde{\mathcal{X}}_q^{\boldsymbol{\epsilon}_q^{\mathrm{sat}}}(\mathbf{x}_{-q})$. Different approaches can be considered to encompass such effect. First, the game analysis may be designed to hold whatever the strategy selected by the player. If this is not possible, then it may be assumed a feasible strategy is selected uniformly at random, the analysis leveraging on this uniform stochastic property.

In this section, another perspective is considered: given that the players equally prefer any strategy fulfilling the constraints, their objective function could be designed so as to guarantee BRD convergence, as provided by the GNEP framework of Chapter 4. Let the designed objective function of the qth player be denoted $d_q(\mathbf{x}_q, \mathbf{x}_{-q})$. Instead of modelising the players' performance, this objective function enables to control their interaction. The game obtained by adding such designed metrics to a constraint satisfaction game is coined in this thesis under the name *designed constraint satisfaction game*, as defined below.

Definition 5.2: Designed constraint satisfaction game

Given the constraint satisfaction game $\tilde{\mathcal{G}}^{\mathbf{E}^{\text{sat}}} \triangleq \left\langle \Omega, \left\{ \tilde{\mathcal{X}}_q^{\boldsymbol{\epsilon}_q^{\text{sat}}} \right\}_{q\in\Omega}, \{1\}_{q\in\Omega} \right\rangle$, and the designed functions $\{d_q\}_{q\in\Omega}$, the designed constraint satisfaction game is the GNEP defined as $\tilde{\mathcal{G}}^{\mathbf{E}^{\text{sat}},\text{des}} \triangleq \left\langle \Omega, \left\{ \tilde{\mathcal{X}}_q^{\boldsymbol{\epsilon}_q^{\text{sat}}} \right\}_{q\in\Omega}, \{d_q\}_{q\in\Omega} \right\rangle$.

The use of constraint satisfaction games to model wireless networks has among others been considered in [133]. In that work, the distinction is made between the so-called *satisfaction equilibria*, and the *efficient satisfaction equilibria*. Such distinction mirrors the one made in this chapter, between all the possible equilibria of the constraint satisfaction game, and the ones of the designed constraint satisfaction games. To tackle such problem, the philosophy of [133] has been to identify the constraint satisfaction games as a constraint potential games, in order to obtain existence and uniqueness results. Instead, in this chapter, the framework of the above chapters is applied in order to obtain BRD convergence guarantees.

To that aim, considering the constraint satisfaction game satisfies the strategy set requirements of Assumptions 4.2 and 4.3, and that the designed functions fulfil the objective function requirements of Assumption 4.1, then the GNEP framework can be applied to the designed constraint satisfaction game if the strategy sets are polyhedral with variable RHSs. In that case, let the convergence matrix associated with $\tilde{\mathcal{G}}^{\mathbf{E}^{\text{sat}},\text{des}}$ be denoted $\mathbf{\Gamma}^{\mathbf{E}^{\text{sat}},\text{des}}$. The convergence matrix related to the constraints only is furthermore introduced as $\mathbf{\Gamma}^{\mathbf{E}^{\text{sat}}} \in \mathbb{R}^{Q\times Q}$, with

$$\left[\mathbf{\Gamma}^{\mathbf{E}^{\text{sat}}}\right]_{qr} \triangleq \begin{cases} \displaystyle\max_{\substack{\mathbf{x}\in\mathcal{X} \\ \mathcal{I}\in\mathfrak{I}_{qr}^{\boldsymbol{\epsilon}_q^{\text{sat}},\dagger}}} \left\{\sigma_{\max}\left(\left(\mathbf{E}_{qr,\mathcal{I}}\mathbf{\Pi}_{qr,\mathcal{I}}\right)^{+}\mathbf{G}_{qr,\mathcal{I}}\left(\mathbf{x}_{-q}\right)\right)\right\} & \text{if } q \neq r, \\ 0 & \text{otherwise,} \end{cases}$$

with $\mathfrak{I}_{qr}^{\boldsymbol{\epsilon}_q^{\text{sat}}}$, $\mathbf{E}_{qr,\mathcal{I}}$, $\mathbf{\Pi}_{qr,\mathcal{I}}$ and $\mathbf{G}_{qr,\mathcal{I}}\left(\mathbf{x}_{-q}\right)$ being defined as in Section 4.3. As stated in the below corollary, this matrix has a spectral radius smaller to the one of any designed constraint satisfaction game which fulfils the constraints.

Corollary 5.1: Designed objective functions

Let $\tilde{\mathcal{G}}^{\mathbf{E}^{\text{sat}},\text{des}}$ be the designed constraint satisfaction game associated with the constraint satisfaction game $\tilde{\mathcal{G}}^{\mathbf{E}^{\text{sat}}}$ and the designed functions $\{d_q\}_{q\in\Omega}$, assumed to fulfil Assumptions 4.1 to 4.3 and to have polyhedral strategy sets with variable RHSs. Then, the convergence matrices satisfy

$$\rho\left(\mathbf{\Gamma}^{\mathbf{E}^{\text{sat}},\text{des}}\right) \geq \rho\left(\mathbf{\Gamma}^{\mathbf{E}^{\text{sat}}}\right).$$

The equality is achieved if $\forall q \in \Omega$,

$$d_q(\mathbf{x}) = \|\mathbf{x}_q - \mathbf{y}_q\|_2^2, \tag{5.6}$$

with $\mathbf{y}_q \in \mathbb{R}^{n_q}$ chosen by each qth player as desired.

Proof. The above directly follows from the convergence matrix definition, from the non-negativity of the objective part of this matrix, as well as from the fact that the condition number of a matrix is greater or equal to 1. □

Building on this corollary, we argue in this thesis that for the GNEP convergence conditions of Theorem 4.1, one of the best choice for the designed objective functions is given by (5.6), for the three following reasons.

- First, from the inequality provided by Corollary 5.1, the square distances objective functions lead to the broadest convergence guarantees for the totally asynchronous BRD, at least for the GNEP framework of Theorem 4.1.

- Secondly, with such an objective, the qth player BR is the projection of $\mathbf{y}_q$ on his strategy set. Such projection can be efficiently obtained with quadratic solvers, or with projection algorithms [119, 120]. Also, many euclidean projections have closed-form, or almost closed-form expressions [103]. The projection points $\mathbf{y}_q$ might moreover be selected by the players in order to lead to a closed-form, or simple projection formulation.

- Finally, the engineered objectives can be chosen in an autonomous way by all the players, and thus no additional side-information is required.

5.5 Application to the multi-function multi-point use-cases

In this section, the MF MP use cases of section 2.4 are studied, modelling the nodes as players interacting through a constraint satisfaction game.

5.5.1 JRC scenario

As discussed in Section 4.4.1, the JRC objective functions however do not translate into polyhedral strategy sets when they are considered as constraints. This emphasises one of the limitations of the developed framework, which prevents the analysis of the JRC constraint satisfaction games.

5.5.2 Multi-level RA scenario

In the constraint satisfaction game associated with the RA MOG defined in Section 2.4.2, the optimisation problem of the qth player reads as

$$\begin{aligned} \text{minimise}_{\mathbf{x}_q} \quad & 1 \\ \text{s.t.} \quad & x_{q,0} \geq 1 - x_{q,\max}, \\ & x_{q,a_q} \geq 0, \quad \forall a_q = 1, \dots, A_q, \\ & \mathbf{r}_q^\top \mathbf{x}_q \geq \tfrac{\epsilon_{q,1}}{\theta_q(\mathbf{x}_{-q})}, \\ & \mathbf{p}_q^\top \mathbf{x}_q \leq \epsilon_{q,2}. \\ & \textstyle\sum_{a_q=0}^{A_q} x_{q,a_q} = 1, \end{aligned} \tag{5.7}$$

with $\epsilon_{q,1}$ and $\epsilon_{q,2}$ the thresholds associated respectively with the normalised rate and power.

For this game, the constraint satisfaction matrix $\mathbf{\Gamma}^{\mathbf{E}^{\text{sat}}}$ is first computed. It ensures BRD convergence if $\rho\left(\mathbf{\Gamma}^{\mathbf{E}^{\text{sat}}}\right) < 1$, and if the designed objective functions have the form (5.6). To that aim, the set-valued mapping elements

(4.1) are identified as $\mathcal{I}_q = \{1, \ldots, A_q + 3\}$,

$$\mathbf{p}_{q,i} = \begin{cases} -\mathbf{e}_i & \forall i = 1, \ldots, A_q + 1, \\ -\mathbf{r}_q & i = A_q + 2, \\ \mathbf{p}_q & i = A_q + 3, \end{cases}$$

$$\gamma_{q,i}\left(\mathbf{x}_{-q}\right) = \begin{cases} x_q^{\max} - 1 & i = 1, \\ 0 & \forall i = 2, \ldots, A_q + 1, \\ -\frac{\epsilon_{q,1}}{\theta_q\left(\mathbf{x}_{-q}\right)} & i = A_q + 2, \\ \epsilon_{q,2} & i = A_q + 3. \end{cases}$$

The equality constraint leads to $\mathcal{J}_q = \{1\}$, $\tilde{\mathbf{p}}_{q,1} = \mathbf{1}_{A_q+1}$, and $\tilde{\gamma}_{q,1}\left(\mathbf{x}_{-q}\right) = 1$. The set of constraints depending on the other players are furthermore defined as $\mathcal{I}_{qr}^{\circ} = \{A_q + 2\}$, $\mathcal{J}_{qr}^{\circ} = \emptyset$. From this, the convergence matrix $\mathbf{\Gamma}$ is build in 5.7.2, its elements reading as

$$[\mathbf{\Gamma}]_{qr} = \frac{\epsilon_{q,1}}{\prod_{p=1}^{Q}\left(1 - x_p^{\max}\right)} \max\left\{C_{qr}^{(1)}, C_{qr}^{(2)}\right\}, \tag{5.8}$$

with

$$C_{qr}^{(1)} = \frac{R_{q,A_q}}{\min_{\substack{\mathcal{I} \subseteq \{1,\ldots,A_q+1\} \\ |\mathcal{I}|=3}} \sqrt{\sum_{a_q \in \mathcal{I}}\left(R_{q,a_q} - \overline{R}_{q,\mathcal{I}}\right)^2} \left|\sin\left(\theta_{q,\mathcal{I}}\right)\right|}, \tag{5.9}$$

$$C_{qr}^{(2)} = \frac{\sqrt{2} R_{q,A_q}}{\min_{a_q=0,\ldots,A_q-1}\left|R_{q,a_q} - R_{q,a_q+1}\right|}, \tag{5.10}$$

and with the mean rate and power vectors, and the angle between the centred vectors, defined as

$$\overline{R}_{q,\mathcal{I}} \triangleq \frac{1}{|\mathcal{I}|} \sum_{a_q \in \mathcal{I}} R_{q,a_q}, \tag{5.11}$$

$$\overline{P}_{q,\mathcal{I}} \triangleq \frac{1}{|\mathcal{I}|} \sum_{a_q \in \mathcal{I}} P_{q,a_q}, \tag{5.12}$$

$$\cos\left(\theta_{q,\mathcal{I}}\right) \triangleq \frac{\sum_{a_q \in \mathcal{I}}\left(R_{q,a_q} - \overline{R}_{q,\mathcal{I}}\right)\left(P_{q,a_q} - \overline{P}_{q,\mathcal{I}}\right)}{\sqrt{\sum_{a_q \in \mathcal{I}}\left(R_{q,a_q} - \overline{R}_{q,\mathcal{I}}\right)^2} \sqrt{\sum_{a_q \in \mathcal{I}}\left(R_{q,a_q} - \overline{P}_{q,\mathcal{I}}\right)^2}}. \tag{5.13}$$

The two elements of the convergence matrix $C_{qr}^{(1)}$ and $C_{qr}^{(2)}$ are related respectively to the case of an active maximum power constraint, and of an inactive one. This latter case correspond thus to the GNEP analysis of Section 4.4.2, with the matrix elements being identical. The $C_{qr}^{(2)}$ case also depends on the rate of the activity levels, but more importantly on the angles between the rate and power vectors.

This analysis thus provides the same insights as the ϵ-constraint version of the multi-level RA scheme. These insights are that BRD convergence is likely to occur when the maximum active probabilities are low, the rate requirements significantly lower than the maximum active probabilities, and when the activity levels have significantly different rates, as given in Insights 4.1 to 4.3. The constraint satisfaction flavour however adds a fourth insight, coming from the $\sin(\theta_{q,\mathcal{I}})$ factors. Indeed, the value of $\sin(\theta_{q,\mathcal{I}})$ can also be interpreted as the square of the sample Pearson correlation coefficient between $\mathbf{r}_q$ and $\mathbf{p}_q$, the coefficient measuring the linear dependency existing between two sets of data.

Insight 5.1: Non-linear rate-power relationship

For the RA constraint satisfaction game with a designed objective function given by (5.6), the BRD is likely to converge when the rates of the activity levels have a non-linear relationship with the power levels.

This convergence analysis should be complemented by determining whether the strategy set assumptions (non-emptiness, constraint qualification and insensitivity) are fulfilled. Moreover, the point selected by the players in their designed objective function could be discussed, as well as the way to compute the resulting BR. This is however left for future works.

5.6 Chapter summary

This chapter has leveraged on the weighted-sum game analysis of Chapter 3, and the GNEP framework of Chapter 4, to study the general case of the hybrid scalarised games. The obtained results are somehow lukewarm.

On the negative side, obtaining convergence conditions for the BRD which do not depend on the constraint thresholds has proven to be challenging. On the positive side however, it has been shown that the convergence conditions can be made independent of the weighted-sum scalarisation weights, by relying on the underlying games associated with a hybrid scalarised game.

The second part of this chapter has focused on the constraint satisfaction games. For such games, it has been considered the players were equipped with a well-designed objective function, which benefits from strong BRD convergence guarantees. It has been shown that square distance objectives were providing at the same time the best possible convergence guarantees, while having attractive properties in terms of BR computations. The developed framework has finally been applied to the multi-level RA, revealing the importance of the non-linear relationship between the rate and power levels for the convergence of the BRD.

This chapter concludes the analysis of the MO interactions between the players. This analysis has been performed under several perspectives, being the different scalarised game flavours. The next chapter provides therefore a synthetic view of the particularities of each scalarisation flavour, as well as the insights gained on the MF MP use-cases.

5.7 Proofs

5.7.1 Proof of Proposition 5.1

Similarly to the full convergence matrices, the objective and constraint parts of the hybrid convergence matrices are denoted for the hybrid scalarised game, and underlying games, as $\mathbf{\Gamma}^{\mathrm{obj},\mathbf{\Lambda}^{(h)}}$, $\mathbf{\Gamma}^{\mathbf{\Lambda}^{(h)}}$, $\mathbf{\Gamma}^{\mathrm{obj},\left(\boldsymbol{\pi}^{(h)}\right)}$, and $\mathbf{\Gamma}^{\left(\boldsymbol{\pi}^{(h)}\right)}$. Following the results of Section 3.7.2, one obtains that whatever $q, r \in \Omega$, $q \neq r$,

$$\left[\mathbf{\Gamma}^{\mathrm{obj},\mathbf{\Lambda}^{(h)}}\right]_{qr} \leq \sum_{\pi_q=1}^{l_q^{(h)}} \lambda_{q,\pi_q}^{(h)} \left[\mathbf{\Gamma}^{\mathrm{obj},\left(\boldsymbol{\pi}^{(h)}\right)}\right]_{qr},$$

$$\left[\mathbf{\Gamma}^{\mathrm{cons},\mathbf{\Lambda}^{(h)}}\right]_{qr} \leq \sum_{\pi_q=1}^{l_q^{(h)}} \lambda_{q,\pi_q}^{(h)} \left[\mathbf{\Gamma}^{\mathrm{cons},\left(\boldsymbol{\pi}^{(h)}\right)}\right]_{qr}.$$

It should be noted that the dependency of the constraint part on $\mathbf{\Lambda}^{(h)}$ comes from the condition number present in its definition (4.9). This condition number being the ratio of the maximum and minimum eigenvalue of the

Hessian of the objective function, it also satisfies the same properties as those proven in Section 3.7.2. Equipped with these inequalities,

$$\begin{aligned}
\left[\boldsymbol{\Gamma}^{\boldsymbol{\Lambda}^{(h)}}\right]_{qr} &= \left\| \begin{bmatrix} \left[\boldsymbol{\Gamma}^{\mathrm{obj},\boldsymbol{\Lambda}^{(h)}}\right]_{qr} \\ \left[\boldsymbol{\Gamma}^{\mathrm{cons},\boldsymbol{\Lambda}^{(h)}}\right]_{qr} \end{bmatrix} \right\|_2 , \\
&\leq \left\| \sum_{\pi_q=1}^{l_q^{(h)}} \lambda_{q,\pi_q}^{(h)} \begin{bmatrix} \left[\boldsymbol{\Gamma}^{\mathrm{obj},\left(\boldsymbol{\pi}^{(h)}\right)}\right]_{qr} \\ \left[\boldsymbol{\Gamma}^{\mathrm{cons},\left(\boldsymbol{\pi}^{(h)}\right)}\right]_{qr} \end{bmatrix} \right\|_2 , \\
&\leq \sum_{\pi_q=1}^{l_q^{(h)}} \lambda_{q,\pi_q}^{(h)} \left\| \begin{bmatrix} \left[\boldsymbol{\Gamma}^{\mathrm{obj},\left(\boldsymbol{\pi}^{(h)}\right)}\right]_{qr} \\ \left[\boldsymbol{\Gamma}^{\mathrm{cons},\left(\boldsymbol{\pi}^{(h)}\right)}\right]_{qr} \end{bmatrix} \right\|_2 = \sum_{\pi_q=1}^{l_q^{(h)}} \left[\boldsymbol{\Gamma}^{,\left(\boldsymbol{\pi}^{(h)}\right)}\right]_{qr} ,
\end{aligned}$$

from the monotonicity of the 2-norm and the triangular inequality [99, Prop. 9.1.2, Def. 9.1.1]. Building on Proposition 3.4 to translate the $\boldsymbol{\Gamma}$ convergence matrices into $\boldsymbol{\Upsilon}$ matrices, one obtains an inequality similar to the one of Lemma 3.1. Finally, the proof given in Section 3.7.3 can be leverage upon to show that the above element-wise inequality ensures that if $\rho\left(\boldsymbol{\Gamma}^{\left(\boldsymbol{\pi}^{(h)}\right)}\right) < 1$ whatever $\boldsymbol{\pi}^{(h)} \in \Pi^{(h)}$, then $\rho\left(\boldsymbol{\Gamma}^{\boldsymbol{\Lambda}^{(h)}}\right) < 1$ whatever $\boldsymbol{\Lambda}^{(h)} \in \Delta^{\times,(h)}$. The converse also holds, since the underlying games are particular scalarised games.

5.7.2 RA scenario analysis

First, the linearly independent constraints sets which can be active at the same time, with at least one constraint depending on the other players, must be identified. Such sets always include the (A_q+2)th constraint since it is the only one depending on the other players. To preserve a linearly independent set, considering an active (A_q+2)th constraint and the active equality constraint, only $A_q - 1$ other constraints can be active. Two cases are possible, depending on whether the power constraint is active, or not. The set $\mathfrak{I}_{qr}^{\dagger}$ is thus given by $\mathfrak{I}_{qr}^{\dagger} = \mathfrak{I}_{qr}^{\dagger,(1)} \cup \mathfrak{I}_{qr}^{\dagger,(2)}$, with

$$\begin{aligned}
\mathfrak{I}_{qr}^{\dagger,(1)} &= \{\mathcal{S} \subseteq \{1,\dots,A_q+1\} | |\mathcal{S}| \leq A_q - 2\} \cup \{A_q+2, A_q+3\} , \\
\mathfrak{I}_{qr}^{\dagger,(2)} &= \{\mathcal{S} \subseteq \{1,\dots,A_q+1\} | |\mathcal{S}| \leq A_q - 1\} \cup \{A_q+2\} .
\end{aligned}$$

The analysis for the constraint sets in $\mathfrak{I}_{qr}^{\dagger,(2)}$ is identical to the one provided in Section 4.6.2, and it leads to

$$\max_{\substack{\mathbf{x}\in\mathcal{X}\\ \mathcal{I}\in\mathfrak{I}_{qr}^{\dagger,(2)}}} \left\{\sigma_{\max}\left(\left(\mathbf{E}_{qr,\mathcal{I}}\mathbf{\Pi}_{qr,\mathcal{I}}\right)^{+}\mathbf{G}_{qr,\mathcal{I}}\left(\mathbf{x}_{-q}\right)\right)\right\}$$
$$= \frac{\epsilon_{q,1}}{\prod_{p\neq q}\left(1-x_p^{\max}\right)}\frac{1}{\left(1-x_r^{\max}\right)}\frac{\sqrt{2}}{\min_{i=0,\dots,A_q-1}\left|r_{q,i}-r_{q,i+1}\right|}. \tag{5.14}$$

The following of the proof focuses thus on the constraint sets in $\mathfrak{I}_{qr}^{\dagger,(1)}$, i.e., those with the maximum power constraint active. Given $\mathcal{I}\in\mathfrak{I}_{qr}^{\dagger,(1)}$, the indices of the active lower-bounds are defined as $\mathcal{I}^{\mathrm{a}}\triangleq\mathcal{I}\setminus\{A_q+2,A_q+3\}$ and their number is denoted by $N\triangleq|\mathcal{I}|-2$. The variables not constrained by the lower bounds are indexed in $\mathcal{I}^{\mathrm{Na}}=\{1,\dots,A_q+1\}\setminus\mathcal{I}^{\mathrm{a}}$, and their number is defined as $m\triangleq A_q+1-N$. The elements of $\mathbf{r}_q$ related respectively to the variables constrained by the lower bounds, and those for which it is not the case, are grouped into $\mathbf{r}_{q,\mathcal{I}^{\mathrm{a}}}$ and $\mathbf{r}_{q,\mathcal{I}^{\mathrm{Na}}}$, and similarly for the vector $\mathbf{p}_q$ which is split into $\mathbf{p}_{q,\mathcal{I}^{\mathrm{a}}}$ and $\mathbf{p}_{q,\mathcal{I}^{\mathrm{Na}}}$. With these definitions, the matrices instrumental to the definition of the convergence matrix are obtained as

$$\mathbf{E}_{qr,\mathcal{I}}=\begin{bmatrix}-\mathbf{r}_{q,\mathcal{I}^{\mathrm{a}}}^{\top} & -\mathbf{r}_{q,\mathcal{I}^{\mathrm{Na}}}^{\top}\end{bmatrix},\quad \mathbf{F}_{qr,\mathcal{I}}=\begin{bmatrix}-\mathbf{I}_N & \mathbf{0}_{N\times m}\\ \mathbf{F}_{qr,\mathcal{I}^{\mathrm{a}}} & \mathbf{F}_{qr,\mathcal{I}^{\mathrm{Na}}}\end{bmatrix},$$
$$\mathbf{G}_{qr,\mathcal{I}}\left(\mathbf{x}_{-q}\right)=\begin{bmatrix}\frac{\epsilon_{q,1}}{\prod_{p\neq q}x_{p,0}}\frac{1}{x_{r,0}},0,\dots,0\end{bmatrix},$$

with

$$\mathbf{F}_{qr,\mathcal{I}^{\mathrm{a}}}=\begin{bmatrix}\mathbf{p}_{q,\mathcal{I}^{\mathrm{a}}}^{\top}\\ \mathbf{1}_N^{\top}\end{bmatrix},\quad \mathbf{F}_{qr,\mathcal{I}^{\mathrm{Na}}}=\begin{bmatrix}\mathbf{p}_{q,\mathcal{I}^{\mathrm{Na}}}^{\top}\\ \mathbf{1}_m^{\top}\end{bmatrix}.$$

The matrix $\mathbf{\Pi}_{qr,\mathcal{I}}$ is the projector onto the null space of $\mathbf{F}_{qr,\mathcal{I}}$, and it is obtained as

$$\mathbf{\Pi}_{qr,\mathcal{I}}=\begin{bmatrix}\mathbf{0}_{N\times N} & \mathbf{0}_{N\times m}\\ \mathbf{0}_{m\times N} & \mathbf{I}_m-\left(\mathbf{F}_{qr,\mathcal{I}^{\mathrm{Na}}}\right)^{+}\mathbf{F}_{qr,\mathcal{I}^{\mathrm{Na}}}\end{bmatrix}.$$

The above is either obtained after lengthy matrix developments which include the use of [99, Fact 2.17.3, Cor. 2.8.8], or by noticing that the projector onto the null space of $\mathbf{F}_{qr,\mathcal{I}}$ must set the first N elements to 0, while the

m last must belong to the null space of $\mathbf{F}_{qr,\mathcal{I}^{\mathrm{Na}}}$, $\mathbf{I}_m - \left(\mathbf{F}_{qr,\mathcal{I}^{\mathrm{Na}}}\right)^+ \mathbf{F}_{qr,\mathcal{I}^{\mathrm{Na}}}$ being the projector onto this null space. Following similar steps as those of Section 4.6.2,

$$\max_{\mathbf{x}\in\mathcal{X}} \sigma_{\max}\left(\left(\mathbf{E}_{qr,\mathcal{I}}\mathbf{\Pi}_{qr,\mathcal{I}}\right)^+ \mathbf{G}_{qr,\mathcal{I}}\left(\mathbf{x}_{-q}\right)\right)$$
$$= \frac{\frac{\epsilon_{q,1}}{\prod_{p\neq q}\left(1-x_p^{\max}\right)}\frac{1}{\left(1-x_r^{\max}\right)}}{\left\|\left(\mathbf{I}_m - \left(\mathbf{F}_{qr,\mathcal{I}^{\mathrm{Na}}}\right)^+ \mathbf{F}_{qr,\mathcal{I}^{\mathrm{Na}}}\right)\mathbf{r}_{q,\mathcal{I}^{\mathrm{Na}}}\right\|_2}.$$

It remains thus to investigate the value of $\left\|\left(\mathbf{I}_m - \left(\mathbf{F}_{qr,\mathcal{I}^{\mathrm{Na}}}\right)^+ \mathbf{F}_{qr,\mathcal{I}^{\mathrm{Na}}}\right)\mathbf{r}_{q,\mathcal{I}^{\mathrm{Na}}}\right\|_2$ in order to determine which constraints set of $\mathfrak{I}_{qr}^{\dagger,(1)}$ lead to the maximum of the above. To that aim, the following notations are introduced:

$$\begin{aligned}
\overline{r}_{q,\mathcal{I}^{\mathrm{Na}}} &\triangleq \frac{\mathbf{1}_m^\top \mathbf{r}_{q,\mathcal{I}^{\mathrm{Na}}}}{m} = \frac{1}{m}\sum_{i\in\mathcal{I}^{\mathrm{Na}}} r_{q,i},\\
\mathbf{r}_{q,\mathcal{I}^{\mathrm{Na}},c} &\triangleq \mathbf{r}_{q,\mathcal{I}^{\mathrm{Na}}} - \overline{r}_{q,\mathcal{I}^{\mathrm{Na}}}\mathbf{1}_m,\\
\overline{p}_{q,\mathcal{I}^{\mathrm{Na}}} &\triangleq \frac{\mathbf{1}_m^\top \mathbf{p}_{q,\mathcal{I}^{\mathrm{Na}}}}{m} = \frac{1}{m}\sum_{i\in\mathcal{I}^{\mathrm{Na}}} p_{q,i},\\
\mathbf{p}_{q,\mathcal{I}^{\mathrm{Na}},c} &\triangleq \mathbf{p}_{q,\mathcal{I}^{\mathrm{Na}}} - \overline{p}_{q,\mathcal{I}^{\mathrm{Na}}}\mathbf{1}_m,\\
\cos\left(\theta_{q,\mathcal{I}^{\mathrm{Na}}}\right) &\triangleq \frac{\mathbf{r}_{q,\mathcal{I}^{\mathrm{Na}},c}^\top \mathbf{p}_{q,\mathcal{I}^{\mathrm{Na}},c}}{\left\|\mathbf{r}_{q,\mathcal{I}^{\mathrm{Na}},c}\right\|_2\left\|\mathbf{p}_{q,\mathcal{I}^{\mathrm{Na}},c}\right\|_2}.
\end{aligned}$$

With the above definition, developing the expression of the 2-norm, it comes that

$$\begin{aligned}
&\left(\mathbf{I}_m - \left(\mathbf{F}_{qr,\mathcal{I}^{\mathrm{Na}}}\right)^+ \mathbf{F}_{qr,\mathcal{I}^{\mathrm{Na}}}\right)\mathbf{r}_{q,\mathcal{I}^{\mathrm{Na}}}\\
&= \mathbf{r}_{q,\mathcal{I}^{\mathrm{Na}}} + \left(\overline{p}_{q,\mathcal{I}^{\mathrm{Na}}}\cos\left(\theta_{q,\mathcal{I}^{\mathrm{Na}}}\right)\frac{\left\|\mathbf{r}_{q,\mathcal{I}^{\mathrm{Na}},c}\right\|_2}{\left\|\mathbf{p}_{q,\mathcal{I}^{\mathrm{Na}},c}\right\|_2} - \overline{r}_{q,\mathcal{I}^{\mathrm{Na}}}\right)\mathbf{1}_m\\
&\qquad - \cos\left(\theta_{q,\mathcal{I}^{\mathrm{Na}}}\right)\frac{\left\|\mathbf{r}_{q,\mathcal{I}^{\mathrm{Na}},c}\right\|_2}{\left\|\mathbf{p}_{q,\mathcal{I}^{\mathrm{Na}},c}\right\|_2}\mathbf{p}_{q,\mathcal{I}^{\mathrm{Na}}},\\
&= \mathbf{r}_{q,\mathcal{I}^{\mathrm{Na}},c} - \cos\left(\theta_{q,\mathcal{I}^{\mathrm{Na}}}\right)\frac{\left\|\mathbf{r}_{q,\mathcal{I}^{\mathrm{Na}},c}\right\|_2}{\left\|\mathbf{p}_{q,\mathcal{I}^{\mathrm{Na}},c}\right\|_2}\mathbf{p}_{q,\mathcal{I}^{\mathrm{Na}},c}.
\end{aligned}$$

Therefore, this leads to

$$\begin{aligned}\left\|\left(\mathbf{I}_m - \left(\mathbf{F}_{qr,\mathcal{I}^{\mathrm{Na}}}\right)^+ \mathbf{F}_{qr,\mathcal{I}^{\mathrm{Na}}}\right) \mathbf{r}_{q,\mathcal{I}^{\mathrm{Na}}}\right\|_2 &= \left\|\mathbf{r}_{q,\mathcal{I}^{\mathrm{Na}},c}\right\|_2 \sqrt{1-\cos^2\left(\theta_{q,\mathcal{I}^{\mathrm{Na}}}\right)},\\ &= \left\|\mathbf{r}_{q,\mathcal{I}^{\mathrm{Na}},c}\right\|_2 \left|\sin\left(\theta_{q,\mathcal{I}^{\mathrm{Na}}}\right)\right|.\end{aligned}$$

It remains to determine which subsets $\mathcal{I}^{\mathrm{Na}}$ lead to the minimal value of $\left\|\mathbf{r}_{q,\mathcal{I}^{\mathrm{Na}},c}\right\|_2 \left|\sin\left(\theta_{q,\mathcal{I}^{\mathrm{Na}}}\right)\right|$. To that aim, the set $\mathcal{I}^{\mathrm{Na}} \setminus \{i_0\}$ is considered, being of size $m-1$. The following then holds

$$\begin{aligned}\mathbf{r}_{q,\mathcal{I}^{\mathrm{Na}},c} &= \begin{bmatrix}\mathbf{r}_{q,\mathcal{I}^{\mathrm{Na}}\setminus\{i_0\},c} - \Delta_r\sqrt{\frac{1}{m(m-1)}}\mathbf{1}_{m-1}\\ \sqrt{\frac{m-1}{m}}\Delta_r\end{bmatrix},\\ \mathbf{p}_{q,\mathcal{I}^{\mathrm{Na}},c} &= \begin{bmatrix}\mathbf{p}_{q,\mathcal{I}^{\mathrm{Na}}\setminus\{i_0\},c} - \Delta_p\sqrt{\frac{1}{m(m-1)}}\mathbf{1}_{m-1}\\ \sqrt{\frac{m-1}{m}}\Delta_p\end{bmatrix},\end{aligned}$$

with $\Delta_r \triangleq (r_{q,i_0} - \overline{r}_{q,\mathcal{I}^{\mathrm{Na}}\setminus\{i_0\}})\sqrt{m-1}/\sqrt{m}$ and $\Delta_p \triangleq (p_{q,i_0} - \overline{p}_{q,\mathcal{I}^{\mathrm{Na}}\setminus\{i_0\}})\sqrt{m-1}/\sqrt{m}$. Therefore,

$$\begin{aligned}&\left\|\mathbf{r}_{q,\mathcal{I}^{\mathrm{Na}},c}\right\|_2^2 = \left\|\mathbf{r}_{q,\mathcal{I}^{\mathrm{Na}}\setminus\{i_0\},c}\right\|_2^2 + \Delta_r^2,\\ &\left\|\mathbf{p}_{q,\mathcal{I}^{\mathrm{Na}},c}\right\|_2^2 = \left\|\mathbf{p}_{q,\mathcal{I}^{\mathrm{Na}}\setminus\{i_0\},c}\right\|_2^2 + \Delta_p^2,\\ &\cos^2\left(\theta_{q,\mathcal{I}^{\mathrm{Na}}}\right) = \frac{\left(\cos\left(\theta_{q,\mathcal{I}^{\mathrm{Na}}\setminus\{i_0\}}\right)\left\|\mathbf{r}_{q,\mathcal{I}^{\mathrm{Na}}\setminus\{i_0\},c}\right\|_2 \left\|\mathbf{p}_{q,\mathcal{I}^{\mathrm{Na}}\setminus\{i_0\},c}\right\|_2 + \Delta_p\Delta_r\right)^2}{\left(\left\|\mathbf{p}_{q,\mathcal{I}^{\mathrm{Na}}\setminus\{i_0\},c}\right\|_2^2 + \Delta_p^2\right)\left(\left\|\mathbf{r}_{q,\mathcal{I}^{\mathrm{Na}}\setminus\{i_0\},c}\right\|_2^2 + \Delta_r^2\right)}.\end{aligned}$$

After manipulating the expressions, this leads to

$$\begin{aligned}&\left\|\mathbf{r}_{q,\mathcal{I}^{\mathrm{Na}},c}\right\|_2^2\left(1-\cos^2\left(\theta_{q,\mathcal{I}^{\mathrm{Na}}}\right)\right) - \left\|\mathbf{r}_{q,\mathcal{I}^{\mathrm{Na}}\setminus\{i_0\},c}\right\|_2^2\left(1-\cos^2\left(\theta_{q,\mathcal{I}^{\mathrm{Na}}\setminus\{i_0\}}\right)\right)\\ &= \frac{\left(\Delta_r\left\|\mathbf{p}_{q,\mathcal{I}^{\mathrm{Na}}\setminus\{i_0\},c}\right\|_2 - \Delta_p\left\|\mathbf{r}_{q,\mathcal{I}^{\mathrm{Na}}\setminus\{i_0\},c}\right\|_2\cos\left(\theta_{q,\mathcal{I}^{\mathrm{Na}}\setminus\{i_0\}}\right)\right)^2}{\left\|\mathbf{p}_{q,\mathcal{I}^{\mathrm{Na}}\setminus\{i_0\},c}\right\|_2^2 + \Delta_p^2}.\end{aligned}$$

The above shows thus that the minimal value of $\left\|\mathbf{r}_{q,\mathcal{I}^{\mathrm{Na}},c}\right\|_2 \left|\sin\left(\theta_{q,\mathcal{I}^{\mathrm{Na}}}\right)\right|$ is obtained with the set $\mathcal{I}^{\mathrm{Na}}$ with the minimal number of elements. Yet, since in $\mathfrak{I}_{qr}^{\dagger,(1)}$, the number of active lower bounds is bounded by $N = |\mathcal{I}| - 2 \leq A_q - 2$, the set $\mathcal{I}^{\mathrm{Na}}$ has a size $m = A_q + 1 - N \geq 3$. Therefore, only the sets of size 3 must be considered. To conclude the analysis, as for the GNEP case, the invertible matrix $\mathbf{T} = \mathrm{Diag}\left(\left[\frac{1}{1-x_1^{\max}}, \ldots, \frac{1}{1-x_Q^{\max}}\right]\right)$ is introduced to obtain

$\rho(\mathbf{\Gamma}) = \rho\left(\mathbf{T}\mathbf{\Gamma}\mathbf{T}^{-1}\right)$ [99, Fact 4.45.xii].

6

Conclusion on the autonomous interference analysis and management

This chapter provides an overview of the results obtained in the analysis of the MO interactions between players. Section 6.1 first synthesises the developed theoretical frameworks, while a bird's eye view of the insights gained for the two MF MP applicative scenarios is given in Section 6.2.

6.1 Bird's eye view of the MOG results

The perspective considered in the above chapters has been to obtain convergence guarantees for the totally asynchronous BRD of the scalarised games associated with a MOG. The obtained theoretical results are summarised in Table 6.1, differentiating the impact of the interactions between the objective functions, and between the strategy sets.

Indeed, the different flavours of scalarised games may either be NEPs or GNEPs, depending on whether the constraints of a player depend on the strategy of the others. While BRD convergence guarantees were existing

	Objective functions	Strategy sets
	$\underset{\mathbf{x}_q}{\text{minimise}} \quad u_q(\mathbf{x})$ $\text{s.t.} \quad \mathbf{P}_q \mathbf{x}_q \leq \boldsymbol{\gamma}_q(\mathbf{x}_{-q})$	
Requirements	Strong convexity 2nd differentiability	Polyhedral with variable RHSs Constraint qualification 1st differentiability Perturbation insensitivity
Convergence condition	$\rho(\boldsymbol{\Gamma}) < 1$ $[\boldsymbol{\Gamma}]_{qr} = \sqrt{\left[\boldsymbol{\Gamma}^{\text{obj}}\right]_{qr}^2 + \left[\boldsymbol{\Gamma}^{\text{cons}}\right]_{qr}^2}$	
Convergence matrix	$\left[\boldsymbol{\Gamma}^{\text{obj}}\right]_{qr} = \max_{\mathbf{x}} \frac{\sigma_{\max}\left(\boldsymbol{\nabla}^2_{\mathbf{x}_r\mathbf{x}_q} u_q(\mathbf{x})\right)}{\lambda_{\min}\left(\boldsymbol{\nabla}^2_{\mathbf{x}_q\mathbf{x}_q} u_q(\mathbf{x})\right)}$	$\left[\boldsymbol{\Gamma}^{\text{cons}}\right]_{qr} = \max_{\mathbf{x},\mathcal{I}} \kappa\left(\boldsymbol{\nabla}^2_{\mathbf{x}_q\mathbf{x}_q} u_q(\mathbf{x})\right) \sigma_{\max}\left(\mathbf{P}^+_{q,\mathcal{I}} \boldsymbol{\nabla}_{\mathbf{x}_r} \boldsymbol{\gamma}_{q,\mathcal{I}}(\mathbf{x}_{-q})\right)$
Interpretation	Measure of the impact of $\mathbf{x}_r$ on the minimiser of u_q	Measure of the impact of $\mathbf{x}_r$ on the RHS constraint terms Measure of the linear dependency of the active constraints
Preference awareness	Preference agnostic if all underlying games satisfy the convergence conditions Polyhedral preference subsets may be considered	Preference aware

Table 6.1 Bird's eye view of the MOG results. The cells with a background colour correspond to the results which were existing in the literature.

in the literature for NEPs [55], they were lacking for the GNEPs. In Chapter 4, a unifying framework has hence been obtained for both NEPs and GNEPs, when their strategy sets are polyhedral with variable RHSs. In this framework, the guarantees are obtained by verifying the spectral radius of a convergence matrix is smaller than one, this matrix measuring at the same time the objective function and the constraint interactions. On the objective function side, the matrix elements are almost identical to those of the literature, measuring how quickly the optimum strategy of a player changes when the other players modify their own strategy. On the constraint side, the convergence matrix elements depend on the speed at which the constraints are translated given a change of strategy of the other players, as well as on the linear dependency which may exist between the active constraints.

The developed GNEP framework enables therefore the study of the scalarised games associated with a MOG. Such analysis however still depends on the specific considered scalarised game, through the weights of the weighted-sum objective function, and through the constraint thresholds. In order to truly encompass the MO character of the nodes, the goal is to obtain guarantees which hold whatever the value of these weights and thresholds, i.e., whatever the preferences of the players. This thus differentiates the *preference-aware* from the *preference-agnostic* analyses. In Chapter 3 and Chapter 5, it is shown that it is possible to obtain conditions ensuring BRD convergence whatever the weighted-sum scalarisation weights. These conditions hinge upon the underlying games associated with the scalarised games, being the games obtain when each player selects a single objective function. On the contrary, Chapter 5 discusses the reasons why obtaining convergence conditions which hold whatever the constraint thresholds is challenging.

6.2 Bird's eye view of the multi-function multi-point use-cases

The developed theoretical framework has been applied on two MF MP scenarios. First, the power allocation on the OFDM tones of a JRC system has been considered, the nodes interacting through the interference generated on each tone. Secondly, a multi-level RA scheme has been studied, the nodes interacting through the collisions occurring between their communications.

JRC scenario A synthesis of the analysis performed on the JRC scenario is presented in Table 6.2. The metrics of this scenario are the radar and communication rates. When kept as objective functions, the strong convexity of these metrics makes possible the analysis of the games. The associated BRs have a waterfilling-like expression, the water level being computed efficiently with binary search methods. As far as the convergence of the BRD is concerned, the analysis reveals that it is likely to occur when the

<table>
<tr><td></td><td colspan="3">$$\begin{aligned} \underset{\mathbf{p}_q}{\text{minimise}} \quad & \begin{bmatrix} \sum_k \ln\left(1 + \frac{p_{q,k}}{\xi_{q,k}(\mathbf{p}_{-q})}\right) \\ \sum_k \ln\left(1 + \frac{p_{q,k}}{\xi^{\star}_{q,k}(\mathbf{p}_{-q})}\right) \end{bmatrix} \\ \text{s.t.} \quad & \mathbf{p}_q \geq \mathbf{0} \\ & \sum_k p_{q,k} = P_q \end{aligned}$$</td></tr>
<tr><td></td><td>Problem transform</td><td>BR computations</td><td>Insights</td></tr>
<tr><td>Weighted-sum</td><td>-</td><td>Waterfilling-like</td><td>Low interference</td></tr>
<tr><td>ϵ-constraint</td><td>-</td><td>Convex solver</td><td>-</td></tr>
<tr><td>Constraint satisfaction</td><td>-</td><td>Convex solver</td><td>-</td></tr>
</table>

Table 6.2 Bird's eye view of the analysis of the interactions in the JRC scenario. The coloured red cells depict the fact that for this scalarised game family, the assumptions required by the developed framework were not fulfilled, and therefore no analysis has been conducted.

interference between the players remain small.

Unfortunately, when set as constraints, the sum-rate metrics do not lead to linear inequalities with variable RHSs. While the BRs can be computed with convex-programming solvers, the developed framework cannot be applied to analyse the players' interaction. Therefore, the parameters which impact the convergence in the ϵ-constraint and constraint scalarisation games remain unknown.

Multi-level RA scenario In the multi-level RA scenario, the metrics of the players are the consumed power and average rate, being linear in the strategy of the considered player. Such linearity however does not fulfil the strong convexity requirements of the developed theoretic framework. To overcome this, a strongly regularisation term is added to the original metrics when they are kept as objective functions. This regularisation term is parameterised by a factor which when increased, makes the strong convexity parameter greater, but leads to coarser approximation of the original rate and power metrics. The autonomous insights are summarised in Table 6.3, and discussed below.

A studied in Section 3.5, in the weighted-sum scalarised game, the BR are

	$\underset{\mathbf{x}_q}{\text{minimise}} \begin{bmatrix} \mathbf{p}_q^\top \mathbf{x}_q \\ -\theta_q\left(\mathbf{x}_{-q}\right) \mathbf{r}_q^\top \mathbf{x}_q \end{bmatrix}$ s.t. $1 - x_q^{\max} \leq x_{q,0}$, $0 \leq x_{q,a_q}$, $\sum_{a_q} x_{q,a_q} = 1$		
	Problem transform	BR computations	Insights
Weighted-sum	Squared 2-norm regularisation	Waterfilling-like	Few activity levels
			Coarse approximation of the metrics
ϵ-constraint (rate maximisation)	Squared 2-norm regularisation	Quadratic solver	Few activity levels
		Alternating projection algorithm	Coarse approximation of the metrics
	Collision-free rate	Linear solver	No interactions
ϵ-constraint (power minimisation)	Squared 2-norm regularisation	Quadratic solver	Low maximum activity probability
		Alternating projection algorithm	Low rate requirement
		Linear solver	Activity levels with different rates
Constraint satisfaction		Quadratic solver	Low maximum activity probability
		Alternating projection algorithm	Low rate requirement
			Activity levels with different rates
			Non-linear rate-power relationship

Table 6.3 Bird's eye view of the analysis of the interactions in the RA scenario. The coloured red cells highlight the problematic insights.

expressed with waterfilling-like expressions, which can therefore efficiently be computed. The analysis reveals that BRD convergence is likely to occur when the players have few activity levels, and when the regularisation parameter is large. Since this latter implies that the rate and power metrics are only approximated coarsely, studying the MO interactions through the weighted-sum scalarised game family is questionable.

The same phenomenon happens when the ϵ-constraint scalarisation is considered, with the power objective is set as constraint. Nevertheless, as described in Section 4.4, the games might be slightly modified by considering the players maximise their rate, regardless of the collisions and thus on their communication success probability. In that case, the players are not interacting anymore, and thus the question of BRD convergence does not apply. The other ϵ-constraint scalarised game considers players minimising their power under a minimum rate requirement. While the power metric must be regularised for the assumptions to hold, the convergence guarantees do not depend on the value of the regularisation parameter, and therefore the approximation can be made as good as wanted. This explains why the players might compute their BR considering the unregularised metrics with a linear solver, if the complexity of the quadratic solver is too high. Regarding the insights, the GNEP analysis reveals that the maximum active probability of the players should be small, that the rate requirements should be small too, and that the activity levels must have significantly different rates.

Finally, the constraint satisfaction games have been studied, considering the players are equipped with designed square distances objective function. The same insights as those of the power minimisation ϵ-constraint game are obtained, yet with the addition of a fourth one. Indeed, for BRD convergence, the rate-power relationship must be as non-linear as possible.

6.3 General conclusion

The theoretical framework summary, as well as the results obtained for the MF MP scenarios, push us to draw the following guidelines for the study of MO interactions.

- As a rule of thumb, the convergence of the BRD is likely to occur when the players are slightly coupled. Therefore, in low to moderate coupling scenarios, the interference between the players may be managed autonomously. Highly coupled nodes however require dedicated centralised solutions, as their interaction might not settle to a stable point.

- When a node is characterised by several metrics, the strongly convex ones should be kept as objective functions, while the linear ones should be set as constraints. Doing so, the developed framework can be applied to analyse the interactions.

- An exception to the above arise when there are many linear functions. As the convergence conditions are harder to fulfil when the linear dependency between two constraints increases, having many constraints degrades the convergence guarantees.

- When a linear function is kept as an objective, it can be regularised by square 2-norm objectives. If another metric of the weighted-sum is strongly convex, then this regularisation can be avoided by considering subset of preferences, which will prevent the linear metric to be optimised alone.

Beside these guidelines, the following research directions are identified.

- The class of MF MP which can be tackled by the developed GNEP framework is limited by the polyhedral structure of the strategy sets. As discussed in the conclusion of Chapter 4, obtaining convergence guarantees for non-polyhedral convex sets is hence one of the key leads for future research.

- The second direction for future works tackles the problem of the constraint thresholds, on which the convergence conditions depend. Obtaining guarantees on the convergence of the BRD whatever the value of these thresholds would enable to have results fully agnostic about the preferences of the players.

- On the applicative side, the study of other MF MP scenarios is obviously of interest. Similarly to what has been done in this thesis, the output of such analysis would enable to identify the key parameters impacting the interactions between the nodes of the considered MF MP systems.

- In some cases, the assumptions required by the GT framework are however not fulfilled by the studied MF MP scenario, or the convergence conditions are not met. In these cases, ad-hoc optimisation-based interference management schemes should be designed. This will be the focus of the next part of this thesis.

Part II

Optimisation-based interference management

7

Coding-aware secure beamforming in cell-free networks

This chapter covers the contributions provided in the following papers of the author [134, 135].

This second thesis part focuses on optimisation-based interference management schemes. In these schemes, the resource allocation of a set of interfering nodes is jointly optimised. This offers the possibility to obtain resource allocation strategies which are globally optimal, contrarily to the equilibrium points reached with the autonomous approach. This may also enable to tackle cases in which the assumptions required by the autonomous approach are not met, or for which the BRD convergence conditions are too stringent.

Nevertheless, the challenges of the optimisation-based approach are twofold. First, the metrics of the nodes must be aggregated into a unique network-wide objective function, i.e., they must be scalarised. Depending on the choice of the scalarisation, the reached Pareto-optimal point may drastically differ. Some scalarisations might favour the performance of one node at the price of decreasing the performance of the others. Others might provide fair solutions, yet they might not leverage on the full potential of some nodes. Designing relevant global objective functions constitutes thus the first difficulty of the optimisation-based approach. The second results from the fact that inherently, the obtained optimisation problem are high-dimensional, since they involve the resources of many nodes. Therefore, the second challenge is to provide efficient way of reaching optimum points of these high-dimensional problems.

In this part, two instances of MF MP networks will be studied through the lens of this optimisation-based interference management. This chapter focuses on providing secure communications in a Cell-Free (CF) network, while Chapter 8 investigates the beamforming design in a JRC network.

7.1 Chapter introduction

This chapter studies the problem of transmitting information from a network of distributed antennas towards several legitimate users, while preventing information leakage towards malicious users, named the *eavesdroppers*. This scenario is therefore an instance of a MF MP network, in which the two functions are the communication and the security, and the multiple points are the legitimate users, the eavesdroppers, and the several transmitters.

The tackled problem falls into the field of *secure communications*, as defined by Claude Shannon in 1949 [136]. The bottom line of this concept is that perfectly secure communications can be achieved when the channel between the transmitter and the legitimate UE is of superior quality than the one towards the eavesdropper. When the transmitter is equipped with several antennas, the beamforming can actively degrade as much as possible the eavesdropper channel while guaranteeing a sufficient channel quality towards the targeted UE [137]. This process however depends on the scene geometry: blinding eavesdroppers located close to a legitimate user might be difficult, and it might be impossible to do so if an eavesdropper is on the Line-of-Sight (LoS) path between the transmitter and the legitimate receiver.

To address this issue, the coding scheme developed in [138] can be leveraged upon, which exploits parallel communication channels. While in the original paper, the parallel channels are obtained with different communication bands, the idea followed in this chapter is to use distributed antennas to provide spatial parallel channels, whose number is denoted

K. Instead of sending the raw signals on each channel, the secure scheme developed in [138] sends K independent linear combinations of the K signals, one combination on each channel. The targeted UE, upon reception of the K linear combinations, is able to recover the K signals by inverting the linear system. However, as soon as an eavesdropper misses one of the combinations, the recovery of the signals is impossible. This impossibility is proven in terms of zero mutual information between the received linear combinations and any of the raw signals [138].

This coding scheme drastically changes the way beamforming is performed. While traditionally, it must be ensured all eavesdroppers misses the signals of all channels, the goal becomes to ensure that each eavesdropper misses the signal of at least one channel. To that aim, frequency-dependent antenna radiation patterns have been leveraged upon in [139], and beamformers have been designed in [140]. In this thesis, we consider the case of the distributed antennas of a CF network [141], and investigate how the distributed nature of this network might enable to blind eavesdroppers even if they benefit from good channel conditions. The detailed contributions are the following.

- A coding-aware beamforming design optimisation problem is formulated, which leverages upon the secure parallel communication scheme of [138], for CF networks with multiple transmitters, receivers and eavesdroppers.

- Locally optimal beamformers are obtained as the output of a successive minimisation algorithm. The sub-problems which must be tackled are reformulated in a standard convex conic form, so that they can efficiently be solved at each iteration.

- The beamforming methods are validated numerically, showing significant gains with respect to traditional secure beamformers. In particular, the security-rate trade-off, as well as the security-eavesdropper closeness trade-off is emphasised.

To that aim, the system model is provided in Section 7.2, as well as the beamforming optimisation problems. The algorithms providing a solution to these problems are presented in Section 7.3, and their performance is numerically evaluated in Section 7.4.

7.2 System model

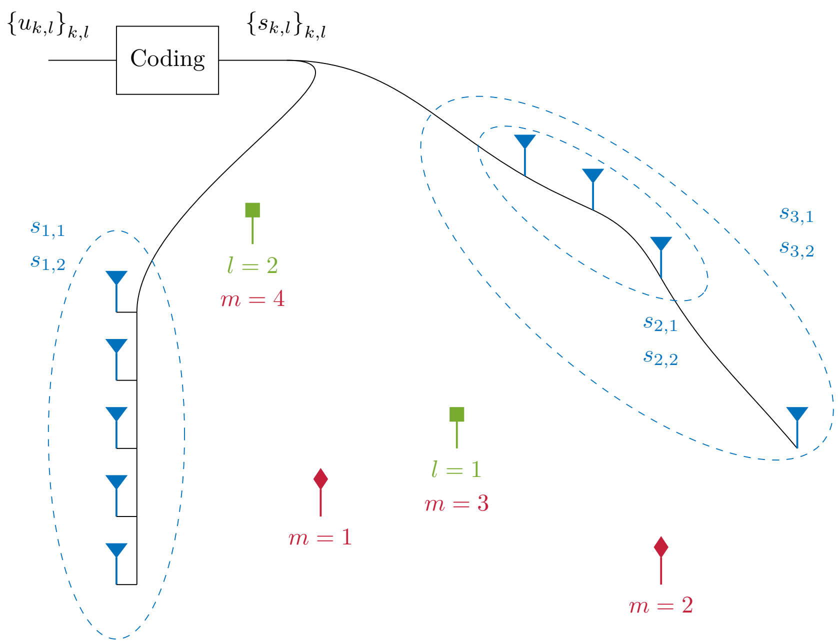

Fig. 7.1 Illustration of the system model of the coding-aware secure beamforming scheme, with L=2 legitimate UEs, $M = 4$ eavesdroppers, and with the information coded onto $K = 3$ symbols. The blue triangular antennas are the emitting antennas, the green square ones are the legitimate UEs while the diamond ones are the eavesdroppers. The blue ellipses represent the groups of antennas associated with one of the resource elements.

CF model A CF network is considered, with L UEs and M eavesdroppers, all equipped with a single-antenna. They are located respectively at the positions $\{\mathbf{y}_l\}_l$, and $\{\mathbf{z}_m\}_m$, the notation $\{\cdot\}_l$ implicitly denoting $\{\cdot\}_{l=1}^{L}$, and similarly for the other indices. The eavesdroppers are associated with positive weights $\{\beta_{l,m}\}_{l,m}$ which depict the relative importance of the mth eavesdropper for the lth UE, $\beta_{l,m} = 0$ implying it is not considered as a malicious user. These weights enable among others to include the UEs in the eavesdroppers' set, but to have a 0 weight for each UE with respect to himself. In the setting of Figure 7.1, these weights could be given by

$$\begin{bmatrix} \beta_{1,1} & \beta_{1,2} & \beta_{1,3} & \beta_{1,4} \\ \beta_{2,1} & \beta_{2,2} & \beta_{2,3} & \beta_{2,4} \end{bmatrix} = \begin{bmatrix} 1 & 1 & 0 & 1 \\ 1 & 1 & 1 & 0 \end{bmatrix},$$

implying that the communication of a UE must be protected against the two eavesdroppers and the other UE.

Communication metrics In order to provide secure communications, the following strategy is investigated. The CF network splits its communication resources into K orthogonal Resource Elements (REs), typically in the time or frequency domain. At each time slot, the CF network processes K symbols for each UE, leading to a total of KL symbols. The kth symbol of each lth UE is denoted $s_{k,l}$, and it is allocated to the kth REs. As the UEs share the same resources, interference occurs on each RE, and thus the different UE locations are exploited to separate them in the space domain thanks to the beamforming design. To that aim, each RE is associated with N_k antennas of the CF network. The sets of antennas serving the different REs might have total, partial or zero overlap. The channel vector of the kth RE towards an antenna at location $\mathbf{p}$ is denoted $\mathbf{h}_{k,(\mathbf{p})}$. Considering LoS propagation, it is given by [142]

$$\mathbf{h}_{k,(\mathbf{p})} = \left[L\left(r^{(1)}_{k,(\mathbf{p})}\right) e^{j\frac{2\pi}{\lambda_k} r^{(1)}_{k,(\mathbf{p})}}, \dots, L\left(r^{(N_k)}_{k,(\mathbf{p})}\right) e^{j\frac{2\pi}{\lambda_k} r^{(N_k)}_{k,(\mathbf{p})}} \right]^{\top},$$

with $r^{(n)}_{k,(\mathbf{p})}$ the distance between the nth antenna of the kth RE and the location $\mathbf{p}$, $L\left(r\right)$ the channel gain function, and λ_k the wavelength associated with the kth RE carrier frequency. The signal received on the kth RE at a location $\mathbf{p}$ reads thus as

$$r_{k,(\mathbf{p})} = \sum_{l=1}^{L} \mathbf{h}^{\mathrm{H}}_{k,(\mathbf{p})} \mathbf{w}_{k,l} s_{k,l} + n_k,$$

with $\mathbf{w}_{k,l} \in \mathbb{C}^{N_k}$ the beamforming vector of the symbol $s_{k,l}$, and n_k the Additive White Gaussian Noise (AWGN) realisation of the kth RE, with variance σ_n^2. Denoting the channel vectors of the lth UE as $\mathbf{h}_{k,l} \triangleq \mathbf{h}_{k,(\mathbf{y}_l)}$, the received signal on the kth resource element at the lth UE reads therefore as

$$r_{k,l} = \mathbf{h}_{k,l}^{\mathrm{H}} \mathbf{w}_{k,l} s_{k,l} + \underbrace{\sum_{l' \neq l} \mathbf{h}_{k,l}^{\mathrm{H}} \mathbf{w}_{k,l'} s_{k,l'}}_{\text{MUI}} + n_k,$$

the Multi-User Interference (MUI) being emphasised. Considering this MUI as noise, the SINR of the kth symbol of the lth UE is thus given by

$$\mathrm{SINR}_{k,l} = \frac{\left|\mathbf{h}_{k,l}^{\mathrm{H}} \mathbf{w}_{k,l}\right|^2}{\sigma_n^2 + \sum_{l' \neq l} \left|\mathbf{h}_{k,l}^{\mathrm{H}} \mathbf{w}_{k,l'}\right|^2}, \tag{7.1}$$

with unit-energy symbols. To mitigate the MUI, techniques such as successive interference cancellation could be employed. Yet, they are difficult to operate in practical settings. Thus, the above SINR expression is considered, providing in any case a lower bound to the actual SINR. On the contrary, to ensure secure communications, the eavesdroppers must be assumed to be performant enough to successfully suppress all the MUI. The mth eavesdropper is thus impacted by the following Signal-to-Noise Ratio (SNR) for the kth symbol of the lth user:

$$\mathrm{SNR}_{k,l,m} = \frac{\left|\mathbf{g}_{k,m}^{\mathrm{H}} \mathbf{w}_{k,l}\right|^2}{\sigma_n^2}, \tag{7.2}$$

with $\mathbf{g}_{k,m} \triangleq \mathbf{h}_{k,(\mathbf{z}_m)}$. The eavesdroppers are associated with an SNR sensitivity δ, or equivalently a power sensitivity $\delta\sigma_n^2$, under which they are unable to perform decoding [138].

Coding scheme Two possibilities are investigated for the symbols $s_{k,l}$. In the traditional case, the symbols $s_{k,l}$ are the information symbols $u_{k,l}$, and they are thus all sensitive to information leakage. In the second-case, the scheme of [138] is employed, meaning the K symbols of the lth UE are obtained as an invertible linear transform of his K information symbols. Such a rate-one linear coding has the following properties: i) upon reception of the K linear combinations, the linear system can be inverted to recover the information messages, and ii) as soon as one of the linear combinations is missing, none of the information symbols $u_{k,l}$ can be recovered [138]. It should be emphasised that such an impossibility can be proven in terms of zero mutual information, and thus that it is an information-theoretic guarantee.

Remark 7.1

In order for the legitimate users to recover the information symbols without errors, error-correcting codes are required. Yet, in order to preserve the zero mutual information property, this step must be performed adequately.
The error-correction mechanism cannot be applied to the information symbols. Indeed, the zero mutual information guarantee is valid if and only if the information symbols are independent one from the others. When this is not the case, an eavesdropper could use the public knowledge of the error-correcting code to break the security of the information.
The error-correction mechanism can neither be applied across the set of coded symbols which are produced at each time slot. If this is the case, then the eavesdropper can benefit from the error-correction provided by the code. Thus, he may be able to recover the information symbols even if he does not get one of the coded symbol.
What can be done, however, is applying the error-correcting code separately for each k and l, across the symbols transmitted at the different time slots. In that case, considering a static scenario, the eavesdropper misses all the symbols corresponding to one (k,l)-pair, and therefore physical layer security is preserved.

Information leakage metrics Given $\mathbf{w} \triangleq \{\mathbf{w}_{k,l}\}_{k,l}$, the information leakage metrics of the lth user towards the mth eavesdropper are defined, respectively in the traditional and coded case, as

$$\overline{\mathcal{L}}_{l,m}(\mathbf{w}) \triangleq \max_{k=1,\ldots K} \max\{\mathrm{SNR}_{k,l,m} - \delta, 0\}, \tag{7.3}$$

$$\underline{\mathcal{L}}_{l,m}(\mathbf{w}) \triangleq \min_{k=1,\ldots K} \max\{\mathrm{SNR}_{k,l,m} - \delta, 0\}. \tag{7.4}$$

In the traditional case, as all symbols contain uncoded sensitive information, the RE with the highest SNR impacts the information leakage, justifying the maximum operator. Contrarily, thanks to the linear coding scheme, the resource with the lowest SNR matters in the second case, hence the minimum over the REs. In both cases, if the metric is equal to 0, then secure communications are guaranteed. As it will be discussed below, minimising $\underline{\mathcal{L}}_{l,m}(\mathbf{w})$ is difficult since it is neither convex, nor convex in the beamforming vectors of one RE, with those of the other REs fixed. Hence, even considering each RE sub-problem leads to a complicated optimisation. The metric $\underline{\mathcal{K}}_{l,m}$ is hence introduced as a proxy to (7.4) as

$$\underline{\mathcal{K}}_{l,m}(\mathbf{w}) \triangleq \prod_{k=1}^{K} \max\left\{\mathrm{SNR}_{k,l,m} - \delta, 0\right\}. \tag{7.5}$$

From the generalised mean inequality, it satisfies $0 \leq \underline{\mathcal{L}}_{l,m} \leq \sqrt[K]{\underline{\mathcal{K}}_{l,m}}$, providing an upper-bound to the information leakage, and ensuring secure communications when $\underline{\mathcal{K}}_{l,m} = 0$. While the above is still not convex, its advantage is that it is convex in each RE beamforming vectors $\{\mathbf{w}_{k,l}\}_{l=1}^{L}$ when the others are considered fixed. This thus opens the way to decentralised methods reaching local optima, such as sequential minimisation [143].

Centralised optimisation problems Given these elements, the beamformers are designed to minimise the information leakage, while fulfilling SINR requirements ensuring that the symbols $s_{k,l}$ are correctly decoded, and with a power constraint for each RE. In the traditional case, it reads thus as

$$\begin{aligned} \min_{\mathbf{w}} \quad & \textstyle\sum_{l=1}^{L}\sum_{m=1}^{M} \beta_{l,m}\overline{\mathcal{L}}_{l,m}(\mathbf{w}) \\ \text{s.t.} \quad & \mathrm{SINR}_{k,l} \geq \theta_l, \forall k, \forall l, \\ & \textstyle\sum_{l=1}^{L} \|\mathbf{w}_{k,l}\|_2^2 \leq 1, \forall k, \end{aligned} \tag{7.6}$$

with θ_l the SINR requirement of the lth UE. In the above, the notations $\forall k$ implicitly denote $\forall k = 1, \ldots, K$, and similarly for the other indices. The optimisation problem in the case of linear coding is obtained in the same manner as

$$\begin{aligned} \min_{\mathbf{w}} \quad & \textstyle\sum_{l=1}^{L}\sum_{m=1}^{M} \beta_{l,m}\underline{\mathcal{K}}_{l,m}(\mathbf{w}) \\ \text{s.t.} \quad & \mathrm{SINR}_{k,l} \geq \theta_l, \forall k, \forall l, \\ & \textstyle\sum_{l=1}^{L} \|\mathbf{w}_{k,l}\|_2^2 \leq 1, \forall k, \end{aligned} \tag{7.7}$$

In the following, (7.7) will be termed the coding-aware beamforming design problem.

Remark 7.2

In both cases, the optimisation problems require knowing the channel vectors $\mathbf{g}_{k,m}$, and thus the eavesdroppers' positions $\mathbf{z}_m$. If the eavesdroppers are active transmitters, such an information may come from their uplink transmissions to the CF network. Moreover, other systems such as camera's could give the locations of the users and equipments present in a scene, identifying them as potential eavesdroppers. Also, in areas such as warehouses, critical spots may be identified, for instance at locations at which visitors may be located. By considering these spots as potential eavesdropper locations, the above problems enable to create safe zones at which no information leakage is guaranteed. Such prior knowledge may moreover be fine-tuned with the weights $\beta_{l,m}$, by setting higher weights for positions which are more likely to be critical.

Remark 7.3

In this chapter, the MF MP resource allocation problem is tackled in a centralised way.
A first set of reasons stem from the application itself. As represented in Figure 7.1, the multiple antennas are connected together through the backhaul network, which provides thus an infrastructure to centralise the optimisation problem's' parameters. Moreover, the security metrics are inherently centralised metrics, since the requirement is that the eavesdroppers get no information on any of the symbols. Therefore, identifying autonomous players would be in this case quite artificial.
The second set of reasons stems from the convexity and differentiability requirements of the autonomous framework. In this case, the objective functions are continuous, yet not differentiable. Hence, as the requirements of the autonomous framework are not met, the centralised approach is preferred.

7.3 Beamforming design algorithms

In this section, methods to solve the optimisation problems (7.6) and (7.7) are designed. First, the optimisation problems are translated into the real domain in Section 7.3.1, and transformed to make the non-convex SINR constraints convex. Then, Section 7.3.2 provides a method to obtain the global optimum of the traditional secure beamforming problem. The coding-aware problem is studied in Section 7.3.3, where an algorithm able to efficiently find a local minimum is designed.

7.3.1 Convex real reformulation

A first challenge coming with problems (7.6) and (7.7) is that the SINR constraint is not convex. To circumvent this, it is noted that in both cases, the optimal beamforming vectors are defined up to a phase shift. Therefore, forcing the phase of $\mathbf{h}_{k,l}^{\mathrm{H}}\mathbf{w}_{k,l}$ to be zero for all k and l, the following constraints can be added to the optimisation problems without changing their optimal value:

$$\mathrm{Re}\left\{\mathbf{h}_{k,l}^{\mathrm{H}}\mathbf{w}_{k,l}\right\} \geq 0, \qquad \mathrm{Im}\left\{\mathbf{h}_{k,l}^{\mathrm{H}}\mathbf{w}_{k,l}\right\} = 0. \tag{7.8}$$

In order to express the above inequalities into the real domain, the following notations are introduced. Given a vector $\mathbf{v}$, its real and imaginary parts are denoted as $\mathbf{v}_{\mathrm{R}} \triangleq \mathrm{Re}\{\mathbf{v}\}$ and $\mathbf{v}_{\mathrm{I}} \triangleq \mathrm{Im}\{\mathbf{v}\}$. The real vectors $\mathbf{b}_{k,l}, \mathbf{c}_{k,l}, \mathbf{x}_{k,l} \in \mathbb{R}^{2N_k}$ are furthermore defined as $\mathbf{b}_{k,l}^{\top} \triangleq \left[\mathbf{h}_{k,l;\mathrm{R}}^{\top}, \mathbf{h}_{k,l;\mathrm{I}}^{\top}\right]$, $\mathbf{c}_{k,l}^{\top} \triangleq \left[-\mathbf{h}_{k,l;\mathrm{I}}^{\top}, \mathbf{h}_{k,l;\mathrm{R}}^{\top}\right]$, and $\mathbf{x}_{k,l}^{\top} \triangleq \left[\mathbf{w}_{k,l;\mathrm{R}}^{\top}, \mathbf{w}_{k,l;\mathrm{I}}^{\top}\right]$, the phase reference constraints (7.8) becoming

$$\mathbf{b}_{k,l}^{\top}\mathbf{x}_{k,l} \geq 0, \qquad \mathbf{c}_{k,l}^{\top}\mathbf{x}_{k,l} = 0.$$

Under the above, the SINR constraint reads as

$$\frac{\mathbf{b}_{k,l}^{\top}\mathbf{x}_{k,l}}{\sqrt{\theta_l}} \geq \sqrt{\sigma_n^2 + \sum_{l'\neq l}\left[\left(\mathbf{b}_{k,l}^{\top}\mathbf{x}_{k,l'}\right)^2 + \left(\mathbf{c}_{k,l}^{\top}\mathbf{x}_{k,l'}\right)^2\right]}, \tag{7.9}$$

being now convex in the vectors $\{\mathbf{x}_{k,l}\}_{k,l}$. The power constraints are handled by noting that $\|\mathbf{w}_{k,l}\|_2 = \|\mathbf{x}_{k,l}\|_2$. For the eavesdroppers' SNRs, the following is introduced

$$\mathbf{A}_{k,m} \triangleq \begin{bmatrix} \mathbf{g}_{k,m;\mathrm{R}}^{\top} & \mathbf{g}_{k,m;\mathrm{I}}^{\top} \\ -\mathbf{g}_{k,m;\mathrm{I}}^{\top} & \mathbf{g}_{k,m;\mathrm{R}}^{\top} \end{bmatrix} \in \mathbb{R}^{2\times 2N_k},$$

leading to $\left|\mathbf{g}_{k,m}^{\mathrm{H}}\mathbf{w}_{k,l}\right|^2 = \|\mathbf{A}_{k,m}\mathbf{x}_{k,l}\|_2^2$, and concluding the translation of (7.6) and (7.7) into the real domain.

7.3.2 Traditional secure beamforming

Under the above transform, (7.6) becomes,

$$\min_{\{\mathbf{x}_{k,l}\}_{k,l}} \sum_{l,m} \beta_{l,m} \max_{k} \max\left\{\frac{\|\mathbf{A}_{k,m}\mathbf{x}_{k,l}\|_2^2}{\sigma_n^2} - \delta, 0\right\} \tag{7.10}$$

$$\begin{aligned}
\text{s.t.} \quad & \frac{\mathbf{b}_{k,l}^{\top}\mathbf{x}_{k,l}}{\sqrt{\theta_l}} \geq \sqrt{\sigma_n^2 + \textstyle\sum_{l'\neq l}\left[\left(\mathbf{b}_{k,l}^{\top}\mathbf{x}_{k,l'}\right)^2 + \left(\mathbf{c}_{k,l}^{\top}\mathbf{x}_{k,l'}\right)^2\right]}, && \forall k,l, \\
& \mathbf{c}_{k,l}^{\top}\mathbf{x}_{k,l} = 0, && \forall k,l, \\
& \textstyle\sum_l \|\mathbf{x}_{k,l}\|_2^2 \leq 1, && \forall k,
\end{aligned}$$

with the inequality $\mathbf{b}_{k,l}^{\top}\mathbf{x}_{k,l} \geq 0$ being encompassed by (7.9). The above is a convex optimisation problem, which can be rewritten in a standard conic form to be solved by conic-programming solvers such as Mosek [119]:

$$\min_{\{\mathbf{x}_{k,l},\xi_{k,l}\}_{k,l},\{\eta_{l,m}\}_{l,m}} \sum_{l,m} \beta_{l,m}\eta_{l,m} \tag{7.11}$$

$$\begin{aligned}
\text{s.t.} \quad & \eta_{l,m} \geq 0, && \forall l,m, \\
& \|\mathbf{A}_{k,m}\mathbf{x}_{k,l}\|_2^2 - \delta\sigma_n^2 \leq \eta_{l,m}\sigma_n^2, && \forall k,l,m, \\
& \frac{\mathbf{b}_{k,l}^{\top}\mathbf{x}_{k,l}}{\sqrt{\theta_l}} \geq \sqrt{\sigma_n^2 + \textstyle\sum_{l'\neq l}\left[\left(\mathbf{b}_{k,l}^{\top}\mathbf{x}_{k,l'}\right)^2 + \left(\mathbf{c}_{k,l}^{\top}\mathbf{x}_{k,l'}\right)^2\right]}, && \forall k,l, \\
& \mathbf{c}_{k,l}^{\top}\mathbf{x}_{k,l} = 0, && \forall k,l, \\
& \textstyle\sum_l \xi_{k,l} \leq 1, && \forall k, \\
& \xi_{k,l} \geq \|\mathbf{x}_{k,l}\|_2^2, && \forall k,l.
\end{aligned}$$

Apart from the above linear constraints, the third one is an instance of a quadratic cone, while the second and sixth ones correspond to a rotated quadratic cone.

7.3.3 Coding-aware secure beamforming

The real form of (7.7) reads as

$$\min_{\{\mathbf{x}_{k,l}\}_{k,l}} \sum_{l,m} \beta_{l,m} \prod_{k} \max\left\{\frac{\|\mathbf{A}_{k,m}\mathbf{x}_{k,l}\|_2^2}{\sigma_n^2} - \delta, 0\right\} \tag{7.12}$$

$$\begin{aligned}
\text{s.t.} \quad & \frac{\mathbf{b}_{k,l}^\top \mathbf{x}_{k,l}}{\sqrt{\theta_l}} \geq \sqrt{\sigma_n^2 + \textstyle\sum_{l' \neq l}\left[\left(\mathbf{b}_{k,l}^\top \mathbf{x}_{k,l'}\right)^2 + \left(\mathbf{c}_{k,l}^\top \mathbf{x}_{k,l'}\right)^2\right]}, && \forall k, l,\\
& \mathbf{c}_{k,l}^\top \mathbf{x}_{k,l} = 0, && \forall k, l,\\
& \textstyle\sum_l \|\mathbf{x}_{k,l}\|_2^2 \leq 1, && \forall k,
\end{aligned}$$

In the above, the constraint set is convex, but the objective function is however not. While obtaining a global optimum is extremely challenging, a local minimum can nevertheless be attained through successive minimisation [143]. In such an algorithm, the beamforming vectors of each RE are alternatively optimised, considering the ones of the other REs as fixed. The sub-problem of the kth RE, denoted $(\mathcal{P}_k)$, is therefore given by

$$(\mathcal{P}_k) \quad \begin{aligned}
\min_{\{\mathbf{x}_{k,l}\}_l} \; & \sum_{l,m} C_{k,l,m} \max\left\{\frac{\|\mathbf{A}_{k,m}\mathbf{x}_{k,l}\|_2^2}{\sigma_n^2} - \delta, 0\right\}\\
\text{s.t.} \quad & \frac{\mathbf{b}_{k,l}^\top \mathbf{x}_{k,l}}{\sqrt{\theta_l}} \geq \sqrt{\sigma_n^2 + \textstyle\sum_{l' \neq l}\left[\left(\mathbf{b}_{k,l}^\top \mathbf{x}_{k,l'}\right)^2 + \left(\mathbf{c}_{k,l}^\top \mathbf{x}_{k,l'}\right)^2\right]}, && \forall l,\\
& \mathbf{c}_{k,l}^\top \mathbf{x}_{k,l} = 0, && \forall l,\\
& \textstyle\sum_l \|\mathbf{x}_{k,l}\|_2^2 \leq 1,
\end{aligned}$$

with $C_{k,l,m} \triangleq \beta_{l,m} \prod_{k' \neq k} \max\left\{\frac{\|\mathbf{A}_{k',m}\mathbf{x}_{k',l}\|_2^2}{\sigma_n^2} - \delta, 0\right\}$ modified weights taking into account the fact eavesdroppers might already be blinded on the other REs. The major advantage of the above is that each sub-problem $(\mathcal{P}_k)$ is convex in $\{\mathbf{x}_{k,l}\}_l$, and can thus efficiently be solved. Moreover, since it is known that the optimal objective value is 0, if the successive minimisation algorithm, described in Algorithm 2, leads to this value, then it is known that a global optimum is achieved. The standard conic form associated with the problems $(\mathcal{P}_k)$ can be obtained similarly as for (7.11), at the difference that only the kth RE beamforming vectors are optimised, the others being considered fixed and included into the weights $C_{k,l,m}$. In Algorithm 2, the initial beamformers $\mathbf{w}_{k,l}^{(\text{init})}$ can be any beamformers fulfilling all the constraints of (7.7). Among others, a reasonable choice is to initialise the sequential minimisation algorithm with the beamformers found through the traditional optimisation problem (7.6).

Algorithm 2 Coding-aware beamforming design

Set $\mathbf{w}_{k,l} = \mathbf{w}_{k,l}^{(\text{init})}$ $\forall k, l$.
Transform the $\{\mathbf{w}_{k,l}\}_{k,l}$ into the $\{\mathbf{x}_{k,l}\}_{k,l}$
while No convergence **do**
  for $k = 1, \ldots, K$ **do**
    Update the $\{\mathbf{x}_{k,l}\}_l$ by solving $(\mathcal{P}_k)$
    Update the weights $\{C_{k,l,m}\}_{k,l,m}$
Obtain the beamformers $\{\mathbf{w}_{k,l}\}_{k,l}$ from the $\{\mathbf{x}_{k,l}\}_{k,l}$

7.4 Numerical analysis

The above section provides solutions to the beamforming design problem, when the information symbols are sent (traditional scheme) or with linearly coded streams. In this section, the performance of the above solutions are illustrated and validated numerically. Unless stated otherwise, the parameters are as follows: $L = 2$ UEs are served on $K = 3$ REs, all with a carrier frequency $f_c = 5\,\text{GHz}$. The scene geometry is depicted in Figure 7.2, with the UE locations being $[-10, 5]$ and $[10, -10]$m. Each RE is associated with a different antenna set, each set being an antenna array with $N_k = 30$ antenna spaced by $\lambda/2$, respectively at $[-25, 0]$, $[0, 25]$, $[0, -25]$m. There are 3 eavesdroppers around each UE, located on a circle of radius $r_{\text{eve}} = 2\,\text{m}$. In total, this leads to $M = 8$, with 6 eavesdroppers and the two 2 UEs. All weights $\beta_{l,m}$ are set to 1, except the weights corresponding to a UE with itself. Considering the worst case scenario, the eavesdropper sensitivity is set to $\delta = 0$. The noise variance, normalised by the transmit power, is $\sigma_n^2 = 0.1$, and the path loss function is given by $L(r) = 625r^{-2}$. The SINR threshold is set to $\theta_l = 14.7\,\text{dB}$.

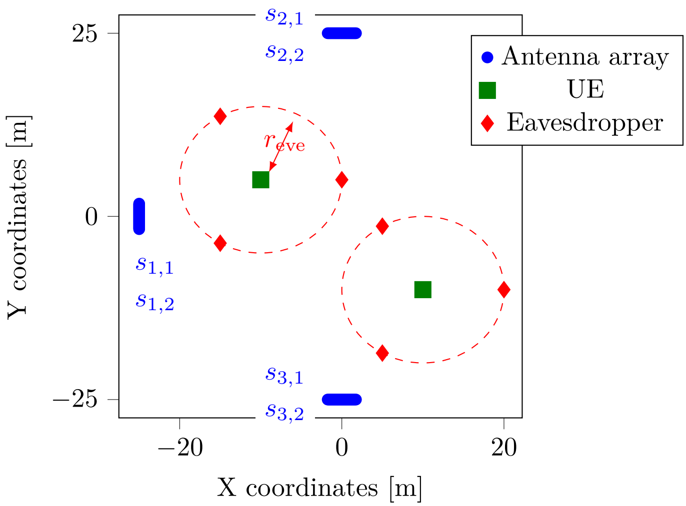

Fig. 7.2 Secure beamforming scene description (not to scale).

7.4.1 Beamformer analysis

First, the beamformers resulting from the optimisation are qualitatively analysed. Figure 7.3 depicts the SNR of the three REs for an antenna located in the region surrounding the first UE, as well as the information leakage metrics. In the upper graphs, the traditional beamformer of each RE tries to avoid all the eavesdroppers. As some of the eavesdroppers are almost aligned with the UE, providing such a security is impossible for each of the REs. In the bottom graphs, it can be observed the coding-aware beamformers act differently, since each eavesdropper must be in the blind region of only one of the REs. Hence, the beamformer of each RE manages to blind two out of the three eavesdroppers, the remaining one being tackled by the beamformers of the other REs. These effects are also observed in the right panels of Figure 7.3, depicting the values of the metrics $\overline{\mathcal{L}}$ and $\sqrt[K]{\underline{\mathcal{K}}}$ in the UE region. As it can be observed, many locations are unsecured in the traditional case, as at least one of the RE beamformer radiates power at that location. Thanks to the coding-aware beamformers, the unsecure region is significantly reduced, and the eavesdroppers get no information.

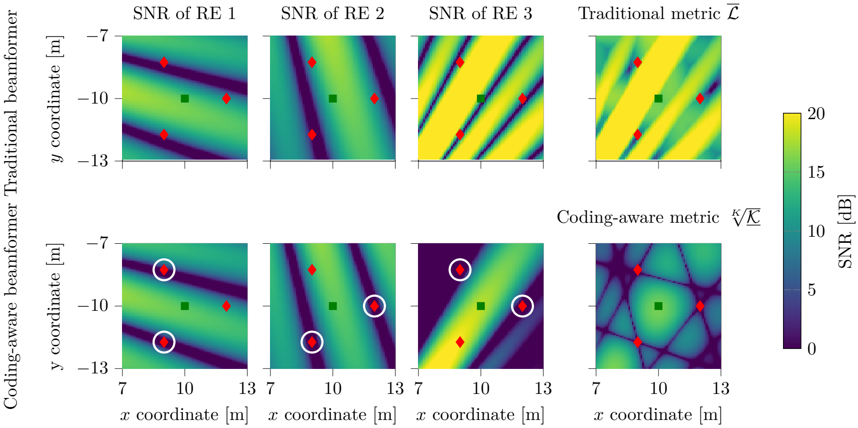

Fig. 7.3 SNR received by an antenna located in the region surrounding the first UE, on the three REs, with the traditional beamformers and with the coding-aware beamformers. The right panels depict the information leakage metrics in the two cases, for an eavesdropper located in (x, y). As in Figure 7.2, the green square denotes the UE location while the red points are the eavesdropper locations. The white circles highlight the eavesdroppers blinded by the coding-aware beamformers, emphasising the differences with respect to the traditional ones.

7.4.2 Security-rate-eavesdropper closeness trade-offs

The qualitative analysis can be complemented by quantitative security-rate trade-offs, by determining the highest possible security level achievable while fulfilling the rate constraint, for given eavesdropper locations. The upper panel of Figure 7.4 depicts such a trade-off, for the two beamforming designs, with 30 eavesdroppers located on each eavesdropper circle. Regarding the SINR axis, it is quantified as the loss with respect to the maximum achievable rate, i.e., when security is not a concern. For the security metrics, they have been normalised with the security value achieved with these security-unaware beamformers. As it can be observed, the coding-aware beamformers significantly improve the considered trade-off, providing security guarantees even in the presence of many eavesdroppers and high rate constraints. Another trade-off can be studied, which amounts to keeping the rate constraint constant while making the eavesdroppers closer through the value of r_{eve}. This is illustrated in the bottom panel of Figure 7.4. Again, the coding-aware beamforming design drastically improves the security guarantees.

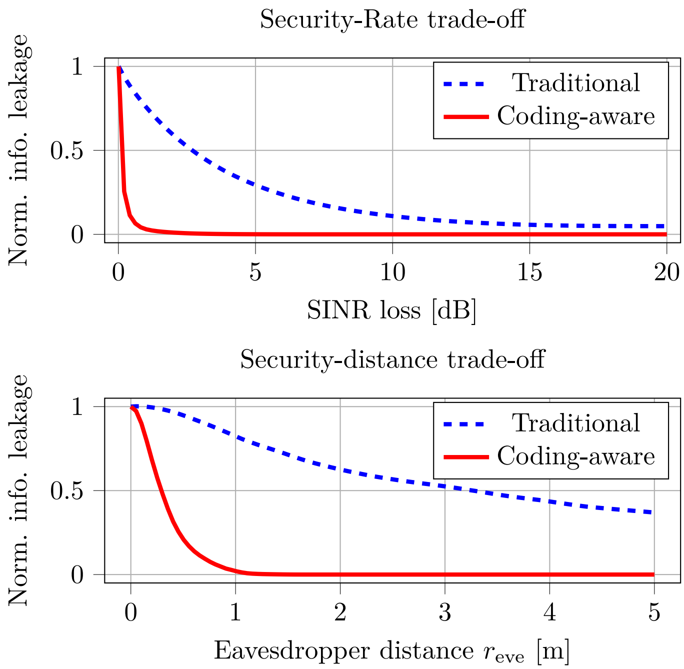

Fig. 7.4 Security-Rate (above) and Security-Distance (below) trade-offs

7.5 Chapter summary

This chapter studies a CF network simultaneously communicating with multiple legitimate UEs while preventing information leakage towards eavesdroppers. To that aim, the CF network splits its communication resource into several REs, and different antenna sets are associated with each RE. This enables to illuminate the scene from different directions, and therefore to blind eavesdroppers which are close to the legitimate UEs.

Two communication cases are considered. In the traditional physical layer security scheme, the symbols sent on the REs are the communication symbols. All REs have therefore sensitive information, which must be protected against the eavesdroppers. In the second case, independent linear combinations of the information symbols are instead sent, following [138]. In that case, information leakage occurs only if an eavesdropper gets all the linear combinations, thereby improving the security guarantees.

Secure beamforming optimisation problems have been formulated in both the traditional and the coding-aware cases. The problems have been translated into the real domain, this enabling to transform the non-convex constraints into convex ones. In the traditional case, the resulting optimisation problem is convex, and it has therefore been cast into a standard conic form which can be handled by specialised solvers. In the coding-aware case, a local minimum is attained by solving a sequence of convex problems. The developed schemes have been illustrated numerically, showing the significant gains provided by the developed coding-aware beamforming scheme. Regarding the application, important research directions include the case of eavesdroppers and UEs with several antennas, as well as the extension to eavesdroppers cooperating together.

On a broader level, the studied scenario is an instance of a MF MP network. The two functions are the communication and the security functions, and the MP character comes from the several transmitting antennas, receivers, and eavesdroppers. The considered downlink beamforming design problem is inherently a centralised problem, and it is therefore solved accordingly. The autonomous approach would anyway fail to apply in this case, since the required assumptions would not be met. The preference for the centralised approach comes therefore both from the application itself, and from mathematical tractability reasons. This will also be the case in the next chapter, in which another instance of a MF MP network is studied in a centralised way. General conclusions on the centralised interference management approach for MF MP networks will also be provided at the end of the next chapter, in Section 8.5.

8

Fair beamforming design for multi-antenna JRC systems

The material of this chapter is the result of a collaboration with François De Saint Moulin, which has lead to the following paper [144]. Both authors have equally contributed to this chapter during the whole research process.

The MF MP scenario investigated in this chapter is an instance of a JRC system. The multiple functions are therefore the communication and the radar tasks, while the multiple points come from the fact that multiple communication users, and several targets are considered. The resources upon which the optimisation is performed are the transmit and receive beamforming vectors, which must address the interference between the radar and communication tasks. This chapter sets the focus on the fairness between the different targets and communication users. Indeed, the propagation conditions may be heterogeneous across these different points. This implies that if the beamforming design problem is formulated inadequately, then the points suffering from poor propagation conditions may be set aside.

Related works The following works can be leveraged upon. In [145], an uplink communication signal is received together with a radar echo, the beamformers being able to nullify the interference between both systems. Motivated by the complexity reduction, [146] and [147] provide suboptimal beamformers, in a downlink scenario with a maximisation of one target SINR, constrained by the SINR of the communication and the other targets. In [148], the radar CRB is minimised with SINR constraints on the UEs. The beamformers are either obtained in closed-form in the single-user case, or the problem is relaxed and solved with numerical methods for multi-user systems. The radar CRB is also considered in [149] and minimised under a communication sum-rate constraint. In [150], an iterative algorithm optimises the radar power and communication rates while ensuring a low self-interference in a full-duplex scenario.

In order to handle the multiplicity of targets and UEs, the above works consider the following approaches. One possible paradigm is to consider one metric as an objective, with the others as constraints [147–149]. Still, choosing adequate constraint thresholds is challenging, and may require multiple iterations to ensure sufficient performance for both functions. Alternatively, a weighted-sum of the radar and communication objectives can be performed [150]. However, such formulation might totally neglect one objective in favour of the others. This issue is tackled in [151], in which a fair optimisation of the downlink communication and radar performance is performed. The proposed approach requires nonetheless to solve a sequence of convex optimisation problems and the computational burden this implies might be incompatible with the real-time tracking mechanisms usually associated with radar beamforming schemes.

Contributions This chapter complements the above works by designing beamforming schemes which are fair across the uplink communication UEs and targets. The detailed contributions are the following.

- The considered metric is the product of the SINR of each UE and target. This product optimisation is independent of the direct channel gains, and it therefore considers fairly both the low- and high-SINR points.

- An iterative beamforming scheme is designed to optimise this SINR product metric, ensured to reach a local optimum. At each iteration, parts of the optimisation variables are optimised upon. The solutions of the considered subproblems are provided, depending on the number of UEs and targets.

- The performance of the developed scheme is numerically evaluated on a JRC scenario. Among others, this numerical comparison highlights the fair character of the designed beamformers compared to a SINR sum metric.

Organisation To that aim, the structure of this chapter is the following. First, the JRC system model is described, and the beamforming design optimisation problem is formulated in Section 8.1. Section 8.2 then provides algorithms attaining local optima of this problem, depending on the number of targets and UEs. Finally, the numerical evaluation of the developed schemes is performed in Section 8.3.

8.1 System model

System overview The considered JRC scenario, depicted in Figure 8.1, involves a multi-antenna JRC system equipped with N_{t} transmit antennas, and N_{r} receive ones. This JRC system must estimate the range and velocity of K targets, and must receive the communication streams of L UEs, the lth one equipped with $N_{\mathrm{t}l}$ antennas.

Emitted waveforms For the radar function, the waveform $x_{\mathrm{R}}(t)$ is transmitted, being beamformed with the vector $\mathbf{u}_{\mathrm{R}} \in \mathbb{C}^{N_{\mathrm{t}}}$. Regarding the communications, the lth UE emits a complex pulse train defined as $x_{\mathrm{C}l}(t) \triangleq \sum_n I_{nl}\, g_l(t-nT)$ with I_{nl} his nth transmitted symbol, $g_l(\cdot)$ his pulse shaping filter, and T the symbol period. This complex pulse train is mapped onto the transmit antennas with the beamforming vector $\mathbf{u}_{\mathrm{C}l} \in \mathbb{C}^{N_{\mathrm{t}l}}$. The sent signals are therefore given by

$$
\begin{aligned}
\mathbf{x}_{\mathrm{R}}(t) &\triangleq \mathbf{u}_{\mathrm{R}} x_{\mathrm{R}}(t), \\
\mathbf{x}_{\mathrm{C}l}(t) &\triangleq \mathbf{u}_{\mathrm{C}l} x_{\mathrm{C}l}(t), \quad \forall l = 1, \ldots, L.
\end{aligned}
$$

Without loss of generality, the communication and radar waveforms are normalised to a unit energy, the symbols I_{nl} have a unit variance, and the

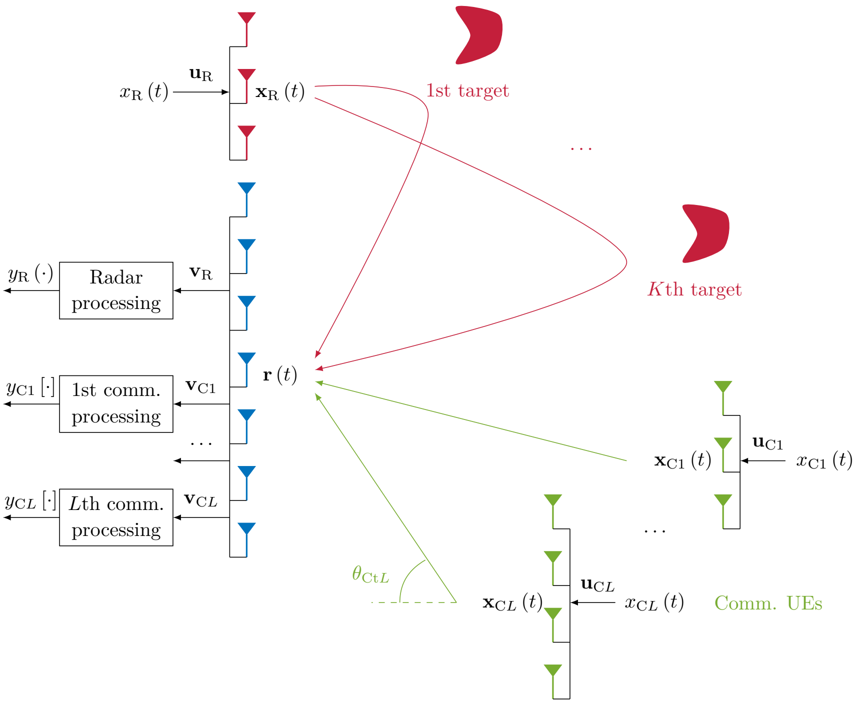

Fig. 8.1 JRC beamforming design scenario. The red colour depicts the parts that are specific to the radar function, the green colour the ones related to the communication function, while the blue colour represents the common parts. The angle of departure of the Lth UE is represented, illustrating the convention followed for the departure and arrival angles.

beamformers have at most a unit power:

$$\int |x_{\mathrm{R}}(t)|^2 \, \mathrm{d}t = 1, \qquad \|\mathbf{u}_{\mathrm{R}}\|_2 \leq 1,$$
$$\int |g_l(t)|^2 \, \mathrm{d}t = 1, \qquad \|\mathbf{u}_{\mathrm{C}l}\|_2 \leq 1, \quad \forall l = 1, \ldots, L.$$

Propagation Frequency-flat Far-Field (FF) LoS channels are considered in this chapter. Each propagation path is thus characterised by a complex channel coefficient, a propagation delay and a Doppler frequency. For each kth target (resp. lth UE), the complex channel coefficient is denoted $\alpha_{\mathrm{R}k}$ (resp. $\alpha_{\mathrm{C}l}$), the propagation delay $\tau_{\mathrm{R}k}$ (resp. $\tau_{\mathrm{C}l}$) and the Doppler frequency $f_{\mathrm{DR}k}$ (resp. $f_{\mathrm{DC}l}$). Regarding the Doppler frequencies, they may either come from the targets or UE movement, or from the frequency offset between one of the emitters and the receiver.

The received signal also depends on the FF steering vectors of the arrays. The transmit vector of the kth target (resp. lth UE) is denoted $\mathbf{a}_{\mathrm{Rt}k} \in \mathbb{C}^{N_{\mathrm{t}}}$ (resp. $\mathbf{a}_{\mathrm{Ct}l} \in \mathbb{C}^{N_{\mathrm{t}l}}$), while the received one is $\mathbf{a}_{\mathrm{Rr}k} \in \mathbb{C}^{N_{\mathrm{r}}}$ (resp. $\mathbf{a}_{\mathrm{Cr}l} \in \mathbb{C}^{N_{\mathrm{r}}}$). For a Uniform Linear Array (ULA) with antenna spacing d, $\mathbf{a}_{\mathrm{Ct}l}$ depends on the departure angle $\theta_{\mathrm{Ct}l}$ as

$$\mathbf{a}_{\mathrm{Ct}l} \triangleq \begin{bmatrix} 1 & e^{-j2\pi\frac{d}{\lambda}\sin(\theta_{\mathrm{Ct}l})} & \dots & e^{-j2\pi\frac{d}{\lambda}(N_{\mathrm{t}l}-1)\sin(\theta_{\mathrm{Ct}l})} \end{bmatrix}^{\top}, \tag{8.1}$$

and similarly for the other steering vectors. With these elements, the received signal reads hence as

$$\begin{aligned} \mathbf{r}(t) = & \sum_{k=1}^{K} \alpha_{\mathrm{R}k}\, e^{j2\pi f_{\mathrm{DR}k} t}\, \mathbf{a}_{\mathrm{Rr}k}\, \mathbf{a}_{\mathrm{Rt}k}^{\mathrm{H}}\, \mathbf{x}_{\mathrm{R}}(t-\tau_{\mathrm{R}k}) \\ & + \sum_{l=1}^{L} \alpha_{\mathrm{C}l}\, e^{j2\pi f_{\mathrm{DC}l} t}\, \mathbf{a}_{\mathrm{Cr}l}\, \mathbf{a}_{\mathrm{Ct}l}^{\mathrm{H}}\, \mathbf{x}_{\mathrm{C}l}(t-\tau_{\mathrm{C}l}) + \mathbf{n}(t), \end{aligned} \tag{8.2}$$

with $\mathbf{n}(t) \in \mathbb{C}^{N_{\mathrm{r}}}$ an AWGN with a baseband Power Spectral Density (PSD) $2N_0$, the noises at each of the antennas being independent:

$$\mathbb{E}\left\{\mathbf{n}(t)\,\mathbf{n}^{\mathrm{H}}(t')\right\} = 2N_0\delta(t-t')\,\mathbf{I}_{N_{\mathrm{r}}}. \tag{8.3}$$

It must be emphasised that in the expression of $\mathbf{r}(t)$, the interference coming from the direct path between the radar transmitter and receiver has been neglected. It is indeed considered the self-interference is negligible compared to the uplink signal and radar echoes power, after an analogue suppression step [150].

Receiver communication processing At the receiver side, a separated processing is performed for each UE, which first involves performing the receive beamforming with the vector $\mathbf{v}_{\mathrm{C}l} \in \mathbb{C}^{N_{\mathrm{R}}}$ for the lth stream. The receive beamformers are normalised to a unit energy: $\|\mathbf{v}_{\mathrm{C}l}\|_2 = 1$. Then, a perfect correction of the delay and frequency offset is carried out, and a matched filtering is applied. After sampling, the decision variable of the lth stream at time instant n is consequently given by

$$
\begin{aligned}
y_{\mathrm{C}l}[n] &= \int_t \mathbf{v}_{\mathrm{C}l}^{\mathrm{H}} \mathbf{r}\left(t+\tau_{\mathrm{C}l}\right)\, e^{-j2\pi f_{\mathrm{DC}l} t}\, g_l^{\star}\left(t-nT\right)\, \mathrm{d}t, \qquad (8.4)\\
&= \alpha_{\mathrm{C}l}\, \mathbf{v}_{\mathrm{C}l}^{\mathrm{H}} \mathbf{a}_{\mathrm{Cr}l} \mathbf{a}_{\mathrm{Ct}l}^{\mathrm{H}} \mathbf{u}_{\mathrm{C}l}\, \chi_{\mathrm{CC}ll}[n] + \sum_{l' \neq l'} \alpha_{\mathrm{C}l'}\, \mathbf{v}_{\mathrm{C}l}^{\mathrm{H}} \mathbf{a}_{\mathrm{Cr}l'} \mathbf{a}_{\mathrm{Ct}l'}^{\mathrm{H}} \mathbf{u}_{\mathrm{C}l'}\, \chi_{\mathrm{CC}l'l}[n]\\
&\quad + \sum_{k=1}^{K} \alpha_{\mathrm{R}k}\, \mathbf{v}_{\mathrm{C}l}^{\mathrm{H}} \mathbf{a}_{\mathrm{Rr}k} \mathbf{a}_{\mathrm{Rt}k}^{\mathrm{H}} \mathbf{u}_{\mathrm{R}}\, \chi_{\mathrm{RC}kl}[n] + w_{\mathrm{C}l}[n].
\end{aligned}
$$

In the above, the correlation functions $\chi_{\mathrm{CC}l'l}[n]$ and $\chi_{\mathrm{RC}kl}[n]$, and the sample noise, are defined as

$$
\begin{aligned}
\chi_{\mathrm{CC}l'l}[n] &\triangleq \int_t x_{\mathrm{C}l'}\left(t+\tau_{\mathrm{C}l}-\tau_{\mathrm{C}l'}\right) g_l^{\star}\left(t-nT\right) e^{j2\pi(f_{\mathrm{DC}l'}-f_{\mathrm{DC}l})t}\, \mathrm{d}t,\\
&= \sum_m I_{ml'} \int_t g_{l'}\left(t-mT+\tau_{\mathrm{C}l}-\tau_{\mathrm{C}l'}\right) g_l^{\star}\left(t-nT\right) e^{j2\pi(f_{\mathrm{DC}l'}-f_{\mathrm{DC}l})t}\, \mathrm{d}t,\\
\chi_{\mathrm{RC}kl}[n] &\triangleq \int_t x_{\mathrm{R}k}\left(t+\tau_{\mathrm{C}l}-\tau_{\mathrm{R}k}\right) g_l^{\star}\left(t-nT\right) e^{j2\pi(f_{\mathrm{DR}k}-f_{\mathrm{DC}l})t}\, \mathrm{d}t,\\
w_{\mathrm{C}l}[n] &\triangleq \int_t \mathbf{v}_{\mathrm{C}l}^{\mathrm{H}} \mathbf{n}\left(t+\tau_{\mathrm{C}l}\right)\, e^{-j2\pi f_{\mathrm{DC}l} t}\, g_l^{\star}\left(t-nT\right)\, \mathrm{d}t.
\end{aligned}
$$

From the expression of $y_{\mathrm{C}l}[n]$, one can identify the interference coming from the other UEs, from the radar targets, and the noise. Regarding the term of the lth UE with himself, it is assumed the filter $g_l\left(t\right)$ fulfils the Nyquist criterion for Inter-Symbol Interference (ISI), implying $\chi_{\mathrm{CC}ll}[n] = I_{nl}\delta[n]$. From (8.3) and the unit-norm property of the receive beamforming vectors, this also implies the sampled noise is white, since

$$
\mathbb{E}\left\{w_{\mathrm{C}l}[n] w_{\mathrm{C}l}^{\star}[n']\right\} = 2N_0 \int_t g_l^{\star}\left(t-nT\right) g_l\left(t-n'T\right) \mathrm{d}t = 2N_0 \delta\left[n-n'\right].
$$

With these elements, the SINR of the lth UE is given by

$$
\mathrm{SINR}_{\mathrm{C}l} = \frac{\beta_{\mathrm{CC}ll}\, \left|\mathbf{v}_{\mathrm{C}l}^{\mathrm{H}} \mathbf{a}_{\mathrm{Cr}l}\right|^2 \left|\mathbf{u}_{\mathrm{C}l}^{\mathrm{H}} \mathbf{a}_{\mathrm{Ct}l}\right|^2}{I_{\mathrm{RC}l} + I_{\mathrm{CC}l} + 1},
$$

with $I_{\mathrm{RC}l}$ and $I_{\mathrm{CC}l}$ the interference arising from the radar signals and other uplink signals:

$$I_{\mathrm{RC}l} = \sum_{k=1}^{K} \beta_{\mathrm{RC}kl} \left|\mathbf{v}_{\mathrm{C}l}^{\mathrm{H}} \mathbf{a}_{\mathrm{Rr}k}\right|^2 \left|\mathbf{u}_{\mathrm{R}}^{\mathrm{H}} \mathbf{a}_{\mathrm{Rt}k}\right|^2, \tag{8.5}$$

$$I_{\mathrm{CC}l} = \sum_{l' \neq l} \beta_{\mathrm{CC}l'l} \left|\mathbf{v}_{\mathrm{C}l}^{\mathrm{H}} \mathbf{a}_{\mathrm{Cr}l'}\right|^2 \left|\mathbf{u}_{\mathrm{C}l'}^{\mathrm{H}} \mathbf{a}_{\mathrm{Ct}l'}\right|^2, \tag{8.6}$$

where the interference coefficients are $\beta_{\mathrm{CC}l'l} = \mathbb{E}\left\{\left|\alpha_{\mathrm{C}l'}\right|^2 \left|\chi_{\mathrm{CC}l'l}[n]\right|^2\right\}/2N_0$, and $\beta_{\mathrm{RC}kl} = \mathbb{E}\left\{\left|\alpha_{\mathrm{R}k}\right|^2 \left|\chi_{\mathrm{RC}kl}[n]\right|^2\right\}/2N_0$. The expectation operations of these coefficients are performed over the symbols I_{nl}, and over the channel power gains in case of fading, considered to be independent.

Receiver radar processing Contrarily to the operations performed for the communication streams, the same beamforming vector $\mathbf{v}_{\mathrm{R}} \in \mathbb{C}^{N_{\mathrm{R}}}$ is applied for all targets, with a unit energy: $\left\|\mathbf{v}_{\mathrm{R}}\right\|_2 = 1$. Then, the Delay-Doppler map is build by correlating the received signal with the radar waveform affected by a putative delay τ and a Doppler frequency f_{D}. This corresponds to traditional range-velocity radar processing, in which a unique Delay-Doppler map is build for all targets, and then these latter are detected using for instance a Neyman-Pearson detector [152]. The Delay-Doppler map is computed as

$$\begin{aligned} y_{\mathrm{R}}\left(\tau, f_{\mathrm{D}}\right) &= \int_t \mathbf{v}_{\mathrm{R}}^{\mathrm{H}} \mathbf{r}\left(t\right)\, x_{\mathrm{R}}^{*}\left(t-\tau\right)\, e^{-j2\pi f_{\mathrm{D}} t}\, \mathrm{d}t, && (8.7) \\ &= \sum_{k=1}^{K} \alpha_{\mathrm{R}k}\, \mathbf{v}_{\mathrm{R}}^{\mathrm{H}} \mathbf{a}_{\mathrm{Rr}k} \mathbf{a}_{\mathrm{Rt}k}^{\mathrm{H}} \mathbf{u}_{\mathrm{R}}\, \chi_{\mathrm{RR}k}\left(\tau, f_{\mathrm{D}}\right) && (8.8) \\ &+ \sum_{l=1}^{L} \alpha_{\mathrm{C}l}\, \mathbf{v}_{\mathrm{R}}^{\mathrm{H}} \mathbf{a}_{\mathrm{Cr}l} \mathbf{a}_{\mathrm{Ct}l}^{\mathrm{H}} \mathbf{u}_{\mathrm{C}l}\, \chi_{\mathrm{CR}l}\left(\tau, f_{\mathrm{D}}\right) + w_{\mathrm{R}}\left(\tau, f_{\mathrm{D}}\right), \end{aligned}$$

with

$$\chi_{\mathrm{RR}k}\left(\tau, f_{\mathrm{D}}\right) \triangleq \int_t x_{\mathrm{R}}\left(t-\tau_{\mathrm{R}k}\right) x_{\mathrm{R}}^*\left(t-\tau\right) e^{j2\pi\left(f_{\mathrm{DR}k}-f_{\mathrm{D}}\right)t}\,\mathrm{d}t,$$

$$\chi_{\mathrm{CR}l}\left(\tau, f_{\mathrm{D}}\right) \triangleq \int_t x_{\mathrm{C}l}\left(t-\tau_{\mathrm{C}l}\right) x_{\mathrm{R}}^*\left(t-\tau\right) e^{j2\pi\left(f_{\mathrm{DC}l}-f_{\mathrm{D}}\right)t}\,\mathrm{d}t,$$

$$w_{\mathrm{R}}\left(\tau, f_{\mathrm{D}}\right) \triangleq \int_t \mathbf{v}_{\mathrm{R}}^{\mathrm{H}}\mathbf{n}\left(t\right)\; x_{\mathrm{R}}^*\left(t-\tau\right)\; e^{-j2\pi f_{\mathrm{D}}t}\,\mathrm{d}t.$$

Levering on (8.3), the covariance of the noise $w_{\mathrm{R}}\left(\tau, f_{\mathrm{D}}\right)$ is given by

$$\mathbb{E}\left\{w_{\mathrm{R}}\left(\tau, f_{\mathrm{D}}\right) w_{\mathrm{R}}^*\left(\tau', f_{\mathrm{D}}'\right)\right\} = 2N_0 \int_t x_{\mathrm{R}}^*\left(t-\tau\right) x_{\mathrm{R}}\left(t-\tau'\right) e^{j2\pi\left(f_{\mathrm{D}}-f_{\mathrm{D}}'\right)t}\,\mathrm{d}t,$$

being independent of the beamforming vector $\mathbf{v}_{\mathrm{R}}$. As $x_{\mathrm{R}}\left(t\right)$ has a unit-energy, the noise variance is hence equal to $2N_0$. The SINR of the kth target is consequently obtained as

$$\mathrm{SINR}_{\mathrm{R}k} = \frac{\beta_{\mathrm{RR}kk}\,\left|\mathbf{v}_{\mathrm{R}}^{\mathrm{H}}\mathbf{a}_{\mathrm{Rr}k}\right|^2\left|\mathbf{u}_{\mathrm{R}}^{\mathrm{H}}\mathbf{a}_{\mathrm{Rt}k}\right|^2}{I_{\mathrm{RR}k}+I_{\mathrm{CR}k}+1}, \tag{8.9}$$

with $I_{\mathrm{RR}k}$ and $I_{\mathrm{CR}k}$ the interferences arising respectively from the other targets and uplink signals:

$$I_{\mathrm{RR}k} = \sum_{k'\neq k}\beta_{\mathrm{RR}k'k}\,\left|\mathbf{v}_{\mathrm{R}}^{\mathrm{H}}\mathbf{a}_{\mathrm{Rr}k'}\right|^2\left|\mathbf{u}_{\mathrm{R}}^{\mathrm{H}}\mathbf{a}_{\mathrm{Rt}k'}\right|^2, \tag{8.10}$$

$$I_{\mathrm{CR}k} = \sum_{l=1}^{L}\beta_{\mathrm{CR}lk}\,\left|\mathbf{v}_{\mathrm{R}}^{\mathrm{H}}\mathbf{a}_{\mathrm{Cr}l}\right|^2\left|\mathbf{u}_{\mathrm{C}l}^{\mathrm{H}}\mathbf{a}_{\mathrm{Ct}l}\right|^2, \tag{8.11}$$

where $\beta_{\mathrm{RR}k'k} \triangleq \mathbb{E}\left\{\left|\alpha_{\mathrm{R}k'}\right|^2\left|\chi_{\mathrm{RR}k'}(\tau_{\mathrm{R}k}, f_{\mathrm{DR}k})\right|^2\right\}/2N_0$ for the radar part, and $\beta_{\mathrm{CR}lk} \triangleq \mathbb{E}\left\{\left|\alpha_{\mathrm{C}l}\right|^2\left|\chi_{\mathrm{CR}l}(\tau_{\mathrm{R}k}, f_{\mathrm{DR}k})\right|^2\right\}/2N_0$. As for the communication processing, the expectations are performed on the communication symbols and channel gains, these latter considered independent.

Beamforming optimisation problem To formulate the beamforming optimisation problem, the $L+K$ SINRs must be condensed into a Single-Objective (SO) optimisation problem, i.e., one must scalarise a MO function. The selected scalarisation is the maximisation of the product of the radar and communication SINRs [81]:

$$\mathcal{M}\left(\mathbf{u}_{\mathrm{R}}, \mathbf{v}_{\mathrm{R}}, \{\mathbf{u}_{\mathrm{C}l}, \mathbf{v}_{\mathrm{C}l}\}_l\right) \triangleq \prod_{k=1}^{K} \mathrm{SINR}_{\mathrm{R}k} \cdot \prod_{l=1}^{L} \mathrm{SINR}_{\mathrm{C}l}, \tag{8.12}$$

the optimisation problem reading thus as

$$\begin{aligned} \max_{\mathbf{u}_{\mathrm{R}}, \mathbf{v}_{\mathrm{R}}, \{\mathbf{u}_{\mathrm{C}l}, \mathbf{v}_{\mathrm{C}l}\}_l} \quad & \mathcal{M}\left(\mathbf{u}_{\mathrm{R}}, \mathbf{v}_{\mathrm{R}}, \{\mathbf{u}_{\mathrm{C}l}, \mathbf{v}_{\mathrm{C}l}\}_l\right) \\ \text{s.t.} \quad & \|\mathbf{u}_{\mathrm{R}}\|_2 \leq 1,\ \|\mathbf{v}_{\mathrm{R}}\|_2 = 1, \\ & \|\mathbf{u}_{\mathrm{C}l}\|_2 \leq 1,\ \|\mathbf{v}_{\mathrm{C}l}\|_2 = 1, \quad \forall l = 1, \dots L. \end{aligned} \tag{8.13}$$

In the above, the notation $\{\cdot\}_l$ implicitly means $\{\cdot\}_{l=1}^{L}$, and similarly for the other indices. The metric $\mathcal{M}$ offers the advantage of fairly considering all targets and communication users, since they all impact in the same manner the objective function. Furthermore, since the direct channel gains can be removed from the optimisation problem, this formulation prevents the targets and UEs with low SINRs to be set aside compared to the high-SINR ones. As it will be emphasised below in Figure 8.3, formulating the above with a sum of SINRs instead of a product might lead to solutions optimising a single SINR at the detriment of the others. Finally, at high SINR, (8.13) is equivalent to a sum-rate maximisation [87].

Remark 8.1: Channel state information

In the above optimisation problem, a perfect Channel State Information (CSI) is assumed. This CSI includes the delays, the Doppler frequencies, and the array steering vectors. One possible way to acquire this knowledge is to consider that periodically, the communication UEs send training sequences which enables the estimation of these parameters, and the radar performs a coarse estimate of the targets parameters. During the next time slots, the beamforming optimisation can be performed, possibly with a refinement of the targets' parameters along the operations. Once the CSI quality becomes tow low, the initial CSI acquisition can be repeated.

Remark 8.2: Downlink communications

The considered system model does not include downlink communications for the sake of simplicity. These communications could be included either by considering a dedicated set of antennas and a dedicated waveform, or with $x_{\mathrm{R}}(t)$ containing the communication information. In both cases, the resulting SINRs could be added to the optimisation problem and the iterative scheme described in Section 8.2 could be adapted.

8.2 Beamforming design schemes

The beamforming optimisation problem (8.13) is tackled in this section. First, Section 8.2.1 translates the problem into a lower-dimensional problem. Then, Sections 8.2.2 to 8.2.6 provide solutions to the subproblems obtained by optimising upon each variable alone. Finally, Section 8.2.7 provides an Alternating Maximisation (AM) maximisation algorithm reaching a local optimum.

8.2.1 Dimensionality reduction

In order to facilitate the optimisation, the beamforming optimisation problem (8.13) can be reduced to a lower-dimensional one. This is achieved by expressing the beamforming vectors as vectors in the spaces of the steering vectors. Let these spaces be defined as

$$\begin{aligned}
\mathcal{S}_{\mathrm{Rt}} &\triangleq \operatorname{span}\left\{\begin{bmatrix}\mathbf{a}_{\mathrm{Rt}1} & \dots & \mathbf{a}_{\mathrm{Rt}K}\end{bmatrix}\right\}, \\
\mathcal{S}_{\mathrm{r}} &\triangleq \operatorname{span}\left\{\begin{bmatrix}\mathbf{a}_{\mathrm{Rr}1} & \dots & \mathbf{a}_{\mathrm{Rr}K} & \mathbf{a}_{\mathrm{Cr}1} & \dots & \mathbf{a}_{\mathrm{Cr}L}\end{bmatrix}\right\}, \\
\mathcal{S}_{\mathrm{Ct}l} &\triangleq \operatorname{span}\left\{\begin{bmatrix}\mathbf{a}_{\mathrm{Ct}l}\end{bmatrix}\right\}, \quad \forall l = 1, \dots, L.
\end{aligned} \tag{8.14}$$

The dimensions of the first two spaces are respectively denoted M_{Rt}, M_{r}, being in general different from the number of steering vectors if these latter are linearly dependent. The communication steering spaces are however always of dimension 1 since a single steering vector is involved. The matrices whose columns provide an orthonormal basis for the corresponding steering space are respectively denoted as $\mathbf{S}_{\mathrm{Rt}} \in \mathbb{C}^{N_{\mathrm{t}} \times M_{\mathrm{Rt}}}$, $\mathbf{S}_{\mathrm{r}} \in \mathbb{C}^{N_{\mathrm{r}} \times M_{\mathrm{r}}}$, and $\mathbf{S}_{\mathrm{Ct}l} \in \mathbb{C}^{N_{\mathrm{t}l}}$. By definition, they are therefore such that

$$\begin{aligned}
&\mathbf{S}_{\mathrm{Rt}}^{\mathrm{H}} \mathbf{S}_{\mathrm{Rt}} = \mathbf{I}_{M_{\mathrm{Rt}}}, && \mathcal{R}\left\{\mathbf{S}_{\mathrm{Rt}}\right\} = \mathcal{S}_{\mathrm{Rt}}, \\
&\mathbf{S}_{\mathrm{r}}^{\mathrm{H}} \mathbf{S}_{\mathrm{r}} = \mathbf{I}_{M_{\mathrm{r}}}, && \mathcal{R}\left\{\mathbf{S}_{\mathrm{r}}\right\} = \mathcal{S}_{\mathrm{r}}, \\
&\mathbf{S}_{\mathrm{Ct}l}^{\mathrm{H}} \mathbf{S}_{\mathrm{Ct}l} = 1, && \mathcal{R}\left\{\mathbf{S}_{\mathrm{Ct}l}\right\} = \mathcal{S}_{\mathrm{Ct}l}, \quad \forall l = 1, \ldots, L.
\end{aligned}$$

In these bases, the coordinates of the original steering vectors are defined as

$$\begin{aligned}
&\tilde{\mathbf{a}}_{\mathrm{Rt}k} \triangleq \mathbf{S}_{\mathrm{Rt}}^{\mathrm{H}} \mathbf{a}_{\mathrm{Rt}k}, && \tilde{\mathbf{a}}_{\mathrm{Rr}k} \triangleq \mathbf{S}_{\mathrm{r}}^{\mathrm{H}} \mathbf{a}_{\mathrm{Rr}k}, \\
&\tilde{a}_{\mathrm{Ct}l} \triangleq \mathbf{S}_{\mathrm{Ct}l}^{\mathrm{H}} \mathbf{a}_{\mathrm{Ct}l}, && \tilde{\mathbf{a}}_{\mathrm{Cr}l} \triangleq \mathbf{S}_{\mathrm{r}}^{\mathrm{H}} \mathbf{a}_{\mathrm{Cr}l}.
\end{aligned}$$

With these elements, the optimisation problem can be expressed in the steering space as follows.

Lemma 8.1: Low-dimensional beamforming optimisation

The optimisation problem (8.13) is equivalent to

$$\begin{aligned}
\max_{\substack{\mathbf{y}_{\mathrm{R}} \in \mathbb{C}^{M_{\mathrm{Rt}}} \\ \mathbf{z}_{\mathrm{R}}, \{\mathbf{z}_{\mathrm{C}l}\}_l \in \mathbb{C}^{M_{\mathrm{r}}} \\ P_{\mathrm{Rt}}, \{P_{\mathrm{Ct}l}\}_l \in \mathbb{R}}} \quad & \mathcal{M}\left(\mathbf{S}_{\mathrm{Rt}} \mathbf{y}_{\mathrm{R}} \sqrt{P_{\mathrm{Rt}}}, \mathbf{S}_{\mathrm{r}} \mathbf{z}_{\mathrm{R}}, \left\{\mathbf{S}_{\mathrm{Ct}l} \sqrt{P_{\mathrm{Ct}l}}, \mathbf{S}_{\mathrm{r}} \mathbf{z}_{\mathrm{C}l}\right\}_l\right) \\
\text{s.t. } & \left\|\mathbf{y}_{\mathrm{R}}\right\|_2^2 = 1, \\
& P_{\mathrm{Rt}} \in [0; 1], \\
& \left\|\mathbf{z}_{\mathrm{R}}\right\|_2^2 = 1, \\
& P_{\mathrm{Ct}l} \in [0; 1], \forall l, \\
& \left\|\mathbf{z}_{\mathrm{C}l}\right\|_2^2 = 1, \forall l,
\end{aligned} \tag{8.15}$$

with the optimal beamformers given by

$$\begin{aligned}
&\mathbf{u}_{\mathrm{R}} = \mathbf{S}_{\mathrm{Rt}} \mathbf{y}_{\mathrm{R}} \sqrt{P_{\mathrm{Rt}}}, && \mathbf{v}_{\mathrm{R}} = \mathbf{S}_{\mathrm{r}} \mathbf{z}_{\mathrm{R}}, \\
&\mathbf{u}_{\mathrm{C}l} = \mathbf{S}_{\mathrm{Ct}l} \sqrt{P_{\mathrm{Ct}l}}, && \mathbf{v}_{\mathrm{C}l} = \mathbf{S}_{\mathrm{r}} \mathbf{z}_{\mathrm{C}l}.
\end{aligned}$$

Proof. See Section 8.6.1. □

Therefore, instead of optimising over $N_{\mathrm{t}} + (L+1) N_{\mathrm{r}} + \sum_l N_{\mathrm{t}l}$ complex variables, the above involves $M_{\mathrm{Rt}} + (L+1)\, M_{\mathrm{r}}$ complex variables and $L+1$ real ones. Since the considered scenarios have much more antennas than the number of targets and UEs, this second formulation significantly reduces the problem dimensionality.

Remark 8.3

The fact that the transmit beamformers might not use all the available power can be surprising. Yet, this happens since the power impacts both the useful receive powers, but also the interference terms. There is thus a trade-off between increasing the useful power and increasing the interference.

The optimisation problem (8.15) is challenging to solve as it is neither convex in its objective function, nor in its constraints. Therefore, the below sections provide solutions for the subproblems which arise when optimising one beamformer or power with the others considered as fixed.

8.2.2 Communication transmit beamformers

First, the optimisation of $P_{\mathrm{Ct}l}$ with the others variables as fixed is considered, the optimum value being denoted $\hat{P}_{\mathrm{Ct}l}$. As described by the below lemmas, the optimal power is either 1, or it can be found with the Golden-Section Search (GSS) method [153], which finds the maximum of a unimodal function over a one-dimensional domain.

Lemma 8.2: Communication transmit power, $K + L \leq 2$

If $K + L \leq 2$, $\hat{P}_{\mathrm{Ct}l} = 1$.

Lemma 8.3: Communication transmit power

For general K and L, the optimal transmit power of the lth UE is a function of $\left(\mathbf{y}_{\mathrm{R}}, P_{\mathrm{Rt}}, \{P_{\mathrm{Ct}l'}, \mathbf{z}_{\mathrm{C}l'}\}_{l' \neq l}\right)$. Given $\left(\mathbf{y}_{\mathrm{R}}, P_{\mathrm{Rt}}, \{P_{\mathrm{Ct}l'}, \mathbf{z}_{\mathrm{C}l'}\}_{l' \neq l}\right)$, the unique maximum of $\mathcal{M}$ can be found with the GSS method [153], since $\mathcal{M}$ is unimodal on the interval $P_{\mathrm{Ct}l} \in [0; 1]$ whatever $\left(\mathbf{y}_{\mathrm{R}}, P_{\mathrm{Rt}}, \{P_{\mathrm{Ct}l'}, \mathbf{z}_{\mathrm{C}l'}\}_{l' \neq l}\right)$.

Proof. See Section 8.6.2. □

8.2.3 Communication receive beamformers

The optimum communication receive beamformer of the lth UE, denoted $\hat{\mathbf{z}}_{\mathrm{C}l}$ in the steering space, has a closed-form expression when the other beamformers are considered fixed. The impact of these other beamformers is gathered into the matrix $\mathbf{B}_{\mathrm{Cr}l}$ defined as

$$\begin{aligned}\mathbf{B}_{\mathrm{Cr}l} \triangleq \mathbf{I}_{M_\mathrm{r}} &+ \sum_{l'\neq l} \beta_{\mathrm{CC}l'l} P_{\mathrm{Ct}l'} \left|\tilde{a}_{\mathrm{Ct}l'}\right|^2 \tilde{\mathbf{a}}_{\mathrm{Cr}l'} \tilde{\mathbf{a}}_{\mathrm{Cr}l'}^{\mathrm{H}} \\ &+ P_{\mathrm{Rt}} \sum_{k=1}^{K} \beta_{\mathrm{RC}kl} \left|\mathbf{y}_{\mathrm{R}}^{\mathrm{H}} \tilde{\mathbf{a}}_{\mathrm{Rt}k}\right|^2 \tilde{\mathbf{a}}_{\mathrm{Rr}k} \tilde{\mathbf{a}}_{\mathrm{Rr}k}^{\mathrm{H}}.\end{aligned} \tag{8.16}$$

Lemma 8.4: Communication receive beamformer

The optimal communication receive beamformer of the lth UE is a function of $\left(\mathbf{y}_{\mathrm{R}}, P_{\mathrm{Rt}}, \{P_{\mathrm{Ct}l'}\}_{l'\neq l}\right)$. Given $\left(\mathbf{y}_{\mathrm{R}}, P_{\mathrm{Rt}}, \{P_{\mathrm{Ct}l'}\}_{l'\neq l}\right)$, it reads as

$$\hat{\mathbf{z}}_{\mathrm{C}l} = \frac{\mathbf{B}_{\mathrm{Cr}l}^{-1} \tilde{\mathbf{a}}_{\mathrm{Cr}l}}{\left\|\mathbf{B}_{\mathrm{Cr}l}^{-1} \tilde{\mathbf{a}}_{\mathrm{Cr}l}\right\|_2}.$$

Proof. See Section 8.6.3. □

8.2.4 Radar receive beamformer

The optimum radar receive beamformer, denoted $\hat{\mathbf{z}}_{\mathrm{R}}$ in the steering space, is more challenging to obtain as it is identical for all targets. Similarly to the communication receive beamformers, the impact of the other optimisation variables is gathered into K matrices defined for the kth one as

$$\begin{aligned}\mathbf{B}_{\mathrm{Rr}k} \triangleq \mathbf{I}_{M_\mathrm{r}} &+ P_{\mathrm{Rt}} \sum_{k'\neq k} \beta_{\mathrm{RR}k'k} \left|\mathbf{y}_{\mathrm{R}}^{\mathrm{H}} \tilde{\mathbf{a}}_{\mathrm{Rt}k'}\right|^2 \tilde{\mathbf{a}}_{\mathrm{Rr}k'} \tilde{\mathbf{a}}_{\mathrm{Rr}k'}^{\mathrm{H}} \\ &+ \sum_{l=1}^{L} \beta_{\mathrm{CR}lk} P_{\mathrm{Ct}l} \left|\tilde{a}_{\mathrm{Ct}l}\right|^2 \tilde{\mathbf{a}}_{\mathrm{Cr}l} \tilde{\mathbf{a}}_{\mathrm{Cr}l}^{\mathrm{H}}.\end{aligned} \tag{8.17}$$

Lemma 8.5: Radar receive beamformer, $K = 1$

If $K = 1$, whatever L, the optimal radar receive beamformer depends on $\{P_{\mathrm{Ct}l}\}_l$. Given $\{P_{\mathrm{Ct}l}\}_l$, it reads as

$$\hat{\mathbf{z}}_{\mathrm{R}} = \frac{\mathbf{B}_{\mathrm{Rr}1}^{-1}\tilde{\mathbf{a}}_{\mathrm{Rr}1}}{\left\|\mathbf{B}_{\mathrm{Rr}1}^{-1}\tilde{\mathbf{a}}_{\mathrm{Rr}1}\right\|_2}.$$

Lemma 8.6: Radar receive beamformer, $K = 2$, $L = 0$

If $K = 2$ and $L = 0$, the optimal radar receive beamformer depends on $(\mathbf{y}_{\mathrm{R}}, P_{\mathrm{Rt}})$. Given $(\mathbf{y}_{\mathrm{R}}, P_{\mathrm{Rt}})$, it reads as

$$\hat{\mathbf{z}}_{\mathrm{R}} = \frac{\lambda\frac{\tilde{\mathbf{a}}_{\mathrm{Rr}1}}{\|\tilde{\mathbf{a}}_{\mathrm{Rr}1}\|_2} + (1-\lambda)\frac{\tilde{\mathbf{a}}_{\mathrm{Rr}2}}{\|\tilde{\mathbf{a}}_{\mathrm{Rr}2}\|_2}e^{j\arg\left\{\tilde{\mathbf{a}}_{\mathrm{Rr}2}^{\mathrm{H}}\tilde{\mathbf{a}}_{\mathrm{Rr}1}\right\}}}{\left\|\lambda\frac{\tilde{\mathbf{a}}_{\mathrm{Rr}1}}{\|\tilde{\mathbf{a}}_{\mathrm{Rr}1}\|_2} + (1-\lambda)\frac{\tilde{\mathbf{a}}_{\mathrm{Rr}2}}{\|\tilde{\mathbf{a}}_{\mathrm{Rr}2}\|_2}e^{j\arg\left\{\tilde{\mathbf{a}}_{\mathrm{Rr}2}^{\mathrm{H}}\tilde{\mathbf{a}}_{\mathrm{Rr}1}\right\}}\right\|_2}.$$

Furthermore, the metric $\mathcal{M}$ is unimodal over $\lambda \in [0; 1]$ whatever $(\mathbf{y}_{\mathrm{R}}, P_{\mathrm{Rt}})$, and the unique maximum of $\mathcal{M}$ can hence be found with the GSS method [153].

Proof. See Section 8.6.4. □

When $K = 2$ and $L \geq 1$, only an approximate solution is obtained, for which some notations must be introduced. The Kronecker product is denoted $\otimes$. Given $\mathbf{U} \in \mathbb{C}^{N\times N}$ and $\mathbf{E} \in \mathbb{C}^{N\times N}$, the matrix $\mathbf{M}_{\mathbf{U}} \in \mathbb{R}^{2N\times 2N}$ and the vector $\mathrm{vec}_{\mathbb{C}}(\mathbf{E}) \in \mathbb{R}^{2N^2}$ are defined as

$$\begin{aligned}\mathbf{M}_{\mathbf{U}} &\triangleq \begin{bmatrix}\mathrm{Re}\{\mathbf{U}\} & -\mathrm{Im}\{\mathbf{U}\}\\ \mathrm{Im}\{\mathbf{U}\} & \mathrm{Re}\{\mathbf{U}\}\end{bmatrix},\\ \mathrm{vec}_{\mathbb{C}}(\mathbf{E}) &\triangleq \begin{bmatrix}\mathrm{vec}^{\top}(\mathrm{Re}\{\mathbf{E}\}) & \mathrm{vec}^{\top}(\mathrm{Im}\{\mathbf{E}\})\end{bmatrix}^{\top},\end{aligned} \tag{8.18}$$

with $\mathrm{vec}(\cdot)$ the vectorisation operator. The inverse operator of $\mathrm{vec}_{\mathbb{C}}(\cdot)$ is denoted $\mathrm{vec}_{\mathbb{C}}^{-1}(\cdot)$. For Hermitian matrices, the half-vectorisation operator $\mathrm{vech}_{\mathbb{C}}(\mathbf{E})$ is defined similarly, but with the duplicate entries excluded. That is, $\mathrm{vech}_{\mathbb{C}}(\mathbf{E})$ is the vector of size $N^2 \times 1$, whose first $N(N+1)/2$ elements are the stacked columns of the upper triangular part of $\mathrm{Re}\{\mathbf{E}\}$, including the diagonal, and the last $N(N-1)/2$ elements are the stacked columns of the upper triangular part of $\mathrm{Im}\left\{\mathbf{E}\right\}$, excluding the diagonal. The duplication matrix $\mathbf{T} \in \mathbb{R}^{2N^2 \times N^2}$ is then introduced as the unique matrix fulfilling $\mathbf{T}\mathrm{vech}_{\mathbb{C}}\left(\mathbf{E}\right) = \mathrm{vec}_{\mathbb{C}}\left(\mathbf{E}\right)$.

Lemma 8.7: Radar receive beamformer, $K = 2$

If $K = 2$, whatever L, the optimal radar receive beamformer depends on $(\mathbf{y}_{\mathrm{R}}, P_{\mathrm{Rt}}, \{P_{\mathrm{Ct}l}\}_l)$. Given $(\mathbf{y}_{\mathrm{R}}, P_{\mathrm{Rt}}, \{P_{\mathrm{Ct}l}\}_l)$, an approximate solution of $\hat{\mathbf{z}}_{\mathrm{R}}$ is given by the eigenvector associated with the largest positive eigenvalue of

$$\hat{\mathbf{X}}_{\mathrm{R}} \triangleq \frac{\mathrm{vec}_{\mathbb{C}}^{-1}\left(\mathbf{T}\hat{\mathbf{f}}\right)}{\mathrm{Tr}\left\{\mathrm{vec}_{\mathbb{C}}^{-1}\left(\mathbf{T}\hat{\mathbf{f}}\right)\right\}},$$

with $\hat{\mathbf{f}}$ the eigenvector associated with the largest eigenvalue of

$$\mathbf{K} \triangleq \left(\mathbf{T}^{\top}\mathbf{M}_{\left(\mathbf{B}_{\mathrm{Rr}1}^{\star} \otimes \mathbf{B}_{\mathrm{Rr}2}\right)}\mathbf{T}\right)^{-1}\mathbf{T}^{\top}\mathbf{M}_{\left(\mathbf{A}_{\mathrm{Rr}1}^{\star} \otimes \mathbf{A}_{\mathrm{Rr}2}\right)}\mathbf{T},$$

where $\mathbf{A}_{\mathrm{Rr}k} \triangleq \tilde{\mathbf{a}}_{\mathrm{Rr}k}\tilde{\mathbf{a}}_{\mathrm{Rr}k}^{\mathrm{H}}$.

Proof. See Section 8.6.5 □

Lemma 8.8: Radar receive beamformer

For general K (and L), the optimal radar receive beamformer depends on $(\mathbf{y}_{\mathrm{R}}, P_{\mathrm{Rt}}, \{P_{\mathrm{Ct}l}\}_l)$. Given $(\mathbf{y}_{\mathrm{R}}, P_{\mathrm{Rt}}, \{P_{\mathrm{Ct}l}\}_l)$, a local optimum can be obtained by performing an AM on the first $M_{\mathrm{r}} - 1$ complex coefficients of $\mathbf{z}_{\mathrm{R}}$, which reads as

$$\mathbf{z}_{\mathrm{R}} \triangleq \begin{bmatrix} z_{\mathrm{R},1} & \dots & z_{\mathrm{R},M_{\mathrm{r}}-1} & \sqrt{1 - \sum_{i=1}^{M_{\mathrm{r}}-1}\left|z_{\mathrm{R},i}\right|^2} \end{bmatrix}^{\top}.$$

Proof. See Section 8.6.5 □

8.2.5 Radar transmit power

Regarding the radar transmit power, it is obtained as follows.

Lemma 8.9: Radar transmit power, $L = 0$

When $L = 0$, whatever $K \geq 1$, the optimal radar transmit power is $\hat{P}_{\mathrm{Rt}} = 1$.

Lemma 8.10: Radar transmit power, $K = 1$, $L = 1$

When $K = L = 1$, the optimal radar transmit power is $\hat{P}_{\mathrm{Rt}} = 1$.

Lemma 8.11: Radar transmit power

For general K and L, the optimal radar transmit power is a function of $(\mathbf{y}_{\mathrm{R}}, \mathbf{z}_{\mathrm{R}}, \{P_{\mathrm{Ct}l}, \mathbf{z}_{\mathrm{C}l}\}_l)$. Given $(\mathbf{y}_{\mathrm{R}}, \mathbf{z}_{\mathrm{R}}, \{P_{\mathrm{Ct}l}, \mathbf{z}_{\mathrm{C}l}\}_l)$, the unique maximum of $\mathcal{M}$ can be found with the GSS method [153], since $\mathcal{M}$ is unimodal on the interval $P_{\mathrm{Rt}} \in [0; 1]$ whatever $(\mathbf{y}_{\mathrm{R}}, \mathbf{z}_{\mathrm{R}}, \{P_{\mathrm{Ct}l}, \mathbf{z}_{\mathrm{C}l}\}_l)$.

Proof. See Section 8.6.6. □

8.2.6 Radar transmit beamformer

Finally, the radar transmit beamformer is studied, the impact of the other variables being grouped into the matrices

$$
\begin{aligned}
\mathbf{B}_{\mathrm{Rt}l} &\triangleq \frac{\sum_{k=1}^{K} \beta_{\mathrm{RC}kl} \left|\mathbf{z}_{\mathrm{C}l}^{\mathrm{H}} \tilde{\mathbf{a}}_{\mathrm{Rr}k}\right|^2 \tilde{\mathbf{a}}_{\mathrm{Rt}k} \tilde{\mathbf{a}}_{\mathrm{Rt}k}^{\mathrm{H}}}{1 + \sum_{l' \neq l} \beta_{\mathrm{CC}l'l} \left|\mathbf{z}_{\mathrm{C}l}^{\mathrm{H}} \tilde{\mathbf{a}}_{\mathrm{Cr}l'}\right|^2 P_{\mathrm{Ct}l'} \left|\tilde{a}_{\mathrm{Ct}l'}\right|^2}, \forall l = 1, \ldots, L, \\
\mathbf{C}_{\mathrm{Rt}k} &\triangleq \frac{\sum_{k' \neq k} \beta_{\mathrm{RR}k'k} \left|\mathbf{z}_{\mathrm{R}}^{\mathrm{H}} \tilde{\mathbf{a}}_{\mathrm{Rr}k'}\right|^2 \tilde{\mathbf{a}}_{\mathrm{Rt}k'} \tilde{\mathbf{a}}_{\mathrm{Rt}k'}^{\mathrm{H}}}{1 + \sum_{l=1}^{L} \beta_{\mathrm{CR}lk} \left|\mathbf{z}_{\mathrm{R}}^{\mathrm{H}} \tilde{\mathbf{a}}_{\mathrm{Cr}l}\right|^2 P_{\mathrm{Ct}l} \left|\tilde{a}_{\mathrm{Ct}l}\right|^2}, \forall k = 1, \ldots, K.
\end{aligned} \tag{8.19}
$$

Lemma 8.12: Radar transmit beamformer, $K = 1$

When $K = 1$, $\hat{y}_{\mathrm{R}} = 1$.

Lemma 8.13: Radar transmit beamformer, $K = 2$, $L = 0$

If $K = 2$ and $L = 0$, the optimal radar transmit beamformer depends on $(P_{\mathrm{Rt}}, \mathbf{z}_{\mathrm{R}})$. Given $(P_{\mathrm{Rt}}, \mathbf{z}_{\mathrm{R}})$, it reads as

$$\hat{\mathbf{y}}_{\mathrm{R}} = \frac{\lambda \frac{\tilde{\mathbf{a}}_{\mathrm{Rt1}}}{\|\tilde{\mathbf{a}}_{\mathrm{Rt1}}\|_2} + (1-\lambda) \frac{\tilde{\mathbf{a}}_{\mathrm{Rt2}}}{\|\tilde{\mathbf{a}}_{\mathrm{Rt2}}\|_2} e^{j \arg\left\{\tilde{\mathbf{a}}_{\mathrm{Rt2}}^{\mathrm{H}} \tilde{\mathbf{a}}_{\mathrm{Rt1}}\right\}}}{\left\| \lambda \frac{\tilde{\mathbf{a}}_{\mathrm{Rt1}}}{\|\tilde{\mathbf{a}}_{\mathrm{Rt1}}\|_2} + (1-\lambda) \frac{\tilde{\mathbf{a}}_{\mathrm{Rt2}}}{\|\tilde{\mathbf{a}}_{\mathrm{Rt2}}\|_2} e^{j \arg\left\{\tilde{\mathbf{a}}_{\mathrm{Rt2}}^{\mathrm{H}} \tilde{\mathbf{a}}_{\mathrm{Rt1}}\right\}} \right\|_2}.$$

Furthermore, the metric $\mathcal{M}$ is unimodal over $\lambda \in [0; 1]$ whatever $(P_{\mathrm{Rt}}, \mathbf{z}_{\mathrm{R}})$, and the unique maximum of $\mathcal{M}$ can hence be found with the GSS method [153].

Lemma 8.14: Radar transmit beamformer

For general K and L, the optimal radar transmit beamformer depends on $(P_{\mathrm{Rt}}, \mathbf{z}_{\mathrm{R}}, \{P_{\mathrm{C}l}, \mathbf{z}_{\mathrm{C}l}\}_l)$. Given $(P_{\mathrm{Rt}}, \mathbf{z}_{\mathrm{R}}, \{P_{\mathrm{C}l}, \mathbf{z}_{\mathrm{C}l}\}_l)$, a local optimum can be obtained by performing an AM on the first $M_{\mathrm{Rt}} - 1$ complex coefficients of $\mathbf{y}_{\mathrm{R}}$ defined as

$$\mathbf{y}_{\mathrm{R}} \triangleq \left[y_{\mathrm{R},1} \quad \ldots \quad y_{\mathrm{R},M_{\mathrm{Rt}}-1} \quad \sqrt{1 - \sum_{i=1}^{M_{\mathrm{Rt}}-1} |y_{\mathrm{R},i}|^2} \right]^{\top}.$$

Proof. See Section 8.6.7. □

Remark 8.4

As discussed in [144], well-designed radar waveforms provide a good separation of the targets if these latter are not too close. In that case, the coefficients $\beta_{\mathrm{RR}kk'}$ can be assumed to be 0 for $k \neq k'$. Then, results similar to those of Lemma 8.7 can be obtained with up to $K = L = 2$ UEs and targets.

8.2.7 Alternating maximisation

Above, solutions to the component-wise optimisation of (8.15) have been provided, as summarised in Table 8.1. This enables to perform an AM of $\mathcal{M}$, as given in Algorithm 3. This AM scheme is ensured to reach a local maximum of $\mathcal{M}$, since each optimisation step maximises this metric. Therefore, the metric value cannot decrease, ensuring the convergence to

	$P_{\mathrm{C}tl}$	$\mathbf{z}_{\mathrm{C}l}$	$\mathbf{z}_{\mathrm{R}}$	$P_{\mathrm{R}t}$	$\mathbf{y}_{\mathrm{R}}$
$K=1$ $L=0$	-	-	1	1 Lemma 8.9	1 Lemma 8.12
$K=0$ $L=1$	1 Lemma 8.2	1	-	-	-
$K=1$ $L=1$	1 Lemma 8.2	Exact Lemma 8.4	Exact Lemma 8.5	1 Lemma 8.10	1 Lemma 8.12
$K=2$ $L=0$	-	-	GSS Lemma 8.6	1 Lemma 8.9	GSS Lemma 8.13
$K=0$ $L=2$	GSS Lemma 8.3	Exact Lemma 8.4	-	-	-
$K=2$ $L=1$	GSS Lemma 8.3	Exact Lemma 8.4	Approx. Lemma 8.7	GSS Lemma 8.11	AM Lemma 8.14
$K=1$ $L=2$	GSS Lemma 8.3	Exact Lemma 8.4	Exact Lemma 8.5	GSS Lemma 8.11	AM Lemma 8.14
$K=2$ $L=2$	GSS Lemma 8.3	Exact Lemma 8.4	Approx. Lemma 8.7	GSS Lemma 8.11	AM Lemma 8.14
K L	GSS Lemma 8.3	Exact Lemma 8.4	AM Lemma 8.8	GSS Lemma 8.11	AM Lemma 8.14

Table 8.1 Summary of the beamforming solutions for the steps of the AM scheme, for different numbers of targets and users. For each variable, it is specified whether it is equal to 1, computed exactly, computed approximatively, computed iteratively with the GSS method, or computed iteratively with an AM scheme. The lemmas providing these results are furthermore referred to. For the two first scenarios, since the steering spaces are all of dimension 1, the beamforming vectors $\mathbf{z}_{\mathrm{C}l}$, $\mathbf{z}_{\mathrm{R}}$ and $\mathbf{y}_{\mathrm{R}}$ are trivially equal to 1.

a local maximum. It should be noted that the order of the variables is arbitrary in the AM algorithm. Also, at the different steps of the algorithm, once the optimal value of a variable is found, it immediately replaces its previous value.

Algorithm 3 Alternating beamforming optimisation

Compute the steering vector bases $\mathbf{S}_{\mathrm{C}tl}$, $\mathbf{S}_{\mathrm{Rt}}$ and $\mathbf{S}_{\mathrm{r}}$
Compute the steering vector coordinates $\{\tilde{\mathbf{a}}_{\mathrm{Rt}k}, \tilde{\mathbf{a}}_{\mathrm{Rr}k}\}_k$, $\{\tilde{a}_{\mathrm{Ct}l}, \tilde{\mathbf{a}}_{\mathrm{Cr}l}\}_l$
Choose the initial beamformers $\mathbf{y}_{\mathrm{R}}, P_{\mathrm{Rt}}, \mathbf{z}_{\mathrm{R}}, \{P_{\mathrm{C}l}, \mathbf{z}_{\mathrm{C}l}\}_l$
for $n = 0 \to \infty$ **do**
  for $l = 1, \dots, L$ **do**
    Compute $\hat{P}_{\mathrm{Ct}l}$ as a function of $\left(\mathbf{y}_{\mathrm{R}}, P_{\mathrm{Rt}}, \{P_{\mathrm{Ct}l'}, \mathbf{z}_{\mathrm{C}l'}\}_{l' \neq l}\right)$
  for $l = 1, \dots, L$ **do**
    Compute $\hat{\mathbf{z}}_{\mathrm{C}l}$ as a function of $\left(\mathbf{y}_{\mathrm{R}}, P_{\mathrm{Rt}}, \{P_{\mathrm{Ct}l'}\}_{l' \neq l}\right)$
  Compute $\hat{P}_{\mathrm{Rt}}$ as a function of $(\mathbf{y}_{\mathrm{R}}, \mathbf{z}_{\mathrm{R}}, \{P_{\mathrm{Ct}l}, \mathbf{z}_{\mathrm{C}l}\}_l)$
  Compute $\hat{\mathbf{y}}_{\mathrm{R}}$ as a function of $(P_{\mathrm{Rt}}, \mathbf{z}_{\mathrm{R}}, \{P_{\mathrm{C}l}, \mathbf{z}_{\mathrm{C}l}\}_l)$
  Compute $\hat{\mathbf{z}}_{\mathrm{R}}$ as a function of $(\mathbf{y}_{\mathrm{R}}, P_{\mathrm{Rt}}, \{P_{\mathrm{Ct}l}\}_l)$
Compute the beamformers $\mathbf{u}_{\mathrm{R}}, \mathbf{v}_{\mathrm{R}}, \{\mathbf{u}_{\mathrm{C}l}, \mathbf{v}_{\mathrm{C}l}\}_l$ as a function of $\mathbf{y}_{\mathrm{R}}, P_{\mathrm{Rt}}, \mathbf{z}_{\mathrm{R}}, \{P_{\mathrm{C}l}, \mathbf{z}_{\mathrm{C}l}\}_l$

Remark 8.5

The convergence of the AM scheme might be jeopardised during the update steps of $\mathbf{z}_{\mathrm{R}}$, when only an approximation of this latter is available, as provided by Lemma 8.7. Indeed, especially when the AM scheme is close to a local maximum, the approximate solution might decrease the value of $\mathcal{M}$ instead of increasing it. To avoid this issue, the approximate solution is considered as valid only if $\mathcal{M}$ is increased, and if not, the previous value of $\mathbf{z}_{\mathrm{R}}$ is kept.

8.3 Numerical analysis

In this section, the developed JRC metric and associated beamforming design schemes are analysed.

8.3.1 Two-targets two-users scenario

The considered scenario involves two targets and two UEs, all equipped with $N_{\mathrm{t}} = N_{\mathrm{t}l} = N_{\mathrm{r}} = 8$ and half-wavelength ULA. The departure and arrival angles are given by

$$\theta_{\mathrm{Rt1}} = \theta_{\mathrm{Rr1}} = 12°, \qquad \theta_{\mathrm{Rt2}} = \theta_{\mathrm{Rr2}} = 43°,$$
$$\theta_{\mathrm{Ct1}} = 0°, \qquad \theta_{\mathrm{Ct2}} = 0°,$$
$$\theta_{\mathrm{Cr1}} = 21°, \qquad \theta_{\mathrm{Cr2}} = -67°,$$

and the FF steering vectors are obtained with (8.1). Regarding the interference coefficients (i.e., the β coefficients), they are set as

$$\beta_{\mathrm{RR}} = \begin{bmatrix} 1 & 0.5 \\ 0.1 & 1 \end{bmatrix}, \qquad \beta_{\mathrm{CR}} = \begin{bmatrix} 1 & 0.1 \\ 0.2 & 1 \end{bmatrix},$$
$$\beta_{\mathrm{CC}} = \begin{bmatrix} 1 & 0.1 \\ 0.2 & 1 \end{bmatrix}, \qquad \beta_{\mathrm{RC}} = \begin{bmatrix} 0.5 & 0.5 \\ 0.1 & 0.1 \end{bmatrix}.$$

For this scenario, Figure 8.2 illustrates the receive communication beampatterns $G_{\mathbf{v}_{\mathrm{C},l}} \triangleq \left|\mathbf{v}_{\mathrm{C},l}^{\mathrm{H}}\mathbf{a}_{\mathrm{r}}(\theta)\right|$, and the radar transmit and receive beampatterns $G_{\mathbf{u}_{\mathrm{R}}} \triangleq \left|\mathbf{u}_{\mathrm{R}}^{\mathrm{H}}\mathbf{a}_{\mathrm{t}}(\theta)\right|$ and $G_{\mathbf{v}_{\mathrm{R}}} \triangleq \left|\mathbf{v}_{\mathrm{R}}^{\mathrm{H}}\mathbf{a}_{\mathrm{r}}(\theta)\right|$, with $\mathbf{a}_{\mathrm{r}}(\theta)$ the receive steering vector in direction θ provided by (8.1). As it can be observed in the bottom panel, the receive communication beamforming vectors manage to provide low power gains in the direction of the radar targets and of the other communication users. In the upper panel, the receive radar beamforming vector blinds the communication users, while providing high power gains for both targets simultaneously.

8.3.2 SINR product metric

Next, the benefits of the SINR product metric are investigated. Figure 8.3 illustrates a scenario with no communication user and two radar targets located at $\theta_{\mathrm{R1}} = 43°$ and $\theta_{\mathrm{R2}} = -43°$, with the interfering coefficients set to $\beta_{\mathrm{RR11}} = \alpha$, $\beta_{\mathrm{RR12}} = 0.1\alpha$, $\beta_{\mathrm{RR21}} = 0.1$ and $\beta_{\mathrm{RR22}} = 1$. The factor α models the path loss ratio between the first and second radar target, i.e., $\alpha < 1$ means that the first target is in less favourable conditions than the second. For a given α, the achievable Pareto-optimal SINR couples $(\mathrm{SINR}_{\mathrm{R0}}, \mathrm{SINR}_{\mathrm{R1}})$ are displayed, as well as the point selected by the SINR product and SINR sum metric. As it can be observed, the product metric always selects a Pareto-optimal point, and fairly considers both targets, even

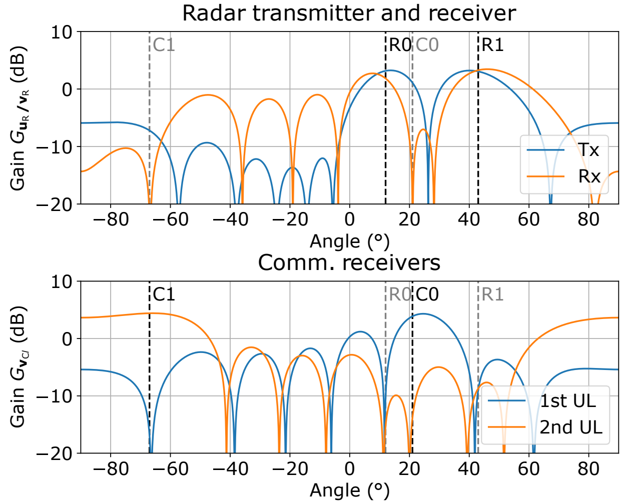

Fig. 8.2 Scenario with two targets and two UEs — radar transmit and receive (top) and communication receive beamforming gains (bottom).

if one suffers from severe channel degradation. In contrast, the SINR sum metric drastically favours the target with the best channel condition, at the detriment of the other. As a result, the SINR sum metric is extremely sensitive to channel changes, as it can be observed by comparing the $\alpha = 0.99$ and $\alpha = 1.01$ results: while the Pareto frontier remains almost unmodified, the SINR of the first target jumps from -23 dB to 18 dB.

8.4 Chapter summary

This chapter has considered the beamforming design for a JRC system, with several communication UEs and several targets. The product of the SINRs of both the UEs and the targets has been considered as the optimised metric, since it enables a fair consideration of the different elements of the JRC system.

Once formulated, the beamforming optimisation scheme has been tackled by first translating it into a low-dimensional problem. Then, an AM scheme has been described, and the solutions to the subproblems have been obtained depending on the number of UEs and targets.

Finally, the obtained beamformers have been qualitatively analysed,

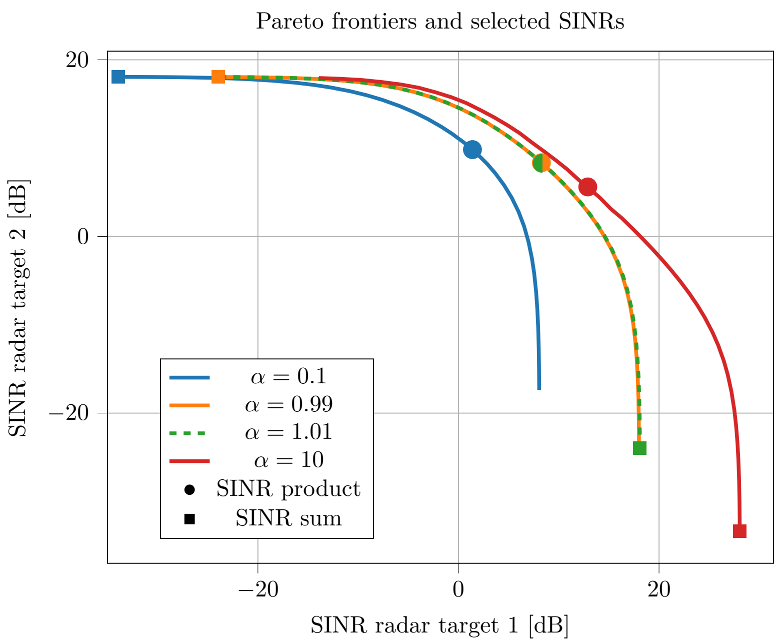

Fig. 8.3 Pareto frontier and selected point for the SINR product and sum metrics, in a scenario with two radar targets. The factor α is the ratio between the path loss of the first radar target and the second.

and the benefit of the SINR product metric over the SINR sum has been emphasised.

Similarly to the secure beamforming scheme developed in Chapter 7, the studied JRC MF MP scenario could not have been tackled through the autonomous perspective of Part I. The first reason is that the problem is inherently a centralised problem, in which one beamformer must be optimised by considered its associated metric, but also the interference it creates for the other functions of the network. The second reason, more practical, is that maximising SINRs under unit-norm constraints is not a convex problem, and therefore the assumptions made in Part I would not hold.

8.5 Conclusion on the optimisation-based interference management

Before moving to the third and last part of this thesis, the optimisation-based interference management approach must be commented.

- First, as it is the case for the two considered scenarios, the centralised approach might naturally stem from the considered scenarios, rather than being a mathematical modelling choice. This is the case for instance when the resources upon which the optimisation is performed are located at the same physical place. This also arises when the infrastructure needed to centralise the information is already required by the network functions.

- One challenge of centralised solutions is that may heavily depend on the formulation of the optimisation problem. It must be decided whether the multiple points and functions have the same relative importance, or whether some of them should be prioritised. However, the benefit is that globally optimal points can be reached, while the autonomous approach only guarantees the convergence to an equilibrium.

- Since it must take into account the multiple functions and points, the centralised optimisation problems are often high-dimensional, and lacking the standard convexity and differentiability properties. However, compared to the autonomous approach, ad-hoc mechanism can be investigated, even if they are only guaranteed to converge to local optima.

In a nutshell, centralise interference management techniques might provide substantial gains, yet their downside is that they often come with a high computational cost. This is why the third part of this thesis investigates another perspective, in which the interference is handled by exploiting the NF effects.

8.6 Proofs

8.6.1 Proof of Lemma 8.1

Given the steering spaces defined in (8.14), the beamformers can be decomposed as

$$\begin{aligned} \mathbf{u}_{\mathrm{R}} &= \mathbf{S}_{\mathrm{Rt}}\mathbf{y}_{\mathrm{R}} + \mathbf{u}_{\mathrm{R}}^{\perp}, & \mathbf{v}_{\mathrm{R}} &= \mathbf{S}_{\mathrm{r}}\mathbf{z}_{\mathrm{R}} + \mathbf{v}_{\mathrm{R}}^{\perp}, \\ \mathbf{v}_{\mathrm{C}l} &= \mathbf{S}_{\mathrm{r}}\mathbf{z}_{\mathrm{C}l} + \mathbf{v}_{\mathrm{C}l}^{\perp}, & \mathbf{u}_{\mathrm{C}l} &= \mathbf{S}_{\mathrm{Ct}l}y_{\mathrm{C}l} + \mathbf{u}_{\mathrm{C}l}^{\perp}, \quad \forall l = 1, \dots, L, \end{aligned}$$

with $\mathbf{y}_{\mathrm{R}} \in \mathbb{C}^{M_{\mathrm{Rt}}}$, $\mathbf{z}_{\mathrm{R}}, \mathbf{z}_{\mathrm{C}l} \in \mathbb{C}^{M_{\mathrm{r}}}$, $y_{\mathrm{C}l} \in \mathbb{C}$, and the parts orthogonal to the steering spaces such that $\mathbf{u}_{\mathrm{R}}^{\perp} \notin \mathcal{S}_{\mathrm{Rt}}$, $\mathbf{v}_{\mathrm{R}}^{\perp}, \mathbf{v}_{\mathrm{C}l}^{\perp} \notin \mathcal{S}_{\mathrm{r}}$, and $\mathbf{u}_{\mathrm{C}l}^{\perp} \notin \mathcal{S}_{\mathrm{Ct}l}$. As the SINR expressions depend on the beamforming vectors through scalar products with the corresponding steering vectors, only the parts lying in the steering spaces impact the metric $\mathcal{M}$:

$$\mathcal{M}\left(\mathbf{u}_{\mathrm{R}}, \mathbf{v}_{\mathrm{R}}, \{\mathbf{u}_{\mathrm{C}l}, \mathbf{v}_{\mathrm{C}l}\}_l\right) = \mathcal{M}\left(\mathbf{S}_{\mathrm{Rt}}\mathbf{y}_{\mathrm{R}}, \mathbf{S}_{\mathrm{r}}\mathbf{z}_{\mathrm{R}}, \{\mathbf{S}_{\mathrm{Ct}l}y_{\mathrm{C}l}, \mathbf{S}_{\mathrm{r}}\mathbf{z}_{\mathrm{C}l}\}_l\right).$$

Regarding the orthogonal parts, they can be set to $\mathbf{0}$ without loss of generality. Indeed, replacing any radar transmit beamformer $\mathbf{u}_{\mathrm{R}}^{(1)} = \mathbf{S}_{\mathrm{Rt}}\mathbf{y}_{\mathrm{R}} + \mathbf{u}_{\mathrm{R}}^{\perp}$ which fulfils the power constraint by $\mathbf{u}_{\mathrm{R}}^{(2)} = \mathbf{S}_{\mathrm{Rt}}\mathbf{y}_{\mathrm{R}}$ leads to the same objective value, while still fulfilling the power constraint since

$$\left\|\mathbf{u}_{\mathrm{R}}^{(2)}\right\|_2^2 = \|\mathbf{y}_{\mathrm{R}}\|_2^2 \leq \|\mathbf{y}_{\mathrm{R}}\|_2^2 + \left\|\mathbf{u}_{\mathrm{R}}^{\perp}\right\|_2^2 = \left\|\mathbf{u}_{\mathrm{R}}^{(1)}\right\|_2^2,$$

and similarly for the communication transmit vectors. As far as the radar receive beamformer is concerned, plugging into $\mathcal{M}$ the normalised vector $\mathbf{v}_{\mathrm{R}}^{(1)} = \left(\mathbf{S}_{\mathrm{r}}\mathbf{z}_{\mathrm{R}} + \mathbf{v}_{\mathrm{R}}^{\perp}\right) / \sqrt{\|\mathbf{z}_{\mathrm{R}}\|_2^2 + \left\|\mathbf{v}_{\mathrm{R}}^{\perp}\right\|_2^2}$, and keeping only the factors depending on this vector, one obtains

$$\mathcal{M} \underset{\mathbf{v}_{\mathrm{R}}^{(1)}}{\propto} \prod_{k=1}^{K} \frac{\left|\mathbf{z}_{\mathrm{R}}^{\mathrm{H}}\mathbf{S}_{\mathrm{r}}^{\mathrm{H}}\tilde{\mathbf{a}}_{\mathrm{Rr}k}\right|^2}{\left\|\mathbf{v}_{\mathrm{R}}^{\perp}\right\|_2^2 + \mathbf{z}_{\mathrm{R}}^{\mathrm{H}}\mathbf{B}_{\mathrm{Rr}k}\mathbf{z}_{\mathrm{R}}},$$

with $\underset{\mathbf{v}_{\mathrm{R}}^{(1)}}{\propto}$ indicating that only the factors depending on $\mathbf{v}_{\mathrm{R}}$ are kept, and $\mathbf{B}_{\mathrm{Rr}k}$ a positive definite matrix defined in (8.17). This shows that replacing $\mathbf{v}_{\mathrm{R}}^{(1)}$ by $\mathbf{v}_{\mathrm{R}}^{(2)} = \mathbf{S}_{\mathrm{r}}\mathbf{z}_{\mathrm{R}}/\left\|\mathbf{z}_{\mathrm{R}}\right\|_2$ provides a higher metric value, and that therefore the orthogonal parts can be set to $\mathbf{0}$. From a similar reasoning, the same applies to the communication receive beamformers. These elements lead to the formulation (8.15), with as a last step the fact that since the beamformers are defined up to a phase shift, $y_{\mathrm{C}l}$ can be selected as real.

8.6.2 Proof of Lemma 8.2 and Lemma 8.3

In order to determine the optimal transmit power of the lth UE, the metric $\mathcal{M}$ is rewritten by only keeping the factor depending on this power. It reads therefore as

$$\mathcal{M} \underset{P_{\mathrm{Ct}l}}{\propto} \left(\frac{1}{P_{\mathrm{Ct}l}}\right)^{K+L-2} \prod_{l'\neq l} \frac{1}{\frac{1}{P_{\mathrm{Ct}l}} + b_{\mathrm{Ct}l'l}} \prod_{k=1}^{K} \frac{1}{\frac{1}{P_{\mathrm{Ct}l}} + c_{\mathrm{Ct}kl}},$$

with the non-negative scalars

$$b_{\mathrm{Ct}l'l} \triangleq \frac{\beta_{\mathrm{CC}ll'}\left|\mathbf{z}_{\mathrm{C}l'}^{\mathrm{H}}\tilde{\mathbf{a}}_{\mathrm{Cr}l}\right|^2\left|\tilde{a}_{\mathrm{Ct}l}\right|^2}{1+\sum_{l''\neq l,l'}\beta_{\mathrm{CC}l''l'}\left|\mathbf{z}_{\mathrm{C}l'}^{\mathrm{H}}\tilde{\mathbf{a}}_{\mathrm{Cr}l''}\right|^2 P_{\mathrm{Ct}l''}\left|\tilde{a}_{\mathrm{Ct}l''}\right|^2+P_{\mathrm{Rt}}\sum_{k=1}^{K}\beta_{\mathrm{RC}kl}\left|\mathbf{z}_{\mathrm{C}l'}^{\mathrm{H}}\tilde{\mathbf{a}}_{\mathrm{Rr}k}\right|^2\left|\mathbf{y}_{\mathrm{R}}^{\mathrm{H}}\tilde{\mathbf{a}}_{\mathrm{Rt}k}\right|^2},$$

$$c_{\mathrm{Ct}kl} \triangleq \frac{\beta_{\mathrm{CR}lk}\left|\mathbf{z}_{\mathrm{R}}^{\mathrm{H}}\tilde{\mathbf{a}}_{\mathrm{Cr}l}\right|^2\left|\tilde{a}_{\mathrm{Ct}l}\right|^2}{1+P_{\mathrm{Rt}}\sum_{k'\neq k}\beta_{\mathrm{RR}k'k}\left|\mathbf{z}_{\mathrm{R}}^{\mathrm{H}}\tilde{\mathbf{a}}_{\mathrm{Rr}k'}\right|^2\left|\mathbf{y}_{\mathrm{R}}^{\mathrm{H}}\tilde{\mathbf{a}}_{\mathrm{Rt}k'}\right|^2+\sum_{l'\neq l}\beta_{\mathrm{CR}l'k}\left|\mathbf{z}_{\mathrm{R}}^{\mathrm{H}}\tilde{\mathbf{a}}_{\mathrm{Cr}l'}\right|^2 P_{\mathrm{Ct}l'}\left|\tilde{a}_{\mathrm{Ct}l'}\right|^2}.$$

This shows that when $K + L \leq 2$, the factor $(1/P_{\mathrm{Ct}l})^{K+L-2}$ increases or stays constant with $P_{\mathrm{Ct}l}$, while the remaining products increases with it, concluding the proof of Lemma 8.2. When $K + L > 2$, the above is rewritten as

$$\mathcal{M} \underset{\mathbf{P}_{\mathrm{Ct}l}}{\propto} \frac{P_{\mathrm{Ct}l}}{\sum_{i=0}^{K+L-1}\kappa_{l,i}P_{\mathrm{Ct}l}^{i}},$$

with positive coefficients $\kappa_{l,i} > 0$ which depend on the $b_{\mathrm{Ct}l'l}$'s and $c_{\mathrm{Ct}kl}$'s. Since the above is differentiable, any unconstrained optimum of $\mathcal{M}$ is at a point with a zero first derivative, fulfilling therefore the condition

$$\kappa_{l,0} - \sum_{i=2}^{K+L-1} \kappa_{l,i} (i-1) P_{\mathrm{C}tl}^{i} = 0,$$

This is a polynomial with a unique sign change, and therefore, from Descarte's rule of sign [99, Fact 11.17.1], there exists a unique positive root. Since the derivative value is positive at $P_{\mathrm{C}tl} = 0$ and negative at $P_{\mathrm{C}tl} = \infty$, this roots correspond to a maximum of $\mathcal{M}$. This therefore also implies that the function is unimodal on the $[0; 1]$ interval, concluding the proof of Lemma 8.3.

8.6.3 Proof of Lemma 8.4

To obtain the optimal lth communication receive beamformer, the factors independent of $\mathbf{z}_{\mathrm{C}l}$ are discarded from the objective function, this leading to

$$\max_{\mathbf{z}_{\mathrm{C}l}} \frac{\mathbf{z}_{\mathrm{C}l}^{\mathrm{H}} \tilde{\mathbf{a}}_{\mathrm{Cr}l} \tilde{\mathbf{a}}_{\mathrm{Cr}l}^{\mathrm{H}} \mathbf{z}_{\mathrm{C}l}}{\mathbf{z}_{\mathrm{C}l}^{\mathrm{H}} \mathbf{B}_{\mathrm{Cr}l} \mathbf{z}_{\mathrm{C}l}} \quad \text{s.t.} \quad \|\mathbf{z}_{\mathrm{C}l}\|_2^2 = 1.$$

This problem is known as a *generalised Rayleigh quotient*, and its solution is given by the Minimum Variance Distortionless Response (MVDR) vector [147], which reads in this case as

$$\hat{\mathbf{z}}_{\mathrm{C}l} = \eta_{\mathrm{C}l} \mathbf{B}_{\mathrm{Cr}l} \tilde{\mathbf{a}}_{\mathrm{Cr}l}, \tag{8.20}$$

with $\eta_{\mathrm{C}l} = 1/\left\|\mathbf{B}_{\mathrm{Cr}l}^{-1} \tilde{\mathbf{a}}_{\mathrm{Cr}l}\right\|_2$, concluding the proof.

8.6.4 Proof of Lemmas 8.5 and 8.6

When $K = 1$, the proof is identical to Section 8.6.3. When $K = 2$ and $L = 0$, the metric $\mathcal{M}$ can be rewritten as

$$\mathcal{M} \underset{\mathbf{z}_{\mathrm{R}}}{\propto} \frac{1}{\frac{1}{\left|\mathbf{z}_{\mathrm{R}}^{\mathrm{H}} \tilde{\mathbf{a}}_{\mathrm{Rr1}}^{\dagger}\right|^2} + C_1} \frac{1}{\frac{1}{\left|\mathbf{z}_{\mathrm{R}}^{\mathrm{H}} \tilde{\mathbf{a}}_{\mathrm{Rr2}}^{\dagger}\right|^2} + C_2},$$

with $C_1 \triangleq P_{\mathrm{Rt}} \beta_{\mathrm{RR12}} \left|\mathbf{y}_{\mathrm{R}}^{\mathrm{H}} \tilde{\mathbf{a}}_{\mathrm{Rt1}}\right|^2 \|\tilde{\mathbf{a}}_{\mathrm{Rr1}}\|_2^2$ and $C_2 \triangleq P_{\mathrm{Rt}} \beta_{\mathrm{RR21}} \left|\mathbf{y}_{\mathrm{R}}^{\mathrm{H}} \tilde{\mathbf{a}}_{\mathrm{Rt2}}\right|^2 \|\tilde{\mathbf{a}}_{\mathrm{Rr2}}\|_2^2$, and with the normalised vectors $\tilde{\mathbf{a}}_{\mathrm{Rr1}}^{\dagger} = \tilde{\mathbf{a}}_{\mathrm{Rr1}} / \|\tilde{\mathbf{a}}_{\mathrm{Rr1}}\|_2^2$, $\tilde{\mathbf{a}}_{\mathrm{Rr2}}^{\dagger} = \tilde{\mathbf{a}}_{\mathrm{Rr2}} / \|\tilde{\mathbf{a}}_{\mathrm{Rr2}}\|_2^2$. By definition, $\mathbf{z}_{\mathrm{R}}$ belongs to span $\left\{\tilde{\mathbf{a}}_{\mathrm{Rr1}}^{\dagger}, \tilde{\mathbf{a}}_{\mathrm{Rr2}}^{\dagger}\right\}$, and it is defined up to a phase shift. It can hence be expressed as

$$\mathbf{z}_{\mathrm{R}} = \frac{\alpha_1 \tilde{\mathbf{a}}^{\dagger}_{\mathrm{Rr1}} + \alpha_2 e^{j\phi} \tilde{\mathbf{a}}^{\dagger}_{\mathrm{Rr2}}}{\left\| \alpha_1 \tilde{\mathbf{a}}^{\dagger}_{\mathrm{Rr1}} + \alpha_2 e^{j\phi} \tilde{\mathbf{a}}^{\dagger}_{\mathrm{Rr2}} \right\|_2} = \frac{\lambda \tilde{\mathbf{a}}^{\dagger}_{\mathrm{Rr1}} + (1-\lambda) e^{j\phi} \tilde{\mathbf{a}}^{\dagger}_{\mathrm{Rr2}}}{\left\| \lambda \tilde{\mathbf{a}}^{\dagger}_{\mathrm{Rr1}} + (1-\lambda) e^{j\phi} \tilde{\mathbf{a}}^{\dagger}_{\mathrm{Rr2}} \right\|_2},$$

with $\alpha_1 \geq 0$, $\alpha_2 \geq 0$ and $\phi \in \mathbb{R}$, and $\lambda = \alpha_1 / (\alpha_1 + \alpha_2) \in [0;1]$. With this vector, letting $\gamma \triangleq \tilde{\mathbf{a}}^{\dagger,\mathrm{H}}_{\mathrm{Rr2}} \tilde{\mathbf{a}}^{\dagger}_{\mathrm{Rr1}}$,

$$\begin{aligned} \frac{1}{\left| \mathbf{z}_{\mathrm{R}}^{\mathrm{H}} \tilde{\mathbf{a}}^{\dagger}_{\mathrm{Rr1}} \right|^2} &= \frac{\alpha_1^2 + \alpha_2^2 + 2\alpha_1\alpha_2 \mathrm{Re}\left\{\gamma e^{-j\phi}\right\}}{\alpha_1^2 + \alpha_2^2 \left|\gamma\right|^2 + 2\alpha_1\alpha_2 \mathrm{Re}\left\{\gamma e^{-j\phi}\right\}}, \\ &= 1 + \frac{\alpha_2^2 \left(1 - \left|\gamma\right|^2\right)}{\alpha_1^2 + \alpha_2^2 \left|\gamma\right|^2 + 2\alpha_1\alpha_2 \mathrm{Re}\left\{\gamma e^{-j\phi}\right\}}, \end{aligned}$$

$$\frac{1}{\left| \mathbf{z}_{\mathrm{R}}^{\mathrm{H}} \tilde{\mathbf{a}}_{\mathrm{Rr2}} \right|^2} = 1 + \frac{\alpha_1^2 \left(1 - \left|\gamma\right|^2\right)}{\alpha_1^2 \left|\gamma\right|^2 + \alpha_2^2 + 2\alpha_1\alpha_2 \mathrm{Re}\left\{\gamma e^{-j\phi}\right\}}.$$

Since the numerators are always positive from the Cauchy-Schwarz inequality, to minimise $1/\left|\mathbf{z}_{\mathrm{R}}^{\mathrm{H}} \tilde{\mathbf{a}}_{\mathrm{Rr2}}\right|^2$ and $1/\left|\mathbf{z}_{\mathrm{R}}^{\mathrm{H}} \tilde{\mathbf{a}}_{\mathrm{Rr2}}\right|^2$, the phase shift should be equal to $\hat{\phi} = \arg\left\{\gamma\right\} = \arg\left\{\tilde{\mathbf{a}}_{\mathrm{Rr2}}^{\mathrm{H}} \tilde{\mathbf{a}}_{\mathrm{Rr1}}\right\}$. Plugging the optimum phase shifts into $\mathcal{M}$, the following is obtained

$$-\log\left(\mathcal{M}\right) = C + \log\left(o_1 + \frac{(1-\lambda)^2}{\left(1 - p_1 (1-\lambda)\right)^2}\right) + \log\left(o_2 + \frac{\lambda^2}{\left(1 - p_2 \lambda\right)^2}\right),$$

with the constants $o_1, o_2 \geq 1$ and $p_1, p_2 \in [0,1]$ and $C \in \mathbb{R}$. The above is convex, since it can be verified the function $f(x) \triangleq \log\left(o + \frac{x^2}{(1-px)^2}\right)$ is convex for $x \in [0,1]$, $o \geq 1$ and $p \in [0,1]$. Therefore, a unique optimum exists implying the function $\mathcal{M}$ is unimodal on $\lambda \in [0;1]$. This concludes the proof of Lemma 8.6.

8.6.5 Proof of Lemmas 8.7 and 8.8

When $K = 2$ and $L \geq 1$, the problem is developed as

$$\begin{aligned}
&\max_{\mathbf{z}_{\mathrm{R}}} \frac{\mathbf{z}_{\mathrm{R}}^{\mathrm{H}}\mathbf{A}_{\mathrm{Rr1}}\mathbf{z}_{\mathrm{R}}}{\mathbf{z}_{\mathrm{R}}^{\mathrm{H}}\mathbf{B}_{\mathrm{Rr1}}\mathbf{z}_{\mathrm{R}}} \frac{\mathbf{z}_{\mathrm{R}}^{\mathrm{H}}\mathbf{A}_{\mathrm{Rr2}}\mathbf{z}_{\mathrm{R}}}{\mathbf{z}_{\mathrm{R}}^{\mathrm{H}}\mathbf{B}_{\mathrm{Rr2}}\mathbf{z}_{\mathrm{R}}} \quad \text{s.t.} \quad \|\mathbf{z}_{\mathrm{R}}\|_2^2 = 1,\\
\iff &\max_{\mathbf{z}_{\mathrm{R}}} \frac{\mathrm{Tr}\left\{\mathbf{z}_{\mathrm{R}}\mathbf{z}_{\mathrm{R}}^{\mathrm{H}}\mathbf{A}_{\mathrm{Rr1}}\mathbf{z}_{\mathrm{R}}\mathbf{z}_{\mathrm{R}}^{\mathrm{H}}\mathbf{A}_{\mathrm{Rr2}}\right\}}{\mathrm{Tr}\left\{\mathbf{z}_{\mathrm{R}}\mathbf{z}_{\mathrm{R}}^{\mathrm{H}}\mathbf{B}_{\mathrm{Rr1}}\mathbf{z}_{\mathrm{R}}\mathbf{z}_{\mathrm{R}}^{\mathrm{H}}\mathbf{B}_{\mathrm{Rr2}}\right\}} \quad \text{s.t.} \quad \mathrm{Tr}\left\{\mathbf{z}_{\mathrm{R}}\mathbf{z}_{\mathrm{R}}^{\mathrm{H}}\right\} = 1,\\
\iff &\max_{\mathbf{X}_{\mathrm{R}} \in \mathbb{C}^{M_{\mathrm{r}} \times M_{\mathrm{r}}}} \frac{\mathrm{Tr}\left\{\mathbf{X}_{\mathrm{R}}\mathbf{A}_{\mathrm{Rr1}}\mathbf{X}_{\mathrm{R}}\mathbf{A}_{\mathrm{Rr2}}\right\}}{\mathrm{Tr}\left\{\mathbf{X}_{\mathrm{R}}\mathbf{B}_{\mathrm{Rr1}}\mathbf{X}_{\mathrm{R}}\mathbf{B}_{\mathrm{Rr2}}\right\}} \quad \text{s.t.} \quad \begin{cases} \mathrm{rank}\left\{\mathbf{X}_{\mathrm{R}}\right\} = 1,\\ \mathbf{X}_{\mathrm{R}} = \mathbf{X}_{\mathrm{R}}^{\mathrm{H}},\\ \mathrm{Tr}\left\{\mathbf{X}_{\mathrm{R}}\right\} = 1. \end{cases}
\end{aligned}$$

Obtaining a solution to the above is however challenging due to the rank-one constraint. An approximate solution is therefore obtained by first relaxing this constraint, and then projecting the obtained solution onto the constraints of the above formulation.

Relaxation The relaxed problem reads as

$$\max_{\mathbf{X}_{\mathrm{R}} \in \mathbb{C}^{M_{\mathrm{r}} \times M_{\mathrm{r}}}} \frac{\mathrm{Tr}\left\{\mathbf{X}_{\mathrm{R}}\mathbf{A}_{\mathrm{Rr1}}\mathbf{X}_{\mathrm{R}}\mathbf{A}_{\mathrm{Rr2}}\right\}}{\mathrm{Tr}\left\{\mathbf{X}_{\mathrm{R}}\mathbf{B}_{\mathrm{Rr1}}\mathbf{X}_{\mathrm{R}}\mathbf{B}_{\mathrm{Rr2}}\right\}} \quad \text{s.t.} \quad \begin{cases} \mathbf{X}_{\mathrm{R}} = \mathbf{X}_{\mathrm{R}}^{\mathrm{H}},\\ \mathrm{Tr}\left\{\mathbf{X}_{\mathrm{R}}\right\} = 1, \end{cases}$$

and it can be translated into the real domain as [99, Fact 7.4.9]

$$\begin{aligned}
\frac{\mathrm{Tr}\left\{\mathbf{X}_{\mathrm{R}}\mathbf{A}_{\mathrm{Rr1}}\mathbf{X}_{\mathrm{R}}\mathbf{A}_{\mathrm{Rr2}}\right\}}{\mathrm{Tr}\left\{\mathbf{X}_{\mathrm{R}}\mathbf{B}_{\mathrm{Rr1}}\mathbf{X}_{\mathrm{R}}\mathbf{B}_{\mathrm{Rr2}}\right\}} &= \frac{\mathrm{vec}\left(\mathbf{X}_{\mathrm{R}}\right)^{\mathrm{H}}\left(\mathbf{A}_{\mathrm{Rr1}}^{\star} \otimes \mathbf{A}_{\mathrm{Rr2}}\right)\mathrm{vec}\left(\mathbf{X}_{\mathrm{R}}\right)}{\mathrm{vec}\left(\mathbf{X}_{\mathrm{R}}\right)^{\mathrm{H}}\left(\mathbf{B}_{\mathrm{Rr1}}^{\star} \otimes \mathbf{B}_{\mathrm{Rr2}}\right)\mathrm{vec}\left(\mathbf{X}_{\mathrm{R}}\right)},\\
&= \frac{\mathrm{vec}_{\mathbb{C}}\left(\mathbf{X}_{\mathrm{R}}\right)^{\top}\mathbf{M}_{\left(\mathbf{A}_{\mathrm{Rr1}}^{\star} \otimes \mathbf{A}_{\mathrm{Rr2}}\right)}\mathrm{vec}_{\mathbb{C}}\left(\mathbf{X}_{\mathrm{R}}\right)}{\mathrm{vec}_{\mathbb{C}}\left(\mathbf{X}_{\mathrm{R}}\right)^{\top}\mathbf{M}_{\left(\mathbf{B}_{\mathrm{Rr1}}^{\star} \otimes \mathbf{B}_{\mathrm{Rr2}}\right)}\mathrm{vec}_{\mathbb{C}}\left(\mathbf{X}_{\mathrm{R}}\right)},\\
&= \frac{\mathrm{vech}_{\mathbb{C}}\left(\mathbf{X}_{\mathrm{R}}\right)^{\top}\mathbf{T}^{\top}\mathbf{M}_{\left(\mathbf{A}_{\mathrm{Rr1}}^{\star} \otimes \mathbf{A}_{\mathrm{Rr2}}\right)}\mathbf{T}\mathrm{vech}_{\mathbb{C}}\left(\mathbf{X}_{\mathrm{R}}\right)}{\mathrm{vech}_{\mathbb{C}}\left(\mathbf{X}_{\mathrm{R}}\right)^{\top}\mathbf{T}^{\top}\mathbf{M}_{\left(\mathbf{B}_{\mathrm{Rr1}}^{\star} \otimes \mathbf{B}_{\mathrm{Rr2}}\right)}\mathbf{T}\mathrm{vech}_{\mathbb{C}}\left(\mathbf{X}_{\mathrm{R}}\right)},
\end{aligned}$$

where the second line follows from the definition of the operators $\mathrm{vec}_{\mathbb{C}}(\cdot)$ and $\mathbf{M}_{\mathbf{U}}$ given in (8.18), and the third from the Hermitian property of $\mathbf{X}_{\mathrm{R}}$. The relaxed problem becomes therefore a generalised Rayleigh quotient problem reading as

$$\max_{\mathbf{f}\in\mathbb{R}^{M_{\mathrm{r}}^2}} \frac{\mathbf{f}^\top\mathbf{T}^\top\mathbf{M}_{\left(\mathbf{A}_{\mathrm{Rr}1}^\star\otimes\mathbf{A}_{\mathrm{Rr}2}\right)}\mathbf{T}\mathbf{f}}{\mathbf{f}^\top\mathbf{T}^\top\mathbf{M}_{\left(\mathbf{B}_{\mathrm{Rr}1}^\star\otimes\mathbf{B}_{\mathrm{Rr}2}\right)}\mathbf{T}\mathbf{f}} \quad \text{s.t.} \quad \mathrm{Tr}\left\{\mathrm{vec}_{\mathbb{C}}^{-1}\left(\mathbf{T}\mathbf{f}\right)\right\} = 1,$$

with $\mathbf{X}_{\mathrm{R}} = \mathrm{vec}_{\mathbb{C}}^{-1}\left(\mathbf{T}\mathbf{f}\right)$. The optimum $\mathbf{f}$ is therefore an eigenvector associated with the largest eigenvalue of $\mathbf{K} = \left(\mathbf{T}^\top\mathbf{M}_{\left(\mathbf{B}_{\mathrm{Rr}1}^\star\otimes\mathbf{B}_{\mathrm{Rr}2}\right)}\mathbf{T}\right)^{-1}\mathbf{T}^\top\mathbf{M}_{\left(\mathbf{A}_{\mathrm{Rr}1}^\star\otimes\mathbf{A}_{\mathrm{Rr}2}\right)}\mathbf{T}$. This eigenvector can always be selected as real since if $\mathbf{g}$ is an eigenvector of the real symmetric matrix $\mathbf{A}$, then $\mathrm{Re}\left\{\mathbf{g}\right\}$ is also an eigenvector of the same matrix associated with the same eigenvalue:

$$\mathbf{A}\mathbf{g} = \lambda\mathbf{g} \implies \mathrm{Re}\left\{\mathbf{A}\mathbf{g}\right\} = \mathrm{Re}\left\{\lambda\mathbf{g}\right\} \implies \mathbf{A}\mathrm{Re}\left\{\mathbf{g}\right\} = \lambda\mathrm{Re}\left\{\mathbf{g}\right\}.$$

Projection To obtain a rank-one matrix, the optimal $\hat{\mathbf{X}}_{\mathrm{R}}$ is projected on the set

$$\mathcal{S} \triangleq \left\{\mathbf{X} = \mathbf{v}\mathbf{v}^{\mathrm{H}} \middle| \mathbf{v} \in \mathbb{C}^{M_{\mathrm{r}}}, \left\|\mathbf{v}\right\|_2 = 1\right\}.$$

The optimisation problem reads as

$$\min_{\mathbf{v}} \left\|\hat{\mathbf{X}}_{\mathrm{R}} - \mathbf{v}\mathbf{v}^{\mathrm{H}}\right\|_F \quad \text{s.t.} \quad \left\|\mathbf{v}\right\|_2 = 1,$$

with $\left\|\cdot\right\|_F$ the Frobenius norm of a matrix. This norm is developed as

$$\begin{aligned}\left\|\hat{\mathbf{X}}_{\mathrm{R}} - \mathbf{v}\mathbf{v}^{\mathrm{H}}\right\|_F &= \mathrm{Tr}\left\{\left(\hat{\mathbf{X}}_{\mathrm{R}} - \mathbf{v}\mathbf{v}^{\mathrm{H}}\right)^{\mathrm{H}}\left(\hat{\mathbf{X}}_{\mathrm{R}} - \mathbf{v}\mathbf{v}^{\mathrm{H}}\right)\right\}, \\ &= \mathrm{Tr}\left\{\hat{\mathbf{X}}_{\mathrm{R}}^{\mathrm{H}}\hat{\mathbf{X}}_{\mathrm{R}}\right\} - 2\mathrm{Re}\left\{\mathrm{Tr}\left\{\hat{\mathbf{X}}_{\mathrm{R}}^{\mathrm{H}}\mathbf{v}\mathbf{v}^{\mathrm{H}}\right\}\right\} + \mathrm{Tr}\left\{\mathbf{v}\mathbf{v}^{\mathrm{H}}\mathbf{v}\mathbf{v}^{\mathrm{H}}\right\}, \\ &= \mathrm{Tr}\left\{\hat{\mathbf{X}}_{\mathrm{R}}^{\mathrm{H}}\hat{\mathbf{X}}_{\mathrm{R}}\right\} - 2\mathrm{Re}\left\{\mathbf{v}^{\mathrm{H}}\hat{\mathbf{X}}_{\mathrm{R}}^{\mathrm{H}}\mathbf{v}\right\} + \left\|\mathbf{v}\right\|_2^4.\end{aligned}$$

The first term is independent of $\mathbf{v}$, while the last is equal to 1 from the unit norm constraint. Regarding the middle term, the Hermitian property of $\hat{\mathbf{X}}_{\mathrm{R}}$ is used to obtain makes it real, showing that the optimal $\mathbf{v}$ is the eigenvector of $\hat{\mathbf{X}}_{\mathrm{R}}$ corresponding to the largest positive eigenvalue. This therefore concludes the proof of Lemma 8.7.

As far as Lemma 8.8 is concerned, the lemma follows from the fact that the beamformer are defined up to a phase shift. Therefore, the last element can be selected as real, and satisfying the unit power constraint.

8.6.6 Proof of Lemmas 8.9 to 8.11

For the radar transmit power, the metric $\mathcal{M}$ can be expressed as

$$\mathcal{M} \underset{P_{\mathrm{Rt}}}{\propto} \prod_{l=1}^{L} \frac{1}{1+P_{\mathrm{Rt}} b_{\mathrm{Rt}l}} \prod_{k=1}^{K} \frac{P_{\mathrm{Rt}}}{1+P_{\mathrm{Rt}} c_{\mathrm{Rt}k}},$$

with the non-negative scalars $\mathbf{b}_{\mathrm{Rt}l} \triangleq \mathbf{y}_{\mathrm{R}}^{\mathrm{H}} \mathbf{B}_{\mathrm{Rt}l} \mathbf{y}_{\mathrm{R}}$ and $\mathbf{c}_{\mathrm{Rt}k} \triangleq \mathbf{y}_{\mathrm{R}}^{\mathrm{H}} \mathbf{C}_{\mathrm{Rt}k} \mathbf{y}_{\mathrm{R}}$, the matrices being defined in (8.19). When $L=0$, $\mathcal{M}$ is therefore an increasing function of P_{Rt} whatever the number of targets. When $K=1$, $c_{\mathrm{Rt}k}=0$ by definition. This implies that when $K=1$ and $L=1$, then $\mathcal{M}$ is also an increasing function of P_{Rt}, concluding the proof of Lemma 8.9. For general K and L, the metric $\mathcal{M}$ is rewritten as

$$\mathcal{M} \underset{P_{\mathrm{Rt}}}{\propto} \frac{P_{\mathrm{Rt}}^{K}}{\sum_{i=0}^{L+K} \kappa_i P_{\mathrm{Rt}}^{i}},$$

with non-negative coefficients κ_i. The unimodality of $\mathcal{M}$ can then be obtained similarly to the proof provided in Section 8.6.2.

8.6.7 Proof of Lemma 8.12

For the radar transmit beamformer, the metric $\mathcal{M}$ can be expressed as

$$\mathcal{M} \underset{\mathbf{y}_{\mathrm{R}}}{\propto} \prod_{l=1}^{L} \frac{1}{1+P_{\mathrm{Rt}} \mathbf{y}_{\mathrm{R}}^{\mathrm{H}} \mathbf{B}_{\mathrm{Rt}l} \mathbf{y}_{\mathrm{R}}} \prod_{k=1}^{K} \frac{\left|\mathbf{y}_{\mathrm{R}}^{\mathrm{H}} \tilde{\mathbf{a}}_{\mathrm{Rt}k}\right|^2}{1+P_{\mathrm{Rt}} \mathbf{y}_{\mathrm{R}}^{\mathrm{H}} \mathbf{C}_{\mathrm{Rt}k} \mathbf{y}_{\mathrm{R}}}.$$

The proof of the lemmas then follows the same steps as those of Section 8.6.5.

Part III

Near-field-based interference analysis

9

Near-Field Multi-Antenna Range Estimation

The material of this chapter is the result of a collaboration with François De Saint Moulin, which has led to the following papers [154–157]. The author acknowledges and warmly thanks François De Saint Moulin for the development of the extended target model which has initiated this line of research. François De Saint Moulin and the author have equally contributed to the development of the range estimator (Sections 9.2 and 9.3), while the author is the principal contributor for the development of the associated performance bounds (Sections 9.4 and 9.5).

IN this last part and chapter of this thesis, a third alternative for handling the interference is studied, beside the autonomous and centralised frameworks considered above.

In these previous frameworks, an optimisation is performed to maximise the performance of the network nodes. This optimisation is either carried out at the node level, or at the network level. In the first case, the interactions between the coupled optimisation problems must be analysed, to ensure they converge to a stable point. This however relies on quite stringent assumptions, as well as on a rather complicated analysis. In the second case, the global optimisation problem modelling the network-level performance is often complex to solve, and it requires to centralise the CSI into a unique point. When either the complexity, the required hypotheses, or the side-information exchange load makes these two approaches unpractical, then one may consider allocate orthogonal resources to the different points of the networks. This enables to suppress the interference between the nodes, and therefore avoids the need for the interaction analysis, or the network-wide optimisation.

The traditional resources are the time, frequency, codes, or the angular domain of multi-antenna arrays. Nevertheless, the higher frequencies, large array dimensions, and small propagation distances envisioned for emerging networks, make possible to leverage on the range domain of multi-antenna arrays, in the so-called NF region. In this region, the wavefront emitted by an antenna must be considered spherical, contrarily to what happens in the FF region, in which a planar approximation can be performed. By exploiting this spherical nature, an antenna array can discriminate between points located at the same angle, but at different ranges. This therefore opens the way to interference management across the range domain.

Contrarily to the other resources, the exploitation of the NF range resource is much more recent, at least for wireless networks. The NF effect has indeed already been exploited in terahertz and imaging applications, in which the goal is to obtain a detailed image of an object or the environment [158, 159]. Among the many works covering imaging applications, the following thesis [160] stands out as an excellent entry point in the literature. In the above works, the high frequencies make the NF effect significant. In a complementary manner, the extremely large array size of synthetic aperture radars has also led to important NF effects [161, 162]. In this two domains, the NF effect has been leveraged upon mainly for imaging tasks, that is, for obtaining a detailed image of the environment. Rather, in NF radar applications, the goal is to estimate a few parameters (position, velocity, etc) of a target. Hence, this limited objective might offer the possibility to design more efficient and accurate estimation algorithms with respect to those existing in the imaging domain.

As the use of the NF effect for wireless communications and positioning has only emerged in the recent years, many questions are still open in the literature, and a complete study of NF MF MP networks is not provided here. Instead, this thesis considers the smaller problem of the radar range estimation of a single point, as well as the associated performance bounds. While this is an instance of a single-function single-point network, the carried out analysis paves the way to the understanding of more complex networks, with possibly multiple points, or with other functions.

9.1 Chapter introduction

To develop such radar range estimation, the works dealing with source positioning can be leveraged upon since the settings are similar. In such a setting, an active point source located in the NF region of an antenna array emits a signal. Based on the received signal, the array can perform source positioning [163]. As no control is exerted on the signal, this latter is either modelled as a parametric or stochastic narrowband signal [164], with the performance depending on the quantities measured by the receiver [165]. The NF effect can also be leveraged upon in radar applications, in which signals are reflected by passive targets. Performance bounds are derived in [166] for 3D localisation. OFDM signals are exploited in [167], the localisation performance being demonstrated experimentally and evaluated with the CRB. An approximate expression of the radar resolution, measured as the half-power width of the ambiguity function, is provided in [168], and applied to narrowband NF radars in [169]. Wideband waveforms are studied in [170], in which the associated CRBs is computed, and the parameter impact emphasised. The above works consider dimensionless Point Targets (PTs), which re-emit the impinging signals isotropically. Yet, when large targets are close to the arrays, such a model might be too simplistic, as noted in [167]. Such large targets are named Extended Targets (ETs), and call for specific signal processing and performance bounds.

This chapter provides therefore the following contributions.

- The maximum likelihood estimator of the range of a target located in the NF region of an antenna array is developed. The considered model encompasses both PTs, and the electromagnetic model developed in [157] for large planar ETs.

- Closed-form ambiguity function expressions are provided, highlighting the cooperation between the NF phase shifts and the classical waveform delay information. Expressions of the radar resolution and the peak-to-side-lobe level ratio are provided, highlighting the parameters' impact. Moreover, the impact of a model mismatch between the signal reflected by an ET, and the range estimation through a PT

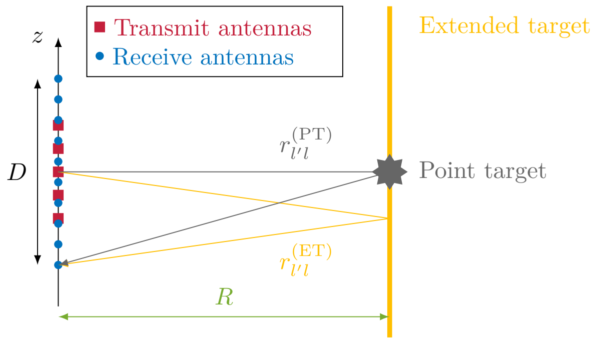

Fig. 9.1 System model

model is analysed. It is shown that such a mismatch leads to a severe performance degradation.

- The CRBs on the range estimation are derived for both PTs and ETs. The obtained expression reveals the impact of the parameters, namely the carrier frequency, and the waveform central frequency, and its root-mean-square bandwidth. The NF effect is shown to depend on the Root-Mean-Square (RMS) value of the propagation distance derivative, scaling with the fourth power of the ratio between the array dimension and the target range.
- Analysing the ambiguity function and the CRBs, an expression of the range at which the NF effect becomes insignificant with respect to the waveform information is obtained. This range delimits the so-called *effective NF region*.

To that aim, Section 9.2 provides the considered system model, while Section 9.3 develops the associated Maximum Likelihood (ML) estimator. The ambiguity function is analysed in Section 9.4, while the CRB is obtained in Section 9.5.

9.2 System model

Scene geometry The scenario of Figure 9.1 is considered, in which a large metallic reflector is located in front of two linear antenna arrays of respectively N_t and N_r antennas, whose maximum dimension is denoted D.

The reflector is parallel to the arrays and located at a distance R, named the target range. The z-axis position of the lth transmit and receive antennas is respectively denoted z_l and y_l. The system operates around a frequency f_c, with hence a wavelength given by $\lambda = c/f_c$ with c the speed of light, and the wave number $k = 2\pi/\lambda$.

Associated with the array dimension and wavelength, the Rayleigh distance is given by [171]

$$R_D \triangleq \frac{2D^2}{\lambda}. \tag{9.1}$$

This distance characterises the transition between the NF and the FF region of the array. In the NF region, the spherical nature of the wavefront must be considered, or in other words, the exact propagation distances matter. On the contrary, in the FF region, the wavefront can locally be seen as a planar one, and therefore the distances can be approximated accordingly.

Emitted waveform In order to estimate the range R, each transmit antenna emits the same waveform $s(t)$ on orthogonal time resources, in a TDMA manner. TDMA indeed leads to an easier implementation than systems in which orthogonality is achieved in other domains, such as frequencies or codes [172]. The waveform has a frequency content ranging from $-B/2$ to $B/2$ with B the bandwidth, and its correlation function, energy, central frequency and RMS bandwidth are respectively denoted and defined as

$$C(\tau) \triangleq \int s(t)\, s^*(t-\tau)\,\mathrm{d}t, \qquad \mathcal{E}_c \triangleq C(0), \tag{9.2}$$

$$f_M \triangleq \frac{1}{\mathcal{E}_c}\int f\,|S(f)|^2\,\mathrm{d}f, \tag{9.3}$$

$$B_{\mathrm{RMS}} \triangleq \sqrt{\frac{1}{\mathcal{E}_c}\int (f-f_M)^2\,|S(f)|^2\,\mathrm{d}f}, \tag{9.4}$$

with $S(f)$ the Fourier transform of $s(t)$.

Received signal At the l'th receive antenna, N_t noisy signals are received, the lth one reading as

$$u_{l'l}(t) = \xi\mu_{l'l;R}(t) + w_{l'l}(t), \tag{9.5}$$

$$\text{with} \quad \mu_{l'l;R}(t) \triangleq e^{-jkr_{l'l}}\, s\left(t - \frac{r_{l'l}}{c}\right). \tag{9.6}$$

In the above, ξ is an unknown complex coefficient common to all antennas, $r_{l'l}$ is the propagation distance between the lth transmit and l'th receive antennas, and $w_{l'l}(t)$ is an AWGN with PSD γ_n.

Remark 9.1: Uniform received power

The coefficient ξ includes both the path loss and the complex coefficient corresponding to the reflection on the target. As ξ is common to all antenna pairs, this implies the path loss is identical for all these pairs. This is a valid model for ranges above the so-called *uniform power distance*, which is within a constant factor of the array dimension D [173]. For targets very close to the antenna array, the antenna-dependent path loss information could nevertheless be leveraged upon to improve the range estimation.

Target models The propagation distances $r_{l'l}$ depend on the target model. Indeed, contrarily to what happens in the FF region, the target size might be significant in the NF one. This implies that depending on the target shape, it may either be a PT, or it may require to be modelled as an ET. For a PT located at $z = 0$, the propagation distance is given by

$$r_{l'l}^{\mathrm{PT}} \triangleq \sqrt{R^2 + z_l^2} + \sqrt{R^2 + y_{l'}^2}, \tag{9.7}$$

as the target reflects the signal isotropically. For large ETs, the propagation occurs instead as if the signal emitted by the lth antenna were reflected in a specular manner by the target [157]. Therefore, the propagation distance $r_{l'l}^{\mathrm{ET}}$ depends on the specular point location, which is the point at which the incident angle equals the reflection angle. In this chapter, the considered ET is a large planar plate, parallel to the antenna arrays, as represented in Figure 9.1. In that case [157],

$$r_{l'l}^{\mathrm{ET}} \triangleq \sqrt{4R^2 + (z_l - y_{l'})^2}. \tag{9.8}$$

Remark 9.2

When $R \gg R_D$, the planar wavefront FF assumption leads to

$$r_{l'l}^{(\mathrm{FF})} \approx 2R,$$

for a target located at $z = 0$, whatever the antenna pair (l, l') and the target model. The received signal can hence be written as

$$u_{l'l}(t) = \tilde{\xi} s\left(t - \frac{2R}{c}\right) + w_{l'l}(t),$$

with $\tilde{\xi} \triangleq \xi e^{-jk2R}$. Therefore, the phase information is absorbed by the unknown complex coefficient ξ, and the range estimation can only leverage upon to waveform time shift.

Remark 9.3

The system model could be generalised to PTs located at $z \neq 0$, as well as to planar ETs which are not parallel to the antenna arrays, or to curved ETs. This constitutes one of the main directions for future works, but this is not tackled in this chapter. In the following, the acronyms PT and ET will consequently refer to the considered specific instances of PTs and ETs.

9.3 ML range estimation

Based on the $N_\mathrm{t} N_\mathrm{r}$ received signals at the times $t \in [-\infty, \infty]$, the radar system estimates the range R of the target. To that aim, the ML range estimator associated with (9.5) reads as

$$\hat{R}, \hat{\xi} = \arg\max_{\tilde{R}, \tilde{\xi}} T_U\left(\{u_{l'l}(t)\}_{l,l',t}; \tilde{R}, \tilde{\xi}\right), \tag{9.9}$$

with $T_U\left(\{u_{l'l}(t)\}_{l,l',t}; \tilde{R}, \tilde{\xi}\right)$ the likelihood function of the received signals $u_{l'l}(t)$ for all antenna pairs (l, l') and all times t, for a candidate range $\tilde{R}$ and candidate complex coefficient $\tilde{\xi}$. The distinction is thus made between the true values R and ξ, the candidate values $\tilde{R}$ and $\tilde{\xi}$, and the estimates $\hat{R}$

and $\hat{\xi}$. Since the noise is complex Gaussian, the likelihood function reads as

$$T_U\left(\{u_{l'l}(t)\}_{l,l',t}; \tilde{R}, \tilde{\xi}\right) \propto \exp\left(-\frac{1}{\gamma_n}\sum_{l'=1}^{N_\mathrm{r}}\sum_{l=1}^{N_\mathrm{t}}\int_t \left|u_{l'l}(t) - \tilde{\xi}\mu_{l'l;\tilde{R}}(t)\right|^2 \mathrm{d}t\right). \tag{9.10}$$

The below lemma then provides the ML estimator of R, denoted $\hat{R}$.

Lemma 9.1: NF Range estimator

The range estimator associated with the received signals (9.5) is given by

$$\hat{R} = \arg\max_{\tilde{R}} \Lambda\left(\tilde{R}\right),$$

with

$$\Lambda\left(\tilde{R}\right) \triangleq \left|\sum_{l'=1}^{N_\mathrm{r}}\sum_{l=1}^{N_\mathrm{t}}\int_t u_{l'l}(t)\,\mu^{\star}_{l'l;\tilde{R}}(t)\,\mathrm{d}t\right|. \tag{9.11}$$

Proof. See Section 9.8.1. □

The above lemma provides a way to estimate the range R by computing $\Lambda\left(\tilde{R}\right)$ and finding its maximum. To understand the behaviour of the range estimator, the associated *ambiguity function* is considered. This function is given by $\Lambda\left(\tilde{R}\right)$, when the received signals are noiseless [174]. Furthermore, without loss of generality, the ambiguity functions are considered normalised to a unit maximum.

Definition 9.1: Range ambiguity function

The *range ambiguity function* associated with the estimator $\hat{R}$ is given by

$$\xi\left(\tilde{R}; R\right) \triangleq \frac{\Lambda\left(\tilde{R}\right)}{\max_\rho \Lambda\left(\rho\right)},$$

with $\Lambda\left(\tilde{R}\right)$ evaluated with the signals $u_{l'l}(t) = \xi\mu_{l'l;R}(t)$.

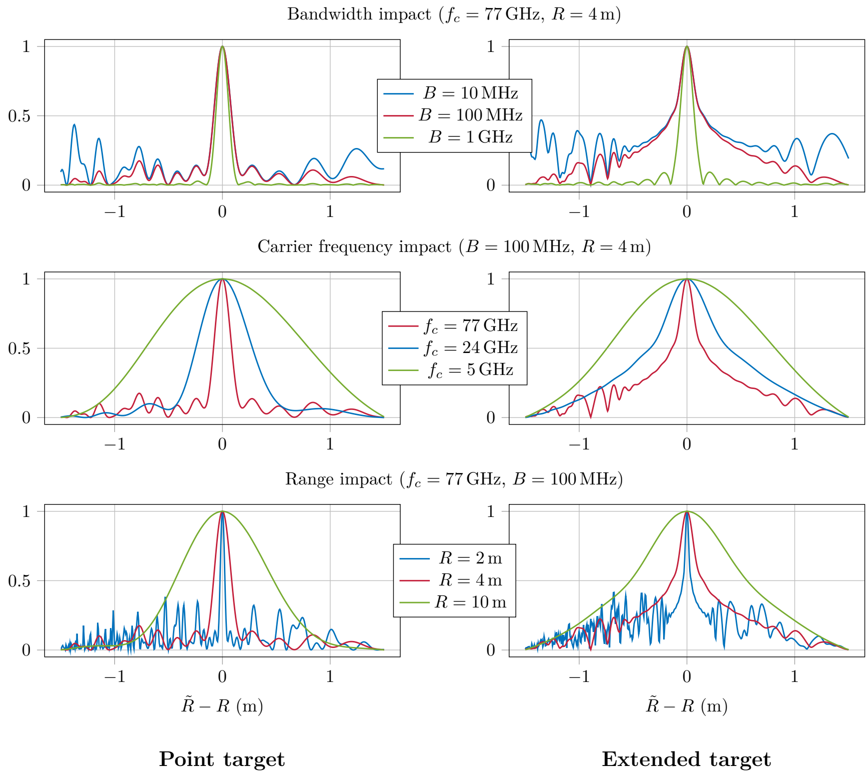

Fig. 9.2 Impact of the parameters on the NF range ambiguity functions, for a PT (left graphs) and an ET (right graphs), in the MIMO case.

Studying the ambiguity function enables to understand the behaviour of the estimator in the presence of noise. Indeed, since $\Lambda\left(\tilde{R}\right)$ is a noisy version of $\xi\left(\tilde{R}; R\right)$, this latter should have a maximum which stays as close as possible to the true range R even in the presence of noise. This thus leads to the twofold requirement of i) having a lobe at the true range value with a sharp maximum, and ii) having low side-lobes.

To provide a qualitative illustration of the range ambiguity function, the following scenario is considered. Two uniform linear arrays of $N_\mathrm{t} = N_\mathrm{r} = 13$ antennas perform the range estimation, with an antenna spacing $\Delta = 0.125\,\mathrm{m}$. The considered waveform is $s(t) = \mathrm{sinc}\left(Bt\right)$ with B the signal bandwidth and the cardinal sine defined as $\mathrm{sinc}\left(x\right) \triangleq \frac{\sin(\pi x)}{\pi x}$. The unknown complex coefficient is set to $\xi = 0.35 + 0.35j$. In Figure 9.2, the ambiguity functions obtained for different sets of bandwidth, carrier frequency and range parameters are represented, either in the case of a PT or of an ET.

As it can be observed, for all sets of parameters, the ambiguity function is indeed maximum at the true range. Regarding the impact of the system parameters, it is observed that the ambiguity function sharpness increases when the bandwidth increases, the carrier frequency increases and the range decreases. As functions with a sharper maximum are more robust to noise, this directly translates into an impact on the estimator performance. Comparing the case of PTs and ETs, it appears that PTs have a tendency to have a lower side-lobes than their ET counterpart. As far as the main lobe sharpness is concerned, no significant difference is observed in the illustrated scenario.

This qualitative analysis calls for a supporting theoretical basis, both regarding the side-lobes and the ambiguity function sharpness. To that aim, Section 9.4 provides closed-form expressions of the ambiguity function of the NF range estimator, while Section 9.5 studies the CRB.

9.4 Ambiguity function

This section studies the ambiguity function associated with the NF range estimator. First, Section 9.4.1 provides a general expression of the ambiguity function, which is particularised to the PT and ET models in Section 9.4.2. These theoretical results enable to provide simple forms for the radar resolution and the side-lobe level in Section 9.4.3. Finally, the impact of a model mismatch is analysed in Section 9.4.4.

9.4.1 Near-field range ambiguity function

In this section, closed-form expressions of the NF range ambiguity functions are obtained. To that aim, the following assumption is introduced.

Assumption 9.1

The ranges satisfy $R \geq R_D \frac{B}{f_c}$.

Under this assumption, the waveform bandwidth is not large enough to resolve the delay differences between the different antenna pairs. Indeed, considering the worst situation where $z_l = D/2$, and $y_{l'} = -D/2$, the delay difference is given for both target models by

$$\frac{r_{l'l} - 2R}{c} = \frac{2R}{c}\left(\sqrt{1 + \frac{R_D \lambda}{8R^2}} - 1\right) \leq \frac{2R}{c}\left(\sqrt{1 + \frac{c}{8BR}} - 1\right),$$
$$\leq \frac{2R}{c}\frac{c}{16BR} = \frac{1}{8B},$$

where the first inequality comes from Assumption 9.1, and the second from $\sqrt{1+x} \leq 1 + x/2$. Therefore, this implies $C\left(r_{l'l}/c\right) \approx C\left(2R/c\right)$. Under this assumption, the range ambiguity function can be expressed as a product of the ambiguity function provided by the waveform delay, and the one provided by the phase differences between the antennas, being defined as follows.

Definition 9.2: Waveform ambiguity function

The waveform ambiguity function is defined as

$$\chi_C\left(\tilde{R} - R\right) \triangleq \left|\frac{C\left(2\frac{\tilde{R}-R}{c}\right)}{\mathcal{E}_c}\right|.$$

Definition 9.3: Phase ambiguity function

The phase ambiguity function is defined as

$$\chi_{\Delta\phi}\left(\tilde{R}; R\right) \triangleq \left|\frac{1}{N_\mathrm{r} N_\mathrm{t}} \sum_{l'=1}^{N_\mathrm{r}} \sum_{l=1}^{N_\mathrm{t}} e^{jk\left(\tilde{r}_{l'l} - r_{l'l}\right)}\right|.$$

In the above definition and in the remaining of this chapter, the notations $\tilde{r}_{l'l}$ refers to the propagation distances (9.7) and (9.8), for a range equal to $\tilde{R}$ instead of R. It can again be noticed that the definition of the ambiguity functions is such that they have a unit maximum at $R = \tilde{R}$. With these definitions, the range ambiguity function is given by the following proposition.

Proposition 9.1: NF range ambiguity function

The ambiguity function of the NF range estimator of Lemma 9.1 is

$$\chi\left(\tilde{R};R\right)=\left|\frac{1}{N_\mathrm{r}N_\mathrm{t}}\sum_{l'=1}^{N_\mathrm{r}}\sum_{l=1}^{N_\mathrm{t}}e^{jk\left(\tilde{r}_{l'l}-r_{l'l}\right)}\frac{C\left(\frac{\tilde{r}_{l'l}-r_{l'l}}{c}\right)}{\mathcal{E}_c}\right|. \tag{9.12}$$

Under Assumption 9.1, (9.12) is approximated as

$$\chi\left(\tilde{R};R\right)\approx\chi_C\left(\tilde{R}-R\right)\chi_{\Delta\phi}\left(\tilde{R};R\right). \tag{9.13}$$

Proof. See Section 9.8.2. □

The product present in (9.13) implies that the global ambiguity function has a main lobe narrower than the one of χ_C and $\chi_{\Delta\phi}$ alone, and smaller side-lobes. It thus appears that the waveform and the phase information act collaboratively to provide the range estimation. It should be noted that the above proposition holds for both target models, since the expression of the propagation distances has not been utilised.

9.4.2 Point and extended targets

While the above proposition provides an efficient of way of computing the range ambiguity function, the impact of the parameters remains elusive. Hence, the expression given in Proposition 9.1 is developed here for the two considered target models, and for two antenna configurations. The two antennas configurations are termed the Single-Input Multiple-Output (SIMO) and MIMO configurations. The SIMO one is with a single transmit antenna located at $z=0$ and a receive array of dimension D, centred at $z=0$. In the MIMO case, the transmit and receive arrays have the same dimension D, are centred at $z=0$ and have a possibly different number of antennas. As described in Section 9.2, the transmit antennas emits in a TDMA manner.

To obtain simplified closed-form expressions of the ambiguity function emphasising the impact of the parameters, two assumptions are leveraged upon.

Assumption 9.2

The ranges satisfy $R \geq 1.2D$ [171].

Under Assumption 9.2, the distance $r_{l'l}$ is well approximated by its second-order Taylor series, denoted $\tilde{r}_{l'l}$ and reading for the two target models as

$$r_{l'l}^{\mathrm{PT}} \approx \tilde{r}_{l'l}^{\mathrm{PT}} = 2R + \frac{z_l^2 + y_{l'}^2}{2R}, \tag{9.14}$$

$$r_{l'l}^{\mathrm{ET}} \approx \tilde{r}_{l'l}^{\mathrm{ET}} = 2R + \frac{(z_l - y_{l'})^2}{4R}, \tag{9.15}$$

these approximations being named the Fresnel approximations.

Assumption 9.3

The array size and the numbers of antennas are such that the summations on the antennas of the arrays can be replaced by integrals [175].

With these assumptions, Proposition 9.2 shows that the phase difference information is captured by the parameter β defined as

$$\beta \triangleq \sqrt{R_D \left| \frac{1}{\tilde{R}} - \frac{1}{R} \right|}. \tag{9.16}$$

This parameter impacts the value of the phase ambiguity function of the transmit array, the receive one, and the coupled ambiguity function, which are respectively defined as

$$\begin{aligned}
\chi_{\Delta\phi,\mathrm{t}}(\beta) &\triangleq \left| \tfrac{1}{N_{\mathrm{t}}} \textstyle\sum_{l=1}^{N_{\mathrm{t}}} e^{j\frac{\pi}{2}\left(\frac{\beta z_l}{D}\right)^2} \right|, \\
\chi_{\Delta\phi,\mathrm{r}}(\beta) &\triangleq \left| \tfrac{1}{N_{\mathrm{r}}} \textstyle\sum_{l'=1}^{N_{\mathrm{r}}} e^{j\frac{\pi}{2}\left(\frac{\beta y_{l'}}{D}\right)^2} \right|, \\
\chi_{\Delta\phi,\mathrm{rt}}(\beta) &\triangleq \left| \tfrac{1}{N_{\mathrm{t}} N_{\mathrm{r}}} \textstyle\sum_{l=1}^{N_{\mathrm{t}}} \sum_{l'=1}^{N_{\mathrm{r}}} e^{j\frac{\pi}{2}\left(\beta \frac{z_l - y_{l'}}{D}\right)^2} \right|.
\end{aligned}$$

These definitions are reminiscent of those obtained to evaluate the performance of beamfocusing in NF communications [175]. As shown below, these functions can be approximated under Assumption 9.3 by expressions involving the Fresnel integral

$$F(x) \triangleq \int_0^x e^{j\frac{\pi}{2}t^2}\mathrm{d}t.$$

Proposition 9.2

The phase ambiguity function of Definition 9.3 is approximated under Assumption 9.2 as

$$\begin{aligned}
\chi_{\Delta\phi}^{\mathrm{PT,SIMO}}\left(\tilde{R};R\right) &\approx \chi_{\Delta\phi,\mathrm{r}}\left(\beta\right),\\
\chi_{\Delta\phi}^{\mathrm{PT,MIMO}}\left(\tilde{R};R\right) &\approx \chi_{\Delta\phi,\mathrm{r}}\left(\beta\right)\chi_{\Delta\phi,\mathrm{t}}\left(\beta\right),\\
\chi_{\Delta\phi}^{\mathrm{ET,SIMO}}\left(\tilde{R};R\right) &\approx \chi_{\Delta\phi,\mathrm{r}}\left(\frac{\beta}{\sqrt{2}}\right),\\
\chi_{\Delta\phi}^{\mathrm{ET,MIMO}}\left(\tilde{R};R\right) &\approx \chi_{\Delta\phi,\mathrm{rt}}\left(\frac{\beta}{\sqrt{2}}\right).
\end{aligned}$$

Moreover, under Assumption 9.3,

$$\begin{aligned}
\chi_{\Delta\phi,\mathrm{t}}\left(\beta\right) \approx \chi_{\Delta\phi,\mathrm{r}}\left(\beta\right) &\approx \left|\frac{2}{\beta}F\left(\frac{\beta}{2}\right)\right|,\\
\chi_{\Delta\phi,\mathrm{rt}}\left(\beta\right) &\approx \left|2\frac{F\left(\beta\right)}{\beta} - e^{j\pi\frac{\beta^2}{4}}\operatorname{sinc}\left(\frac{\beta^2}{4}\right)\right|.
\end{aligned}$$

Proof. See Section 9.8.3. □

The above proposition provides the following insights. First, for large numbers of antennas, $\chi_{\Delta\phi}^{\mathrm{PT,MIMO}} = \left(\chi_{\Delta\phi}^{\mathrm{PT,SIMO}}\right)^2$, showing that the side-lobes are greatly reduced in the MIMO case. In the SIMO case, it appears that the PT and the ET model have a similar ambiguity function, yet with the β factor divided by $\sqrt{2}$ for the ETs. These effects can be observed in Figure 9.3, where the asymptotic (i.e., for a large number of antennas) closed-form phase ambiguity functions are depicted as a function of β. They are represented both in natural scale, and in dB-scale.

As expected, the ambiguity functions of a PT have smaller side-lobes than their ET counterpart. They have also a sharper maximum, the difference being significant in the SIMO case, while it is less pronounced in the MIMO case. This latter is the setting of the qualitative analysis provided by Figure 9.2, hence explaining the observed behaviour. The fact that PTs

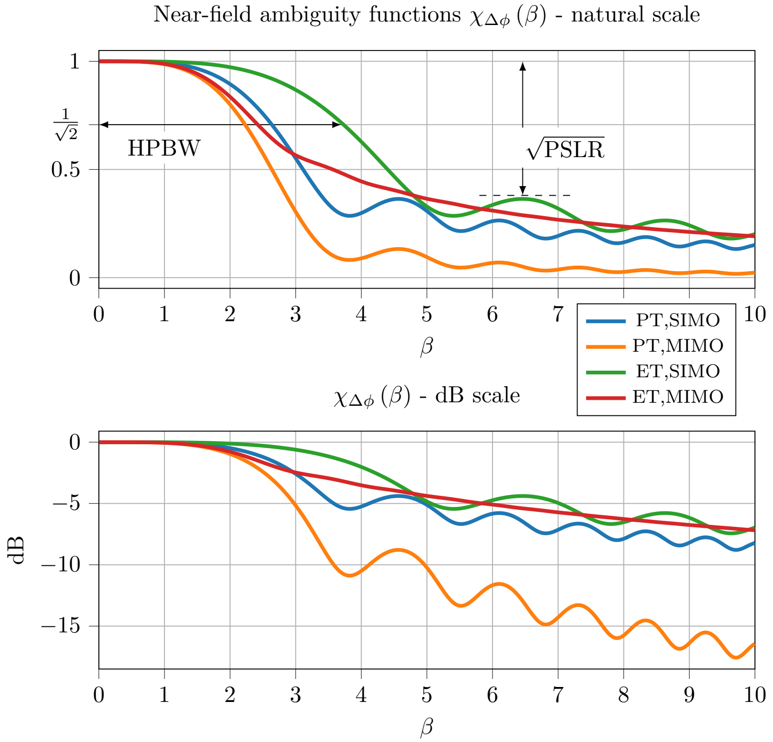

Fig. 9.3 Phase ambiguity function of Proposition 9.2 as a function of β. For the ET SIMO case, the half-power beamwidth and the peak-to-side-lobe level ratio are illustrated.

lead to an easier estimation than ETs can be understood as follows. Due to presence of ξ, only the phase difference between the antennas can be measured. Considering the Fresnel approximations (9.14) and (9.15), the phase difference of a PT scales in $1/2R$, while the one of a ET is in $1/4R$. This implies that a change of R has a smaller impact on the measured phase difference for an ET, and therefore that the range estimation is less performant.

In the above figure, the asymptotic ambiguity functions have been provided, i.e., for a theoretically infinite number of antennas. The impact of the number of antennas is analysed in the SIMO case for an ET, the obtained results being similar for the others cases. In order to validate both Proposition 9.1 and Proposition 9.2, the ambiguity function $\chi^{\text{ET,SIMO}}\left(\tilde{R}; R\right)$

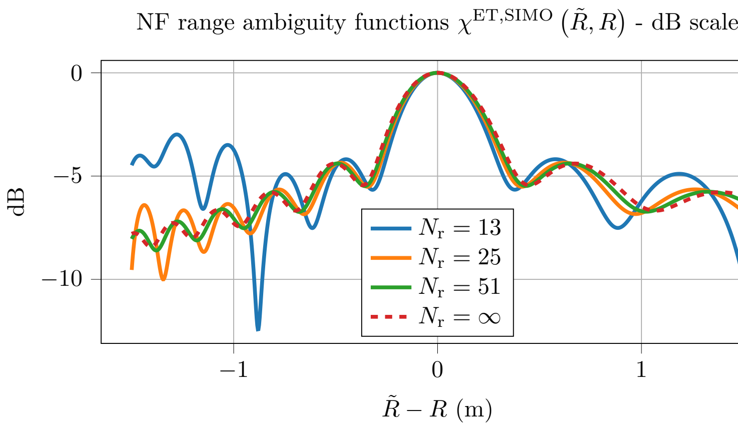

Fig. 9.4 Impact of the number of antennas on the NF range ambiguity function, in the SIMO configuration and with an ET. The parameters are $R = 4\,\mathrm{m}$, $B = 10\,\mathrm{MHz}$, $f_c = 77\,\mathrm{GHz}$, $D = 1.5\,\mathrm{m}$, $\xi = 0.35 + 0.35j$, with a cardinal sine waveform.

is represented, including both the waveform delay information and the phase shifts. For a constant antenna dimension $D_\mathrm{r} = 1.5\,\mathrm{m}$, the number of antennas is varied, considering uniform spacing between the antennas. As it can be observed, even for small numbers of antennas, the main lobe of the ambiguity function is well-approximated by the asymptotic closed-form formula. Differently, higher side-lobes appear for small number of antennas, but they quickly stick to the asymptotic formula when the number of antennas increases. It is stressed out that even with $N_\mathrm{r} = 51$, the antenna spacing is $3\,\mathrm{cm}$, which is much higher than the wavelength of $3.9\,\mathrm{mm}$ in this case. In other words, the antenna arrays must not have $\lambda/2$ spacing as far as the range estimation is concerned.

9.4.3 Range resolution and side-lobes

The results provided by Proposition 9.1 and Proposition 9.2 enable to evaluate the achieved radar resolution, as well as the side-lobe level of the ambiguity function.

Range resolution The radar resolution can be measured with the Half-Power BeamWidth (HPBW), which is the width of the main lobe of $\chi(\tilde{R}; R)$

measured at $\chi\left(\tilde{R};R\right) = 1/\sqrt{2}$ [168], or in other words the width of the main lobe of $\chi^2\left(\tilde{R};R\right)$ at half the maximum power. Invoking the product expression of Proposition 9.1, the range resolution ΔR is bounded as

$$\Delta R \leq \min\left\{\Delta R_C, \Delta R_{\Delta\phi}\right\}, \tag{9.17}$$

with ΔR_C the range resolution of the waveform ambiguity function $\chi_C\left(\tilde{R}-R\right)$, and $\Delta R_{\Delta\phi}$ the one of the phase ambiguity function $\chi_{\Delta\phi}\left(\tilde{R};R\right)$. This thus once again highlights the cooperation between the waveform information, and the phase information, since the best of the two is obtained by the NF range estimation.

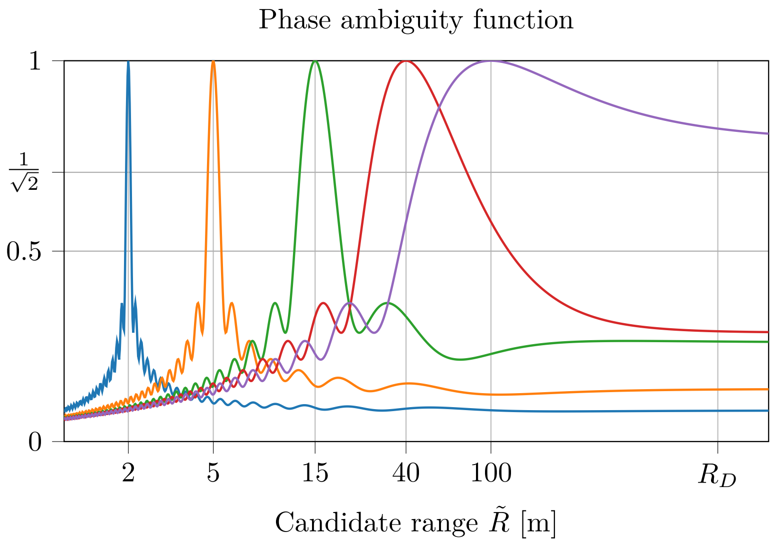

Fig. 9.5 Phase ambiguity function of Proposition 9.2 as a function of the candidate range $\tilde{R}$, for different true ranges R. The radar resolution can be measured at $1/\sqrt{2}$.

Regarding $\Delta R_{\Delta\phi}$, the asymptotic closed-form expressions of Proposition 9.2 are represented in Figure 9.5, for different true range values R, and with $R_D = 1156\,\text{m}$. As expected, the width of the main lobe increases when the true range increases, and it can even become infinite for large ranges. This comes from the fact that when $\tilde{R} \to \infty$, $\beta \to \sqrt{R_D/R}$ which is a finite value. Let β_{HPBW} be the value of β corresponding to the HPBW, which can be computed from Figure 9.3 as

$$\begin{aligned}\beta_{\mathrm{HPBW}}^{\mathrm{PT,SIMO}} &\approx 2.63,\\ \beta_{\mathrm{HPBW}}^{\mathrm{PT,MIMO}} &\approx 2.23,\\ \beta_{\mathrm{HPBW}}^{\mathrm{ET,SIMO}} &\approx 3.73,\\ \beta_{\mathrm{HPBW}}^{\mathrm{ET,MIMO}} &\approx 2.43.\end{aligned}$$

One can observe the $\sqrt{2}$ factor between the PT SIMO case and the ET SIMO case, coming from the expressions given by Proposition 9.2. Given these values, the range resolution can be obtained by finding the ranges at which $\beta = \beta_{\mathrm{HPBW}}$, leading to

$$\Delta R_{\Delta\phi} = \begin{cases} \infty & \text{if } \frac{R_D}{\beta_{\mathrm{HPBW}}^2} \leq R, \\ \frac{2}{\frac{R_D}{R^2\beta_{\mathrm{HPBW}}^2} - \frac{\beta_{\mathrm{HPBW}}^2}{R_D}} & \text{otherwise.} \end{cases}$$

In the above, the infinity value depict the ranges for which the ambiguity function does not fall below $1/\sqrt{2}$ after the maximum. This happens when $R \geq R_D/\beta_{\mathrm{HPBW}}^2$, showing that the Rayleigh distance overestimates the NF region with a factor β_{HPBW}^2. This echoes the conclusion obtained in [176], in which a similar analysis has been performed.

These elements motivate the definition of an *effective NF region*, which is the region in which the phase information provides a better resolution than the waveform resolution ΔR_C. This upper range of this region, denoted $R_{\mathrm{NF,eff}}^{\mathrm{res}}$ is hence obtained as

$$R_{\mathrm{NF,eff}}^{\mathrm{res}} = \sqrt{\frac{1}{\frac{2\beta_{\mathrm{HPBW}}^2}{R_D\Delta R_C} + \frac{\beta_{\mathrm{HPBW}}^4}{R_D^2}}} \approx \sqrt{\frac{R_D\Delta R_C}{2\beta_{\mathrm{HPBW}}^2}}, \tag{9.18}$$

the approximation holding when $\Delta R_C \ll R_D/\beta_{\mathrm{HPBW}}^2$, as it is the case when the waveform bandwidth is sufficiently large. Plugging the values of β_{HPBW}, this gives

$$\begin{aligned}
R_{\mathrm{NF,eff}}^{\mathrm{res,PT,SIMO}} &\approx \sqrt{\frac{R_D \Delta R_C}{13.8}}, \\
R_{\mathrm{NF,eff}}^{\mathrm{res,PT,MIMO}} &\approx \sqrt{\frac{R_D \Delta R_C}{9.94}}, \\
R_{\mathrm{NF,eff}}^{\mathrm{res,ET,SIMO}} &\approx \sqrt{\frac{R_D \Delta R_C}{27.8}}, \\
R_{\mathrm{NF,eff}}^{\mathrm{res,ET,MIMO}} &\approx \sqrt{\frac{R_D \Delta R_C}{11.8}}. \qquad (9.19)
\end{aligned}$$

In the PT SIMO case, this distance is almost identical to the one obtained in [169, Equation (3)], in which the authors have a 14 factor instead of 13.8. Nevertheless, their 14 factor has been fitted through numerical experiments, while it is obtained theoretically in our case.

Peak-to-side-lobe level ratio The obtained theoretical results also enable to study the side-lobes of the ambiguity function, which can be measured with the Peak-to-Side-lobe Level Ratio (PSLR). Since the ambiguity function has been normalised, this PSLR is the square value of the ambiguity function at the first side-lobe. Proposition 9.1 ensures that the PSLR of $\chi\left(\tilde{R}; R\right)$ satisfies

$$\mathrm{PSLR} \leq \min\left\{\mathrm{PSLR}_C, \mathrm{PSLR}_{\Delta\phi}\right\}, \qquad (9.20)$$

with PSLR_C and $\mathrm{PSLR}_{\Delta\phi}$ the PSLR respectively of the waveform ambiguity function and of the phase ambiguity function. With the analytical expressions of Proposition 9.2, the PSLR can be obtained as

$$\begin{aligned}
\mathrm{PSLR}_{\Delta\phi}^{\mathrm{PT,SIMO}} &= 8.79\,\mathrm{dB}, \\
\mathrm{PSLR}_{\Delta\phi}^{\mathrm{PT,MIMO}} &= 17.57\,\mathrm{dB}, \\
\mathrm{PSLR}_{\Delta\phi}^{\mathrm{ET,SIMO}} &= 8.79\,\mathrm{dB}, \\
\mathrm{PSLR}_{\Delta\phi}^{\mathrm{ET,MIMO}} &= \text{undefined}.
\end{aligned}$$

From Proposition 9.2, the PSLR is identical in the PT SIMO and in the ET SIMO cases, while it is doubled (in dB scale) for the PT MIMO case. Surprisingly, in the ET MIMO case, no side-lobes are observed for large number of antennas.

9.4.4 Impact of a model mismatch

This section investigates the effect of using the PT model when the target is an ET, or conversely, focusing on the SIMO case. This may happen when the range a large planar target is estimated considering it is instead a PT. In the opposite case, if the target is for instance a small sphere, then it can accurately be modelled as a PT, and estimating its range with a planar ET model leads to a model mismatch.

To evaluate the impact of these effects, the mismatched ambiguity function is defined as

$$\chi^{\text{Mis}}\left(\tilde{R}; R\right) \triangleq \frac{\Lambda\left(\tilde{R}\right)}{N_{\text{r}} N_{\text{t}} \mathcal{E}_c \left|\xi\right|},$$

with $\Lambda\left(\tilde{R}\right)$ evaluated with the noise-free signals $u_{l'l}(t) = \xi \mu_{l'l;R}(t)$, in which the true distance are given by $r^{\text{ET}}_{l'l}$, while the candidate ones are $r^{\text{PT}}_{l'l}$, and conversely. It can be observed the mismatched ambiguity function has been normalised with the factor $N_{\text{r}} N_{\text{t}} \mathcal{E}_c \left|\xi\right|$ which is the normalisation factor of the ambiguity functions without mismatch, instead of normalising it to a unit maximum. THaving the same normalisation factor enables to compare the ambiguity function maximum values, differences in these values corresponding to different SNRs. Corollary 9.1 provides the analytical expression of the ambiguity function in the SIMO case.

Corollary 9.1

In the case of a model mismatch, the ambiguity function, in the SIMO case, is given by

$$\chi^{\text{Mis,SIMO}}\left(\tilde{R}; R\right) \approx \chi_C\left(\tilde{R} - R\right) \chi_{\Delta\phi,\text{r}}\left(\frac{\gamma}{\sqrt{2}}\right),$$

with

- $\gamma \triangleq \sqrt{R_D \left|\frac{2}{\tilde{R}} - \frac{1}{R}\right|}$ when the range of an ET is estimated with a PT model;
- $\gamma \triangleq \sqrt{R_D \left|\frac{2}{R} - \frac{1}{\tilde{R}}\right|}$ when the range of a PT is estimated with an ET model.

Proof. The ambiguity function is obtained by studying the phase ambiguity function of Definition 9.3 with $\tilde{r}_{l'l}$ given by $\tilde{r}_{l'l}^{\mathrm{PT}}$, but with $r_{l'l}$ given by $r_{l'l}^{\mathrm{ET}}$, as provided by (9.14) and (9.15). Then, the proof is similar to the one of Proposition 9.2. □

This corollary shows that in case of a model mismatch, the phase ambiguity function has a similar form as those of Proposition 9.2, yet with the parameter β replaced by γ. Focusing on the first case (ET model estimated with an PT model), the waveform information then gives an information which is in contradiction with the phase shift information, since $\chi_C\left(\tilde{R}-R\right)$ has its maximum at $\tilde{R}=R$, while $\chi_{\Delta\phi,\mathrm{r}}\left(\gamma\right)$ has its maximum at $\tilde{R}=2R$.

This can be explained using (9.14) and (9.15). Indeed, the phase difference between the signal received at the antenna l' and l'' is given by $\Delta_\phi^{\mathrm{PT}}=k(y_{l'}^2-y_{l''}^2)/2R$ and $\Delta_\phi^{\mathrm{ET}}=k(y_{l'}^2-y_{l''}^2)/4R$ for a PT and an ET, z_l being 0 in the SIMO case. For the same phase difference, the estimated range will thus be affected by a factor 2 if the erroneous model is considered. Contrarily, the waveform delay of each antenna pair can be measured in an absolute manner, since the emitter and receiver are considered synchronised in time. For a given time delay, the range estimation will thus mainly be obtained from the $2R$ terms in (9.14) and (9.15) as they are much larger than the term in $\mathcal{O}(1/R)$. The $2R$ terms being identical for both target models, the waveform ambiguity function is not impacted by the model mismatch.

Examples of mismatched ambiguity functions are provided in Figure 9.6, for the SIMO and MIMO case, and for two different bandwidths, when the range of an ET is estimated with a PT model. The other parameters are $R=4\,\mathrm{m}$, $N_{\mathrm{r}}=201$, $N_{\mathrm{t}}=1$ or 201 depending on the cases, $D=1.5\,\mathrm{m}$, $f_c=77\,\mathrm{GHz}$, $\xi=0.35+0.35j$, and the waveform is a cardinal sine. As it can be observed, the insights provided by Corollary 9.1 are the following in the SIMO case. The mismatched ambiguity function is the product of the waveform and phase ambiguity functions, which have their respective maximum at $\tilde{R}=R$ and $\tilde{R}=2R$. Therefore, the maximum of the mismatched ambiguity function is located close to one of these points. The maximum of the two depends on the side-lobe levels, since $\chi^{\mathrm{Mis,SIMO}}\left(R;R\right)=\chi_{\Delta\phi,\mathrm{r}}\left(\sqrt{\frac{R_D}{2R}}\right)$, and $\chi^{\mathrm{Mis,SIMO}}\left(2R;R\right)=\chi_C\left(R\right)$. This is why for a low bandwidth, the maximum is located close to $\tilde{R}=2R$, while for a large bandwidth, it is located close to $\tilde{R}=R$. Even if the maximum is located close to the true range, the amplitude of the ambiguity function will be approximately

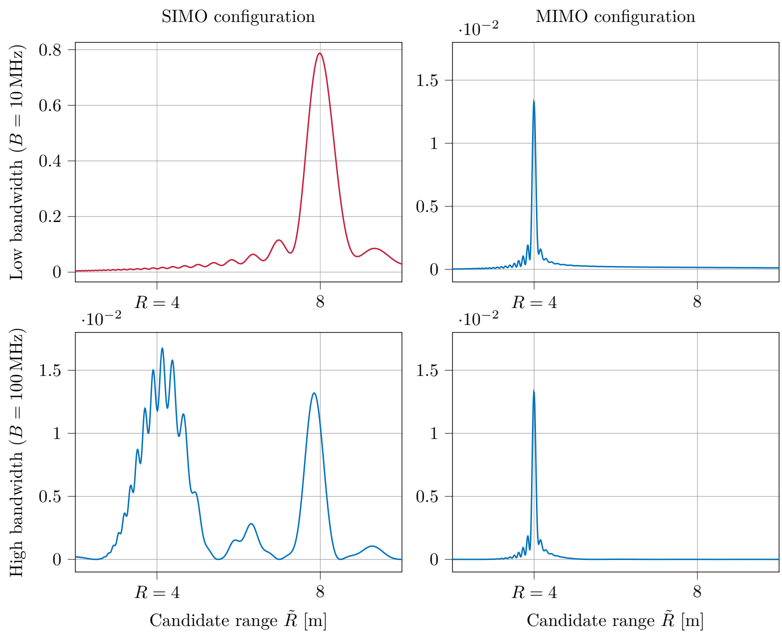

Fig. 9.6 Impact of a target model mismatch on the ambiguity function, in the SIMO and MIMO cases, and for a low and high bandwidth. The left upper panel is depicted in red to highlight the fact the scale of the y-axis is different from the other panels.

$\chi_{\Delta\phi,\mathrm{r}}\left(\sqrt{\frac{R_D}{2R}}\right)$ at the maximum. In the NF region, Figure 9.3 shows that this value is much smaller than one. Since the same normalisation as for the matched ambiguity function has been considered, this translates into a noise which impacts much more the obtained maximum. This can be observed in the y-axis scale of Figure 9.6. For the considered parameters, the loss is around 20 dB.

In the FF region, $\chi_{\Delta\phi,\mathrm{r}}\left(\frac{\gamma}{\sqrt{2}}\right)$ has still a maximum at $\tilde{R} = 2R$. Yet, at that point, $\chi^{\mathrm{Mis,SIMO}}\left(\tilde{R}; R\right) \approx \chi_C\left(R\right)$, which is low for a waveform with a sufficiently large bandwidth. At $\tilde{R} = R$, however, $\chi^{\mathrm{Mis,SIMO}}\left(\tilde{R}; R\right) \approx \chi_{\Delta\phi,\mathrm{r}}\left(\sqrt{\frac{R_D}{2R}}\right) \approx \chi_{\Delta\phi,\mathrm{r}}\left(0\right) = 1$. Thus, the maximum remains at the true range, with an amplitude close to one. This thus translates the fact that the target model has almost no impact in the FF region.

In Figure 9.6, the MIMO case is already represented, even if it has not been studied theoretically. The results shows that the maximum seems to stay at the true range, but that the loss of amplitude is also around 20 dB. Providing a theoretical basis for these observations in the MIMO case is an interesting research direction.

9.5 Cramér-Rao bound

In this section, a general expression of the NF range CRB is developed in Section 9.5.1, and closed-form expressions specific the considered target models are provided in Section 9.5.2.

9.5.1 NF range CRBs

The below proposition provides an expression of the NF range CRB, which depends on the waveform side on f_M and B_{RMS} defined in (9.3) and (9.4), and on the NF phase information side on the η and β factors defined as

$$\eta \triangleq \frac{1}{N_\mathrm{r} N_\mathrm{t}} \sum_{l'=1}^{N_\mathrm{r}} \sum_{l=1}^{N_\mathrm{t}} \left(\frac{1}{2} \frac{\partial r_{l'l}}{\partial R} \right)^2, \tag{9.21}$$

$$\beta \triangleq \frac{1}{N_\mathrm{r} N_\mathrm{t}} \sum_{l'=1}^{N_\mathrm{r}} \sum_{l=1}^{N_\mathrm{t}} \left(\frac{1}{2} \frac{\partial r_{l'l}}{\partial R} \right). \tag{9.22}$$

It is furthermore inversely proportional to the SNR given by $\mathrm{SNR} \triangleq \frac{|\xi|^2 \mathcal{E}_c}{\gamma_n}$.

Proposition 9.3: NF range Cramér-Rao bound

The CRB on the NF range estimation is given by

$$\mathrm{CRB}_R = \frac{(N_\mathrm{r} N_\mathrm{t} \mathrm{SNR})^{-1}}{\frac{32\pi^2}{c^2} \left((\eta - \beta^2)\,(f_c + f_M)^2 + \eta B_{\mathrm{RMS}}^2 \right)}. \tag{9.23}$$

Proof. See Section 9.8.4. □

In (9.23), one can identify the array gain $N_\mathrm{r} N_\mathrm{t}$ which multiplies the SNR. This expression also highlights the cooperation existing between the NF phase term $(f_c + f_M)^2(\eta - \beta^2)$, and the waveform term ηB_{RMS}^2, similarly to what has been observed for the ambiguity functions. The phase effect depends on the carrier frequency and waveform central frequency, while the waveform information depends on its RMS bandwidth. The phase effect also depends on the scene geometry through the $\sqrt{\eta - \beta^2}$ term, which is the RMS value of the propagation distance derivatives, since it can be written as

$$\eta - \beta^2 = \frac{1}{N_\mathrm{r} N_\mathrm{t}} \sum_{l'=1}^{N_\mathrm{r}} \sum_{l=1}^{N_\mathrm{t}} \left(\frac{1}{2} \frac{\partial r_{l'l}}{\partial R} - \beta \right)^2 . \tag{9.24}$$

While significant in the NF region, this term goes to 0 in the FF region of an array, as all propagation distance derivatives becomes identical when R is large.

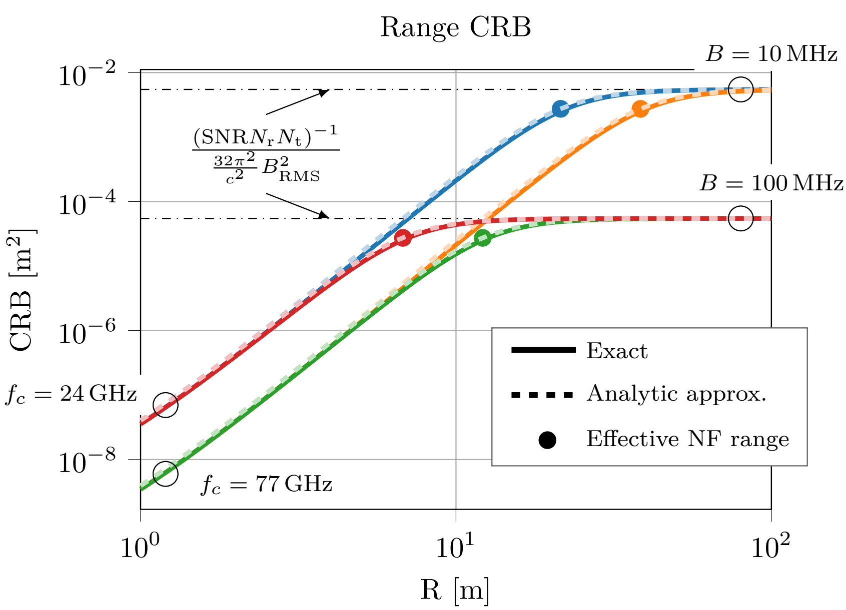

Fig. 9.7 CRB for the ET MIMO case, for two bandwidths and carrier frequencies, with $N_\mathrm{t} = N_\mathrm{r} = 25$, $D = 1.5\,\mathrm{m}$, and $\mathrm{SNR} = 10\,\mathrm{dB}$. The corresponding Rayleigh distances are respectively 360 m and 1156 m. The considered waveform is a cardinal sine, for which $f_M = 0\,\mathrm{Hz}$ and $B_\mathrm{RMS} = B/\sqrt{12}$. The dashed lines correspond to the analytical expressions of Proposition 9.4. The circles depict the ranges at which the NF information vanishes with respect to the waveform one, as given by (9.26).

Figure 9.7 illustrates the range CRB for an ET in the MIMO case, for two bandwidths and carrier frequencies. One can observe that for small ranges, the NF phase information is dominant, depending on the carrier frequency. For large ranges, the NF effect vanishes compared to the waveform information. Therefore, the CRB saturates to the waveform limit.

Remark 9.4

It must be stressed out that the obtained CRB is exact for the model described by Equation (9.6). In particular, it does not require considering $B/f_c \leq R/R_D$ (Assumption 9.1), to leverage on the Fresnel approximation (Assumption 9.2), or to have a high number of antennas (Assumption 9.3).

Up to know, the sharpness of the likelihood function at $\tilde{R} = R$ has been intuitively linked with the CRB value. For many problems, an exact relationship, or an approximate one [168] can be obtained. This is also the case in the considered scenario, as provided by the below corollary.

Corollary 9.2

The CRB on the NF range estimation given in Proposition 9.3, and the ambiguity function defined in Definition 9.1, satisfy

$$\mathrm{CRB}_R = \frac{1}{N_\mathrm{r} N_\mathrm{t} \mathrm{SNR}} \frac{-1}{\left.\frac{\partial^2 \chi^2(\tilde{R};R)}{\partial \tilde{R}^2}\right|_{\tilde{R}=R}}.$$

Proof. See Section 9.8.5. □

9.5.2 Point and extended targets

As for the ambiguity functions, the CRB expression depends on terms depending on the scene geometry. In this case, these terms are the η and β parameters, which measure the RMS value of the propagation distance derivatives. Closed-form expressions are hence provided in this section, under Assumption 9.3, i.e. with a large number of antennas. The following proposition gives these closed-form formulas.

Proposition 9.4

With Assumption 9.3, the factors η and β only depend on $u \triangleq R/D$ as follows:

$$\begin{cases} \eta^{\text{PT,SIMO}} & \approx \frac{1}{4} + \frac{u}{2}\text{atan}\left(\frac{1}{2u}\right) + u\,\text{asinh}\left(\frac{1}{2u}\right), \\ \beta^{\text{PT,SIMO}} & \approx \frac{1}{2} + u\,\text{asinh}\left(\frac{1}{2u}\right), \end{cases}$$
$$\begin{cases} \eta^{\text{PT,MIMO}} & \approx u\,\text{atan}\left(\frac{1}{2u}\right) + 2u^2\text{asinh}^2\left(\frac{1}{2u}\right), \\ \beta^{\text{PT,MIMO}} & \approx 2u\,\text{asinh}\left(\frac{1}{2u}\right), \end{cases}$$
$$\begin{cases} \eta^{\text{ET,SIMO}} & \approx 4u\,\text{atan}\left(\frac{1}{4u}\right), \\ \beta^{\text{ET,SIMO}} & \approx 4u\,\text{asinh}\left(\frac{1}{4u}\right), \end{cases}$$
$$\begin{cases} \eta^{\text{ET,MIMO}} & \approx 4u\,\text{atan}\left(\frac{1}{2u}\right) - 4u^2\log\left(1+\frac{1}{4u^2}\right), \\ \beta^{\text{ET,MIMO}} & \approx 4u\,\text{asinh}\left(\frac{1}{2u}\right) - 8u^2\left(\sqrt{1+\frac{1}{4u^2}}-1\right). \end{cases}$$

Proof. See Section 9.8.6 □

The above shows that the ratio R/D is the key parameter for the CRB. As it can be observed in Figure 9.7, the analytic approximations are in very close agreement with the exact CRB expressions even for low antenna densities, e.g., 25 antennas over 1.5 m in this case. This validates the ambiguity function analysis, for which the main lobe was observed to be closely approximated even for low to very low numbers of antennas. Focusing on the NF geometry term $\eta - \beta^2$, the analytic expressions of Proposition 9.4 are depicted in Figure 9.8. As it can be observed, while the above functions are intricate, the CRB term evolves almost linearly, in log-scale, when $R \geq D$. This observation is formalised in the below corollary, which provides a Taylor series expansion of the CRB for $R \geq D$.

Corollary 9.3

If Assumption 9.2 holds,

$$\text{CRB}_R \approx \frac{(N_\text{r}N_\text{t}\text{SNR})^{-1}}{\frac{32\pi^2}{c^2}\left(\frac{\alpha(f_c+f_M)^2}{11520}\left(\frac{D}{R}\right)^4 + B^2_{\text{RMS}}\right)}, \tag{9.25}$$

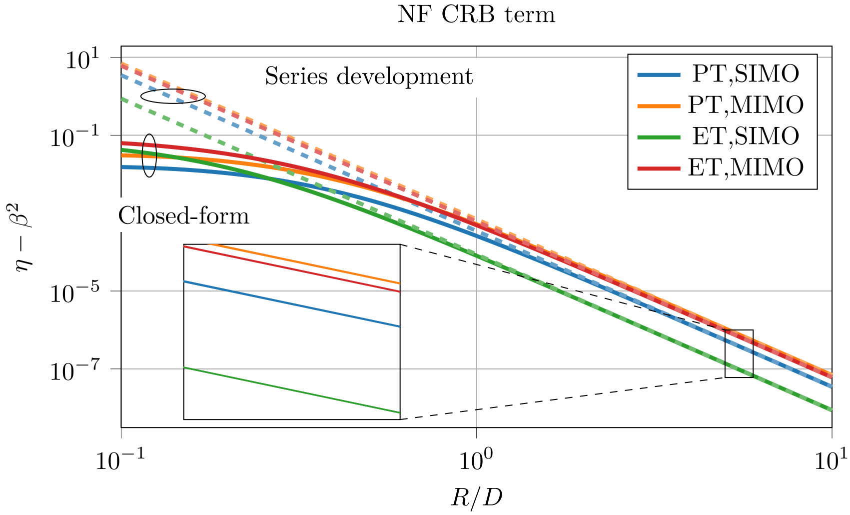

Fig. 9.8 Analytic expressions of Proposition 9.4 for the NF term $\eta - \beta^2$ of the range CRB, as a function of $\frac{R}{D}$. The series developments of Corollary 9.3 are depicted with dashed lines.

with the factor $\alpha = 4$ (resp. 8, 1, 7) in the PT SIMO case (resp. PT MIMO, ET SIMO, ET MIMO).

Proof. See Section 9.8.7 □

The above corollary enables to obtain simple closed-form expressions of the NF CRBs for $R \geq D$. In all cases (SIMO and MIMO, PT and ET), the NF effect evolves in $(D/R)^4$. Yet, a constant vertical offset differentiates the cases, which mirrors the difference in curvatures observed in Figure 9.3. This offset depends on the value of the factor α: in order to achieve the same CRB as the one of a MIMO array of size D with a PT (i.e. the best case), the array size must be equal to $D\sqrt[4]{8/\alpha}$, leading to $1.03D$ for the MIMO ET for instance. From Corollary 9.2, this factor α can be directly linked to the sharpness of the main lobe of the likelihood function, as studied in Figure 9.2 and Figure 9.3. In the MIMO case, the α factor is respectively equal to 8 and 7 for a PT and an ET, explaining why both ambiguity functions ware having an almost identical main lobe.

The above expression of the CRB can yet be rewritten in another manner.

To that aim, let the range waveform precision σ_C and range phase precision $\sigma_{\Delta\phi}$ be defined as

$$\sigma_C \triangleq \frac{c}{\sqrt{32}\pi B_{\mathrm{RMS}}},$$
$$\sigma_{\Delta\phi} \triangleq \frac{c\sqrt{360}}{\pi\sqrt{\alpha}\,(f_C + f_M)} \frac{R^2}{D^2}.$$

The CRB reads then as

$$\mathrm{CRB}_R \approx (N_{\mathrm{r}} N_{\mathrm{t}} \mathrm{SNR})^{-1} \frac{1}{\frac{1}{\sigma^2_{\Delta\phi}} + \frac{1}{\sigma^2_C}}.$$

This directly shows that the combined precision will be dominated by the best precision among the waveform and phase shift one.

Another insight provided by Corollary 9.3 is the range at which the NF effect vanishes with respect to the waveform effect, and thus the performance saturates to the FF performance. Similarly to the effective NF resolution range defined in (9.18), this range is defined as the effective NF precision range, and denoted $R^{\mathrm{prec}}_{\mathrm{NF,eff}}$. It is obtained as the range at which $\sigma_C = \sigma_{\Delta\phi}$, leading to

$$R^{\mathrm{prec}}_{\mathrm{NF,eff}} = D\sqrt{\frac{f_c + f_M}{B_{\mathrm{RMS}}}}\sqrt[4]{\frac{\alpha}{11520}}. \tag{9.26}$$

These ranges are highlighted in Figure 9.7, showing their ability to predict the region in which NF gains are significant. Considering a centred faveform, (i.e., $f_M = 0$), the effective precision range can be rewritten as

$$R^{\mathrm{prec}}_{\mathrm{NF,eff}} = \sqrt{\frac{R_D \sigma_C}{\sqrt{\frac{1440}{\pi^2\alpha}}}}. \tag{9.27}$$

Up to a constant factor, this provides therefore the same insights as (9.18). Interestingly, this shows that the range at which the NF effect vanishes with respect to the classical FF information evolves with the root square of the Rayleigh distance, and with the root square of the radar FF precision. This observation echoes the one of [169].

To conclude the above analysis, (9.27) can be computed for a cardinal sine, for which $\Delta R_C = 0.44c/B$, and $B_{\mathrm{RMS}} = B/\sqrt{12}$. It has thus $\sigma_C \approx$

$0.443\Delta R_C$, and consequently,

$$
\begin{aligned}
R_{\mathrm{NF,eff}}^{\mathrm{prec,PT,SIMO}} &= \sqrt{\frac{R_D B}{13.63}}, \\
R_{\mathrm{NF,eff}}^{\mathrm{prec,PT,MIMO}} &= \sqrt{\frac{R_D B}{9.64}}, \\
R_{\mathrm{NF,eff}}^{\mathrm{prec,ET,SIMO}} &= \sqrt{\frac{R_D B}{27.27}}, \\
R_{\mathrm{NF,eff}}^{\mathrm{prec,ET,MIMO}} &= \sqrt{\frac{R_D B}{10.30}}.
\end{aligned}
$$

These relationships are very close to the ones obtain in (9.19), showing the complementarity of the ambiguity function and CRB analyses [168], as predicted by Corollary 9.2.

9.6 Chapter summary

In this chapter, the ML estimator for the multi-antenna radar range estimation ôf PTs and ETs in the NF region is obtained. Closed-form performance bounds are derived, being the ambiguity function and the CRB. Both metrics reveal a cooperation between the NF phase information and the waveform delay information. For the considered settings, the obtained performance bounds have particularly simple forms from which the parameter impact can be evaluated. This enables to obtain expressions of the radar resolution and the PSLR. As far as the CRB is concerned, the analysis shows that the NF CRBs improve with the RMS value of the propagation distance derivatives. Moreover, an expression of the range at which the NF effect vanishes with respect to the FF information is provided. Future works include the study of other antenna configurations, and performance bounds for the problem of range and angle estimation. The mismatch analysis also calls for the investigation of other target geometries, such as a cylindrical target. By varying the curvature of the cylinder, it would enable to bridge the planar target model (infinite radius) and the point target model (zero radius).

9.7 Conclusion on the NF-based interference management

The radar resolution and precision obtained in this part enable to have an approximate idea of the spatial separation which must exist between targets so that they can be distinguished one from each other. In other words, it determines when the range resource can be exploited to manage the interference between points.

This hence constitutes a first step towards the understanding on how the range resource can be exploited in MF MP networks. Future directions include the study of the communication function, such as in [142], as well as multi-target radar scenarios.

9.8 Proofs

9.8.1 Proof of Lemma 9.1

Starting with Equation (9.9) and the Probability Density Function (PDF) given in (9.10),

$$\begin{aligned}\hat{R}, \hat{\xi} &= \underset{\tilde{R}, \tilde{\xi}}{\arg\min} \sum_{l'=1}^{N_\mathrm{r}} \sum_{l=1}^{N_\mathrm{t}} \int_t \left| u_{l'l}(t) - \tilde{\xi} \mu_{l'l;\tilde{R}}(t) \right|^2 \mathrm{d}t, \\ &= \underset{\tilde{R}, \tilde{\xi}}{\arg\min} \sum_{l'=1}^{N_\mathrm{r}} \sum_{l=1}^{N_\mathrm{t}} \int_t \left| u_{l'l}(t) \right|^2 \mathrm{d}t + |\tilde{\xi}|^2 \sum_{l'=1}^{N_\mathrm{r}} \sum_{l=1}^{N_\mathrm{t}} \int_t \left| \mu_{l'l;\tilde{R}}(t) \right|^2 \mathrm{d}t \\ &\qquad - 2\mathrm{Re}\left\{ \tilde{\xi}^\star \sum_{l'=1}^{N_\mathrm{r}} \sum_{l=1}^{N_\mathrm{t}} \int_t u_{l'l}(t)\, \mu^\star_{l'l;\tilde{R}}(t)\, \mathrm{d}t \right\}.\end{aligned}$$

The first term is independent of $\tilde{R}$ and $\tilde{\xi}$, and the second can be developed as

$$\int_t \left| \mu_{l'l;\tilde{R}}(t) \right|^2 \mathrm{d}t = \int_t \left| s\left(t - \frac{r_{l'l}}{c}\right) \right|^2 \mathrm{d}t = \mathcal{E}_c.$$

This leads to

$$\hat{R}, \hat{\xi} = \arg\min_{\tilde{R}, \tilde{\xi}} \left|\tilde{\xi}\right|^2 N_{\mathrm{t}} N_{\mathrm{r}} \mathcal{E}_c - 2\left|\tilde{\xi}\right| \mathrm{Re}\left\{ e^{-j\arg\{\tilde{\xi}\}} \sum_{l'=1}^{N_{\mathrm{r}}} \sum_{l=1}^{N_{\mathrm{t}}} \int_t u_{l'l}(t)\, \mu^{\star}_{l'l;\tilde{R}}(t)\,\mathrm{d}t \right\},$$

from which one extracts

$$\arg\left\{\hat{\xi}\left(\tilde{R}\right)\right\} = \arg\left\{ \sum_{l'=1}^{N_{\mathrm{r}}} \sum_{l=1}^{N_{\mathrm{t}}} \int_t u_{l'l}(t)\, \mu^{\star}_{l'l;\tilde{R}}(t)\,\mathrm{d}t \right\},$$

$$\left|\hat{\xi}\left(\tilde{R}\right)\right| = \frac{1}{N_{\mathrm{t}} N_{\mathrm{r}} \mathcal{E}_c} \left| \sum_{l'=1}^{N_{\mathrm{r}}} \sum_{l=1}^{N_{\mathrm{t}}} \int_t u_{l'l}(t)\, \mu^{\star}_{l'l;\tilde{R}}(t)\,\mathrm{d}t \right|.$$

Plugging this back into the optimisation problem, the lemma is obtained.

9.8.2 Proof of Proposition 9.1

By developing (9.11) for noise-free signals, one obtains

$$\Lambda\left(\tilde{R}\right) = |\xi|\, N_{\mathrm{r}} N_{\mathrm{t}} \mathcal{E}_c \chi\left(\tilde{R}; R\right).$$

Moreover, from the Cauchy-Schwarz inequality

$$\begin{aligned}
\chi\left(\tilde{R}; R\right) &= \frac{1}{N_{\mathrm{r}} N_{\mathrm{t}} \mathcal{E}_c} \left| \sum_{l'=1}^{N_{\mathrm{r}}} \sum_{l=1}^{N_{\mathrm{t}}} \int_t \mu_{l'l;R}(t)\, \mu^{\star}_{l'l;\tilde{R}}(t)\,\mathrm{d}t \right|, \\
&\leq \frac{1}{N_{\mathrm{r}} N_{\mathrm{t}} \mathcal{E}_c} \sqrt{\sum_{l'=1}^{N_{\mathrm{r}}} \sum_{l=1}^{N_{\mathrm{t}}} \int_t \left|\mu_{l'l;R}(t)\right|^2 \mathrm{d}t} \sqrt{\sum_{l'=1}^{N_{\mathrm{r}}} \sum_{l=1}^{N_{\mathrm{t}}} \int_t \left|\mu_{l'l;\tilde{R}}(t)\right|^2 \mathrm{d}t}, \\
&= 1,
\end{aligned}$$

with this maximum attained at $R = \tilde{R}$. This thus proves (9.12). Under Assumption 9.1,

$$C\left(\frac{\tilde{r}_{l'l} - r_{l'l}}{c}\right) \approx C\left(\frac{2\tilde{R} - 2R}{c}\right),$$

leading to the second desired result.

9.8.3 Proof of Proposition 9.2

The proof is performed for a PT in the SIMO case, the other configurations following from the same steps. Plugging the approximate distances (9.14) into the definition Definition 9.3, one obtains

$$\begin{aligned}
\chi_{\Delta\phi}^{\mathrm{PT,SIMO}}\left(\tilde{R};R\right) &\approx \left|\frac{1}{N_{\mathrm{r}}}\sum_{l'=1}^{N_{\mathrm{r}}} e^{jk\left(2\tilde{R}+\frac{z_l^2}{2\tilde{R}}-2R-\frac{z_l^2}{2R}\right)}\right|, \\
&= \left|\frac{e^{jk\left(2\tilde{R}-2R\right)}}{N_{\mathrm{r}}}\sum_{l'=1}^{N_{\mathrm{r}}} e^{jk\frac{z_l^2}{2}\left|\frac{1}{\tilde{R}}-\frac{1}{R}\right|\mathrm{sign}\left(\frac{1}{\tilde{R}}-\frac{1}{R}\right)}\right|, \\
&= \left|\frac{1}{N_{\mathrm{r}}}\sum_{l'=1}^{N_{\mathrm{r}}} e^{j\frac{\pi}{2}\frac{z_l^2}{D^2}\frac{2D^2}{\lambda}\left|\frac{1}{\tilde{R}}-\frac{1}{R}\right|}\right|,
\end{aligned}$$

concluding the first part of the proof. For the second part, replacing the sum by an integral, one obtains

$$\begin{aligned}
\chi_{\Delta\phi,\mathrm{r}}\left(\beta\right) &\approx \left|\frac{1}{D}\int_{-D/2}^{D/2} e^{j\frac{\pi}{2}\left(\frac{\beta z}{D}\right)^2}\mathrm{d}z\right|, \\
&= \left|\frac{2}{\beta}\int_{0}^{\beta/2} e^{j\frac{\pi}{2}t^2}\mathrm{d}t\right|,
\end{aligned}$$

concluding the proof.

9.8.4 Proof of Proposition 9.3

Associated with the estimation problem (9.9), the Fisher information matrix is given by

$$I = -\mathbb{E}\{\begin{bmatrix}
\frac{\partial^2 \log T_U}{\partial \xi_{\mathcal{R}}^2} & \frac{\partial^2 \log T_U}{\partial \xi_{\mathcal{R}}\partial \xi_{\mathcal{I}}} & \frac{\partial^2 \log T_U}{\partial \xi_{\mathcal{R}}\partial R} \\
\frac{\partial^2 \log T_U}{\partial \xi_{\mathcal{I}}\partial \xi_{\mathcal{R}}} & \frac{\partial^2 \log T_U}{\partial \xi_{\mathcal{I}}^2} & \frac{\partial^2 \log T_U}{\partial \xi_{\mathcal{I}}\partial R} \\
\frac{\partial^2 \log T_U}{\partial R\partial \xi_{\mathcal{R}}} & \frac{\partial^2 \log T_U}{\partial R\partial \xi_{\mathcal{I}}} & \frac{\partial^2 \log T_U}{\partial R^2}
\end{bmatrix}\},$$

with $\xi_{\mathcal{R}}$ and $\xi_{\mathcal{I}}$ the real and imaginary parts of ξ, and T_U the PDF of the received signal given in (9.10). The log-likelihood function is developed as

$$\begin{aligned}\log T_U &= K - \frac{1}{\gamma_n}\sum_{l'=1}^{N_\mathrm{r}}\sum_{l=1}^{N_\mathrm{t}}\int_t \left|u_{l'l}(t) - \xi\mu_{l'l;R}(t)\right|^2 \mathrm{d}t,\\ &= \tilde{K} - \frac{\xi_{\mathcal{R}}^2 N_\mathrm{r}N_\mathrm{t}\mathcal{E}_c}{\gamma_n} - \frac{\xi_{\mathcal{I}}^2 N_\mathrm{r}N_\mathrm{t}\mathcal{E}_c}{\gamma_n}\\ &\quad + \frac{2\xi_{\mathcal{R}}}{\gamma_n}\mathrm{Re}\left\{\sum_{l'=1}^{N_\mathrm{r}}\sum_{l=1}^{N_\mathrm{t}}\int_t u_{l'l}(t)\,\mu^{\star}_{l'l;R}(t)\,\mathrm{d}t\right\}\\ &\quad + \frac{2\xi_{\mathcal{I}}}{\gamma_n}\mathrm{Im}\left\{\sum_{l'=1}^{N_\mathrm{r}}\sum_{l=1}^{N_\mathrm{t}}\int_t u_{l'l}(t)\,\mu^{\star}_{l'l;R}(t)\,\mathrm{d}t\right\}.\end{aligned}$$

This leads to the following elements of the Fisher information matrix:

$$I = \frac{8N_\mathrm{r}N_\mathrm{t}\mathcal{E}_c}{\gamma_n}\begin{bmatrix} \frac{1}{4} & 0 & -\frac{\mathrm{Re}\{\xi N\}}{2}\\ 0 & \frac{1}{4} & -\frac{\mathrm{Im}\{\xi N\}}{2}\\ -\frac{\mathrm{Re}\{\xi N\}}{2} & -\frac{\mathrm{Im}\{\xi N\}}{2} & -|\xi|^2\,\mathrm{Re}\{M\}\end{bmatrix},$$

with N and M defined as

$$N \triangleq \frac{1}{2N_\mathrm{r}N_\mathrm{t}\mathcal{E}_c}\sum_{l'=1}^{N_\mathrm{r}}\sum_{l=1}^{N_\mathrm{t}}\int_t \mu_{l'l;R}(t)\,\frac{\partial\mu^{\star}_{l'l;R}}{\partial R}(t)\,\mathrm{d}t, \tag{9.28}$$

$$M \triangleq \frac{1}{4N_\mathrm{r}N_\mathrm{t}\mathcal{E}_c}\sum_{l'=1}^{N_\mathrm{r}}\sum_{l=1}^{N_\mathrm{t}}\int_t \mu_{l'l;R}(t)\,\frac{\partial^2\mu^{\star}_{l'l;R}}{\partial R^2}(t)\,\mathrm{d}t. \tag{9.29}$$

Partitioning the matrix and using the block-matrix inversion lemma [99, Fact 2.17.3], the CRB is obtained as

$$\mathrm{CRB}_R = \frac{1}{\frac{8|\xi|^2\mathcal{E}_c N_\mathrm{r}N_\mathrm{t}}{\gamma_n}\left(-\mathrm{Re}\{M\} - |N|^2\right)}. \tag{9.30}$$

It remains to develop the expressions of M and N for the model (9.6). To that aim, the following notations are introduced:

$$X \triangleq \int_t s(t) \frac{\partial s^\star(t)}{\partial t} \mathrm{d}t,$$
$$B \triangleq \int_t \left| \frac{\partial s(t)}{\partial t} \right|^2 \mathrm{d}t = -\int_t s(t) \frac{\partial s^\star(t)}{\partial t^2} \mathrm{d}t,$$

the last equality being obtained by integration by part. From the same argument, it can be observed X is purely imaginary: $X = j\mathrm{Im}\{X\}$, while B is real by definition. Moreover, from Parseval theorem,

$$\frac{jX}{\mathcal{E}_c} = 2\pi f_M, \quad \frac{B}{\mathcal{E}_c} - \frac{|X|^2}{\mathcal{E}_c^2} = 4\pi^2 B_{\mathrm{RMS}}^2. \tag{9.31}$$

The following is furthermore introduced:

$$\gamma \triangleq \frac{1}{2N_\mathrm{r}N_\mathrm{t}} \sum_{l'=1}^{N_\mathrm{r}} \sum_{l=1}^{N_\mathrm{t}} \frac{\partial^2 r_{l'l}}{\partial R^2}.$$

Equipped with these notations, the model derivatives are obtained as

$$\frac{\partial \mu_{l'l;R}(t)}{\partial R} = -e^{-jkr_{l'l}} \frac{\partial r_{l'l}}{\partial R} \left(jks\left(t - \frac{r_{l'l}}{c}\right) + \frac{1}{c} \frac{s\left(t - \frac{r_{l'l}}{c}\right)}{\partial t} \right),$$
$$\begin{aligned}\frac{\partial^2 \mu_{l'l;R}(t)}{\partial R^2} = e^{-jkr_{l'l}} \Bigg[&\left(-k^2 \left(\frac{\partial r_{l'l}}{\partial R} \right)^2 - jk \frac{\partial^2 r_{l'l}}{\partial R^2} \right) s\left(t - \frac{r_{l'l}}{c}\right) \\ &+ \left(\frac{2jk}{c} \left(\frac{\partial r_{l'l}}{\partial R} \right)^2 - \frac{1}{c} \frac{\partial^2 r_{l'l}}{\partial R^2} \right) \frac{\partial s\left(t - \frac{r_{l'l}}{c}\right)}{\partial t} \\ &+ \frac{1}{c^2} \left(\frac{\partial r_{l'l}}{\partial R} \right)^2 \frac{\partial^2 s\left(t - \frac{r_{l'l}}{c}\right)}{\partial t^2} \Bigg].\end{aligned}$$

This leads to

$$\begin{aligned}
&\int_t \mu_{l'l;R}(t) \frac{\partial^2 \mu^\star_{l'l;R}}{\partial R^2}(t)\,\mathrm{d}t \\
&= \left(-k^2\left(\frac{\partial r_{l'l}}{\partial R}\right)^2 + jk\frac{\partial^2 r_{l'l}}{\partial R^2}\right)\mathcal{E}_c \\
&+ \left(\frac{-2jk}{c}\left(\frac{\partial r_{l'l}}{\partial R}\right)^2 - \frac{1}{c}\frac{\partial^2 r_{l'l}}{\partial R^2}\right)X - \frac{1}{c^2}\left(\frac{\partial r_{l'l}}{\partial R}\right)^2 B.
\end{aligned}$$

Plugging the above into M,

$$\begin{aligned}
\mathcal{R}\{M\} &= \mathcal{R}\left\{-k^2\eta + 2jk\gamma + \left(\frac{2k}{c}\eta - \frac{2j}{c}\gamma\right)\frac{\mathcal{I}\{X\}}{\mathcal{E}_c} - \frac{\eta}{c^2}\frac{B}{\mathcal{E}_c}\right\}, \\
&= -k^2\eta + \frac{2k}{c}\eta\frac{\mathcal{I}\{X\}}{\mathcal{E}_c} - \frac{1}{c^2}\eta\frac{B}{\mathcal{E}_c}.
\end{aligned}$$

For the second term, it comes that

$$\int_t \mu_{l'l;R}(t)\frac{\partial \mu^\star_{l'l;R}}{\partial R}(t)\,\mathrm{d}t = j\left(k\mathcal{E}_c - \frac{1}{c}\mathcal{I}\{X\}\right)\frac{\partial r_{l'l}}{\partial R},$$

leading to

$$N = j\beta\left(k - \frac{1}{c}\frac{\mathcal{I}\{X\}}{\mathcal{E}_c}\right).$$

Therefore,

$$\begin{aligned}
-\mathcal{R}\{M\} - |N|^2 &= \left(\eta - \beta^2\right)\left(k - \frac{1}{c}\frac{\mathcal{I}\{X\}}{\mathcal{E}_c}\right)^2 + \frac{\eta}{c^2}\left(\frac{B}{\mathcal{E}_c} - \frac{|X|^2}{\mathcal{E}_c^2}\right), \\
&= \left(\eta - \beta^2\right)\frac{4\pi^2}{c^2}\left(f_c + f_M\right)^2 + \eta\frac{4\pi^2}{c^2}B^2_{\mathrm{RMS}},
\end{aligned}$$

concluding the proof.

9.8.5 Proof of Corollary 9.2

The squared exact ambiguity function expression given in (9.12) can be rewritten as

$$\chi^2\left(\tilde{R};R\right)=\left|\frac{1}{N_\mathrm{r}N_\mathrm{t}\mathcal{E}_c}\sum_{l'=1}^{N_\mathrm{r}}\sum_{l=1}^{N_\mathrm{t}}\int_t \mu_{l'l;R}\left(t\right)\mu^\star_{l'l;\tilde{R}}\left(t\right)\mathrm{d}t\right|^2.$$

The second derivative of a squared modulus is given by

$$\frac{\partial^2\left|f\left(\tilde{R}\right)\right|^2}{\partial\tilde{R}^2}=2\left|\frac{\partial f\left(\tilde{R}\right)}{\partial\tilde{R}}\right|^2+2\mathrm{Re}\left\{f^\star\left(\tilde{R}\right)\frac{\partial^2 f\left(\tilde{R}\right)}{\partial\tilde{R}^2}\right\}$$

Consequently,

$$\begin{aligned}\left.\frac{\partial^2\chi^2\left(\tilde{R};R\right)}{\partial\tilde{R}}\right|_{\tilde{R}=R}&=8\left|\frac{1}{2N_\mathrm{r}N_\mathrm{t}\mathcal{E}_c}\sum_{l'=1}^{N_\mathrm{r}}\sum_{l=1}^{N_\mathrm{t}}\int_t \mu_{l'l;R}\left(t\right)\frac{\partial\mu^\star_{l'l;R}\left(t\right)}{\partial R}\mathrm{d}t\right|^2\\&\quad+8\mathrm{Re}\left\{\frac{\chi^\star\left(R,R\right)}{4N_\mathrm{r}N_\mathrm{t}\mathcal{E}_c}\sum_{l'=1}^{N_\mathrm{r}}\sum_{l=1}^{N_\mathrm{t}}\int_t \mu_{l'l;R}\left(t\right)\frac{\partial^2\mu^\star_{l'l;R}\left(t\right)}{\partial R^2}\mathrm{d}t\right\},\end{aligned}$$

where M and N defined in (9.29) and (9.28) can be identified, leading to

$$\left.\frac{\partial^2\chi^2\left(\tilde{R};R\right)}{\partial\tilde{R}}\right|_{\tilde{R}=R}=8\left|N\right|^2+8\mathrm{Re}\left\{M\right\}.$$

Considering the CRB expression given in (9.30), the corollary is obtained.

9.8.6 Proof of Proposition 9.4

In the case of a PT, the range derivative is given by

$$\frac{\partial r^{\mathrm{PT}}_{l'l}}{\partial R}=\frac{R}{\sqrt{R^2+z_l^2}}+\frac{R}{\sqrt{R^2+y_{l'}^2}}.$$

Thus,

$$\eta^{\mathrm{PT}} = \frac{1}{4N_{\mathrm{t}}} \sum_{l=1}^{N_{\mathrm{t}}} \frac{1}{1+\left(\frac{z_l}{R}\right)^2} + \frac{1}{4N_{\mathrm{r}}} \sum_{l'=1}^{N_{\mathrm{r}}} \frac{1}{1+\left(\frac{y_{l'}}{R}\right)^2} + \frac{1}{4N_{\mathrm{r}}N_{\mathrm{t}}} \sum_{l=1}^{N_{\mathrm{t}}} \sum_{l'=1}^{N_{\mathrm{r}}} \frac{2}{\sqrt{1+\left(\frac{z_l}{R}\right)^2}\sqrt{1+\left(\frac{y_{l'}}{R}\right)^2}},$$

$$\beta^{\mathrm{PT}} = \frac{1}{2N_{\mathrm{t}}} \sum_{l=1}^{N_{\mathrm{t}}} \frac{1}{\sqrt{1+\left(\frac{z_l}{R}\right)^2}} + \frac{1}{2N_{\mathrm{r}}} \sum_{l'=1}^{N_{\mathrm{r}}} \frac{1}{\sqrt{1+\left(\frac{y_{l'}}{R}\right)^2}},$$

When the number of antennas is large, the above sums are approximated as

$$\frac{1}{4N_{\mathrm{t}}} \sum_{l=1}^{N_{\mathrm{t}}} \frac{1}{1+\left(\frac{z_l}{R}\right)^2} \approx \frac{R}{2D} \int_0^{\frac{D}{2R}} \frac{1}{1+u^2} \mathrm{d}u = \frac{R}{2D} \mathrm{atan}\left(\frac{D}{2R}\right),$$

$$\frac{1}{2N_{\mathrm{t}}} \sum_{l=1}^{N_{\mathrm{t}}} \frac{1}{\sqrt{1+\left(\frac{z_l}{R}\right)^2}} \approx \frac{R}{D} \int_0^{\frac{D}{2R}} \frac{1}{\sqrt{1+u^2}} \mathrm{d}u = \frac{R}{D} \mathrm{asinh}\left(\frac{D}{2R}\right),$$

providing the desired result. In the case of an extended target model, the range derivative is given by

$$\frac{\partial r_{l'l}^{\mathrm{ET}}}{\partial R} = \frac{2}{\sqrt{1+\left(\frac{z_l - y_{l'}}{2R}\right)^2}}.$$

Thus,

$$\eta^{\mathrm{ET,SIMO}} = \frac{1}{N_{\mathrm{r}}} \sum_{l'=1}^{N_{\mathrm{r}}} \frac{1}{1+\left(\frac{y_{l'}}{2R}\right)^2} \approx \frac{4R}{D} \mathrm{atan}\left(\frac{D}{4R}\right),$$

$$\beta^{\mathrm{ET,SIMO}} = \frac{1}{N_{\mathrm{r}}} \sum_{l'=1}^{N_{\mathrm{r}}} \frac{1}{\sqrt{1+\left(\frac{y_{l'}}{2R}\right)^2}} \approx \frac{4R}{D} \mathrm{asinh}\left(\frac{D}{4R}\right),$$

approximating the sum as an integral under Assumption 9.3. In the MIMO case,

$$\begin{aligned}\eta^{\mathrm{ET,MIMO}} &= \frac{1}{N_{\mathrm{r}}N_{\mathrm{t}}}\sum_{l'=1}^{N_{\mathrm{r}}}\sum_{l=1}^{N_{\mathrm{t}}}\frac{1}{1+\left(\frac{z_l-y_{l'}}{2R}\right)^2},\\ &\approx \frac{4R^2}{D^2}\int_{-\frac{D}{4R}}^{\frac{D}{4R}}\int_{-\frac{D}{4R}}^{\frac{D}{4R}}\frac{1}{1+(u-v)^2}\mathrm{d}u\mathrm{d}v,\\ &= \frac{4R}{D}\mathrm{atan}\left(\frac{D}{2R}\right)-\frac{4R^2}{D^2}\log\left(1+\left(\frac{D}{2R}\right)^2\right),\end{aligned}$$

$$\begin{aligned}\beta^{\mathrm{ET,MIMO}} &= \frac{1}{N_{\mathrm{r}}N_{\mathrm{t}}}\sum_{l'=1}^{N_{\mathrm{r}}}\sum_{l=1}^{N_{\mathrm{t}}}\frac{1}{\sqrt{1+\left(\frac{z_l-y_{l'}}{2R}\right)^2}},\\ &\approx \frac{4R^2}{D^2}\int_{-\frac{D}{4R}}^{\frac{D}{4R}}\int_{-\frac{D}{4R}}^{\frac{D}{4R}}\frac{1}{\sqrt{1+(u-v)^2}}\mathrm{d}u\mathrm{d}v,\\ &= \frac{4R}{D}\mathrm{asinh}\left(\frac{D}{2R}\right)-\frac{8R^2}{D^2}\left(\sqrt{1+\frac{D^2}{4R^2}}-1\right),\end{aligned}$$

concluding the proof.

9.8.7 Proof of Corollary 9.3

Developing the above expressions with Taylor series around $D/R = 0$, one obtains

$$\begin{aligned}\eta^{\mathrm{PT,SIMO}}-\left(\beta^{\mathrm{PT,SIMO}}\right)^2 &= \frac{D^4}{2880R^4}+\mathcal{O}\left(\frac{D^6}{R^6}\right),\\ \eta^{\mathrm{PT,SIMO}} &= 1+\mathcal{O}\left(\frac{D^2}{R^2}\right).\end{aligned}$$

Under Assumption 9.2, the higher order terms are negligible, concluding the proof in the SIMO case. The proof is performed similarly in the MIMO case, leading to

$$\eta^{\mathrm{PT,SIMO}} - \left(\beta^{\mathrm{PT,SIMO}}\right)^2 = \frac{2D^4}{2880R^4} + \mathcal{O}\left(\frac{D^6}{R^6}\right),$$
$$\eta^{\mathrm{PT,MIMO}} = 1 + \mathcal{O}\left(\frac{D^2}{R^2}\right).$$

Again developing the above with Taylor series, the following is obtained

$$\eta^{\mathrm{ET,SIMO}} - \left(\beta^{\mathrm{ET,SIMO}}\right)^2 = \frac{D^4}{11520R^4} + \mathcal{O}\left(\frac{D^6}{R^6}\right),$$
$$\eta^{\mathrm{ET,SIMO}} = 1 + \mathcal{O}\left(\frac{D^2}{R^2}\right),$$
$$\eta^{\mathrm{ET,MIMO}} - \left(\beta^{\mathrm{ET,MIMO}}\right)^2 = \frac{7D^4}{11520R^4} + \mathcal{O}\left(\frac{D^6}{R^6}\right),$$
$$\eta^{\mathrm{ET,MIMO}} = 1 + \mathcal{O}\left(\frac{D^2}{R^2}\right).$$

10 Conclusion

THIS thesis analyses and manages the interference in MF MP networks along three perspectives. These three approaches correspond to the three thesis parts, being the autonomous, optimisation-based, and NF-based approaches. They are relevant in different situations, and they provide different types of insights, as detailed in this conclusion.

10.1 Summary of the contributions

Autonomous interference analysis and management In this perspective, the nodes are considered as selfish, optimising their own performance without caring about the other nodes' performance. The interactions between the nodes translate in the mathematical domain into the BRD of a game. The first element which must be pointed out is that in this approach, the behaviour of the players and the associated BRD are consequences of the studied scenario. This implies that the goal is not to optimise the interactions, or the reached equilibrium, but rather to obtain conditions ensuring the convergence of the BRD towards an equilibrium point. With these conditions obtained, **the macro-parameters which are levers controlling the interactions can be identified, these parameters being the objective of the autonomous interference analysis and management.** In that spirit, this approach lies both in the analysis part (identifying the levers) and the management part (the players optimise their own performance).

This thesis contributes to this goal by studying the interactions between MF nodes, while the wireless literature is mostly concerned about SF nodes. Therefore, a dedicated theoretical framework has been developed, whose aim is to provide conditions ensuring BRD convergence whatever the preferences of the players among their objective functions, as stated in Chapter 2. To that aim, the players' preferences have been modelled in different ways, corresponding to the different flavours of scalarised games. These different flavours differ in the metrics kept in the weighted-sum objective function of the players' optimisation problem, and in those set as constraints. For the metrics kept in the objective function, convergence conditions agnostic about the players' preferences have been obtained in chapter 3. For those in the constraints, this has however not been achieved. In fact, even the BRD convergence conditions for fixed preferences was lacking in the literature. Therefore, a theoretical framework has been developed in Chapter 4 to fill this gap. Finally, Chapter 5 has bridged the results obtained for the two extreme scalarisation flavours (all metrics in the weighted-sum objective, or all but one in the constraints) to the intermediate cases, as well as the case of players having all metrics in their constraints and none as an objective.

This developed theoretical framework has been applied to two instances of MF MP networks, which are a JRC network and a multi-level RA protocol. The analysis of the JRC network reveals that the nodes reach an equilibrium point when the interference levels remain moderate. The associated macro-parameter is thus the node density, which can be controlled by assigning less or more orthogonal resources to the nodes present in an area. For the multi-level RA protocol, the identified levers are the number of activity levels of the nodes, their maximum probability to be active at a time slot, as well as the rate and transmission power corresponding to the different levels.

Optimisation-based interference management In this second approach, the resource allocation of clusters of nodes is optimised cooperatively. To that aim, these nodes gather their performance metrics and the associated parameters in a joint optimisation problem, which must then be solved. Contrarily to the autonomous perspective, **the goal of this approach is to actively design the joint optimisation problem and the associated solution schemes.** Once such steps are done, the nodes can implement the resulting resource allocation. Such approach heavily depends on the considered MF MP scenarios. Indeed, the studied application dictates how the metrics of the different nodes and functions must be articulated in the optimisation problem. The solution methods depending on the optimisation problem structure, they are also specific on the MF MP network which is analysed. The advantage of such specificity is that the interference management schemes can take into account the peculiarities of the network, while general methods may fail to do so. The drawback is however that the conclusions stemming from one scenario cannot be transferred to other settings.

Two instances of MF MP systems have been designed using this approach. The first one, studied in Chapter 7, provides physical layer security in a CF network through beamforming design. To build the optimisation problem, information leakage metrics which take into account the coding operation across the antennas of the networks are first designed. Then, a beamforming design scheme is designed, which reaches a local optimum of the considered optimisation problem. The second instance, studied in Chapter 8, also considers a beamforming design problem, yet in a JRC network. The critical requirement in that case is that the beamforming design is asked to fairly consider all radar targets and communication signals. This is achieved by considering a SINR-product metric. A solution procedure is designed for this problem, which consists in alternating between the different involved beamformers till a local optimum is reached.

NF-based interference analysis In the third considered approach, the space resource is explored as a way to separate points. While angular separation is classic in the wireless literature, this part considers the range separation capability which can be obtained in the NF region of an antenna array. As a first step towards interference management, the focus is set to **the radar range estimation of a target, and the analysis of the associated performance bounds.** These performance bounds then enable to **understand how the network parameters impact the range estimation capability of the radar system.** This opens the way to determining when several targets can be distinguished one from the others, or when they interfere with each other.

In Chapter 9, two target models have been considered, namely the PT and ET models. First, the ML range estimator has been developed. Then, the associated ambiguity functions have been obtained in closed-form for the two target models, from which the range resolution and the PSLRs have been deduced. The impact of a mismatch between the actual target and the considered target model has also been investigated. To assess the precision of the range estimator, the CRB has been derived and simplified till an expression in which the impact of the parameters is explicit. These performance bounds have lead to the definition of an effective NF region, which is the region in which the NF phase information is dominant with respect to the range information coming from the waveform delay.

10.2 Future works

Autonomous interference analysis and management In this line of research, evident future works are the study of other MF MP networks with the developed theoretical frameworks. This lead lies thus on the applicative level. On the theoretical level, three main directions are considered to be of particular interest.

- All the obtained BRD convergence conditions are sufficient conditions. Therefore, there may be a significant gap between them and the actual convergence of the BRD. This thus calls for the development of necessary conditions, which would then enable to identify cases in which the BRD does not converge.
- A second research direction comes from the fact that the equilibrium quality is not considered in the developed framework. Even though the obtained conditions ensure the equilibrium is unique, obtaining information about its quality, such as the *price-of-anarchy*, would complement the convergence analysis.
- Regarding the developed GNEP framework, it is limited to the class of GNEPs with polyhedral strategy sets and variable RHSs. Extending it to other classes of strategy sets would enable to study a broader range of GNEPs.

Optimisation-based interference management As far as this research direction is concerned, the future works depend on the considered scenarios.

For the secure beamforming scenario, one of the research directions is the study of multi-antenna receivers and eavesdroppers. Also, as this could jeopardise the provided security guarantees, the case of eavesdroppers cooperating together forces one to adapt the information leakage metrics, and the subsequent beamforming design. For the fair beamforming design, the numerical complexity of the beamforming scheme for large number of targets and UE calls for the study of dedicated solution methods. A second research question is whether theoretical guarantees can be provided regarding the fairness of the SINR product metric.

NF-based interference analysis Regarding the NF aspects, the future works can be separated in those focusing on a single-target scenario, and those considering multiple targets.

For a single radar target, the main research direction consists in studying the joint estimation of the angle and the range, in order to perform a true localisation. Other extended target geometries should also be studied, for instance considering a cylindrical target. By varying the radius of the cylinder, this would enable to bridge the planar target model (infinite radius) and the point target model (zero radius).

When there are multiple targets, the elements obtained in the single-target case (radar resolution, PSLR, effective NF distance) should be leveraged upon in order to analyse the radar interference between the targets.

Interplay between the research directions To conclude these future works and this thesis, a last research direction consists in investigating the possible synergies between the three considered approaches. For instance, the interactions between clusters of nodes could be analysed, a joint optimisation being performed within these clusters. Another question would be to determine to which extent the NF effect could be leveraged upon in order to diminish the coupling between autonomous nodes, and thus to improve the convergence of the interactions.

List of Publications

Conference publications

- [16] G. Thiran, I. Stupia, and L. Vandendorpe, "Multi-objective game theory for multi-user OFDM integrated radar waveform design," in *2022 42nd Symposium on Information Theory and Signal Processing in the Benelux (SITB)*, 2022
- [17] G. Thiran, I. Stupia, and L. Vandendorpe, "QoS satisfaction game for random access resource management," in *2023 43rd Symposium on Information Theory and Signal Processing in the Benelux (SITB)*, 2023
- [134] G. Thiran and L. Vandendorpe, "Absolutely secure beamforming in non-coherent cell-free networks," in *INTERACT 7th Technical Meeting*, 2024
- [135] G. Thiran and L. Vandendorpe, "Coding-aware secure beamforming in cell-free networks," in *(Accepted to) 2024 IEEE 25th international workshop on signal processing advances in wireless communications (SPAWC)*, IEEE, 2024
- [144] F. De Saint Moulin, G. Thiran, C. Oestges, and L. Vandendorpe, "Fair beamforming design for MIMO ISAC systems," in *2024 19th International Symposium on Wireless Communication Systems (ISWCS)*, pp. 1–6, 2024
- [154] F. D. S. Moulin, G. Thiran, C. Craeye, L. Vandendorpe, and C. Oestges, "Near-field EM-based multistatic radar range estimation," in *INTERACT 7th Technical Meeting*, 2024

- [155] F. D. S. Moulin, G. Thiran, C. Craeye, L. Vandendorpe, and C. Oestges, “Near-field EM-based multistatic radar range estimation,” in *(Accepted to) 2024 32nd European Signal Processing Conference (EUSIPCO)*, IEEE, 2024 with the arXiv version available at [157]

- [156] G. Thiran, F. D. S. Moulin, C. Oestges, and L. Vandendorpe, “Performance bounds for near-field multi-antenna range estimation of extended targets,” in *(Accepted to) 2024 IEEE 25th international workshop on signal processing advances in wireless communications (SPAWC)*, IEEE, 2024 with the arXiv version available at [177]

Journal publications

- [18] G. Thiran, I. Stupia, and L. Vandendorpe, “Best response dynamics convergence for generalized nash equilibrium problems: An opportunity for autonomous multiple access design in federated learning,” *IEEE Internet of Things Journal*, vol. 11, no. 10, pp. 18463–18482, 2024

Bibliography

[1] D. Kimura and H. Seki, "Inter-cell interference coordination (ICIC) technology," *Fujitsu Scientific & Technical Journal*, vol. 48, no. 1, pp. 89–94, 2012.

[2] F. Jameel, Z. Hamid, F. Jabeen, S. Zeadally, and M. A. Javed, "A survey of device-to-device communications: Research issues and challenges," *IEEE Communications Surveys & Tutorials*, vol. 20, no. 3, pp. 2133–2168, 2018.

[3] S. Zeadally, J. Guerrero, and J. Contreras, "A tutorial survey on vehicle-to-vehicle communications," *Telecommunication Systems*, vol. 73, no. 3, pp. 469–489, 2020.

[4] A. Alalewi, I. Dayoub, and S. Cherkaoui, "On 5G-V2X use cases and enabling technologies: A comprehensive survey," *Ieee Access*, vol. 9, pp. 107710–107737, 2021.

[5] C. Isaia and M. P. Michaelides, "A review of wireless positioning techniques and technologies: From smart sensors to 6G," *Signals*, vol. 4, no. 1, pp. 90–136, 2023.

[6] W. Jiang, Q. Zhou, J. He, M. A. Habibi, S. Melnyk, M. El-Absi, B. Han, M. Di Renzo, H. D. Schotten, F.-L. Luo, *et al.*, "Terahertz communications and sensing for 6G and beyond: A comprehensive review," *IEEE Communications Surveys & Tutorials*, 2024.

[7] U. Singh, J.-F. Determe, F. Horlin, and P. De Doncker, "Crowd monitoring: State-of-the-art and future directions," *IETE Technical Review*, vol. 38, no. 6, pp. 578–594, 2021.

[8] M. Mitev, A. Chorti, H. V. Poor, and G. P. Fettweis, "What physical layer security can do for 6G security," *IEEE Open Journal of Vehicular Technology*, vol. 4, pp. 375–388, 2023.

[9] H. Zhang, N. Shlezinger, F. Guidi, D. Dardari, M. F. Imani, and Y. C. Eldar, "Near-field wireless power transfer for 6G internet of everything mobile networks: Opportunities and challenges," *IEEE communications magazine*, vol. 60, no. 3, pp. 12–18, 2022.

[10] X. Tang, C. Cao, Y. Wang, S. Zhang, Y. Liu, M. Li, and T. He, "Computing power network: The architecture of convergence of computing and networking towards 6G requirement," *China communications*, vol. 18, no. 2, pp. 175–185, 2021.

[11] G. Cheng, C. Jiang, B. Yue, R. Wang, B. Alzahrani, and Y. Zhang, "AI-driven proactive content caching for 6G," *IEEE Wireless Communications*, vol. 30, no. 3, pp. 180–188, 2023.

[12] I. Rojek, P. Kotlarz, J. Dorożyński, and D. Mikołajewski, "Sixth-generation (6G) networks for improved machine-to-machine (M2M) communication in industry 4.0," *Electronics*, vol. 13, no. 10, p. 1832, 2024.

[13] H. He, X. Yu, J. Zhang, S. Song, and K. B. Letaief, "Cell-free massive MIMO for 6G wireless communication networks," *Journal of Communications and Information Networks*, vol. 6, no. 4, pp. 321–335, 2021.

[14] E. Hossain, M. Rasti, H. Tabassum, and A. Abdelnasser, "Evolution toward 5G multi-tier cellular wireless networks: An interference management perspective," *IEEE Wireless communications*, vol. 21, no. 3, pp. 118–127, 2014.

[15] D. Fudenberg and J. Tirole, *Game theory.* MIT press, 1991.

[16] G. Thiran, I. Stupia, and L. Vandendorpe, "Multi-objective game theory for multi-user OFDM integrated radar waveform design," in *2022 42nd Symposium on Information Theory and Signal Processing in the Benelux (SITB)*, 2022.

[17] G. Thiran, I. Stupia, and L. Vandendorpe, "QoS satisfaction game for random access resource management," in *2023 43rd Symposium*

on Information Theory and Signal Processing in the Benelux (SITB), 2023.

[18] G. Thiran, I. Stupia, and L. Vandendorpe, "Best response dynamics convergence for generalized nash equilibrium problems: An opportunity for autonomous multiple access design in federated learning," *IEEE Internet of Things Journal*, vol. 11, no. 10, pp. 18463–18482, 2024.

[19] S. Lasaulce and H. Tembine, *Game theory and learning for wireless networks: fundamentals and applications.* Academic Press, 2011.

[20] R. Etkin, A. Parekh, and D. Tse, "Spectrum sharing for unlicensed bands," *IEEE Journal on selected areas in communications*, vol. 25, no. 3, pp. 517–528, 2007.

[21] G. Debreu, "A social equilibrium existence theorem," *Proceedings of the National Academy of Sciences*, vol. 38, no. 10, pp. 886–893, 1952.

[22] K. J. Arrow and G. Debreu, "Existence of an equilibrium for a competitive economy," *Econometrica: Journal of the Econometric Society*, pp. 265–290, 1954.

[23] J. B. Rosen, "Existence and uniqueness of equilibrium points for concave n-person games," *Econometrica: Journal of the Econometric Society*, pp. 520–534, 1965.

[24] F. Facchinei and C. Kanzow, "Generalized Nash equilibrium problems," *Annals of Operations Research*, vol. 175, no. 1, pp. 177–211, 2010.

[25] E. Koutsoupias and C. Papadimitriou, "Worst-case equilibria," in *Annual symposium on theoretical aspects of computer science*, pp. 404–413, Springer, 1999.

[26] G. W. Brown, "Iterative solution of games by fictitious play," *Act. Anal. Prod Allocation*, vol. 13, no. 1, p. 374, 1951.

[27] J.-S. Pang, G. Scutari, F. Facchinei, and C. Wang, "Distributed power allocation with rate constraints in Gaussian parallel interference channels," *IEEE Transactions on Information Theory*, vol. 54, no. 8, pp. 3471–3489, 2008.

[28] G. Scutari, D. P. Palomar, and S. Barbarossa, "Asynchronous Iterative Water-Filling for Gaussian Frequency-Selective Interference Channels," *IEEE Transactions on Information Theory*, 2008.

[29] J.-S. Pang, G. Scutari, D. P. Palomar, and F. Facchinei, "Design of Cognitive Radio Systems Under Temperature-Interference Constraints: A Variational Inequality Approach," *IEEE Transactions on Signal Processing*, 2010.

[30] M. K. Jensen, "Aggregative games and best-reply potentials," *Economic theory*, vol. 43, no. 1, pp. 45–66, 2010.

[31] O. L. De Silva, S. Lasaulce, I.-C. Morărescu, and V. S. Varma, "A game theory analysis of decentralized epidemic management with opinion dynamics," *IEEE Transactions on Control of Network Systems*, 2024.

[32] G. Scutari and D. P. Palomar, "MIMO Cognitive Radio: A Game Theoretical Approach," *IEEE Transactions on Signal Processing*, 2010.

[33] D. Bertsekas and J. Tsitsiklis, "Parallel and distributed computation : numerical methods," *SERBIULA (sistema Librum 2.0)*, 1989.

[34] G. J. Foschini and Z. Miljanic, "A simple distributed autonomous power control algorithm and its convergence," *IEEE Transactions on Vehicular Technology*, 1993.

[35] D. Mitra, "An Asynchronous Distributed Algorithm for Power Control in Cellular Radio Systems," *null*, 1994.

[36] R. D. Yates, "A framework for uplink power control in cellular radio systems," *IEEE Journal on Selected Areas in Communications*, 1995.

[37] H. Ji and C.-Y. Huang, "Non-cooperative uplink power control in cellular radio systems," *Wireless Networks*, 1998.

[38] T. Alpcan, T. Basar, R. Srikant, and E. Altman, "CDMA uplink power control as a noncooperative game," *null*, 2001.

[39] C. U. Saraydar, N. B. Mandayam, and D. J. Goodman, "Efficient power control via pricing in wireless data networks," *IEEE Transactions on Communications*, 2002.

[40] M. Xiao, N. B. Shroff, and E. K. P. Chong, "A utility-based power-control scheme in wireless cellular systems," *IEEE ACM Transactions on Networking*, 2003.

[41] K. K. Leung, C. W. Sung, W. S. Wong, and T.-M. Lok, "Convergence theorem for a general class of power-control algorithms," *IEEE Transactions on Communications*, 2004.

[42] C. W. Sung and K.-K. Leung, "A generalized framework for distributed power control in wireless networks," *IEEE Transactions on Information Theory*, 2005.

[43] K. B. Song, S. T. Chung, G. Ginis, G. Ginis, and J. M. Cioffi, "Dynamic spectrum management for next-generation DSL systems," *IEEE Communications Magazine*, 2002.

[44] W. Yu, G. Ginis, G. Ginis, and J. M. Cioffi, "Distributed multiuser power control for digital subscriber lines," *IEEE Journal on Selected Areas in Communications*, 2002.

[45] S. T. Chung, S.-J. Kim, J. Lee, and J. M. Cioffi, "A game-theoretic approach to power allocation in frequency-selective Gaussian interference channels," *null*, 2003.

[46] G. Scutari, S. Barbarossa, and D. Ludovici, "On the maximum achievable rates in wireless meshed networks: centralized versus decentralized solutions," *null*, 2004.

[47] N. Yamashita and Z.-Q. Luo, "A nonlinear complementarity approach to multiuser power control for digital subscriber lines," *Optimization Methods & Software*, 2004.

[48] Z.-Q. Luo and J.-S. Pang, "Analysis of iterative waterfilling algorithm for multiuser power control in digital subscriber lines," *EURASIP Journal on Advances in Signal Processing*, 2006.

[49] G. Scutari, D. P. Palomar, and S. Barbarossa, "Simultaneous iterative water-filling for Gaussian frequency-selective interference channels," in *2006 IEEE International Symposium on Information Theory*, pp. 600–604, IEEE, 2006.

[50] G. Scutari, D. P. Palomar, and S. Barbarossa, "Asynchronous Iterative Water-Filling for Gaussian Frequency-Selective Interference Channels: A Unified Framework," *null*, 2006.

[51] G. Scutari, D. P. Palomar, and S. Barbarossa, "Distributed Totally Asynchronous Iterative Waterfilling for Wideband Interference Channel with Time/Frequency Offset," *2007 IEEE International Conference on Acoustics, Speech and Signal Processing - ICASSP '07*, 2007.

[52] G. Scutari, D. P. Palomar, and S. Barbarossa, "Optimal Linear Precoding Strategies for Wideband Noncooperative Systems Based on Game Theory—Part I: Nash Equilibria," *IEEE Transactions on Signal Processing*, 2008.

[53] G. Scutari, D. P. Palomar, and S. Barbarossa, "Optimal linear precoding strategies for wideband non-cooperative systems based on game theory—Part II: Algorithms," *IEEE Transactions on Signal Processing*, vol. 56, no. 3, pp. 1250–1267, 2008.

[54] G. Scutari, D. P. Palomar, and S. Barbarossa, "The MIMO iterative waterfilling algorithm," *IEEE Transactions on Signal Processing*, vol. 57, no. 5, pp. 1917–1935, 2009.

[55] G. Scutari, F. Facchinei, J.-S. Pang, and D. P. Palomar, "Real and complex monotone communication games," *IEEE Transactions on Information Theory*, vol. 60, no. 7, pp. 4197–4231, 2014.

[56] C. Shi, F. Wang, M. Sellathurai, and J. Zhou, "Game theoretic power allocation for coexisting multistatic radar and communication systems," in *2018 14th IEEE International Conference on Signal Processing (ICSP)*, pp. 872–877, IEEE, 2018.

[57] A. Garnaev, A. Petropulu, W. Trappe, and H. V. Poor, "A power control problem for a dual communication-radar system facing a jamming threat," in *2020 IEEE Radar Conference (RadarConf20)*, pp. 1–6, IEEE, 2020.

[58] J. Huang, C.-c. Xing, and M. Guizani, "Power allocation for D2D communications with SWIPT," *IEEE Transactions on Wireless Communications*, vol. 19, no. 4, pp. 2308–2320, 2020.

[59] Y. Liu, Z. Wen, N. C. Beaulieu, D. Liu, and X. Liu, "Power allocation for SWIPT in full-duplex AF relay interference channels using game theory," *IEEE Communications Letters*, vol. 24, no. 3, pp. 608–611, 2020.

[60] J. Myung, K. Kim, and Y.-J. Ko, "Transmit power control game with a sum power constraint in cell-free massive MIMO downlink," *IEEE Wireless Communications Letters*, vol. 11, no. 3, pp. 632–635, 2021.

[61] A. U. Rahman, M. A. Kishk, and M.-S. Alouini, "A game-theoretic framework for coexistence of wifi and cellular networks in the 6-GHz unlicensed spectrum," *IEEE Transactions on Cognitive Communications and Networking*, 2022.

[62] R. Gupta and J. Gupta, "Federated learning using game strategies: State-of-the-art and future trends," *Comput. Networks*, 2023.

[63] X. Tu, K. Zhu, N. C. Luong, D. Niyato, Y. Zhang, and J. Li, "Incentive mechanisms for federated learning: From economic and game theoretic perspective," *IEEE Transactions on Cognitive Communications and Networking*, 2021.

[64] A. Richardson, A. Filos-Ratsikas, and B. Faltings, "Budget-bounded incentives for federated learning," *Federated Learning: Privacy and Incentive*, pp. 176–188, 2020.

[65] C. W. Zaw and C. S. Hong, "A decentralized game theoretic approach for energy-aware resource management in federated learning," *International Conference on Big Data and Smart Computing*, 2021.

[66] L. S. Shapley and F. D. Rigby, "Equilibrium points in games with vector payoffs," *Naval Research Logistics Quarterly*, vol. 6, no. 1, pp. 57–61, 1959.

[67] M. Zeleny, "Games with multiple payoffs," *International Journal of game theory*, vol. 4, no. 4, pp. 179–191, 1975.

[68] P. Borm, S. Tijs, and J. Van Den Aarssen, "Pareto equilibria in multi-objective games," *Methods of Operations Research*, vol. 60, pp. 302–312, 1988.

[69] A. Charnes, Z. Huang, J. J. Rousseau, and Q. L. Wei, "Cone extremal solutions of multi-payoff games with cross-constrained strategy sets," *Optimization*, vol. 21, no. 1, pp. 51–69, 1990.

[70] D. Ghose, "A necessary and sufficient condition for Pareto-optimal security strategies in multicriteria matrix games," *Journal of Optimization Theory and Applications*, vol. 68, no. 3, pp. 463–481, 1991.

[71] J. Zhao, "The equilibria of a multiple objective game," *International Journal of Game Theory*, vol. 20, no. 2, pp. 171–182, 1991.

[72] S. Wang, "Existence of a Pareto equilibrium," *Journal of Optimization Theory and Applications*, vol. 79, no. 2, pp. 373–384, 1993.

[73] J. Yu and G.-Z. Yuan, "The study of Pareto equilibria for multiobjective games by fixed point and Ky Fan minimax inequality methods," *Computers & Mathematics with Applications*, vol. 35, no. 9, pp. 17–24, 1998.

[74] J. Puerto, M. Hinojosa, A. Mármol, L. Monroy, and F. Fernández, "Solution concepts for multiple objective N-person games," *Investigaçao Operacional*, vol. 19, pp. 193–209, 1999.

[75] J. Dubra, F. Maccheroni, and E. A. Ok, "Expected utility theory without the completeness axiom," *Journal of Economic Theory*, vol. 115, no. 1, pp. 118–133, 2004.

[76] D. Lozovanu, D. Solomon, and A. Zelikovsky, "Multiobjective games and determining Pareto-Nash equilibria," *Buletinul Academiei de Ştiinţe a Moldovei. Matematica*, vol. 49, no. 3, pp. 115–122, 2005.

[77] S. Bade, "Nash equilibrium in games with incomplete preferences," *Economic Theory*, vol. 26, no. 2, pp. 309–332, 2005.

[78] A. M. Mármol, L. Monroy, M. Caraballo, and A. Zapata, "Equilibria with vector-valued utilities and preference information. the analysis of a mixed duopoly," *Theory and Decision*, vol. 83, no. 3, pp. 365–383, 2017.

[79] A. Zapata, A. Mármol, L. Monroy, and M. Caraballo, "A maxmin approach for the equilibria of vector-valued games," *Group Decision and Negotiation*, vol. 28, no. 2, pp. 415–432, 2019.

[80] J. Park, "Decision making and games with vector outcomes," *The BE Journal of Theoretical Economics*, vol. 20, no. 1, 2020.

[81] E. Bjornson, E. A. Jorswieck, M. Debbah, and B. Ottersten, "Multiobjective signal processing optimization: The way to balance conflicting metrics in 5G systems," *IEEE Signal Processing Magazine*, vol. 31, no. 6, pp. 14–23, 2014.

[82] R. T. Marler and J. S. Arora, "Survey of multi-objective optimization methods for engineering," *Structural and multidisciplinary optimization*, vol. 26, no. 6, pp. 369–395, 2004.

[83] R. Kasimbeyli, Z. K. Ozturk, N. Kasimbeyli, G. D. Yalcin, and B. I. Erdem, "Comparison of some scalarization methods in multiobjective optimization: comparison of scalarization methods," *Bulletin of the Malaysian Mathematical Sciences Society*, vol. 42, pp. 1875–1905, 2019.

[84] M. Ehrgott and M. M. Wiecek, "Multiobjective programming," *Multiple criteria decision analysis: State of the art surveys*, vol. 78, pp. 667–708, 2005.

[85] K. Klamroth and T. Jørgen, "Constrained optimization using multiple objective programming," *Journal of Global Optimization*, vol. 37, pp. 325–355, 2007.

[86] A. R. Chiriyath, B. Paul, and D. W. Bliss, "Radar-communications convergence: Coexistence, cooperation, and co-design," *IEEE Transactions on Cognitive Communications and Networking*, vol. 3, no. 1, pp. 1–12, 2017.

[87] Y. Liu, G. Liao, J. Xu, Z. Yang, and Y. Zhang, "Adaptive OFDM integrated radar and communications waveform design based on information theory," *IEEE Communications Letters*, vol. 21, no. 10, pp. 2174–2177, 2017. Publisher: IEEE.

[88] R. Xu, L. Peng, W. Zhao, W. Zhao, Z. Mi, and Z. Mi, "Radar mutual information and communication channel capacity of integrated radar-communication system using MIMO," *ICT Express*, 2015.

[89] N. Bekkali, M. Benammar, S. Bidon, and D. Roque, "Optimal Power Allocation in Monostatic OFDM Joint Radar Communications Systems," in *2022 IEEE Radar Conference (RadarConf22)*, pp. 1–6, IEEE, 2022.

[90] V. Karimi, R. Mohseni, and S. Samadi, "OFDM waveform design based on mutual information for cognitive radar applications," *The Journal of Supercomputing*, vol. 75, no. 5, pp. 2518–2534, 2019. Publisher: Springer.

[91] Y. Liu, G. Liao, and Z. Yang, "Robust OFDM integrated radar and communications waveform design based on information theory," *Signal Processing*, vol. 162, pp. 317–329, 2019. Publisher: Elsevier.

[92] Y. Liu, G. Liao, Y. Zhiwei, Z. Yang, and J. Xu, "Multiobjective optimal waveform design for OFDM integrated radar and communication systems," *Signal Processing*, 2017.

[93] R. A. Romero, J. Bae, and N. A. Goodman, "Theory and application of SNR and mutual information matched illumination waveforms," *IEEE Transactions on Aerospace and Electronic Systems*, vol. 47, no. 2, pp. 912–927, 2011. Publisher: IEEE.

[94] Y. Yang and R. S. Blum, "MIMO radar waveform design based on mutual information and minimum mean-square error estimation," *IEEE Transactions on Aerospace and electronic systems*, vol. 43, no. 1, pp. 330–343, 2007. Publisher: IEEE.

[95] M. R. Bell, "Information theory and radar waveform design," *IEEE Transactions on Information Theory*, vol. 39, no. 5, pp. 1578–1597, 1993. Publisher: IEEE.

[96] Z. Zhu, S. Kay, R. S. Raghavan, and R. S. Raghavan, "Information-Theoretic Optimal Radar Waveform Design," *IEEE Signal Processing Letters*, 2017.

[97] J. G. Metcalf, "An Examination of the Spectral Utility of Radar," in *2022 IEEE Radar Conference (RadarConf22)*, pp. 1–6, IEEE, 2022.

[98] A. Leshem, O. Naparstek, and A. Nehorai, "Information Theoretic Adaptive Radar Waveform Design for Multiple Extended Targets," *IEEE Journal of Selected Topics in Signal Processing*, 2007.

[99] D. S. Bernstein, *Matrix mathematics.* Princeton university press, 2009.

[100] R. J. Plemmons, "M-matrix characterizations. I—nonsingular M-matrices," *Linear Algebra and its Applications*, vol. 18, no. 2, pp. 175–188, 1977.

[101] P. Mertikopoulos, E. V. Belmega, A. L. Moustakas, and S. Lasaulce, "Dynamic power allocation games in parallel multiple access channels," in *Proceedings of the 5th International ICST Conference on Performance Evaluation Methodologies and Tools*, VALUETOOLS '11, (Brussels, BEL), p. 332–341, ICST (Institute for Computer Sciences, Social-Informatics and Telecommunications Engineering), 2011.

[102] P. Mertikopoulos, E. V. Belmega, A. L. Moustakas, and S. Lasaulce, "Distributed learning policies for power allocation in multiple access channels," *IEEE Journal on Selected Areas in Communications*, vol. 30, no. 1, pp. 96–106, 2011.

[103] A. Beck, *First-order methods in optimization.* SIAM, 2017.

[104] C. Dutang, "A survey of GNE computation methods: theory and algorithms," 2013.

[105] A. Fischer, M. Herrich, and K. Schönefeld, "Generalized Nash equilibrium problems-recent advances and challenges," *Pesquisa Operacional*, vol. 34, no. 3, pp. 521–558, 2014.

[106] F. Facchinei and S. Sagratella, "On the computation of all solutions of jointly convex generalized Nash equilibrium problems," *Optimization Letters*, vol. 5, no. 3, pp. 531–547, 2011.

[107] A. Dreves, F. Facchinei, C. Kanzow, and S. Sagratella, "On the solution of the KKT conditions of generalized Nash equilibrium problems," *SIAM Journal on Optimization*, vol. 21, no. 3, pp. 1082–1108, 2011.

[108] F. Facchinei, C. Kanzow, and S. Sagratella, "Solving quasi-variational inequalities via their KKT conditions," *Mathematical Programming*, vol. 144, no. 1, pp. 369–412, 2014.

[109] J.-S. Pang and M. Fukushima, "Quasi-variational inequalities, generalized Nash equilibria, and multi-leader-follower games," *Computational Management Science*, vol. 2, pp. 21–56, 2005.

[110] F. Facchinei, A. Fischer, and V. Piccialli, "Generalized Nash equilibrium problems and Newton methods," *Mathematical Programming*, vol. 117, no. 1-2, pp. 163–194, 2009.

[111] A. Singh and D. Ghosh, "A globally convergent improved BFGS method for generalized Nash equilibrium problems," *SeMA Journal*, pp. 1–27, 2023.

[112] F. Facchinei and C. Kanzow, "Penalty methods for the solution of generalized Nash equilibrium problems," *SIAM Journal on Optimization*, vol. 20, no. 5, pp. 2228–2253, 2010.

[113] T. Migot and M.-G. Cojocaru, "A decomposition method for a class of convex generalized Nash equilibrium problems," *Optimization and Engineering*, vol. 22, pp. 1653–1679, 2021.

[114] J. G. Kim, "Equilibrium computation of generalized Nash games: A new Lagrangian-based approach," *arXiv preprint arXiv:2106.00109*, 2021.

[115] F. Facchinei, V. Piccialli, and M. Sciandrone, "Decomposition algorithms for generalized potential games," *Computational Optimization and Applications*, vol. 50, no. 2, pp. 237–262, 2011.

[116] I. Stupia, L. Sanguinetti, G. Bacci, and L. Vandendorpe, "Power control in networks with heterogeneous users: A quasi-variational inequality approach," *IEEE Transactions on Signal Processing*, vol. 63, no. 21, pp. 5691–5705, 2015.

[117] G. Thiran, I. Stupia, and L. Vandendorpe, "Energy efficient competitive resource allocation in MIMO networks," *arXiv preprint arXiv:2012.07312*, 2020.

[118] J. Nie, X. Tang, and L. Xu, "The Gauss–Seidel method for generalized Nash equilibrium problems of polynomials," *Computational Optimization and Applications*, vol. 78, pp. 529–557, 2021.

[119] M. F. Anjos and J. B. Lasserre, *Handbook on semidefinite, conic and polynomial optimization*, vol. 166. Springer Science & Business Media, 2011.

[120] J. P. Boyle and R. L. Dykstra, "A method for finding projections onto the intersection of convex sets in hilbert spaces," in *Advances in Order Restricted Statistical Inference* (R. Dykstra, T. Robertson, and F. T. Wright, eds.), (New York, NY), pp. 28–47, Springer New York, 1986.

[121] S. Boyd, S. P. Boyd, and L. Vandenberghe, *Convex optimization*. Cambridge university press, 2004.

[122] H. Whitney, "Analytic extensions of differentiable functions defined in closed sets," *Hassler Whitney Collected Papers*, pp. 228–254, 1992.

[123] S. M. Robinson, "Stability theory for systems of inequalities. part I: Linear systems," *SIAM Journal on Numerical Analysis*, vol. 12, no. 5, pp. 754–769, 1975.

[124] D. P. Bertsekas, "Nonlinear programming," *Journal of the Operational Research Society*, vol. 48, no. 3, pp. 334–334, 1997.

[125] G. Giorgi *et al.*, "A guided tour in constraint qualifications for nonlinear programming under differentiability assumptions," tech. rep., University of Pavia, Department of Economics and Management, 2018.

[126] R. Janin, "Directional derivative of the marginal function in nonlinear programming," in *Sensitivity, Stability and Parametric Analysis*, pp. 110–126, Springer, 1984.

[127] J. Liu, "Sensitivity analysis in nonlinear programs and variational inequalities via continuous selections," *SIAM Journal on Control and Optimization*, vol. 33, no. 4, pp. 1040–1060, 1995.

[128] J. E. Spingarn and R. T. Rockafellar, "The generic nature of optimality conditions in nonlinear programming," *Mathematics of Operations Research*, vol. 4, no. 4, pp. 425–430, 1979.

[129] A. V. Fiacco *et al.*, *Introduction to sensitivity and stability analysis in nonlinear programming*, vol. 165. Academic press, 1983.

[130] F. H. Clarke, "Generalized gradients of Lipschitz functionals," *Advances in Mathematics*, vol. 40, no. 1, pp. 52–67, 1981.

[131] F. H. Clarke, *Optimization and nonsmooth analysis.* SIAM, 1990.

[132] R. T. Rockafellar and R. J.-B. Wets, *Variational analysis*, vol. 317. Springer Science & Business Media, 2009.

[133] S. M. Perlaza, H. Tembine, S. Lasaulce, and M. Debbah, "Quality-of-service provisioning in decentralized networks: A satisfaction equilibrium approach," *IEEE Journal of Selected Topics in Signal Processing*, vol. 6, no. 2, pp. 104–116, 2012.

[134] G. Thiran and L. Vandendorpe, "Absolutely secure beamforming in non-coherent cell-free networks," in *INTERACT 7th Technical Meeting*, 2024.

[135] G. Thiran and L. Vandendorpe, "Coding-aware secure beamforming in cell-free networks," in *(Accepted to) 2024 IEEE 25th international workshop on signal processing advances in wireless communications (SPAWC)*, IEEE, 2024.

[136] C. E. Shannon, "Communication theory of secrecy systems," *The Bell system technical journal*, vol. 28, no. 4, pp. 656–715, 1949.

[137] H. Sharma, N. Kumar, and R. Tekchandani, "Physical layer security using beamforming techniques for 5G and beyond networks: A systematic review," *Physical Communication*, vol. 54, p. 101791, 2022.

[138] A. Cohen, R. G. L. D'Oliveira, C.-Y. Yeh, H. Guerboukha, R. Shrestha, Z. Fang, E. W. Knightly, M. Médard, and D. M. Mittleman, "Absolute security in terahertz wireless links," 2023.

[139] Y. Shiri, C.-Y. Yeh, Z. Fang, R. Shrestha, H. Guerboukha, J. Malowicki, N. Thawdar, and D. M. Mittleman, "Absolute security with diffraction grating in terahertz communication links," in *2023 48th International Conference on Infrared, Millimeter, and Terahertz Waves (IRMMW-THz)*, pp. 1–2, IEEE, 2023.

[140] C.-Y. Yeh, M. Médard, and D. M. Mittleman, "Absolute security with digital beamforming for high-frequency links," in *2023 48th International Conference on Infrared, Millimeter, and Terahertz Waves (IRMMW-THz)*, pp. 1–2, 2023.

[141] S. Elhoushy, M. Ibrahim, and W. Hamouda, "Cell-free massive MIMO: A survey," *IEEE Communications Surveys & Tutorials*, vol. 24, no. 1, pp. 492–523, 2021.

[142] E. Björnson, O. T. Demir, and L. Sanguinetti, "A primer on near-field beamforming for arrays and reconfigurable intelligent surfaces," in *2021 55th Asilomar Conference on Signals, Systems, and Computers*, pp. 105–112, 2021.

[143] R. Sargent and D. Sebastian, "On the convergence of sequential minimization algorithms," *Journal of Optimization Theory and Applications*, vol. 12, pp. 567–575, 1973.

[144] F. De Saint Moulin, G. Thiran, C. Oestges, and L. Vandendorpe, "Fair beamforming design for MIMO ISAC systems," in *2024 19th International Symposium on Wireless Communication Systems (ISWCS)*, pp. 1–6, 2024.

[145] A. Hassanien, C. Sahin, J. Metcalf, and B. Himed, "Uplink signaling and receive beamforming for dual-function radar communications," in

2018 IEEE 19th International Workshop on Signal Processing Advances in Wireless Communications (SPAWC), pp. 1–5, IEEE, 2018.

[146] F. Dong, W. Wang, Z. Hu, and T. Hui, "Low-complexity beamformer design for joint radar and communications systems," *IEEE Communications Letters*, vol. 25, no. 1, pp. 259–263, 2020. Publisher: IEEE.

[147] Y. Ni, Z. Wang, and Q. Huang, "Joint Transceiver Beamforming for Multi-Target Single-User Joint Radar and Communication," *IEEE Wireless Communications Letters*, vol. 11, no. 11, pp. 2360–2364, 2022. Publisher: IEEE.

[148] F. Liu, Y.-F. Liu, A. Li, C. Masouros, and Y. C. Eldar, "Cramér-Rao bound optimization for joint radar-communication beamforming," *IEEE Transactions on Signal Processing*, vol. 70, pp. 240–253, 2021. Publisher: IEEE.

[149] M. Zhu, L. Li, S. Xia, and T.-H. Chang, "Information and sensing beamforming optimization for multi-user multi-target MIMO ISAC systems," *EURASIP Journal on Advances in Signal Processing*, vol. 2023, no. 1, p. 15, 2023. Publisher: Springer.

[150] Z. Liu, S. Aditya, H. Li, and B. Clerckx, "Joint transmit and receive beamforming design in full-duplex integrated sensing and communications," *IEEE Journal on Selected Areas in Communications*, vol. 41, no. 9, pp. 2907–2919, 2023.

[151] L. Chen, F. Liu, W. Wang, and C. Masouros, "Joint radar-communication transmission: A generalized Pareto optimization framework," *IEEE Transactions on Signal Processing*, vol. 69, pp. 2752–2765, 2021. Publisher: IEEE.

[152] W. Yuan, L. Zhou, S. K. Dehkordi, S. Li, P. Fan, G. Caire, and H. V. Poor, "From OTFS to DD-ISAC: Integrating sensing and communications in the delay doppler domain," *arXiv preprint arXiv:2311.15215*, 2023.

[153] J. Kiefer, "Sequential minimax search for a maximum," *Proceedings of the American mathematical society*, vol. 4, no. 3, pp. 502–506, 1953.

[154] F. D. S. Moulin, G. Thiran, C. Craeye, L. Vandendorpe, and C. Oestges, "Near-field EM-based multistatic radar range estimation," in *INTERACT 7th Technical Meeting*, 2024.

[155] F. D. S. Moulin, G. Thiran, C. Craeye, L. Vandendorpe, and C. Oestges, "Near-field EM-based multistatic radar range estimation," in *(Accepted to) 2024 32nd European Signal Processing Conference (EUSIPCO)*, IEEE, 2024.

[156] G. Thiran, F. D. S. Moulin, C. Oestges, and L. Vandendorpe, "Performance bounds for near-field multi-antenna range estimation of extended targets," in *(Accepted to) 2024 IEEE 25th international workshop on signal processing advances in wireless communications (SPAWC)*, IEEE, 2024.

[157] F. De Saint Moulin, G. Thiran, C. Craeye, L. Vandendorpe, and C. Oestges, "Near-field EM-based multistatic radar range estimation," *arXiv preprint arXiv:2403.09258*, 2024.

[158] S. Hunsche, M. Koch, I. Brener, and M. Nuss, "THz near-field imaging," *Optics communications*, vol. 150, no. 1-6, pp. 22–26, 1998.

[159] D. Sheen, D. McMakin, and T. Hall, "Near-field three-dimensional radar imaging techniques and applications," *Appl. Opt.*, vol. 49, pp. E83–E93, Jul 2010.

[160] S. S. Ahmed, *Electronic microwave imaging with planar multistatic arrays.* Logos Verlag Berlin GmbH, 2014.

[161] J. Laviada, A. Arboleya-Arboleya, Y. Alvarez-Lopez, C. Garcia-Gonzalez, and F. Las-Heras, "Phaseless synthetic aperture radar with efficient sampling for broadband near-field imaging: Theory and validation," *IEEE Transactions on Antennas and Propagation*, vol. 63, no. 2, pp. 573–584, 2014.

[162] X. Yang, Y. R. Zheng, M. T. Ghasr, and K. M. Donnell, "Microwave imaging from sparse measurements for near-field synthetic aperture radar," *IEEE Transactions on Instrumentation and Measurement*, vol. 66, no. 10, pp. 2680–2692, 2017.

[163] Y. Begriche, M. Thameri, and K. Abed-Meraim, "Exact conditional and unconditional Cramér–Rao bounds for near field localization," *Digital Signal Processing*, vol. 31, pp. 45–58, 2014.

[164] M. N. El Korso, R. Boyer, A. Renaux, and S. Marcos, "Conditional and unconditional Cramér–Rao bounds for near-field source localization,"

IEEE Transactions on Signal Processing, vol. 58, no. 5, pp. 2901–2907, 2010.

[165] A. Chen, L. Chen, Y. Chen, C. You, G. Wei, and F. R. Yu, "Cramér-Rao bounds of near-field positioning based on electromagnetic propagation model," *IEEE Transactions on Vehicular Technology*, 2023.

[166] H. Hua, J. Xu, and Y. C. Eldar, "Near-field 3D localization via MIMO radar: Cramér-Rao bound analysis and estimator design," *arXiv preprint arXiv:2308.16130*, 2023.

[167] A. Sakhnini, S. De Bast, M. Guenach, A. Bourdoux, H. Sahli, and S. Pollin, "Near-field coherent radar sensing using a massive MIMO communication testbed," *IEEE Transactions on Wireless Communications*, vol. 21, no. 8, pp. 6256–6270, 2022.

[168] A. Sakhnini, A. Albaba, A. Bourdoux, and S. Pollin, "A general technique for radar resolution analysis based on a quadratic approximation," *IEEE Transactions on Radar Systems*, vol. 2, pp. 251–262, 2024.

[169] A. Sakhnini, M. Wachowiak, A. Bourdoux, and S. Pollin, "An approximation of the range resolution in the near-field of a distributed antenna array," *IEEE Wireless Communications Letters*, pp. 1–1, 2024.

[170] H. Wang, Z. Xiao, and Y. Zeng, "Cramér-Rao bounds for near-field sensing with extremely large-scale MIMO," *IEEE Transactions on Signal Processing*, 2024.

[171] E. Björnson, Ö. T. Demir, and L. Sanguinetti, "A primer on near-field beamforming for arrays and reconfigurable intelligent surfaces," in *2021 55th Asilomar Conference on Signals, Systems, and Computers*, pp. 105–112, IEEE, 2021.

[172] F. Xu, S. A. Vorobyov, and F. Yang, "Transmit beamspace DDMA based automotive MIMO radar," *IEEE Transactions on Vehicular Technology*, vol. 71, no. 2, pp. 1669–1684, 2021.

[173] H. Lu and Y. Zeng, "Communicating with extremely large-scale array/surface: Unified modeling and performance analysis," *IEEE Transactions on Wireless Communications*, vol. 21, no. 6, pp. 4039–4053, 2021.

[174] M. A. Richards *et al.*, *Fundamentals of radar signal processing*, vol. 1. Mcgraw-hill New York, 2005.

[175] M. Cui and L. Dai, “Channel estimation for extremely large-scale MIMO: Far-field or near-field?,” *IEEE Transactions on Communications*, vol. 70, no. 4, pp. 2663–2677, 2022.

[176] Z. Wang, P. Ramezani, Y. Liu, and E. Björnson, “Near-field localization and sensing with large-aperture arrays: From signal modeling to processing,” *arXiv preprint arXiv:2406.10941*, 2024.

[177] G. Thiran, F. D. S. Moulin, C. Oestges, and L. Vandendorpe, “Performance bounds for near-field multi-antenna range estimation of extended targets,” *arXiv preprint arXiv:2404.06949*, 2024.